Barrier properties of human skin equivalents : rising to the surface

Thakoersing, V.S.

BARRIER PROPERTIES OF HUMAN SKIN EQUIVALENTS: RISING TO THE SURFACE

VARSHA THAKOERSING

Barrier properties of human skin equivalents: rising to the surface

Varsha Thakoersing

PhD thesis with summary in Dutch

June 2012

Cover design by Jetish Hardwarsing

Printed by Proefschrift Maken

BARRIER PROPERTIES OF HUMAN SKIN EQUIVALENTS: RISING TO THE SURFACE

Proefschrift

ter verkrijging van
de graad van Doctor aan de Universiteit Leiden,
op gezag van Rector Magnificus prof. mr. P.F. van der Heijden,
volgens besluit van het College voor Promoties
te verdedigen op donderdag 7 juni
klokke 10.00 uur

door

Varsha Sakina Thakoersing
Geboren te Paramaribo, Suriname
in 1984

Promotiecommissie

Promotor:	Prof. Dr. J.A. Bouwstra
Copromotor:	Dr. A. El Ghalbzouri
Overige leden:	Prof. Dr. M. Danhof
	Prof. Dr. T. Hankemeier
	Prof. Dr. R. Sandhoff
	Prof. Dr. J. Schalkwijk
	Dr. M. Boncheva

The investigations described in this thesis have been co-supervised by Dr. M. Ponec and were performed at the department of Drug Delivery Technology at the Leiden/Amsterdam Center for Drug Research (LACDR), Leiden University, Leiden, The Netherlands.

This research is supported by the Dutch Technology Foundation STW (grant no. 7503), which is part of the Netherlands Organisation for Scientific Research (NWO) and partly funded by the Ministry of Economic Affairs, Agriculture and Innovation. Additionally, the printing of this thesis was financially supported by STW.

Opgedragen aan mijn ouders...

...voor al jullie steun en liefde

STELLINGEN

Behorende bij het proefschrift

Barrier properties of human skin equivalents: rising to the surface

1. The culture conditions play a crucial role in determining the stratum corneum barrier properties of human skin equivalents. *(this thesis)*

2. Human skin equivalents are able to synthesize all skin barrier lipids, including the twelve ceramide subclasses present in human stratum corneum. *(this thesis)*

3. The reduced free fatty acid level and its altered composition may play an important role in the decreased permeability barrier observed for human skin equivalents. *(this thesis)*

4. The detection of increased levels of mono-unsaturated fatty acids in the stratum corneum of human skin equivalents offers new opportunities to mimic the stratum corneum lipid properties of human skin more closely. *(this thesis)*

5. The mammalian stratum corneum is a remarkable structure that appears lifeless and trivial to the histologist but in reality has almost unbelievable complexities, subtleties, and importance. (*Marks, R., J Nutr 134, 2017S, 2004)*

6. The important role of ceramide EOS in the formation of the 13.4 nm lamellar phase and the transition from a hexagonal to an orthorhombic phase induced by free fatty acids have been observed in mixtures prepared with isolated SC lipids as well as in intact human stratum corneum. *(Bouwstra, J. et al., Skin PharmacolAppl Skin Physiol 14 Suppl 1, 52, 2001)*

7. It is the stated goal of all manufacturers to fit their skin models with a barrier similar to human skin *in vivo*, but it is not foreseeable if or when they will succeed. *(Netzlaff, F. et al., Eur J Pharm Biopharm 60, 167, 2005)*

8. While I have tried to discuss some of what is known about the role of lipids in the formation of this complex stratum corneum lamellar membrane that mediates permeability barrier function, it should be obvious to the reader that much work remains to be done to fully understand the formation and regulation of the epidermal permeability barrier. *(Feingold, K.R., J Lipid Res 48, 2531, 2007)*

9. The beginning of knowledge is the discovery of something we do not understand. *(Frank Herbert)*

10. Employ your time in improving yourself by other men's writings, so that you shall gain easily what others have labored hard for. *(Socrates)*

11. I am among those who think that science has great beauty. A scientist in his laboratory is not only a technician: he is also a child placed before natural phenomena which impress him like a fairy tale. *(Marie Curie)*

12. Being a graduate student is like becoming all of the Seven Dwarves. In the beginning you're Dopey and Bashful. In the middle, you are usually sick (Sneezy), tired (Sleepy), and irritable (Grumpy). But at the end, they call you Doc, and then you're Happy. *(Ronald T. Azuma)*

TABLE OF CONTENTS

1

Essentials of the Skin Barrier

FUNCTION AND STRUCTURE OF THE SKIN

The skin is the largest organ of the body with a surface area of approximately 1.5 m^2 in adults and accounts for roughly 15% of the body weight [1]. The principal function of the skin is to protect the body's interior from the external environment. It prevents the entry of pathogens and exogenous substances into the body and regulates heat and water loss from the body. The stratum corneum (SC) is the uppermost layer of the skin and has a very hydrophobic character. Due to this property it forms an excellent physical barrier against penetration of foreign substances and is concomitantly able to prevent excessive water loss [2, 3]. When exogenous substances partition into the viable skin, defence mechanisms provided by the immunological and biochemical barrier (e.g. detoxification by metabolic enzymes) play an important role [4, 5]. To maintain the body's core temperature the skin exchanges heat with its surrounding through moisture and sweat evaporation at the skin surface [6]. The skin also functions as a sensory organ and detects stimuli such as heat, cold, pressure and pain [7]. The skin has a complex structure consisting of three main regions (from inside out): the dermis, the basement membrane and the epidermis (figure 1).

The dermis

The dermis has a thickness up to 3 mm and can be subdivided into two layers: the papillary and reticular layer. The papillary layer is located 100 to 150 μm underneath the skin surface, while the reticular layer is located in the lower part of the dermis. Blood and lymphatic vessels, nerve endings, hair follicles, sebaceous and sweat glands are all embedded within the dermis. The nerve endings provide the sense of touch and heat. The vascular network of the skin provides oxygen and nutrients to the surrounding tissue and removes toxins and waste products. The vasculature of the skin also plays a role in thermoregulation and wound repair. The main cell type in the dermis is the fibroblast. Fibroblasts secrete collagen, which is the main protein in the dermis, and elastin to generate an extracellular matrix [8, 9].

The collagen fibres give the dermis its toughness and resistance to strain, while elastin is responsible for the elastic properties of the dermis. In addition to fibroblasts, the dermis also contains endothelial cells, mast cells, macrophages, dendritic cells, T-lymphocytes and neutrophils. The various immune cells present in the dermis provide a defence mechanism against intruded pathogens and exogenous substances.

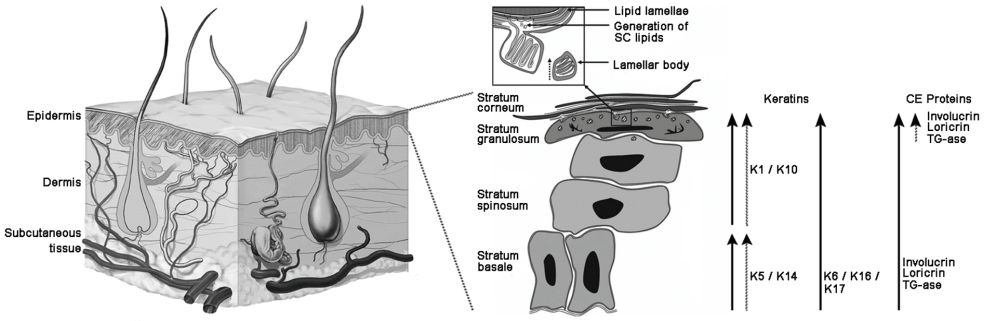

Figure 1. Schematic overview of the structure of human skin. The dermis contains the skin appendages (sweat glands, sebaceous glands and hair follicles), blood and lymphatic vessels and nerve endings. The epidermis is the most superficial layer of the skin and can be subdivided into four strata: the stratum basale, stratum spinosum, stratum granulosum and stratum corneum. During the migration from the basal layer to the stratum corneum, the keratinocytes show the expression of several keratins (K1, K5, K6, K10, K14, K16, K17) and cornified envelope (CE) proteins in specific layers of the epidermis (dotted arrows). The expression of these proteins may be altered in skin disorders (black arrows). At the stratum granulosum-SC interface lamellar bodies containing lipid precursors are extruded. After enzymatic processing, the SC lipids form neatly arranged lipid lamellae around the corneocytes. TG-ase = transglutaminase. This figure is modified from [3, 143].

The basement membrane

The cutaneous basement membrane zone, also known as the dermal-epidermal junction (DEJ), is located between the dermis and the epidermis [10, 11]. The DEJ consists of four distinctive zones: the cell membrane of the basal keratinocytes, the lamina lucida, the lamina densa and the sub-basal lamina. The cell membranes of

the keratinocytes contain hemidesmosomes, which attach keratin filaments to the basolateral epidermal surface. The hemidesmosomes also firmly attach the cell membranes of keratinocytes, the lamina lucida and lamina densa together, by connecting to anchoring filaments that originate from the lamina densa and traverse the lamina lucida. Anchoring fibrils in the lamina densa extend into the dermis and loop back into the lamina densa or are inserted into electron-dense anchoring plaques in the dermis. The existence of anchoring plaques, however, is controversial. The tight connection of the different zones in the DEJ maintains the structural integrity of the skin, provides support for the epidermis and influences keratinocyte polarity, proliferation, differentiation and migration. The DEJ selectively permits the passage of molecules between the dermis and epidermis based on their size and charge. However, migrating or invading cells, such as melanocytes, Langerhans cells and lymphocytes are able to pass freely.

The epidermis

The epidermis is the uppermost layer of the skin. It contains no blood vessels, but is nourished by the diffusion of nutrients from the blood capillaries in the upper dermis. Keratinocytes are the predominant cell types found in the epidermis, although other cells such as Langerhans cells, melanocytes, Merkel cells and T-lymphocytes are also present. The epidermis can be subdivided into four different strata (from inside out): the stratum basale, stratum spinosum, stratum granulosum and SC (figure 1). The transit of keratinocytes through the different epidermal layers is a very dynamic process. The journey of a keratinocyte starts in the basal layer, which contains the proliferating cells of the skin. After a mitotic division, a daughter cell will remain in the basal layer while the other newly formed cell will transiently migrate upwards and start to differentiate [12, 13]. During the differentiation process the keratinocytes will start to express several early and late differentiation markers. This coincides with the gradual change of keratinocyte function (figure 1). In the stratum spinosum the keratinocytes express keratin 10.

Simultaneously the keratinocytes start to produce lipid-enriched lamellar bodies. In the upper spinous layers the keratinocytes become flatter and move into the direction of the stratum granulosum. Once in the stratum granulosum, the keratinocytes accumulate keratohyalin granules, which contain a number of barrier proteins, such as profilaggrin, loricrin and involucrin [14, 15]. Additionally, the production of lamellar bodies is enhanced. At the stratum granulosum/SC interface the keratinocytes initiate the terminal differentiation programme and many processes take place in a very short period. The keratin filaments aggregate into a keratin matrix after interaction with the filaggrin subunit of profilaggrin. Additionally, enzymes will start to degrade the cell components, such as the nucleus and cell organelles. Furthermore, desmosomes, which link the keratinocytes together, are transformed into corneodesmosomes and a cornified envelope is formed around the plasma membrane. The cornified envelope is composed of several structural proteins like involucrin, loricrin and the small-proline rich proteins, which are cross-linked by transglutaminases. The lipid and enzymatic content of the lamellar bodies is extruded via exocytosis at the stratum granulosum/SC interface (figure 1) and a major change in lipid composition occurs [16, 17]. All these changes in the keratinocytes and the secretion of the lipids into the intercellular regions consequently lead to the formation of the SC. The SC consists of dead flattened cells, referred to as corneocytes, which are embedded in a continuous hydrophobic lipid matrix. The corneocytes in the SC are devoid of a nucleus and have replaced the plasma membrane with the highly impermeable cornified envelope, which is chemically coated by a lipid envelope. Corneodesmosomes, which are incorporated in the cornified envelope, link the corneocytes together to maintain SC cohesion. The formation of the SC is a fundamental process that leads to the development of a barrier against excessive water evaporation and protection against penetration of exogenous substances. It generally comprises 10-15 cell layers and is 10-20 μm thick [18, 19]. During the movement of the corneocytes into the direction of the skin surface, the

corneodesmosomes are gradually degraded. This finally leads to shedding of the superficial cells from the skin surface, which is referred to as the desquamation process.

PROPERTIES OF THE STRATUM CORNEUM

Although the SC consists of dead cells, it is considered as a very dynamic tissue due to the continuous formation of new SC layers and the many enzymatic processes that take place. The following sections will provide a more detailed description of the SC structure and mechanisms that maintain the SC properties.

Stratum corneum lipid composition

The corneocytes contain a densely cross-linked protein envelope that is surrounded by a covalently attached lipid layer, also known as the lipid envelope [20]. The major constituents of the lipid envelope are ω-hydroxyceramides, which have a long ω-hydroxy fatty acid that is linked to sphingosine (ceramide A) [21] or 6-hydroxy-4-sphingenine (ceramide B) [22] through an amide bond. The lipid envelope is thought to serve as a scaffold for the proper arrangement of the intercellular SC lipids.

The densely cross-linked protein envelope is rather impermeable, which reduces the partitioning of most substances into the corneocytes . Therefore, the pathway for compound penetration is thought to mainly proceed via the SC lipid domains [23, 24]. The composition and organization of the SC lipids is therefore essential for the permeability barrier of the skin. Changes in the composition and consequently the organization of the SC lipids are known to have detrimental effects on the barrier function of the skin [25]. The SC lipid matrix is composed of cholesterol, free fatty acids and ceramides in an approximately equimolar ratio [16, 17]. Human SC consists of heterogeneous species of free fatty acids and ceramides. The free fatty acids mostly have a saturated acyl chain with a chain length varying from 14 carbon

atoms up to 32 carbon atoms. The most abundant free fatty acid species in human SC are lignoceric acid (C24:0) and cerotic acid (C26:0) [26, 27]. Free fatty acids are generated by the catabolism of phospholipids, which are extruded from lamellar bodies, by phospholipases [16, 28]. Ceramides have a sphingoid base to which a fatty acid is linked. Human SC contains twelve ceramide subclasses [29], which are named according to their chemical structure [30, 31]. Ceramides can have a sphingosine (S), dihydrosphingosine (dS), phytosphingosine (P) or 6-hydroxysphingosine (H) base to which an esterified ω-hydroxy (EO), α-hydroxy (A) or non-hydroxy (N) fatty acid with a varying acyl chain length is linked (figure 2). Among the SC ceramides the acylceramides (EO ceramides) have a unique structure. They have a very long ω-hydroxy fatty acid chain containing up to 34 carbon atoms to which linoleic acid (C18:2) is linked [32]. Human SC ceramides are generated from two different lipid precursors present in the lamellar bodies, namely glucosphingolipids and sphingomyelin [33, 34], by the action of β-glucocerebrosidase [35] and sphingomyelinase [36] respectively.

Fatty acid / Sphingoid	Non-hydroxy fatty acid [N]	α-hydroxy fatty acid [A]	Esterified ω-hydroxy fatty acid [EO]
Dihydrosphingosine [DS]	CER[NDS]	CER[ADS]	CER[EODS]
Sphingosine [S]	CER[NS]	CER[AS]	CER[EOS]
Phytosphingosine [P]	CER[NP]	CER[AP]	CER[EOP]
6-hydroxy sphingosine [H]	CER[NH]	CER[AH]	CER[EOH]

Figure 2. The structure and nomenclature of ceramide subclasses present in human SC. This figure is adopted from [30].

Stratum corneum lipid organization

Cholesterol, free fatty acids and ceramides form neatly arranged lipid layers (i.e. lipid lamellae) that are stacked on top of each other oriented approximately parallel to the skin surface (figure 3). The distance over which a lipid layer is repeated is referred to as the repeat distance. In native human SC two types of lipid lamellae are observed, each with a different repeat distance. The long periodicity phase (LPP) has a repeat distance of approximately 13 nm and the short periodicity phase (SPP) has a repeat distance of around 6 nm [37-41]. The LPP is considered to be important for the barrier function of the skin, as its presence is detected in the SC of all species studied so far. Additionally, recent studies have shown that the LPP plays an essential role in the barrier function of the skin [42, 43].

The packing of the lipids within the lipid lamellae is referred to as the lateral organization. This packing is also of importance for the barrier function of the skin (figure 3). The liquid, hexagonal and orthorhombic packing have an increasing packing density. At a physiological temperature the SC lipids are mostly arranged in an orthorhombic lattice, although some lipids also form the hexagonal or liquid packing [44-46].

Epidermal lipid metabolism

The viable epidermis is an active site for lipid synthesis, since it requires the production of a considerable amount of lipids to form the SC. Additionally, many of these lipid species are unique and are only synthesized in the skin. Fatty acids can be synthesized *de novo* by keratinocytes or originate from dietary sources. Linoleic acid (C18:2) and arachidonic acid (C20:4) are two essential fatty acids that cannot be synthesized by keratinocytes and are therefore derived from external sources. Fatty acid synthase synthesizes fatty acids up to 16 carbon atoms [47]. The elongation of fatty acids is a four step reaction, which are all executed by fatty acid synthase. The elongation of fatty acids with 16 carbon atoms or more principally

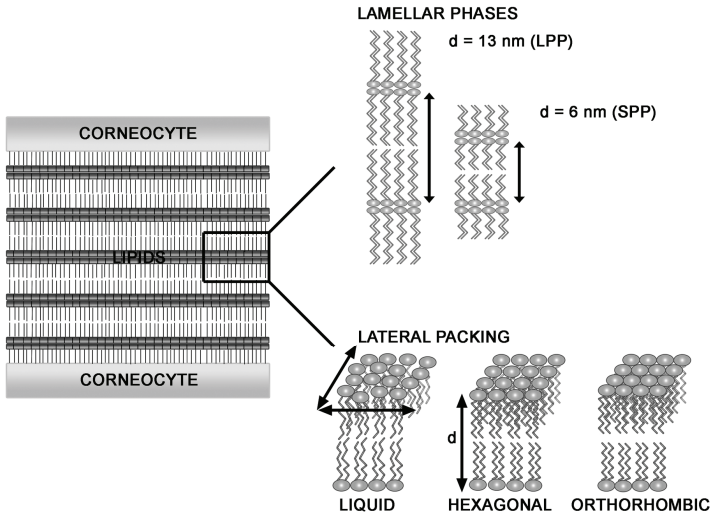

Figure 3. Schematic overview of the lamellar and lateral lipid organization of human SC lipids. Human SC contains lipid lamellae with a repeat distance (d) of 13 nm or 6 nm, referred to as the long periodicity phase (LPP) and short periodicity phase (SPP), respectively. The lipids in the lipid lamellae predominantly form the dense orthorhombic packing in native human SC, although some lipid populations also form the hexagonal or liquid packing. This figure is adapted from [118].

involve the same processes, but requires four distinct enzymes. The first step in the elongation cycle is performed by elongases (ELOVLs) and is also the rate-limiting step. In mammals seven ELOVLs have been identified, which all have their own fatty acid substrate specificity [47-49]. ELOVL1 and ELOVL4 are the two main elongases that have been shown to elongate fatty acids with ≥ 24 carbon atoms, suggesting that they play an important role in the formation of very long chain fatty acids of the SC. The fatty acids intended for the SC lipid matrix are converted to phospholipids and are packed into lamellar bodies.

The formation of ceramides also involves a four step cycle. The variety in ceramide subclasses is generated in the final two steps of this cycle. Dihydrosphingosine, which is formed by the first two steps in the ceramide biosynthesis, is acylated by one of the six ceramide synthases (CERS1-6) [50, 51]. Each CERS shows specificity in

the chain length and degree of saturation of fatty acids that it attaches to dihydrosphingosine [51]. CERS3 is the highest expressed CERS member in the epidermis and has a broad preference for fatty acids, including very long chain fatty acids. Moreover, it has recently been demonstrated that CERS3 is essential in the formation of acylceramides [52]. In the final step, the dihydrosphingosine based ceramide can be converted to sphingosine, phytosphingosine or 6-hydroxysphingosine. *De novo* synthesis of ceramides occurs at the cytosolic leaflet of the endoplasmatic reticulum. After the final synthesis step, the ceramides are transferred to the Golgi apparatus where they are converted to glucosphingolipids by linking glucose moieties to the primary hydroxy group of the ceramides, or to sphingomyelin by linking a phosphocholine head group to this hydroxy group [50]. The SC lipid precursors are then packed into lamellar bodies.

Keratinocytes are able to sense the cellular lipid levels through peroxisome proliferator-activated receptors (PPARs). PPARs are transcription factors that belong to the nuclear hormone receptor family, just as liver X receptor (LXR). PPARs are activated by fatty acids and their derivatives, while LXRs are activated by oxysterols [53]. PPARs and LXR control many key events in keratinocytes, like the expression of differentiation markers and lipid metabolism [54-56]. In the latter case it is demonstrated that PPAR and LXR stimulation leads to increased lipid synthesis, lamellar body formation, lamellar body secretion and extracellular lipid processing in the SC. This indicates that PPARs and LXR play an important role in the formation of the SC.

Stratum corneum hydration

The water content of the SC is important since it affects its physical properties, such as its permeability and flexibility, and the activity of several enzymes. The hydration level of the SC is regulated by small hygroscopic molecules, such as amino acids and their derivatives (e.g. pyrrolidone carboxylic acid and urocanic acid) and non amino-acid derived molecules such as lactate, glycerol, potassium,

sodium and calcium. These molecules are collectively referred to as 'natural moisturizing factors' (NMFs) [57-60]. Some of these NMFs are derived from sweat or the sebaceous lipids, while other NMFs are generated through the hydrolysis of filaggrin. The latter process is regulated by the SC moisture content and the external relative humidity. The SC contains approximately 30% of water, while at the interface between the SC and viable epidermis the water content increases to around 70% [61]. The water transport into the viable cells is facilitated by aquaporines. Aquaporin 3 (AQP3) is found in the membranes of keratinocytes in the viable epidermis and acts as a selective water and glycerol transporter [62].

Desquamation

In order to maintain a proper skin barrier function, the corneocytes in the upper layers of the SC are shed by a process referred to as desquamation. For this process to occur corneodesmosomes, the structures that link the corneocytes together, have to be degraded. Corneodesmosomes consist of several transmembrane proteins, such as desmoglein 1 and desmocollin 1. Additionally, corneodesmosin localizes to the extracellular parts of the corneodesmosomes and is covalently linked to the cornified envelope [63, 64]. The degradation of desmoglein 1, desmocollin 1 and corneodesmosin is an essential step in the desquamation process. The degradation of the corneodesmosomes is performed by kallikreins and cathepsins [63, 64]. At least eight kallikreins are expressed and extruded at the stratum granulosum/SC extracellular space. Kallikrein 5 (KLK 5; SC tryptic enzyme) and kallikrein 7 (KLK7; SC chymotryptic enzyme) are thought to be the primary enzymes involved in this process [65-67]. KLK 5 is auto-activated, but its activity is immediately inhibited by binding of Lympho-epithelial Kazal type related inhibitor (LEKTI) to prevent premature corneodesmolysis. The activity of the KLKs is thereby restricted to the upper layers of the SC. The association of LEKTI to KLKs is regulated in a pH dependent manner [68]. The activity of the desquamatory enzymes is also dependent on the SC water content. A very low and

a very high hydration level in the SC will result in a suboptimal desquamation rate [69]. After degradation of the corneodesmosomes, the corneocytes are shed at the skin surface due to friction between the skin and the external environment.

HUMAN SKIN EQUIVALENTS

Active ingredients developed for topical skin formulations, either for therapeutic purposes or personal care, need to be assessed for their efficacy and safety. Before they are made available to the general public, the permeation of the formulation, its irritancy, corrosivity, toxicity and conversion to potential harmful metabolites by the skin has to be investigated. *Ex vivo* human or animal skin from rat, hairless mouse, guinea pig, pig and other species have extensively been used for these purposes [70-72]. However, data obtained from these studies are difficult to extrapolate to the *in vivo* situation. Additionally, a reduction of the use of animals for testing of pharmaceutical, chemical, personal care, cosmetic, household and food products is demanded by the general public, as well as by the relevant authorities. The EU passed a ban on the use of animals in cosmetics testing starting in 2009, and a complete sales ban of products tested on animals effective in 2013. Together these factors indicate the need for a suitable replacement of human skin. A very attractive candidate is the three-dimensional human skin equivalent (HSE).

Application of human skin equivalents

HSEs may have only an epidermal compartment [73-75] or both a dermal and epidermal compartment [76-80]. Commercially available HSEs (e.g. EpiDerm™ from MatTek, USA; RHE™ from SkinEthic, France), which mostly consist of only an epidermal compartment, are successfully used to predict skin corrosivity, skin irritation and phototoxicity of compounds [73, 81-83]. Since HSEs are relatively easy to handle, they can also be used to investigate the transdermal application of

promising compounds. Additionally, several skin diseases (e.g. eczema, psoriasis and cancer) can be mimicked with HSEs. This makes it possible to use HSEs to screen for new drugs, test the efficacy of lead compounds or to investigate mechanisms underlying skin abnormalities [84-89]. HSEs are currently also used to screen for compounds that show beneficial effects on wound healing, aging and skin pigmentation [90-92]. The skin has also been recognized for its metabolic capacity [5]. It is therefore possible that active ingredients that permeate into the skin are metabolized to compounds that have toxic, irritating or sensitizing properties. The use of HSEs to examine the formation of potential dangerous metabolites is currently under investigation. Studies performed so far have demonstrated that many of the skin's metabolic enzymes are expressed in HSEs [93-98]. The HSEs also offer an attractive tool for clinical purposes. Since the late eighties autologous and allogenic HSEs have already been used to treat chronic wounds and severe skin burns by permanently covering the wounds to accelerate skin regeneration and repair [99, 100]. Finally, HSEs also offer the possibility to gain more fundamental insight into biological processes in the skin and are therefore excellent candidates to study the interaction between cells, and the interaction of the skin with its environment [101, 102].

Development and generation of human skin equivalents

The first human epidermal equivalents were generated by growing keratinocytes under submerged conditions in culture vessels. The resulting epidermis had a disorganized and irregular epithelium and an incomplete differentiation pattern indicated by the absence of keratohyalin granules, lamellar bodies and a SC [77, 103]. In order to create more physiological culture conditions, keratinocytes seeded on collagen gels or collagen-coated filters were generated at the air-liquid interface [103]. This resulted in the generation of cultures with a higher degree of differentiation, as indicated by the presence of a homogenous keratinization profile, the presence of more suprabasal layers and lamellar vesicles. An important development in the

generation of HSEs was the combination of epidermal cells with dermal elements. Keratinocytes seeded on human de-epidermized dermis (DED) were cultured at the air-liquid interface [103-105]. Alternatively, HSEs were also generated by seeding keratinocytes onto collagen gels embedded with fibroblasts [106, 107]. These cultures had a better tissue architecture, an improved expression and distribution of terminal differentiation markers and showed the extracellular deposition of lamellar body content. Further optimization of the culture conditions, such as the use of serum-free medium and supplementation of the culture medium with lipids [108], growth factors [109] and vitamins [110] have resulted in further improvements in tissue architecture, SC lipid content and organization. Supplementation of these factors is crucial for the development of human epidermal skin models. With respect to the SC lipid composition of HSEs, major improvements were made by supplementing the culture medium with vitamin C. Ponec *et al* [110] showed that addition of vitamin C to the culture medium i) markedly increased the level of glucosylceramides, ceramide AP and AH, and ii) improved lamellar body formation, extrusion and thus the intercellular lipid lamellae formation and organization in the SC of HSEs.

Nowadays HSEs are principally generated from only keratinocytes or both keratinocytes and fibroblasts, which are obtained from juvenile foreskin or excised skin obtained from donors undergoing abdomen or mammary reduction. The cells are isolated after separation of the dermis from the epidermis. The keratinocyte and fibroblast cell suspensions are produced by digestion of the epidermis and dermis, respectively [111-113]. Both cell types are separately expanded in monolayer cultures. After reaching an appropriate confluency, the cells are either subcultured, stored deep-frozen or used to generate HSEs. The dermal compartment of HSEs may comprise fibroblasts, endothelial cells [114], myofibroblasts [115] and T-cells [85] or only a biological matrix, which may consist of different types of collagen. HSEs containing melanocytes and Langerhans cells in the epidermis are now also successfully generated [116, 117]. Some of the developed HSEs are commercially available. In the initial stage of HSE generation, the cultures are grown under

submerged conditions to stimulate cell proliferation. To induce basement membrane formation, differentiation of the keratinocytes and formation of the different epidermal strata present in human skin, the HSEs are exposed to the air by lifting them to the air-liquid interface [103]. For the remaining culture period the HSEs are kept air-exposed and are nourished with nutrients in the medium that diffuse upwards from the basolateral side. A schematic overview of the procedure to generate HSEs is provided in figure 4.

In this thesis four different types of HSEs have been generated, including two recently developed HSEs [73, 76, 118]. The full thickness collagen model (FTM) is generated by seeding keratinocytes onto a fibroblast-populated collagen type I matrix. The novel fibroblast-derived matrix model (FDM) is established by seeding fibroblast on an inert filter to allow them to secrete their own extracellular matrix. Hereafter, keratinocytes are seeded onto the developed dermal compartment. The Leiden epidermal model (LEM), also a recently developed HSE, is generated by seeding keratinocytes directly onto an inert filter. The fourth model is generated by expanding small skin biopsies of native human skin on a fibroblast-populated collagen matrix.

Morphology and expression of differentiation markers in human skin equivalents

Modification of the culture conditions over the past years have resulted in the generation of HSEs that closely mimic many aspects of native human skin [103, 108, 110, 119-122]. Nowadays, HSEs can easily be grown for 6-7 weeks or even more than 3 months before a decrease in number of viable cell layers is observed [76, 123]. Morphological examination of commercial and in-house HSEs has demonstrated that these cultures have a fully stratified epidermis, which includes a SC. The stratum granulosum contains keratohyalin granules and lamellar bodies [26, 124, 125]. Additionally, the proliferation index of HSEs is comparable to native human skin [76, 126, 127]. Furthermore, HSEs express several early and late differentiation markers,

such as keratin 10, filaggrin, loricrin and involucrin, similarly as healthy human skin [120, 124, 127, 128]. However, HSEs generally also have features of a hyperproliferative epidermis indicated by the presence of hyperproliferation-associated markers like keratin 6, 16 and 17. The expression of the latter keratins in HSEs may be dependent on the number of fibroblasts present in the dermal layer [120]. This demonstrates that epidermal homeostasis is not completely reached in several of the HSEs.

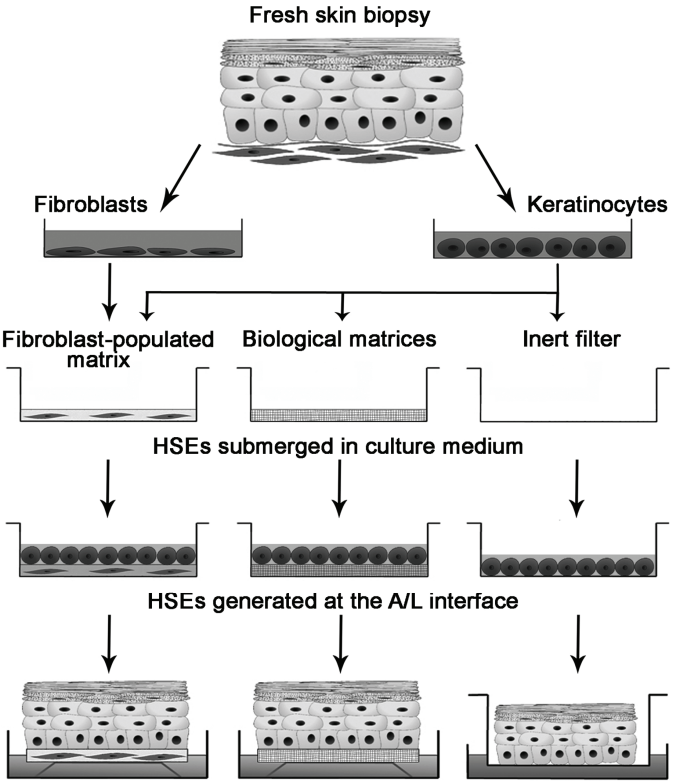

Figure 4. Keratinocytes and fibroblasts isolated from fresh human skin biopsies are cultured separately in monolayer cultures. Dermal substrates are generated by e.g. incorporation of fibroblasts in a collagen type I matrix. Keratinocytes are seeded on different cellular or acellular (biological) substrates. The cultures are initially grown under submerged conditions to stimulate keratinocyte proliferation. Hereafter, the cultures are lifted to the air-liquid (A/L) interface to induce keratinocyte differentiation. This results in the formation of a HSE with a completely stratified epidermis.

Stratum corneum barrier properties of human skin equivalents

HSEs mimic human skin in many aspects. However, they have not extensively been used for permeation testing of substances due to their overestimation of compound penetration, even though improvements in their SC barrier function has been established [129-136]. The SC barrier properties of several HSEs have been investigated to determine the cause of their decreased barrier function. Characterization of the SC barrier properties has mainly been limited to assessing the SC lipid composition, with only few studies focusing on the SC lipid organization. The evolution of the SC barrier properties of HSEs will be described together with improvements made in culture conditions. HSEs generated with serum and epidermal growth factor (EGF), but without vitamin C in the culture medium showed the presence of cholesterol, free fatty acids and ceramides in their SC [137, 138]. These HSEs had an incomplete lamellar body extrusion process, a less uniform distribution of extracellular SC lipids and a poor lamellar ordering compared to native human SC [137, 138]. The lateral lipid organization of these HSEs occasionally showed the presence of some orthorhombic domains in their SC, but the majority of the lipids were thought to form a hexagonal or liquid packing. Optimization of the culture medium by omitting serum (and reduction of supplemented EGF) resulted in an a lipid profile that more closely resembled that of native human SC [122]. Additionally, the LPP was detected in the SC of these HSEs. Further optimization of the culture medium by addition of vitamin C profoundly improved the glucosphingolipid, ceramide AP and AH content in the SC of HSEs [110]. Additionally, the lamellar body extrusion process was complete and the extruded SC lipids were processed into lipid lamellae. Moreover, the presence of the LPP could clearly be demonstrated in the investigated HSEs, indicative of an improved SC lamellar lipid organization. HSEs generated with vitamin C were shown to have a mainly hexagonal packing [139]. When focussing on the commercially available HSEs, it is not possible to discuss the composition of the medium as this is largely unknown. However, it should be noted that the SC

barrier properties of these HSEs was investigated after the beneficial effects of vitamin C supplementation was demonstrated. It is therefore possible that the culture medium contained vitamin C. Examination of the SC lipid composition revealed that the commercial HSEs contain the three main lipid classes, cholesterol, free fatty acids and ceramides in their SC [26, 83, 124, 125]. However, ceramide AH was absent in all models, and ceramides AS and AP were present in low quantities compared to native human SC. Additionally, in some commercial models the processing of lamellar bodies was disturbed [125]. In all HSEs lipid lamellae were observed in the SC. These lipid lamellae formed the LPP, although in some commercial models the population of lipids forming an LPP was limited [125].

During the last decades the SC barrier properties have greatly improved since the first establishment of HSEs. However, the SC lipid composition and organization of HSEs show some differences when compared to native human SC. A common difference observed between HSEs and human skin is a reduced free fatty acid content in the SC [110, 122, 125, 131, 138, 140]. Additionally, HSEs have a pronounced hexagonal packing as opposed to the dense orthorhombic packing observed in human SC [44]. The reduced free fatty acid content and the predominant hexagonal packing are observed in HSEs irrespective of the substrates or cell types that are used to generate the HSEs. With regard to the lamellar lipid organization, HSEs only show the presence of the LPP, while human SC shows the presence of both the LPP and SPP [37]. The SC barrier properties of HSEs were determined in only a few studies that were conducted more than a decade ago, indicating that little is known about their current status. Furthermore, the results from these studies demonstrated that the SC barrier properties of some of the commercial HSEs were known to show large deviations from the SC barrier properties of native human skin. Another limitation relating to the SC barrier properties of HSEs is the impaired desquamation process observed in all HSEs developed so far [141, 142]. As a result, the SC of the HSEs increases in thickness as the culture period is prolonged.

Since the SC forms the main barrier for diffusion of substances across the skin, the use of HSEs in penetration studies may lead to an unreliable *in vitro - in vivo* correlation.

THIS THESIS

The HSEs developed so far generally show a high resemblance to native human skin, but have an unreliable *in vitro- in vivo* correlation for permeation studies [129, 131, 133-136] due to their decreased SC barrier function and impaired desquamation process [141, 142]. Improvement of the culture conditions of HSEs during the past years have led to major advances in epidermal organization and differentiation and consequently SC barrier function. However, more research is needed to generate HSEs that harbor a competent SC barrier that even more closely resembles the SC barrier function of native human skin than the current HSEs. Nevertheless, relatively little research is devoted to the optimization of SC barrier properties of HSEs. Additionally, only a few studies are published in which the SC barrier properties of HSEs are investigated in detail [26, 83, 110, 125, 137]. In this thesis the suitability of two novel in-house HSEs for the replacement of human skin for permeation studies is examined. Furthermore, the SC lipid organization of several in-house HSEs is investigated in detail and correlated to the SC lipid composition. Using novel sophisticated techniques new insights into the SC lipid composition of HSEs have been obtained, which provide new opportunities to optimize the SC barrier properties of HSEs. In addition, the cause of the impaired desquamation process in HSEs is investigated as well.

Objectives

The main goal of this thesis was to answer the following questions:

1. Do the SC barrier properties of our novel in-house HSEs resemble the SC barrier properties of native human skin?
2. How does the SC lipid composition of the in-house HSEs relate to their SC lipid organization?
3. To what extent do the culture conditions influence the SC barrier properties of HSEs?
4. How can the SC barrier properties of HSEs be improved?

Outline

In chapter 2 a method to generate HSEs with a fully differentiated epidermis, while closely mimicking the *in utero* environment, is presented. The developed model is used to study the epidermal development '*in utero*' and to determine whether air-exposure is a requirement to generate a proper HSE. The expression of differentiation markers and the epidermal lipid content of HSEs submerged in amniotic fluid or culture medium are investigated and compared to HSEs generated at the air-liquid interface.

In chapter 3 studies are reported focussing on three in-house developed HSEs. The barrier properties of these HSEs are compared to the barrier properties of native human SC. The barrier function of the HSEs and native human SC are examined by performing diffusion studies using benzocaine as a model drug. The barrier function of the HSEs is also correlated to the SC lipid composition and organization.

In chapter 4 studies are described aiming to determine whether culture conditions or the isolation of keratinocytes are the main factor for the abnormalities in the skin barrier properties of HSEs. Native human skin explants were expanded *in vitro* under the same conditions as the HSEs described in chapter 2. The expression of differentiation markers and the SC lipid composition and organization of the

epidermis that grew from the skin explants are examined and compared to properties observed for native human skin and the HSEs reported in chapter 2.

In chapter 5 a comprehensive analysis of the lipid composition of the HSEs is provided. A novel LC/MS method is used to determine the free fatty acid and ceramide (subclass) chain length distribution and degree of saturation, while HPTLC is used to quantify the SC lipid (sub)classes.

Based on the results of the free fatty acid profiles obtained with LC/MS, in *chapter 6* studies are reported aiming to improve the SC free fatty acid composition and lipid organization. In these studies, HSEs were generated with a modified medium composition.

In chapter 7 the desquamation process in HSEs is reported. The expression pattern of specific desquamatory enzymes is investigated in several HSEs, *ex vivo* human skin and native human skin. Additionally, the activity of KLK5 and KLK7 in the superficial SC layers of the full thickness collagen model and *in vivo* skin are compared.

In chapter 8 the results of this thesis are summarized and discussed and suggestions for future research are provided.

REFERENCES

1. Burton, R.F. Estimating body surface area from mass and height: theory and the formula of Du Bois and Du Bois. Ann Hum Biol **35,** 170, 2008.
2. Madison, K.C. Barrier function of the skin: "la raison d'etre" of the epidermis. J Invest Dermatol **121,** 231, 2003.
3. Proksch, E., Brandner, J.M. and Jensen, J.M. The skin: an indispensable barrier. Exp Dermatol **17,** 1063, 2008.
4. Glenn, G.M., Kenney, R.T., Ellingsworth, L.R., Frech, S.A., Hammond, S.A. and Zoeteweij, J.P. Transcutaneous immunization and immunostimulant strategies: capitalizing on the immunocompetence of the skin. Expert Rev Vaccines **2,** 253, 2003.
5. Oesch, F., Fabian, E., Oesch-Bartlomowicz, B., Werner, C. and Landsiedel, R. Drug-metabolizing enzymes in the skin of man, rat, and pig. Drug Metab Rev **39,** 659, 2007.
6. Blatteis, C.M. Age-Dependent Changes in Temperature Regulation. Gerontology 2011.
7. Schmelz, M. Neuronal sensitivity of the skin. Eur J Dermatol **21 Suppl 2,** 43, 2011.
8. Keene, D.R., Marinkovich, M.P. and Sakai, L.Y. Immunodissection of the connective tissue matrix in human skin. Microsc Res Tech **38,** 394, 1997.
9. Kielty, C.M. and Shuttleworth, C.A. Microfibrillar elements of the dermal matrix. Microsc Res Tech **38,** 413, 1997.
10. Burgeson, R.E. and Christiano, A.M. The dermal-epidermal junction. Curr Opin Cell Biol **9,** 651, 1997.
11. Ghohestani, R.F., Li, K., Rousselle, P. and Uitto, J. Molecular organization of the cutaneous basement membrane zone. Clin Dermatol **19,** 551, 2001.
12. Eckert, R.L. and Rorke, E.A. Molecular biology of keratinocyte differentiation. Environ Health Perspect **80,** 109, 1989.
13. Fuchs, E. Epidermal differentiation: the bare essentials. J Cell Biol **111,** 2807, 1990.
14. Ishida-Yamamoto, A., Hohl, D., Roop, D.R., Iizuka, H. and Eady, R.A. Loricrin immunoreactivity in human skin: localization to specific granules (L-granules) in acrosyringia. Arch Dermatol Res **285,** 491, 1993.
15. Steven, A.C., Bisher, M.E., Roop, D.R. and Steinert, P.M. Biosynthetic pathways of filaggrin and loricrin--two major proteins expressed by terminally differentiated epidermal keratinocytes. J Struct Biol **104,** 150, 1990.
16. Feingold, K.R. The outer frontier: the importance of lipid metabolism in the skin. J Lipid Res **50 Suppl,** S417, 2009.

17. Wertz, P.W. Lipids and barrier function of the skin. Acta Derm Venereol Suppl (Stockh) **208,** 7, 2000.
18. Holbrook, K.A. and Odland, G.F. Regional differences in the thickness (cell layers) of the human stratum corneum: an ultrastructural analysis. J Invest Dermatol **62,** 415, 1974.
19. Russell, L.M., Wiedersberg, S. and Delgado-Charro, M.B. The determination of stratum corneum thickness: an alternative approach. Eur J Pharm Biopharm **69,** 861, 2008.
20. Nemes, Z. and Steinert, P.M. Bricks and mortar of the epidermal barrier. Exp Mol Med **31,** 5, 1999.
21. Wertz, P.W., Madison, K.C. and Downing, D.T. Covalently bound lipids of human stratum corneum. J Invest Dermatol **92,** 109, 1989.
22. Robson, K.J., Stewart, M.E., Michelsen, S., Lazo, N.D. and Downing, D.T. 6-Hydroxy-4-sphingenine in human epidermal ceramides. J Lipid Res **35,** 2060, 1994.
23. Johnson, M.E., Blankschtein, D. and Langer, R. Evaluation of solute permeation through the stratum corneum: lateral bilayer diffusion as the primary transport mechanism. J Pharm Sci **86,** 1162, 1997.
24. Meuwissen, M.E., Janssen, J., Cullander, C., Junginger, H.E. and Bouwstra, J.A. A cross-section device to improve visualization of fluorescent probe penetration into the skin by confocal laser scanning microscopy. Pharm Res **15,** 352, 1998.
25. Bouwstra, J.A. and Ponec, M. The skin barrier in healthy and diseased state. Biochim Biophys Acta **1758,** 2080, 2006.
26. Ponec, M., Gibbs, S., Pilgram, G., Boelsma, E., Koerten, H., Bouwstra, J. and Mommaas, M. Barrier function in reconstructed epidermis and its resemblance to native human skin. Skin Pharmacol Appl Skin Physiol **14 Suppl 1,** 63, 2001.
27. Norlen, L., Nicander, I., Lundsjo, A., Cronholm, T. and Forslind, B. A new HPLC-based method for the quantitative analysis of inner stratum corneum lipids with special reference to the free fatty acid fraction. Arch Dermatol Res **290,** 508, 1998.
28. Mao-Qiang, M., Feingold, K.R., Jain, M. and Elias, P.M. Extracellular processing of phospholipids is required for permeability barrier homeostasis. J Lipid Res **36,** 1925, 1995.
29. Van Smeden, J., Hoppel, L., van der Heijden, R., Hankemeier, T., Vreeken, R.J. and Bouwstra, J.A. LC/MS analysis of stratum corneum lipids: ceramide profiling and discovery. J Lipid Res **52,** 1211, 2011.

30. Masukawa, Y., Narita, H., Shimizu, E., Kondo, N., Sugai, Y., Oba, T., Homma, R., Ishikawa, J., Takagi, Y., Kitahara, T., Takema, Y. and Kita, K. Characterization of overall ceramide species in human stratum corneum. J Lipid Res **49,** 1466, 2008.
31. Motta, S., Monti, M., Sesana, S., Caputo, R., Carelli, S. and Ghidoni, R. Ceramide composition of the psoriatic scale. Biochim Biophys Acta **1182,** 147, 1993.
32. Wertz, P.W. and Downing, D.T. Glucosylceramides of pig epidermis: structure determination. J Lipid Res **24,** 1135, 1983.
33. Hamanaka, S., Hara, M., Nishio, H., Otsuka, F., Suzuki, A. and Uchida, Y. Human epidermal glucosylceramides are major precursors of stratum corneum ceramides. J Invest Dermatol **119,** 416, 2002.
34. Uchida, Y., Hara, M., Nishio, H., Sidransky, E., Inoue, S., Otsuka, F., Suzuki, A., Elias, P.M., Holleran, W.M. and Hamanaka, S. Epidermal sphingomyelins are precursors for selected stratum corneum ceramides. J Lipid Res **41,** 2071, 2000.
35. Holleran, W.M., Takagi, Y., Menon, G.K., Legler, G., Feingold, K.R. and Elias, P.M. Processing of epidermal glucosylceramides is required for optimal mammalian cutaneous permeability barrier function. J Clin Invest **91,** 1656, 1993.
36. Schmuth, M., Man, M.Q., Weber, F., Gao, W., Feingold, K.R., Fritsch, P., Elias, P.M. and Holleran, W.M. Permeability barrier disorder in Niemann-Pick disease: sphingomyelin-ceramide processing required for normal barrier homeostasis. J Invest Dermatol **115,** 459, 2000.
37. Bouwstra, J.A., Gooris, G.S., van der Spek, J.A. and Bras, W. Structural investigations of human stratum corneum by small-angle X-ray scattering. J Invest Dermatol **97,** 1005, 1991.
38. Janssens, M., van Smeden, J., Gooris, G.S., Bras, W., Portale, G., Caspers, P.J., Vreeken, R.J., Kezic, S., Lavrijsen, A.P. and Bouwstra, J.A. Lamellar Lipid Organization and Ceramide Composition in the Stratum Corneum of Patients with Atopic Eczema. J Invest Dermatol 2011.
39. Bouwstra, J., Pilgram, G., Gooris, G., Koerten, H. and Ponec, M. New aspects of the skin barrier organization. Skin Pharmacol Appl Skin Physiol **14 Suppl 1,** 52, 2001.
40. McIntosh, T.J., Stewart, M.E. and Downing, D.T. X-ray diffraction analysis of isolated skin lipids: reconstitution of intercellular lipid domains. Biochemistry **35,** 3649, 1996.
41. White, S.H., Mirejovsky, D. and King, G.I. Structure of lamellar lipid domains and corneocyte envelopes of murine stratum corneum. An X-ray diffraction study. Biochemistry **27,** 3725, 1988.

42. Groen, D., Poole, D.S., Gooris, G.S. and Bouwstra, J.A. Is an orthorhombic lateral packing and a proper lamellar organization important for the skin barrier function? Biochim Biophys Acta 2010.
43. De Jager, M., Groenink, W., Bielsa i Guivernau, R., Andersson, E., Angelova, N., Ponec, M. and Bouwstra, J. A novel in vitro percutaneous penetration model: evaluation of barrier properties with p-aminobenzoic acid and two of its derivatives. Pharm Res **23,** 951, 2006.
44. Damien, F. and Boncheva, M. The extent of orthorhombic lipid phases in the stratum corneum determines the barrier efficiency of human skin in vivo. J Invest Dermatol **130,** 611, 2010.
45. Goldsmith, L.A. and Baden, H.P. Uniquely oriented epidermal lipid. Nature **225,** 1052, 1970.
46. Bouwstra, J.A., Gooris, G.S., Dubbelaar, F.E. and Ponec, M. Phase behavior of lipid mixtures based on human ceramides: coexistence of crystalline and liquid phases. J Lipid Res **42,** 1759, 2001.
47. Jakobsson, A., Westerberg, R. and Jacobsson, A. Fatty acid elongases in mammals: their regulation and roles in metabolism. Prog Lipid Res **45,** 237, 2006.
48. Ohno, Y., Suto, S., Yamanaka, M., Mizutani, Y., Mitsutake, S., Igarashi, Y., Sassa, T. and Kihara, A. ELOVL1 production of C24 acyl-CoAs is linked to C24 sphingolipid synthesis. Proc Natl Acad Sci U S A **107,** 18439, 2010.
49. Uchida, Y. The role of fatty acid elongation in epidermal structure and function. Dermatoendocrinol **3,** 65, 2011.
50. Gault, C.R., Obeid, L.M. and Hannun, Y.A. An overview of sphingolipid metabolism: from synthesis to breakdown. Adv Exp Med Biol **688,** 1, 2010.
51. Mizutani, Y., Mitsutake, S., Tsuji, K., Kihara, A. and Igarashi, Y. Ceramide biosynthesis in keratinocyte and its role in skin function. Biochimie **91,** 784, 2009.
52. Jennemann, R., Rabionet, M., Gorgas, K., Epstein, S., Dalpke, A., Rothermel, U., Bayerle, A., van der Hoeven, F., Imgrund, S., Kirsch, J., Nickel, W., Willecke, K., Riezman, H., Grone, H.J. and Sandhoff, R. Loss of ceramide synthase 3 causes lethal skin barrier disruption. Hum Mol Genet **21,** 586, 2012.
53. Michael, L.F., Schkeryantz, J.M. and Burris, T.P. The pharmacology of LXR. Mini Rev Med Chem **5,** 729, 2005.
54. Feingold, K.R. and Jiang, Y.J. The mechanisms by which lipids coordinately regulate the formation of the protein and lipid domains of the stratum corneum: Role of fatty acids,

oxysterols, cholesterol sulfate and ceramides as signaling molecules. Dermatoendocrinol **3,** 113, 2011.

55. Michalik, L. and Wahli, W. Peroxisome proliferator-activated receptors (PPARs) in skin health, repair and disease. Biochim Biophys Acta **1771,** 991, 2007.
56. Schmuth, M., Jiang, Y.J., Dubrac, S., Elias, P.M. and Feingold, K.R. Thematic review series: skin lipids. Peroxisome proliferator-activated receptors and liver X receptors in epidermal biology. J Lipid Res **49,** 499, 2008.
57. Rawlings, A.V. and Harding, C.R. Moisturization and skin barrier function. Dermatol Ther **17 Suppl 1,** 43, 2004.
58. Verdier-Sevrain, S. and Bonte, F. Skin hydration: a review on its molecular mechanisms. J Cosmet Dermatol **6,** 75, 2007.
59. Fluhr, J.W., Darlenski, R. and Surber, C. Glycerol and the skin: holistic approach to its origin and functions. Br J Dermatol **159,** 23, 2008.
60. Nakagawa, N., Sakai, S., Matsumoto, M., Yamada, K., Nagano, M., Yuki, T., Sumida, Y. and Uchiwa, H. Relationship between NMF (lactate and potassium) content and the physical properties of the stratum corneum in healthy subjects. J Invest Dermatol **122,** 755, 2004.
61. Caspers, P.J., Lucassen, G.W., Carter, E.A., Bruining, H.A. and Puppels, G.J. In vivo confocal Raman microspectroscopy of the skin: noninvasive determination of molecular concentration profiles. J Invest Dermatol **116,** 434, 2001.
62. Hara-Chikuma, M. and Verkman, A.S. Roles of aquaporin-3 in the epidermis. J Invest Dermatol **128,** 2145, 2008.
63. Ishida-Yamamoto, A., Igawa, S. and Kishibe, M. Order and disorder in corneocyte adhesion. J Dermatol **38,** 645, 2011.
64. Ishida-Yamamoto, A. and Kishibe, M. Involvement of corneodesmosome degradation and lamellar granule transportation in the desquamation process. Med Mol Morphol **44,** 1, 2011.
65. Borgono, C.A., Michael, I.P., Komatsu, N., Jayakumar, A., Kapadia, R., Clayman, G.L., Sotiropoulou, G. and Diamandis, E.P. A potential role for multiple tissue kallikrein serine proteases in epidermal desquamation. J Biol Chem **282,** 3640, 2007.
66. Egelrud, T. Desquamation in the stratum corneum. Acta Derm Venereol Suppl (Stockh) **208,** 44, 2000.
67. Eissa, A. and Diamandis, E.P. Human tissue kallikreins as promiscuous modulators of homeostatic skin barrier functions. Biol Chem **389,** 669, 2008.

68. Deraison, C., Bonnart, C., Lopez, F., Besson, C., Robinson, R., Jayakumar, A., Wagberg, F., Brattsand, M., Hachem, J.P., Leonardsson, G. and Hovnanian, A. LEKTI fragments specifically inhibit KLK5, KLK7, and KLK14 and control desquamation through a pH-dependent interaction. Mol Biol Cell **18,** 3607, 2007.

69. Watkinson, A., Harding, C., Moore, A. and Coan, P. Water modulation of stratum corneum chymotryptic enzyme activity and desquamation. Arch Dermatol Res **293,** 470, 2001.

70. Panchagnula, R., Stemmer, K. and Ritschel, W.A. Animal models for transdermal drug delivery. Methods Find Exp Clin Pharmacol **19,** 335, 1997.

71. Barbero, A.M. and Frasch, H.F. Pig and guinea pig skin as surrogates for human in vitro penetration studies: a quantitative review. Toxicol In Vitro **23,** 1, 2009.

72. Godin, B. and Touitou, E. Transdermal skin delivery: predictions for humans from in vivo, ex vivo and animal models. Adv Drug Deliv Rev **59,** 1152, 2007.

73. El Ghalbzouri, A., Siamari, R., Willemze, R. and Ponec, M. Leiden reconstructed human epidermal model as a tool for the evaluation of the skin corrosion and irritation potential according to the ECVAM guidelines. Toxicol In Vitro **22,** 1311, 2008.

74. Rosdy, M. and Clauss, L.C. Terminal epidermal differentiation of human keratinocytes grown in chemically defined medium on inert filter substrates at the air-liquid interface. J Invest Dermatol **95,** 409, 1990.

75. Tinois, E., Tiollier, J., Gaucherand, M., Dumas, H., Tardy, M. and Thivolet, J. In vitro and post-transplantation differentiation of human keratinocytes grown on the human type IV collagen film of a bilayered dermal substitute. Exp Cell Res **193,** 310, 1991.

76. El Ghalbzouri, A., Commandeur, S., Rietveld, M.H., Mulder, A.A. and Willemze, R. Replacement of animal-derived collagen matrix by human fibroblast-derived dermal matrix for human skin equivalent products. Biomaterials **30,** 71, 2009.

77. Ponec, M., Weerheim, A., Kempenaar, J., Mommaas, A. M., Nugteren, D. H. Lipid composition of cultured human keratinocytes in relation to their differentiation. J Lipid Res **29,** 949, 1988.

78. Bell E., Rosenberg M., Kemp P., Gay R., Green G. D., Muthukumaran N. and C., N. Recipes for reconstituting skin. J Biomech Eng **113,** 113, 1991.

79. Smola, H., Thiekotter, G. and Fusenig, N.E. Mutual induction of growth factor gene expression by epidermal-dermal cell interaction. J Cell Biol **122,** 417, 1993.

80. Boyce, S., Michel, S., Reichert, U., Shroot, B. and Schmidt, R. Reconstructed skin from cultured human keratinocytes and fibroblasts on a collagen-glycosaminoglycan biopolymer substrate. Skin Pharmacol **3,** 136, 1990.

81. Alepee, N., Tornier, C., Robert, C., Amsellem, C., Roux, M.H., Doucet, O., Pachot, J., Meloni, M. and de Brugerolle de Fraissinette, A. A catch-up validation study on reconstructed human epidermis (SkinEthic RHE) for full replacement of the Draize skin irritation test. Toxicol In Vitro **24,** 257, 2010.

82. Gibbs, S. In vitro irritation models and immune reactions. Skin Pharmacol Physiol **22,** 103, 2009.

83. Netzlaff, F., Lehr, C.M., Wertz, P.W. and Schaefer, U.F. The human epidermis models EpiSkin, SkinEthic and EpiDerm: an evaluation of morphology and their suitability for testing phototoxicity, irritancy, corrosivity, and substance transport. Eur J Pharm Biopharm **60,** 167, 2005.

84. Carlson, M.W., Alt-Holland, A., Egles, C. and Garlick, J.A. Three-dimensional tissue models of normal and diseased skin. Curr Protoc Cell Biol **Chapter 19,** Unit 19 9, 2008.

85. Engelhart, K., El Hindi, T., Biesalski, H.K. and Pfitzner, I. In vitro reproduction of clinical hallmarks of eczematous dermatitis in organotypic skin models. Arch Dermatol Res **297,** 1, 2005.

86. Garlick, J.A. Engineering skin to study human disease--tissue models for cancer biology and wound repair. Adv Biochem Eng Biotechnol **103,** 207, 2007.

87. Kamsteeg, M., Bergers, M., de Boer, R., Zeeuwen, P.L., Hato, S.V., Schalkwijk, J. and Tjabringa, G.S. Type 2 helper T-cell cytokines induce morphologic and molecular characteristics of atopic dermatitis in human skin equivalent. Am J Pathol **178,** 2091, 2011.

88. Kalish, R.S., Simon, M., Harrington, R., Gottlieb, A.B. and Gilhar, A. Skin equivalent and natural killer cells: a new model for psoriasis and GVHD. J Invest Dermatol **129,** 773, 2009.

89. Tjabringa, G., Bergers, M., van Rens, D., de Boer, R., Lamme, E. and Schalkwijk, J. Development and validation of human psoriatic skin equivalents. Am J Pathol **173,** 815, 2008.

90. Xie, Y., Upton, Z., Richards, S., Rizzi, S.C. and Leavesley, D.I. Hyaluronic acid: evaluation as a potential delivery vehicle for vitronectin:growth factor complexes in wound healing applications. J Control Release **153,** 225, 2011.

91. Hakozaki, T., Minwalla, L., Zhuang, J., Chhoa, M., Matsubara, A., Miyamoto, K., Greatens, A., Hillebrand, G.G., Bissett, D.L. and Boissy, R.E. The effect of niacinamide on reducing cutaneous pigmentation and suppression of melanosome transfer. Br J Dermatol **147,** 20, 2002.

92. Denda, S., Denda, M., Inoue, K. and Hibino, T. Glycolic acid induces keratinocyte proliferation in a skin equivalent model via TRPV1 activation. J Dermatol Sci **57,** 108, 2010.

93. Gibbs, S., van de Sandt, J.J., Merk, H.F., Lockley, D.J., Pendlington, R.U. and Pease, C.K. Xenobiotic metabolism in human skin and 3D human skin reconstructs: a review. Curr Drug Metab **8,** 758, 2007.

94. Harris, I.R., Siefken, W., Beck-Oldach, K., Brandt, M., Wittern, K.P. and Pollet, D. Comparison of activities dependent on glutathione S-transferase and cytochrome P-450 IA1 in cultured keratinocytes and reconstructed epidermal models. Skin Pharmacol Appl Skin Physiol **15 Suppl 1,** 59, 2002.

95. Hu, T., Khambatta, Z.S., Hayden, P.J., Bolmarcich, J., Binder, R.L., Robinson, M.K., Carr, G.J., Tiesman, J.P., Jarrold, B.B., Osborne, R., Reichling, T.D., Nemeth, S.T. and Aardema, M.J. Xenobiotic metabolism gene expression in the EpiDermin vitro 3D human epidermis model compared to human skin. Toxicol In Vitro **24,** 1450, 2010.

96. Jackh, C., Blatz, V., Fabian, E., Guth, K., van Ravenzwaay, B., Reisinger, K. and Landsiedel, R. Characterization of enzyme activities of Cytochrome P450 enzymes, Flavin-dependent monooxygenases, N-acetyltransferases and UDP-glucuronyltransferases in human reconstructed epidermis and full-thickness skin models. Toxicol In Vitro **25,** 1209, 2011.

97. Luu-The, V., Duche, D., Ferraris, C., Meunier, J.R., Leclaire, J. and Labrie, F. Expression profiles of phases 1 and 2 metabolizing enzymes in human skin and the reconstructed skin models Episkin and full thickness model from Episkin. J Steroid Biochem Mol Biol **116,** 178, 2009.

98. Neis, M.M., Wendel, A., Wiederholt, T., Marquardt, Y., Joussen, S., Baron, J.M. and Merk, H.F. Expression and induction of cytochrome p450 isoenzymes in human skin equivalents. Skin Pharmacol Physiol **23,** 29, 2010.

99. Ehrlich, H.P. Understanding experimental biology of skin equivalent: from laboratory to clinical use in patients with burns and chronic wounds. Am J Surg **187,** 29S, 2004.

100. Bello, Y.M., Falabella, A.F. and Eaglstein, W.H. Tissue-engineered skin. Current status in wound healing. Am J Clin Dermatol **2,** 305, 2001.

101. Bernerd, F. Human skin reconstructed in vitro as a model to study the keratinocyte, the fibroblast and their interactions: photodamage and repair processes. J Soc Biol **199,** 313, 2005.

102. Bouwstra J. A., Groenink H. W., Kempenaar J. A., Romeijn S. G. and M., P. Water distribution and natural moisturizer factor content in human skin equivalents are regulated by environmental relative humidity. J Invest Dermatol **128,** 378, 2008.

103. Prunieras, M., Regnier, M. and Woodley, D. Methods for cultivation of keratinocytes with an air-liquid interface. J Invest Dermatol **81,** 28s, 1983.

104. Mackenzie, I.C. and Fusenig, N.E. Regeneration of organized epithelial structure. J Invest Dermatol **81,** 189s, 1983.

105. Régnier, M., Pruniéras, M. and Woodley, D. Growth and differentiation of adult human epidermal cells on dermal substrates. Front Matrix Biol **9,** 35, 1981.

106. Bell, E., Ivarsson, B. and Merrill, C. Production of a tissue-like structure by contraction of collagen lattices by human fibroblasts of different proliferative potential in vitro. Proc Natl Acad Sci U S A **76,** 1274, 1979.

107. Coulomb, B., Lebreton, C. and Dubertret, L. Influence of human dermal fibroblasts on epidermalization. J Invest Dermatol **92,** 122, 1989.

108. Boyce, S.T. and Williams, M.L. Lipid supplemented medium induces lamellar bodies and precursors of barrier lipids in cultured analogues of human skin. J Invest Dermatol **101,** 180, 1993.

109. Gibbs, S., Silva Pinto, A.N., Murli, S., Huber, M., Hohl, D. and Ponec, M. Epidermal growth factor and keratinocyte growth factor differentially regulate epidermal migration, growth, and differentiation. Wound Repair Regen **8,** 192, 2000.

110. Ponec, M., Weerheim, A., Kempenaar, J., Mulder, A., Gooris, G.S., Bouwstra, J. and Mommaas, A.M. The formation of competent barrier lipids in reconstructed human epidermis requires the presence of vitamin C. J Invest Dermatol **109,** 348, 1997.

111. Prunieras, M., Delescluse, C. and Regnier, M. The culture of skin. A review of theories and experimental methods. J Invest Dermatol **67,** 58, 1976.

112. Tsuji, T. and Karasek, M. A procedure for the isolation of primary cultures of melanocytes from newborn and adult human skin. J Invest Dermatol **81,** 179, 1983.

113. Rheinwald, J.G. and Green, H. Serial cultivation of strains of human epidermal keratinocytes: the formation of keratinizing colonies from single cells. Cell **6,** 331, 1975.

114. Ponec, M., El Ghalbzouri, A., Dijkman, R., Kempenaar, J., van der Pluijm, G. and Koolwijk, P. Endothelial network formed with human dermal microvascular endothelial cells in autologous multicellular skin substitutes. Angiogenesis **7,** 295, 2004.

115. Moulin, V., Auger, F.A., Garrel, D. and Germain, L. Role of wound healing myofibroblasts on re-epithelialization of human skin. Burns **26,** 3, 2000.

116. Gibbs, S., Murli, S., De Boer, G., Mulder, A., Mommaas, A.M. and Ponec, M. Melanosome capping of keratinocytes in pigmented reconstructed epidermis--effect of ultraviolet radiation and 3-isobutyl-1-methyl-xanthine on melanogenesis. Pigment Cell Res **13,** 458, 2000.

117. Ouwehand, K., Spiekstra, S.W., Waaijman, T., Scheper, R.J., de Gruijl, T.D. and Gibbs, S. Technical advance: Langerhans cells derived from a human cell line in a full-thickness skin equivalent undergo allergen-induced maturation and migration. J Leukoc Biol **90,** 1027, 2011.

118. Thakoersing, V.S., Gooris, G., Mulder, A.A., Rietveld, M., El Ghalbzouri, A. and Bouwstra, J.A. Unravelling Barrier Properties of Three Different In-House Human Skin Equivalents. Tissue Eng Part C Methods **In press,** In press, 2011.

119. Fartasch, M. and Ponec, M. Improved barrier structure formation in air-exposed human keratinocyte culture systems. J Invest Dermatol **102,** 366, 1994.

120. El Ghalbzouri, A., Lamme, E. and Ponec, M. Crucial role of fibroblasts in regulating epidermal morphogenesis. Cell Tissue Res **310,** 189, 2002.

121. Mak, V.H., Cumpstone, M.B., Kennedy, A.H., Harmon, C.S., Guy, R.H. and Potts, R.O. Barrier function of human keratinocyte cultures grown at the air-liquid interface. J Invest Dermatol **96,** 323, 1991.

122. Gibbs, S., Vicanova, J., Bouwstra, J., Valstar, D., Kempenaar, J. and Ponec, M. Culture of reconstructed epidermis in a defined medium at 33 degrees C shows a delayed epidermal maturation, prolonged lifespan and improved stratum corneum. Arch Dermatol Res **289,** 585, 1997.

123. Boehnke, K., Mirancea, N., Pavesio, A., Fusenig, N.E., Boukamp, P. and Stark, H.J. Effects of fibroblasts and microenvironment on epidermal regeneration and tissue function in long-term skin equivalents. Eur J Cell Biol **86,** 731, 2007.

124. Ponec, M., Boelsma, E., Gibbs, S. and Mommaas, M. Characterization of reconstructed skin models. Skin Pharmacol Appl Skin Physiol **15 Suppl 1,** 4, 2002.

125. Ponec, M., Boelsma, E., Weerheim, A., Mulder, A., Bouwstra, J. and Mommaas, M. Lipid and ultrastructural characterization of reconstructed skin models. Int J Pharm **203,** 211, 2000.

126. El Ghalbzouri, A., Gibbs, S., Lamme, E., Van Blitterswijk, C.A. and Ponec, M. Effect of fibroblasts on epidermal regeneration. Br J Dermatol **147,** 230, 2002.

127. Stark, H.J., Boehnke, K., Mirancea, N., Willhauck, M.J., Pavesio, A., Fusenig, N.E. and Boukamp, P. Epidermal homeostasis in long-term scaffold-enforced skin equivalents. J Investig Dermatol Symp Proc **11,** 93, 2006.

128. Boelsma, E., Gibbs, S., Faller, C. and Ponec, M. Characterization and comparison of reconstructed skin models: morphological and immunohistochemical evaluation. Acta Derm Venereol **80,** 82, 2000.

129. Ackermann, K., Borgia, S.L., Korting, H.C., Mewes, K.R. and Schafer-Korting, M. The Phenion full-thickness skin model for percutaneous absorption testing. Skin Pharmacol Physiol **23,** 105, 2010.

130. Asbill, C., Kim, N., El-Kattan, A., Creek, K., Wertz, P. and Michniak, B. Evaluation of a human bio-engineered skin equivalent for drug permeation studies. Pharm Res **17,** 1092, 2000.

131. Batheja, P., Song, Y., Wertz, P. and Michniak-Kohn, B. Effects of growth conditions on the barrier properties of a human skin equivalent. Pharm Res **26,** 1689, 2009.

132. Marjukka Suhonen, T., Pasonen-Seppanen, S., Kirjavainen, M., Tammi, M., Tammi, R. and Urtti, A. Epidermal cell culture model derived from rat keratinocytes with permeability characteristics comparable to human cadaver skin. Eur J Pharm Sci **20,** 107, 2003.

133. Netzlaff, F., Kaca, M., Bock, U., Haltner-Ukomadu, E., Meiers, P., Lehr, C.M. and Schaefer, U.F. Permeability of the reconstructed human epidermis model Episkin in comparison to various human skin preparations. Eur J Pharm Biopharm **66,** 127, 2007.

134. Schafer-Korting, M., Bock, U., Diembeck, W., Dusing, H.J., Gamer, A., Haltner-Ukomadu, E., Hoffmann, C., Kaca, M., Kamp, H., Kersen, S., Kietzmann, M., Korting, H.C., Krachter, H.U., Lehr, C.M., Liebsch, M., Mehling, A., Muller-Goymann, C., Netzlaff, F., Niedorf, F., Rubbelke, M.K., Schafer, U., Schmidt, E., Schreiber, S., Spielmann, H., Vuia, A. and Weimer, M. The use of reconstructed human epidermis for skin absorption testing: Results of the validation study. Altern Lab Anim **36,** 161, 2008.

135. Schmook, F.P., Meingassner, J.G. and Billich, A. Comparison of human skin or epidermis models with human and animal skin in in-vitro percutaneous absorption. Int J Pharm **215,** 51, 2001.

136. Zghoul, N., Fuchs, R., Lehr, C.M. and Schaefer, U.F. Reconstructed skin equivalents for assessing percutaneous drug absorption from pharmaceutical formulations. Altex **18,** 103, 2001.

137. Bouwstra, J.A., Gooris, G.S., Weerheim, A., Kempenaar, J. and Ponec, M. Characterization of stratum corneum structure in reconstructed epidermis by X-ray diffraction. J Lipid Res **36,** 496, 1995.

138. Kennedy, A.H., Golden, G.M., Gay, C.L., Guy, R.H., Francoeur, M.L. and Mak, V.H. Stratum corneum lipids of human epidermal keratinocyte air-liquid cultures: implications for barrier function. Pharm Res **13,** 1162, 1996.

139. Pilgram, G. A close look at the stratum corneum lipid organization by cryo-electron diffraction [PhD Book]. Division of Pharmaceutical Technology, Leiden University, Leiden, 2000.

140. Pappinen, S., Hermansson, M., Kuntsche, J., Somerharju, P., Wertz, P., Urtti, A. and Suhonen, M. Comparison of rat epidermal keratinocyte organotypic culture (ROC) with intact human skin: lipid composition and thermal phase behavior of the stratum corneum. Biochim Biophys Acta **1778,** 824, 2008.

141. Ponec, M., Kempenaar, J. and Weerheim, A. Lack of desquamation - the Achilles heel of the reconstructed epidermis. Int J Cosmet Sci **24,** 263, 2002.

142. Vicanova, J., Mommaas, A.M., Mulder, A.A., Koerten, H.K. and Ponec, M. Impaired desquamation in the in vitro reconstructed human epidermis. Cell Tissue Res **286,** 115, 1996.

143. Elghalbzouri, A. Reconstructed human skin equivalents: fibroblasts and their role in epidermal morphogenesis [PhD Department of Dermatology, Leiden University Medical Center, Leiden University, Leiden, 2004.

2

GENERATION OF HUMAN SKIN EQUIVALENTS UNDER SUBMERGED CONDITIONS – MIMICKING THE *IN UTERO* ENVIRONMENT

Varsha S. Thakoersing, Maria Ponec and Joke A. Bouwstra

Department of Drug Delivery Technology, Leiden/ Amsterdam Center for Drug Research, Leiden University, Leiden, The Netherlands

Adapted from Tissue Engineering Part A. 2010 Apr;16(4):1433-41.

ABSTRACT

In this study, we generated human skin equivalents (HSEs) under submerged conditions to mimic the aqueous *in utero* environment and investigated the morphology and differentiation process of the formed epidermis. Furthermore, the skin barrier, which resides in the stratum corneum (SC), was characterized by its lipid content, hydration level and natural moisturizing factor level. The submerged HSEs show comparable tissue morphology and similar expression of several differentiation markers and SC lipid composition compared to HSEs grown at the air-liquid interface and native human skin. The SC of the submerged HSEs, however, contained more free water and less natural moisturizing factors compared to the air-exposed counterparts. These results show that the presented cell culture method can be utilized to generate HSEs under submerged conditions to study the epidermal formation under aqueous conditions.

INTRODUCTION

The epidermis is the most superficial layer of the skin and can be subdivided into four different strata: stratum basale, stratum spinosum, stratum granulosum and stratum corneum (SC). The SC is in direct contact with the external environment and therefore forms the first and most important barrier against foreign substances and micro-organisms.

It is ironic to notice that the barrier that protects the human body from desiccation develops in an aqueous environment, i.e. the amniotic fluid. The formation of human skin starts early during embryogenesis and at first consists of only one cell layer of multipotent epithelial cells. This epithelium is covered by a second epidermal layer, called the periderm, which serves as a protective shield between the amniotic fluid and the epidermis while it keratinizes [1, 2]. The periderm is shed at approximately 24 weeks of estimated gestational age (EGA) when the epidermis is fully differentiated and comprises the first few SC layers. During the third trimester the SC is fully exposed to the surrounding amniotic fluid while it matures. At 34 weeks EGA barrier formation is complete. Full-term neonates (40 weeks EGA) are therefore born with a competent skin barrier that resembles that of adults.

Several attempts have been made to simulate the intrauterine epidermal development by culturing keratinocytes under submerged conditions in petri dishes or culture flasks [3-7]. In these culture systems the medium was only supplied from the apical side of the keratinocytes. The resulting cultures, referred to as human skin equivalents (HSEs), show drastic differences with human skin, such as a disorganized epithelium and an incomplete differentiation indicated by the lack of a SC, the absence of keratohyalin and membrane-coating granules or the lack of expression of high-molecular-weight keratins. Only when keratinocytes are seeded on an appropriate substrate and are subsequently cultured at the air-liquid interface do HSEs show high resemblance to human skin in many aspects like morphology, the expression of several differentiation markers and formation of a SC [7-15]. As the

microenvironment of a HSE affects its differentiation process, *in utero* epidermal development may differ from epidermal development at the air-liquid interface. In the present study we have developed a novel method to generate HSEs under aqueous conditions by submerging HSEs in culture media, ensuring that the apical and basolateral side of the developing epidermis are surrounded by an aqueous environment, which mimics the *in utero* environment very closely. The morphology and differentiation process of the epidermis generated under these submerged conditions was examined by determining the expression of various differentiating markers. As the lipids of the SC are crucial for maintaining a proper barrier function, the lipid composition of the SC was examined as well. In addition, the natural moisturizing factor (NMF) and hydration level in SC were determined. Our studies showed for the first time that under submerged conditions a well organized epidermis, including a SC, can be formed.

MATERIALS AND METHODS

Cell culture

Normal human keratinocytes (NHKs) and human dermal fibroblasts were obtained from adult donors undergoing mammary or abdomen surgery and were established as described previously [16].

Dermal equivalents

Dermal equivalents were generated as described earlier [16, 17]. In brief, 1 mL of a 1 mg/mL collagen type I solution was pipetted into filter inserts (Corning Transwell cell culture inserts, membrane diameter 24 mm, pore size 3 μm; Sigma, Zwijndrecht, The Netherlands) and was allowed to polymerize for 15 minutes at 37°C. Subsequently, 3 mL of a 2 mg/mL collagen type I solution, with a fibroblast suspension reaching a final density of 0.4 x 10^5 cells/mL collagen, was pipetted into the inserts. After polymerization, DMEM (Invitrogen, Breda, The

Netherlands) supplemented with 5% FBS (Hyclone, Utah, USA), 1% penicillin/streptomycin and 0.45 mM vitamin C (Sigma, Zwijdrecht, The Netherlands) was added to each culture. The dermal compartments were kept under submerged conditions for 1 week. During this period the medium was refreshed once.

Human skin equivalents (HSEs)

Generated on dermal equivalents: HSEs grown on collagen matrices were generated as described before [9, 16]. First or secondary NHKs were seeded onto fibroblast-populated collagen gels (0.5-1 x 10^6 cells/gel). To mimic the aqueous *in utero* environment, the cultures were kept under submerged conditions during the entire culture period. To investigate the epidermal development under submerged conditions over time, HSEs were grown for 8, 16 and 24 days, after seeding of the NHKs, at 37°C, 93% relative humidity and 8% CO_2. As a control HSEs were also generated under air exposed conditions by seeding keratinocytes on the dermal compartment and lifting them to the air-liquid interface 1 day hereafter. During the culturing period the submerged and air-exposed HSEs were nourished with media as described by Bouwstra *et al.* [16]

Generated on inert filter: to generate HSEs under submerged conditions NHKs (1.0 x 10^6 cells/filter) were seeded directly onto cell culture inserts (Corning Transwell cell culture inserts, membrane diameter 24 mm, pore size 0.4 μm; Corning, The Netherlands). After 4 days the culture medium was supplemented with 1 ng/mL epidermal growth factor (Sigma, Zwijdrecht, The Netherlands) during the remaining culture period, using the same incubator conditions as the HSEs generated on the collagen substrate. As a control NHKs were also seeded onto cell culture inserts and were lifted to the air-liquid interface after 4 days. The filter HSEs were fed with the same media as the collagen HSEs.

Amniotic fluid-treated human skin equivalents

Human amniotic fluid samples were obtained from amniocentesis, provided by Leiden University Medical Centre, from women undergoing caesarean section at 37-39 weeks of pregnancy. Amniotic fluid samples were centrifuged for 6 minutes at 1000 rpm to obtain a cell free solution and were stored at -20°C until use. To closely mimic the *in utero* environment HSEs generated on a collagen substrate were kept submerged with medium or grown at the air-liquid interface for 8 days. Hereafter, a metal ring with a diameter of 10 mm was placed on top of the HSEs and 200 μL amniotic fluid of one donor was applied at the apical side of the HSE until day 24. Amniotic fluid was refreshed twice a week. The amniotic fluid-treated HSEs were nourished with the same media as the collagen HSEs.

Morphology and immunohistochemistry

Harvested HSEs were fixed in 4% (w/v) paraformaldehyde (Lommerse Pharma, Oss, The Netherlands) overnight and sequentially dehydrated in 70%, 80%, 90%, 96% and 100% ethanol, xylene and liquid paraffin for 1 hour each. The dehydrated samples were subsequently embedded in paraffin. 5 μm sections were cut, deparaffinized and rehydrated in preparation for morphological analysis and immunohistochemical staining of keratin 10 and 16, filaggrin, involucrin and loricrin. The primary and secondary antibodies used in this study are listed in table 1. Morphological analysis was performed by light microscopic examination of haematoxylin and eosin stained sections. Immunohistochemical analysis for keratin 10, keratin 16 and filaggrin was performed as described before [16]. Staining of involucrin and loricrin was performed as described with the following modifications: treatment with the citrate buffer was omitted, an additional wash with 0.5% Triton X-100 (Sigma, Zwijndrecht, The Netherlands) was performed prior to the incubation with human serum, and incubation with the first antibody was performed for 1 hour at room temperature.

Table 1 Primary and secondary antibodies for immunohistochemical staining

Antibodies	*Clone*	*Dilution*	*Company*
Primary antibodies			
Mouse cytokeratin 10 Ab-2	DEK10	1:100	Neomarkers, USA
Mouse cytokeratin 16 Ab-1	LL0025	1:20	Neomarkers, USA
Mouse filaggrin Ab-1	FLG01	1:150	Neomarkers, USA
Mouse involucrin	SY5	1:200	Sanbio, The Netherlands
Rabbit loricrin	AF62	1:400	Covance, USA
Secondary antibodies			
Biotinylated goat anti-mouse		1:200	Dako, The Netherlands
Biotinylated swine anti-rabbit		1:300	Dako, The Netherlands

Lipid extraction and analysis

The lipids from human epidermis and the epidermis of HSEs were consecutively extracted according to a modified Bligh and Dyer procedure [18] with the addition of 0.25M KCl to extract polar lipids. The extracted lipids were redissolved in a suitable volume of chloroform: methanol (2:1) and stored at -20°C until use. The lipid extracts of three HSEs generated under the same culture conditions were pooled to obtain a sufficient amount of lipids for analysis. Amniotic fluid of 3 donors was extracted accordingly. The extracted lipids were analyzed by means of one-dimensional high performance thin layer chromatography (HPTLC) as described previously [19] with the solvent systems provided in table 2A and 2B. Co-chromatography of a standard lipid mixture was performed to identify the various lipid classes.

Table 2A Solvent system used for barrier lipids analysis

Eluent	*Composition (v/v)*	*Distance*
1	DCM: EA: A: M (80: 8: 4: 1)	40 mm
2	C: A: M (76: 8: 16)	20 mm
3	H: C: A: M (6: 80: 12: 2)	70 mm
4	H: C: HA: A: M (6: 80: 0.1: 10: 4)	95 mm

A: acetone, C: chloroform, DCM: dichloromethane, DE: diethyl ether, E: ethanol, EA: ethyl acetate, H: hexane, HA: hexyl acetate, M: methanol.

Table 2B Solvent system used for total lipid analysis

Eluent	*Composition (v/v)*	Distance
1	DCM: EA; A: M (88: 8: 4: 1)	40 mm
2	C: A: M (76: 8: 16)	10 mm
3	H: C: HA: A: M (6: 80: 0.1: 10: 4)	70 mm
4	C: EA: EMK: 2P: E: M: W: AA (36: 6: 6: 6: 16: 28: 2: 1)	20 mm
5	C: EA: EMK: 2P: E: M: W (48: 6: 6: 6: 6: 24: 4)	25 mm
6	H: C: A: M (2: 80: 10: 8)	80 mm
7	H: DE: EA (78: 18: 4)	95 mm

2P: 2-propanol, A: acetone, C: chloroform, DCM: dichloromethane, DE: diethyl ether, E: ethanol, EA: ethyl acetate, EMK: ethyl methyl ketone, H: hexane, HA: hexyl acetate, M: methanol, W: water.

Cryo-scanning electron microscopy (Cryo-SEM)

The harvested HSEs were processed as described elsewhere [16]. In brief, the samples were cryo-fixed at -180°C and planed perpendicular to the skin surface. The surface of the samples was visualized at -190°C with a field scanning electron microscope (Jeol 6400F, Japan). As a control dermatomed human skin (300 μm) was incubated for 24 hours at 37°C and 93% RH. Cryo-SEM images of at least 4 different HSEs were taken per culture condition.

Natural moisturizing factor (NMF) content determination

The pyrrolidone carboxylic acid (PCA) content, one of the main components of NMF, in HSEs was determined. The HSEs were clamped between two plates with an opening of 1 cm in diameter in the upper plate and tape-stripped with Scotch Magic Tape 810 tape-strips (3M, Zoeterwoude, The Netherlands). The PCA and the protein content per strip were determined as described previously [16].

RESULTS

Formation of a fully differentiated epidermis, including a SC, under submerged conditions

To determine whether all the epidermal layers are generated under conditions mimicking the *in utero* environment, HSEs were cultured under submerged conditions with amniotic fluid or medium. As a control HSEs were also generated under air-exposed conditions. Vertical sections stained with haematoxylin and eosin were used to evaluate the general tissue architecture. At day 24 the amniotic fluid-treated and submerged HSEs show the presence of all epidermal strata, including a SC. These HSEs show a similar appearance as the air-exposed HSEs, although some small differences are noticed (figure 1).

HSEs were also harvested after 8 and 16 days to investigate the epidermal morphogenesis over time. HSEs generated on a collagen substrate under submerged conditions with medium contained all epidermal cell layers including the stratum basale, stratum spinosum, stratum granulosum and even a few SC layers at day 8, similar to the air-exposed HSEs (figure 1). The number of viable cell layers, however, was less compared to the air-exposed counterparts. At day 16 these submerged HSEs have a fully differentiated epidermis, including a clearly visible SC. No difference is detected in the number of viable cell layers between day 8 and 16. Between day 16 and 24 the SC of the submerged HSEs increased in

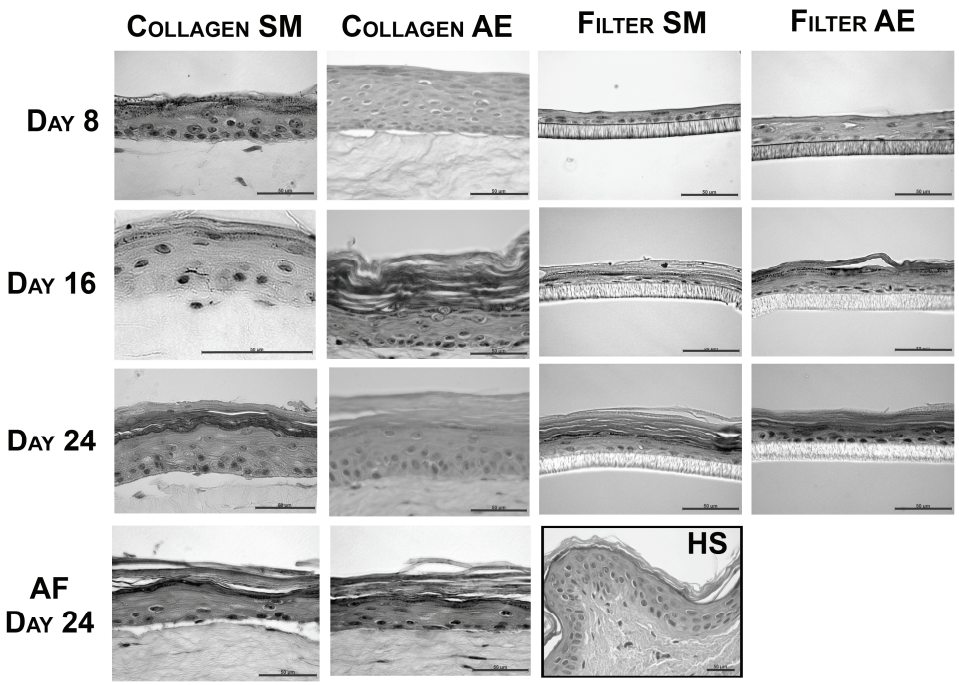

Figure 1. Haematoxylin and eosin staining of HSEs generated under submerged conditions with amniotic fluid (AF) or medium (SM), and air-exposed (AE) conditions harvested after 8, 16 and 24 days after seeding normal human keratinocytes on a fibroblast-populated collagen matrix (Collagen) or inert filter (Filter). The morphology of at least three HSEs per culture condition was examined. HS = human skin. Scale bars represent 50 μm.

thickness, while the number of viable cell layers again did not change. HSEs generated under air-exposed conditions show a decrease in the number of viable cell layers from day 8 to 16, whereas the number of SC layers increases. Although the submerged and air-exposed HSEs develop differently over time, at day 24 the submerged and air-exposed HSEs show many similarities: all viable epidermal cell layers and the SC were generated resembling the morphology of human skin.

The submerged HSEs generated on a filter consisted of only 3 to 4 cell layers at day 8, similarly to the air-exposed HSEs generated on filter (figure 1). At this time point a stratum granulosum and SC were not yet uniformly present. However, at

day 16 all the strata in the submerged and air-exposed HSEs were formed, including the stratum granulosum and the SC. Nevertheless, the stratum spinosum consisted of only 1 to 2 cell layers and the stratum granulosum was thicker than observed in human skin. At day 24, the submerged and air-exposed HSEs generated on filters show a similar morphology. Under both culture conditions the number of stratum spinosum cell layers did not normalize at the end of the culture period.

Submerged and air-exposed HSEs show similar expression of protein differentiation markers

To determine whether the differentiation process of the HSEs that were kept submerged with amniotic fluid or medium was similar to that of the air-exposed HSEs and human skin, the expression of several specific differentiation markers was investigated. Only HSEs treated with amniotic fluid from day 8 to day 24 were stained to examine the effect of amniotic fluid on the differentiation process. Furthermore, HSEs generated on a filter which were harvested after 8 days were not stained as these cultures did not develop a fully differentiated epidermis yet.

HSEs generated on a collagen substrate that were kept submerged with amniotic fluid or medium showed similar expression of the protein differentiation markers keratin 10, keratin 16, filaggrin, loricrin and involucrin as the air-exposed HSEs irrespective of the culture period (figure 2). Keratin 10, a differentiation-specific marker, was located in all the viable cell layers, except the basal layer, whereas filaggrin and loricrin expression was confined to the granular layer. The expression of these proteins is similar to the expression detected in human skin. In contrast, the expression of involucrin and keratin 16 differed from the expression observed in human skin. The submerged as well as the air-exposed HSEs showed suprabasal expression of keratin 16 and involucrin at day 16 and day 24. In human skin involucrin is only expressed in the stratum granulosum and keratin 16 is only expressed under pathological conditions.

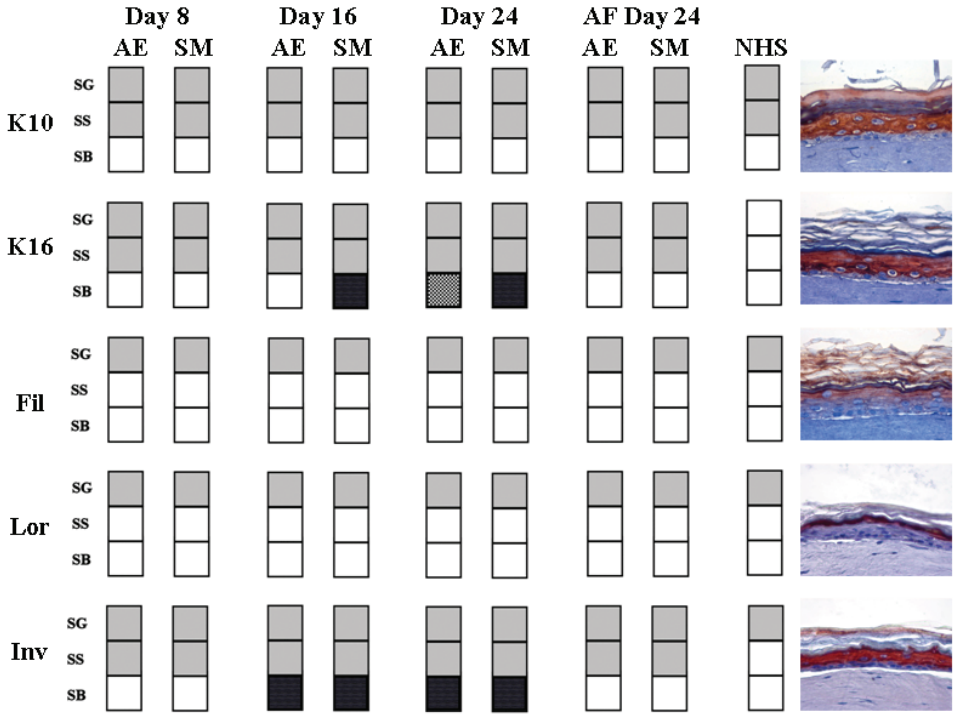

Figure 2. Immunohistochemical staining of keratin 10 (K10), keratin 16 (K16), filaggrin (Fil), loricrin (Lor) and involucrin (Inv) of HSEs generated under air-exposed and submerged conditions either on fibroblast-populated collagen matrices or on filters, and collagen HSEs treated with amniotic fluid. Grey-coloured squares indicate that the differentiation marker is expressed in the corresponding layer of the viable epidermis. The expression of the majority of proteins was similar irrespective of the dermal substrate used, with the exception of K16, where the (half-tone) black-coloured squares indicate that expression of this differentiation marker was additionally detected in the basal cell layer in HSEs generated on an inert filter. HSEs generated on filter and harvested after 8 days are not included in this figure. Examples of submerged collagen HSE sections are shown. SG = stratum granulosum, SS = stratum spinosum, SB = stratum basal, AE = air-exposed, SM = submerged, AF = amniotic fluid.

The submerged HSEs generated on filters also showed similar expression of keratin 10, filaggrin and loricrin as the air-exposed HSEs and human skin from day 16 to day 24 (figure 2). Again the expression pattern of involucrin and keratin 16 in HSEs generated on filters differed from the expression detected in human skin. From day 16 to day 24 involucrin could be detected throughout the entire viable epidermis of both the submerged and air-exposed HSEs. At day 16 keratin 16 expression was also detected in the entire viable epidermis of the submerged HSEs, but only in the suprabasal layers of the air-exposed HSEs. However, at day 24 the air-exposed HSEs also showed weak keratin 16 expression in the basal layer.

Submerged and air-exposed HSEs have similar SC lipid profiles

The lipid profiles of the HSEs generated under submerged conditions with amniotic fluid or culture medium and under air-exposed conditions were investigated to determine whether qualitative changes occurred when culturing under different conditions. Lipid analyses show that the SC lipid profiles of HSEs grown submerged in culture medium and air-exposed conditions, both in the case of HSEs generated on a collagen substrate or filter, are very similar at day 24 (figure 3A). The lipid profiles of the submerged and air-exposed HSEs reveal the presence of all barrier lipids - cholesterol, free fatty acids and ceramides - that are also present in human SC. Moreover, all ceramide subclasses are present in the submerged and air-exposed HSEs, but the free fatty acid levels in the HSEs are lower than in the native tissue. Furthermore, the lipid profile of the submerged HSEs shows a lower level of free fatty acids and ceramide EOS than the air-exposed counterparts. Additionally, when cultured on a collagen substrate, the presence of an additional ceramide with a R_f value between that of ceramide EOS and ceramide NS-A can be detected in the submerged HSEs. The detailed structure of the unidentified lipid remains to be established.

Lipid analyses of amniotic fluid-treated HSEs (figure 3B) show the presence of all barrier lipids, which appeared to be present in slightly higher amounts than in HSEs that were not treated with amniotic fluid (data not shown). However, further analysis showed that all barrier lipids were also present in amniotic fluid (figure 3B).

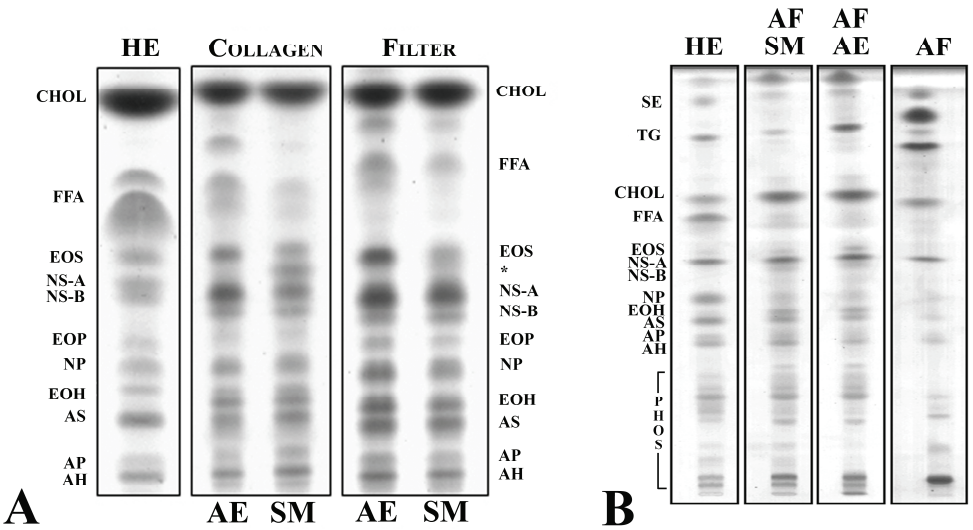

Figure 3. Lipid profiles of human epidermis (HE), submerged (SM) HSEs, generated on fibroblast-populated collagen matrices (Collagen) or an inert filter (Filter) and air-exposed (AE) HSEs harvested after 24 days of culturing are shown in figure A. The lipids were fractionated according to the solvent system provided in table 2A. Figure B shows the lipids present in amniotic fluid-treated collagen HSEs and amniotic fluid extracts. The amniotic fluid-treated HSEs were generated for 8 days under submerged (AF SM) or air-exposed (AF AE) conditions prior to application of amniotic fluid. The lipid extracts from these cultures were fractionated according to the solvent system provided in table 2B. Extracted lipids from 3 HSEs generated under the same conditions were pooled and separated using HPTLC. CHOL = cholesterol, FFA = free fatty acids, * = unidentified ceramide, SE = squalene esters, TG = triglycerides, PHOS = phospholipids.

Submerged and air-exposed HSEs acquire more barrier lipids as the culture period is prolonged

The lipid profiles of HSEs submerged with medium and air-exposed HSEs were quite similar at day 24. In order to investigate the generation of the epidermal barrier in time under submerged and air-exposed conditions, the changes in barrier lipid content were also monitored. For this purpose the HSEs were harvested after 8, 16 and 24 days of culturing. HSEs generated on a filter and harvested after 8 days were not examined, since these HSEs had not formed a SC yet.

The HSEs generated on collagen substrates and filters, grown under submerged and air-exposed conditions, show an increase in all barrier lipid classes over time (figure 4). The HSEs generated on a collagen substrate even clearly show the presence of ceramide NS-A and NS-B at day 8. However, the HSEs show a difference in one ceramide subclass over time. At day 8 both the submerged and air-exposed collagen HSEs show the presence of the unidentified lipid with an R_f value between that of ceramide EOS and NS-A. In the submerged HSEs the presence of this lipid diminishes at day 16, but increases again at day 24. Under air-exposed conditions, the collagen HSEs show the presence of this lipid only at day 8.

Analysis of the phospholipids in the submerged and air-exposed collagen HSEs at day 8, 16 and 24 show that the phospholipids form the major lipid fraction in the early phase of epidermal development. However, their presence decreases over time (data not shown), especially from day 16 to day 24. The ceramide precursors, (acyl)glucosphingolipids (AGC and GSL, respectively), are both present at day 8. The overall GSL content does not change with increasing culturing time, while the AGC content shows a decrease after day 16. The level of both lipid classes is higher in submerged cultures than in the air-exposed cultures.

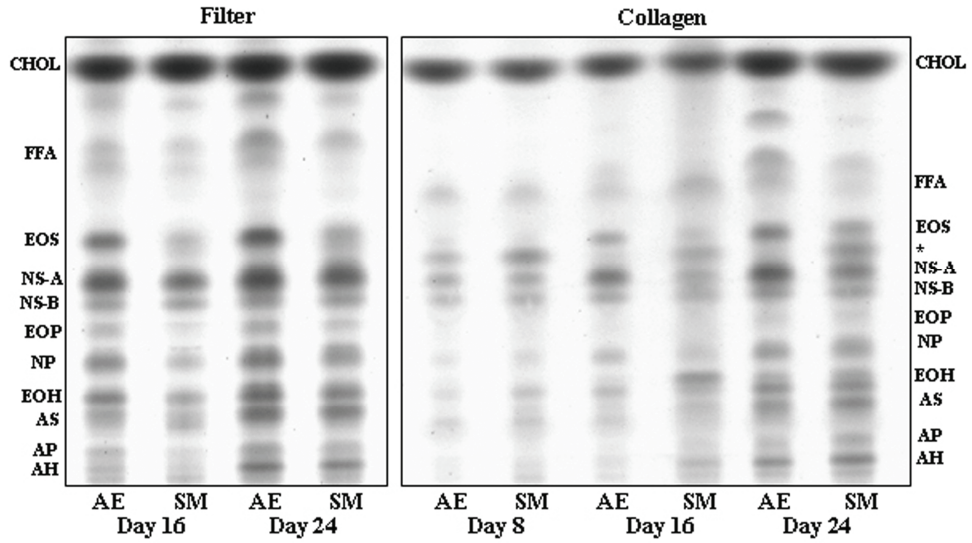

Figure 4. Lipid profiles of air-exposed (AE) and submerged (SM) cultures generated on fibroblast-populated collagen matrices or inert filters harvested after 8, 16 and 24 days of culturing. Lipid extracts of 3 HSEs grown under the same conditions were pooled. CHOL = cholesterol, FFA = free fatty acids, * = unidentified ceramide.

Generating HSEs under submerged conditions increases the hydration level of SC

To investigate whether the culture conditions affect the water level and water distribution in SC, cryo-SEM images were made of HSEs generated under submerged conditions with medium and of air-exposed HSEs harvested after 16 and 24 days. These time points were chosen because morphological examination showed a substantial SC layer. Since the composition of amniotic fluid varies, the amniotic fluid-treated HSEs were not analyzed. Human skin equilibrated in an incubator at 37°C and 93% RH for 24 hours served as a control, as the HSEs were also generated under these conditions.

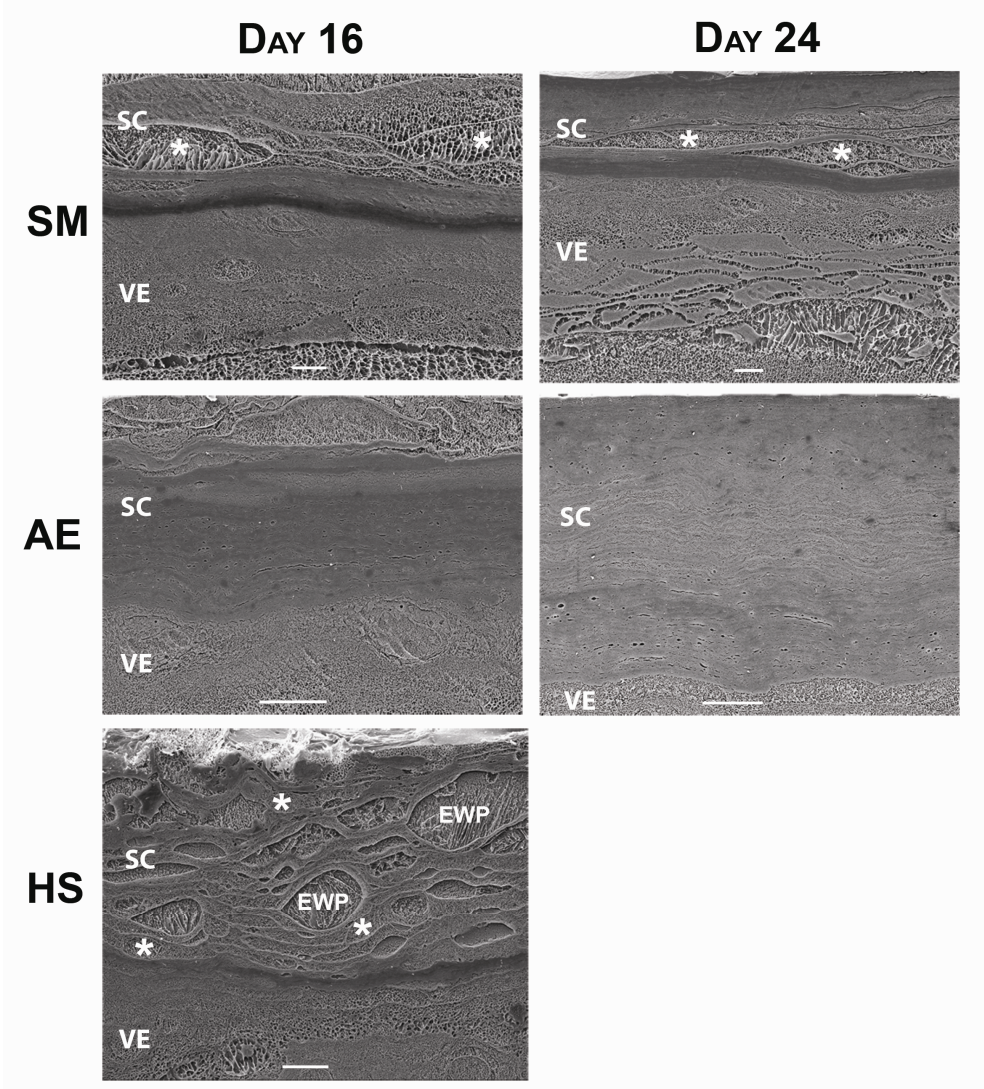

Figure 5. Cryo-SEM images of submerged (SM) and air-exposed (AE) collagen HSEs harvested at day 16 or at day 24, and human skin (HS) equilibrated in an incubator for 24 hours. Scale bars represent 10 μm. SC = stratum corneum, VE = viable epidermis, EWP = extracellular water pool, * = water-containing corneocyte.

Cryo-SEM images can be interpreted by the contrast in an image, which is created at the planed surface by the sublimation of free water. Regions with contrast correspond to areas where free water was located prior to its evaporation. Areas without free water appear as low contrast regions in the image. The HSEs generated on a collagen substrate and grown under submerged conditions reveal a high SC hydration level (figure 5). At day 16 the upper layers of the SC are hydrated, while the inner most layers show low levels of water. The water present in the hydrated regions is mainly present within the corneocytes at this time point. At day 24, the submerged HSEs show a high hydration level in the central region of the SC. The water in the hydrated central region of the SC was mainly present inside the corneocytes, but was occasionally also observed in the intercellular space. The SC of collagen HSEs grown under air-exposed conditions increases in thickness between day 16 and 24, but continues to have low water levels throughout the entire SC, as indicated by the low contrast in the images. Similar results were obtained from submerged and air-exposed HSEs generated on a filter (data not shown).

Corneocytes in SC of human skin equilibrated in the incubator for 24 hours appear swollen and show a high contrast intracellularly, indicating that these cells contain a considerable amount of free water. The corneocytes in the inner part of the SC contain almost no free water, as these cells show almost no contrast.

Generating HSEs under submerged conditions leads to decreased NMF levels

As the NMF level is reported to be one of the factors that influences the hydration level of the SC [20], its content in the SC of the submerged and air-exposed HSEs generated on a collagen substrate was also determined. The NMF level is expressed as the PCA/protein ratio, in which PCA is one of the main components of the NMFs. Figure 6 shows that HSEs grown under submerged conditions have a lower total PCA/protein ratio compared to the HSEs grown under air-exposed

conditions. This indicates that the submerged HSEs contain less NMFs compared to the air-exposed HSEs. However, both air-exposed and submerged HSEs contain less NMF than human skin.

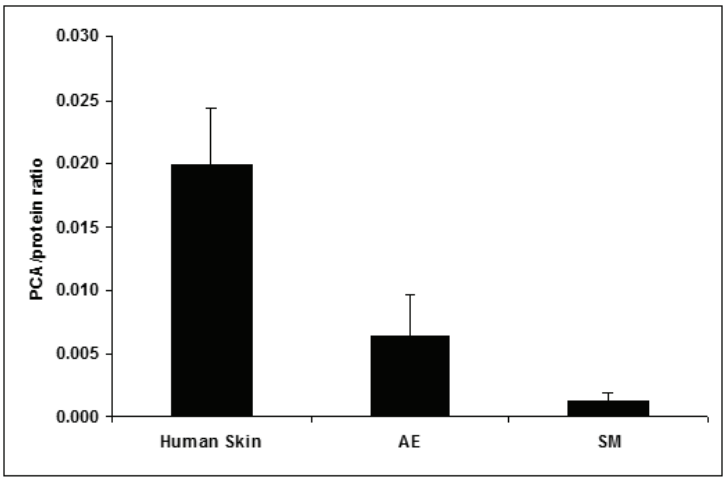

Figure 6. Total SC NMF content, represented by PCA/protein ratios, of human skin, air-exposed (AE) (n=18) and submerged (SM) (n=9) HSEs. All HSEs were generated on fibroblast-populated collagen matrices and harvested after 24 days of culturing. The PCA/protein ratio for human skin was obtained from Bouwstra *et al.* [16]. The error bars represent standard deviations.

DISCUSSION

Several studies have been performed in which human keratinocytes have been cultured in petri dishes or culture flasks under submerged conditions [3-7]. However, the degree of stratification or the organization and lipid content of the SC of these submerged cultures generally showed key differences between cultures grown at the air-liquid interface and human skin. In this study we have developed a culturing method to mimic the aqueous conditions found *in utero* more closely than in previous studies to determine whether a fully differentiated epidermis can also be formed under submerged conditions *in vitro*. The most important result was that the submerged HSEs, generated on a collagen substrate or filter, were able to form

a fully differentiated epidermis that contained all the strata present in human epidermis, including a SC. The submerged HSEs generated on a collagen substrate even showed the presence of all viable epidermal layers as well as a few SC layers after 8 days of culturing. Furthermore, not only all main lipid classes were present in HSEs generated under submerged conditions, but even all the ceramide subclasses were synthesized under these conditions. To mimic the *in utero* environment even closer, additional studies were performed with HSEs generated on a collagen substrate that were kept submerged with amniotic fluid at the apical side. These amniotic fluid-treated HSEs showed a fully differentiated epidermis with a similar morphology, a similar expression of the differentiation markers and lipid profile as the HSEs that were kept submerged with culture medium. However, as the biological amniotic fluid varies in composition, it was decided to carry out most of our studies under well defined medium conditions.

It has been shown that the expression of several receptors is related to the differentiation state of keratinocytes [21, 22]. Basal keratinocytes in submerged cultures grown in petri dishes or culture flasks receive nutrients only from the apical side. Therefore, the epidermal layers that develop above the basal layer in these cultures may decrease the availability of essential nutrients from the culture medium towards the basal keratinocytes, which may hamper the epidermal development. In our present studies keratinocytes receive stimulating factors, which are present in the medium or secreted by fibroblasts, at the basal side in addition to the apical side. This tissue culture method mimics the *in utero* situation closer than the described method in petri dishes or culture flasks. Feeding of the keratinocytes from the basal side might therefore be a crucial prerequisite to develop a fully stratified epidermis under submerged conditions. This hypothesis is in agreement with previous studies that reported an incomplete differentiation of submerged keratinocyte cultures that received nutrients only from the apical side [3-7].

This study also shows that HSEs generated on an inert filter are also able to form a differentiated epidermis under submerged conditions in the absence of fibroblasts.

This finding further supports our hypothesis that feeding of keratinocytes from the basal and apical side is important to generate a differentiated epidermis. However, it should be noted that the presence of fibroblasts improves the epidermal morphology. Several literature findings indicate that fibroblasts have a stimulatory effect on keratinocyte proliferation and appearance of the epidermis [9, 10, 23, 24].

Although the submerged and air-exposed HSEs show similarities in their morphology, some differences were observed concerning the expression of several differentiation markers and SC lipid composition. In the early stage of epidermal development the submerged HSEs generated on a collagen substrate had fewer viable epidermal layers compared to the air-exposed HSEs. This indicates that exposure of HSEs to air results in enhanced proliferation and differentiation of the keratinocytes in the first few days compared to the submerged conditions.

At present the function of each ceramide class remains to be elucidated. However, it is suggested that ceramide EOS is important for the barrier properties of the skin, as this ceramide promotes the formation of the characteristic 13 nm long periodicity phase [25, 26]. Furthermore, free fatty acids are also thought to play a crucial role in the tight packing of the SC lipids [27]. The lower level of ceramide EOS and free fatty acids in the submerged HSEs may therefore lead to decreased barrier properties compared to the air-exposed HSEs. The higher ceramide precursor levels in the submerged HSEs may be a result of the aqueous environment surrounding the developing epidermis.

The submerged HSEs had a much higher SC water content and a paradoxally lower NMF level compared to the air-exposed HSEs. Both the submerged and air-exposed HSEs were grown at a relative humidity of 93%. This environment has a higher humidity level than generally found *in vivo*. As the humidity of the surrounding environment directs the conversion of filaggrin to NMFs, it is plausible that the current culturing conditions lead to decreased NMF levels in the HSEs compared to human SC [20]. However, it is likely that the SC water content of the submerged HSEs nevertheless increased due to the direct contact with culture

medium. This increased water level could consequently have led to a further decrease in the conversion of filaggrin to NMFs.

CONCLUSION

This study shows for the first time that HSEs grown under submerged conditions are able to form a fully differentiated epidermis. The submerged HSEs show similar expression of many differentiation markers and comparable lipid profiles as the air-exposed HSEs and human epidermis. During the last weeks of pregnancy, the developed epidermis is fully exposed to the surrounding amniotic fluid. The described culture method mainly mimics this stage of epidermal development and can therefore be used to study the effect of an aqueous environment on the development of the epidermis during that period. In addition, the presented culturing method may also provide information on the changes that occur in the epidermis during the transition from an aqueous to a terrestrial environment.

ACKNOWLEDGEMENTS

The authors would like to thank Hendrik W. Groenink and Nazmoen Mahmood for their technical assistance.

REFERENCES

1. Zghoul, N., Fuchs, R., Lehr, C.M. and Schaefer, U.F. Reconstructed skin equivalents for assessing percutaneous drug absorption from pharmaceutical formulations. Altex **18,** 103, 2001.
2. Holbrook KA and GF, O. The fine structure of developing human epidermis: light, scanning, and tranmission electron microscopy of the periderm. J Invest Dermatol **65,** 16, 1975.
3. Breiden, B., Gallala, H., Doering, T. and Sandhoff, K. Optimization of submerged keratinocyte cultures for the synthesis of barrier ceramides. Eur J Cell Biol **86,** 657, 2007.
4. Ponec, M., Weerheim, A., Kempenaar, J., Mommaas, A.M. and Nugteren, D.H. Lipid composition of cultured human keratinocytes in relation to their differentiation. J Lipid Res **29,** 949, 1988.
5. Riva, F., Casasco, A., Nespoli, E., Cornaglia, A.I., Casasco, M., Faga, A., Scevola, S., Mazzini, G. and Calligaro, A. Generation of human epidermal constructs on a collagen layer alone. Tissue Eng **13,** 2769, 2007.
6. Uchida, Y., Behne, M., Quiec, D., Elias, P. and Holleran, W. Vitamin C stimulates sphingolipid production and markers of barrier formation in submerged humankeratinocyte cultures. J Invest Dermatol **117,** 1307, 2001.
7. Prunieras, M., Regnier, M. and Woodley, D. Methods for cultivation of keratinocytes with an air-liquid interface. J Invest Dermatol **81,** 28s, 1983.
8. Boelsma, E., Gibbs, S., Faller, C. and Ponec, M. Characterization and comparison of reconstructed skin models: morphological and immunohistochemical evaluation. Acta Derm Venereol **80,** 82, 2000.
9. El Ghalbzouri, A., Lamme, E. and Ponec, M. Crucial role of fibroblasts in regulating epidermal morphogenesis. Cell Tissue Res **310,** 189, 2002.
10. El-Ghalbzouri, A., Gibbs, S., Lamme, E., Van Blitterswijk, C.A. and Ponec, M. Effect of fibroblasts on epidermal regeneration. Br J Dermatol **147,** 230, 2002.
11. Bell E., Rosenberg M., Kemp P., Gay R., Green G. D., Muthukumaran N. and C., N. Recipes for reconstituting skin. J Biomech Eng **113,** 113, 1991.
12. El Ghalbzouri, A., Siamari, R., Willemze, R. and Ponec, M. Leiden reconstructed human epidermal model as a tool for the evaluation of the skin corrosion and irritation potential according to the ECVAM guidelines. Toxicol In Vitro **22,** 1311, 2008.

13. Regnier, M., Desbas, C., Bailly, C. and Darmon, M. Differentiation of normal and tumoral human keratinocytes cultured on dermis: reconstruction of either normal or tumoral architecture. In Vitro Cell Dev Biol **24,** 625, 1988.
14. Stark, H.J., Boehnke, K., Mirancea, N., Willhauck, M.J., Pavesio, A., Fusenig, N.E. and Boukamp, P. Epidermal homeostasis in long-term scaffold-enforced skin equivalents. J Investig Dermatol Symp Proc **11,** 93, 2006.
15. Tinois, E., Tiollier, J., Gaucherand, M., Dumas, H., Tardy, M. and Thivolet, J. In vitro and post-transplantation differentiation of human keratinocytes grown on the human type IV collagen film of a bilayered dermal substitute. Exp Cell Res **193,** 310, 1991.
16. Bouwstra, J.A., Groenink, H.W., Kempenaar, J.A., Romeijn, S.G. and Ponec, M. Water distribution and natural moisturizer factor content in human skin equivalents are regulated by environmental relative humidity. J Invest Dermatol **128,** 378, 2008.
17. Smola, H., Thiekotter, G. and Fusenig, N.E. Mutual induction of growth factor gene expression by epidermal-dermal cell interaction. J Cell Biol **122,** 417, 1993.
18. Bligh, E.G. and Dyer, W.J. A rapid method of total lipid extraction and purification. Can J Biochem Physiol **37,** 911, 1959.
19. Ponec, M., Weerheim, A., Lankhorst, P. and Wertz, P. New acylceramide in native and reconstructed epidermis. J Invest Dermatol **120,** 581, 2003.
20. Rawlings, A.V. and Harding, C.R. Moisturization and skin barrier function. Dermatol Ther **17 Suppl 1,** 43, 2004.
21. Boonstra, J., De Laat, S.W. and Ponec, M. Epidermal growth factor receptor expression related to differentiation capacity. Exp Cell Res **161,** 421, 1985.
22. Ponec, M., Te Pas, M.F., Havekes, L., Boonstra, J., Mommaas, A.M., Vermeer, B.J. LDL receptors in keratinocytes. J Invest Dermatol 1992 Jun;98(6 Suppl):50S-56S **98,** 50, 1992.
23. Boehnke, K., Mirancea, N., Pavesio, A., Fusenig, N.E., Boukamp, P. and Stark, H.J. Effects of fibroblasts and microenvironment on epidermal regeneration and tissue function in long-term skin equivalents. Eur J Cell Biol **86,** 731, 2007.
24. Lee D. Y. and H., C.K. The effects of epidermal keratinocytes and dermal fibroblasts on the formation of cutaneous basement membrane in three-dimensional culture systems. Arch Dermatol Res **296,** 296, 2005.
25. Bouwstra, J.A., Gooris, G.S., Dubbelaar, F.E. and Ponec, M. Phase behavior of stratum corneum lipid mixtures based on human ceramides: the role of natural and synthetic ceramide 1. J Invest Dermatol **118,** 606, 2002.

26. McIntosh, T.J., Stewart, M.E. and Downing, D.T. X-ray diffraction analysis of isolated skin lipids: reconstitution of intercellular lipid domains. Biochemistry **35,** 3649, 1996.

27. Bouwstra, J., Pilgram, G., Gooris, G., Koerten, H. and Ponec, M. New aspects of the skin barrier organization. Skin Pharmacol Appl Skin Physiol **14 Suppl 1,** 52, 2001.

3

UNRAVELING BARRIER PROPERTIES OF THREE DIFFERENT IN-HOUSE HUMAN SKIN EQUIVALENTS

Varsha S. Thakoersing[1], Gerrit S. Gooris[1], Aat Mulder[1], Marion Rietveld[2], Abdoelwaheb El Ghalbzouri[2], Joke A. Bouwstra[1]

[1] Leiden/Amsterdam Center for Drug Research, Department of Drug Delivery Technology, Gorlaeus Laboratories, Leiden University, 2333 CC Leiden, The Netherlands.

[2] Leiden University Medical Center, Department of Dermatology, Leiden University, 2333 ZA Leiden, The Netherlands

Adapted from Tissue Engineering Part C Methods. 2012 Jan;18(1):1-11.

ABSTRACT

Human skin equivalents (HSEs) are three dimensional culture models that are used as a model for native human skin. In this study the barrier properties of two novel HSEs, the Fibroblast Derived matrix Model (FDM) and the Leiden Epidermal Model (LEM), were compared with the Full Thickness collagen Model (FTM) and human skin. As the main skin barrier is located in the lipid regions of the upper layer of the skin, the stratum corneum (SC), we investigated the epidermal morphology, expression of differentiation markers, SC permeability, lipid composition and lipid organization of all HSEs and native human skin. Our results demonstrate that the barrier function of the FDM and LEM improved compared to that of the FTM, but all HSEs are more permeable than human skin. Furthermore, the FDM and LEM have a relatively lower free fatty acid content than the FTM and human skin. Several similarities between the FDM, LEM and FTM were observed: 1) the morphology and the expression of the investigated differentiation markers were similar to that observed in native human skin, except for the observed expression of keratin 16 and premature expression of involucrin which were detected in all HSEs 2) the lipids in the SC of all HSEs were arranged in lipid lamellae, similar to human skin, but show an increase in the number of lipid lamellae in the intercellular regions, and 3) the SC lipids of all HSEs show a less densely packed lateral lipid organization compared to human SC. These findings indicate that the HSEs mimic many aspects of native human skin, but differ in their barrier properties.

INTRODUCTION

The skin provides a possible delivery route of active compounds either to the various skin layers or to the systemic circulation. Penetration studies with preferably *ex vivo* human skin can be performed to investigate whether compounds show promise for dermal or transdermal application. However, the use of *ex-vivo* skin is not always possible due to practical issues. The use of human skin equivalents (HSEs) can therefore provide an alternative for native human skin. HSEs have already been used for various applications such as the treatment of burn wounds [1-3], cutaneous irritation and toxicity testing of substances [4-7] and the generation of diseased skin models [8-11]. Many HSEs have a fairly similar morphology and a comparable expression of several differentiation markers as native human skin [12-17]. However, when HSEs are evaluated for their resemblance to native human skin it is also important to examine their barrier properties. The stratum corneum (SC), which is the outermost layer of the epidermis, forms the first and main barrier of the skin against penetration of exogenous substances. The SC consists of protein rich dead cells that are embedded in a lipid matrix. As the lipids form a continuous pathway in the SC, the lipid domains play a crucial role in the barrier properties of the skin. The SC consists of three main lipid classes, which are cholesterol, free fatty acids and ceramides. These lipids form two lamellar phases with a repeat distance of approximately 13 nm or 6 nm, referred to as the long periodicity phase (LPP) and short periodicity phase (SPP), respectively (see figure 1A) [18-21]. Besides the lamellar organization the lateral packing is also important for a proper barrier function of the SC. The lateral packing discloses information about the density of the lipids within the lipid lamellae. In native human skin, the majority of the SC lipids within the lipid lamellae form crystalline phases. A large fraction of lipids forms the very dense orthorhombic packing, but a small population of lipids also forms the less dense hexagonal or even liquid packing [21-24]. A schematic presentation of these crystalline and liquid phases is shown in figure 1A.

When HSEs are used for *in vitro* permeation studies they generally show a higher permeability compared to human skin, indicative of an impaired barrier function [25-32]. Several studies have been performed in which the barrier properties of various HSEs were examined. However, these studies mainly focused on the SC lipid composition. They showed that HSEs are prone to have a reduced free fatty acid content [14, 25, 33-36]. The few studies in which the SC lateral and lamellar organization of some HSEs have been examined were performed more than a decade ago. These studies mostly showed a predominantly hexagonal packing [34, 37] in HSEs and the presence of the LPP [33, 35, 37]. However, not all models showed a continuous presence of lipid lamellae in the SC or the presence of the LPP [14].

In this study we evaluated the barrier properties of two recently developed HSEs - the fibroblasts derived matrix model (FDM) and the Leiden Epidermal Model (LEM) and compared their barrier properties, which have not been investigated before, with the Full Thickness collagen Model (FTM). The FDM model consists of a dermal compartment based on a human fibroblast-derived matrix [38], while the dermal equivalent of FTM consists of rat-tail collagen populated with fibroblasts [39]. The LEM is an epidermal equivalent generated on an inert filter. To evaluate to which extent these three HSEs mimic the barrier properties of native human skin and to assess their suitability for e.g. permeability testing, we have examined their SC lipid composition, lipid organization and permeability and compared that with native human skin.

Figure 1. A: The SC lipids are organized into lipid layers (i.e. lamellae) stacked on top of each other, referred to as the lamellar phase. The most important parameter to characterize this phase is the repeat distance (d). This is distance over which the molecular structure is repeated. In native human SC the lipids are organized into two lamellar phases, the long periodicity phase (LPP) and the short periodicity phase (SPP) with repeat distances of around 13 and 6 nm, respectively. In the plane perpendicular to

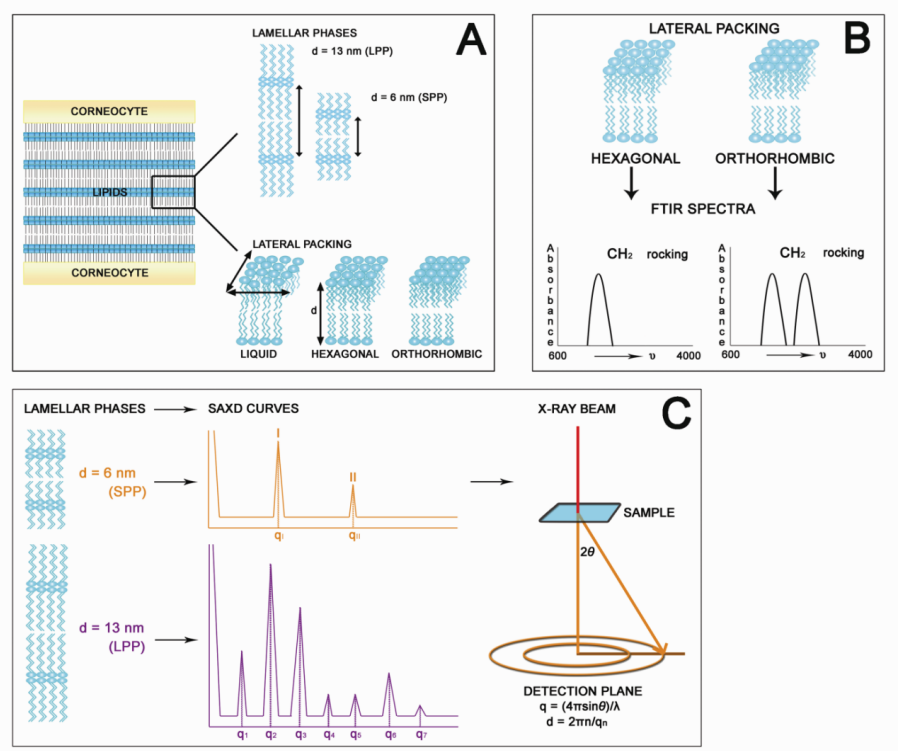

the direction of the lamellar repeats the lipid organization is referred to as the lateral packing. The lateral packing is liquid, hexagonal or orthorhombic. The liquid packing is the least dense packing, while the orthorhombic packing has the highest density of lipids. B: Due to atom bond vibrations, molecules absorb infrared light at characteristic wavenumbers. This absorption provides information about inter- and intramolecular interactions. The CH_2 rocking vibration of the hydrocarbon chains provides information about the lateral packing of the lipids. A single contour at around 719 cm^{-1} is observed when lipids are arranged in a hexagonal packing, while two peaks (around 719 and 730 cm^{-1}) are characteristic for an orthorhombic packing. C: X-rays that pass a sample are scattered by the sample, resulting in a characteristic diffraction pattern. The scattered intensity is plotted as a function of q, the scattering vector. q is defined as $4\pi\sin\theta/\lambda$, in which θ is the scattering angle and λ is the wavelength of the X-rays. In case of a lamellar phase the diffraction peaks in the pattern are all at the same interpeak distance. The position of the peaks (q_1, q_2, q_3,…,q_n, n being the order of the peak) are related to the repeat distance of a lamellar phase by $d=2\pi n/q_n$. As this is a reciprocal relationship, the 1st and 2nd order peak of the SPP is located at higher q-values that that of the LPP.

MATERIALS AND METHODS

Cell culture

Normal human keratinocytes (NHKs) and human dermal fibroblasts were obtained from adult donors undergoing mammary or abdomen surgery and were established as described previously [39]. NHKs used to create HSEs with only an epidermal compartment were generated with the Dermalife K medium complete kit (Lifeline Cell Technology, Walkersville, MD). The NHKs were grown to a maximum confluency of 80% before trypsin digestion. First and second passage NHKs were used to generate HSEs.

Dermal equivalents

Collagen-type I containing dermal equivalents: collagen-type I containing dermal equivalents were generated as described earlier [39]. Collagen was isolated from rat tails and dissolved in 0.1% acetic acid to a concentration of 4 mg/mL. This solution was mixed at 4ºC with Hank's Buffered Salt Solution (HBSS) (Invitrogen, Leek, The Netherlands), 0.1% acetic acid, 1M NaOH and fetal bovine serum (FBS) (Hyclone, Logan, UT) to obtain a final collagen concentration of 1 mg/mL. One mL of the mixture was pipetted into a filter insert (Corning transwell cell culture inserts, membrane diameter 24 mm, pore size 3 μm, Corning Life Sciences, Amsterdam, The Netherlands) and was allowed to polymerize for 15 minutes at 37ºC. Hereafter, a 2 mg/mL collagen solution was prepared at 4ºC with the 4 mg/mL collagen stock solution, HBSS, 0.1% acetic acid, 1M NaOH and a fibroblasts containing FBS solution (final fibroblast cell density of $0.4x10^5$ cells/mL collagen solution). Three mL of this mixture was pipetted onto the previously polymerized collagen layer. The new collagen layer was placed at 37ºC to polymerize. After the final polymerization step the dermal equivalents were placed in a 6-well deep-well plate (Organogensis, Canton, MA) and submerged in medium consisting of Dulbecco's Modified Eagle Medium (DMEM; Invitrogen, Leek, The Netherlands), 5% FBS, 1% penicillin/streptomycin (Sigma) and fresh

supplementation with 45 mM vitamin C (Sigma). The medium was refreshed twice a week.

Fully human dermal equivalents: the dermal compartment of the FDMs were generated as described before [38]. Briefly, $0.4x10^6$ fibroblasts were seeded onto filter inserts (Corning Transwell culture inserts, membrane diameter 24 mm, pore size 0.4 μm; Corning Life Sciences, Amsterdam, The Netherlands). The fibroblasts were nourished with the medium described for the collagen type I containing dermal equivalents for 3 weeks, during which the cells generated a dermal matrix. The medium was refreshed twice a week.

Generation of human skin equivalents (HSEs)

HSEs generated on collagen dermal equivalents referred to as Full Thickness collagen Model (FTM): One week after generation of the collagen dermal equivalents, $0.5x10^6$ NHKs were seeded onto each dermal equivalent. The HSEs were kept submerged for 2 or 3 days with a 3:1 mixture of DMEM and Ham's F12 medium supplemented with 5% FBS, 1% penicillin/streptomycin solution, 0.5 μM hydrocortisone, 1 μM isoproterenol and 0.5 μg/mL insulin. Hereafter, the HSEs were kept submerged for an additional 2 days with medium in which the FBS was reduced to 1% and the medium was additionally supplemented with 0.053 μM selenious acid (Johnson Matthey, Maastricht, The Netherlands), 10 mM L-serine (Sigma), 10 μM L-carnitine (Sigma), 1 μM α-tocopherol acetate (Sigma), 25 mM vitamin C and a lipid mixture of 3.5 μM arachidonic acid (Sigma), 30 μM linoleic acid (Sigma) and 25 μM palmitic acid (Sigma). This medium is referred to as K^1-medium. The HSEs were subsequently lifted to the air-liquid interface. For the remaining culture period the HSEs were fed with a medium similar to K^1-medium except that the FBS was omitted and the arachidonic acid concentration was increased to 7 μM. The culture medium was refreshed twice a week. The HSEs were grown for 16 days after seeding the NHKs.

HSEs generated on fully human dermal equivalents referred to as Fibroblast Derived matrix Model (FDM): three weeks after seeding fibroblasts onto filter inserts, $0.5x10^6$ NHKs were seeded onto each dermal equivalent. The HSEs were further cultured as described for the FTMs.

HSEs generated on inert filter, referred to as Leiden Epidermal Model (LEM): LEM was generated with minor modifications of the culture conditions described by El Ghalbzouri *et al.* [7]. NHKs (0.2 x 10^6 cells/filter) were seeded directly onto cell culture inserts (Corning Transwell cell culture inserts, membrane diameter 12 mm, pore size 0.4 μm; Corning Life Sciences, Amsterdam, The Netherlands) and were kept submerged in Dermalife medium until confluency. Hereafter the HSEs were kept submerged in CnT medium (CellnTec, Bern, Switzerland), which was supplemented according to the manufacturer's protocol, and 1% penicillin/streptomycin solution (Sigma, Zwijdrecht, The Netherlands), 1 μM α-tocopherol acetate (Sigma), 25 mM vitamin C (Sigma) and a lipid mixture of 7 μM arachidonic acid (Sigma), 30 μM linoleic acid (Sigma) and 25 μM palmitic acid (Sigma). After two days the HSEs were lifted to the air-liquid interface. The LEMs were cultured at the air-liquid interface for 12 days before harvesting.

Morphology and immunohistochemistry

Harvested HSEs were fixed in 4% (w/v) paraformaldehyde (Lommerse Pharma, Oss, The Netherlands), dehydrated and subsequently embedded in paraffin. 5 μm sections were cut, deparaffinized, rehydrated and stained with haematoxylin and eosin for analysis by light microscopy. Immunohistochemical staining of keratin 10, keratin 16, filaggrin, loricrin and involucrin was performed on paraffin sections as described before [39, 40]. Immunofluorescent staining of aquaporin 3 (Santa Cruz Biotechnology, Santa Cruz, CA) was performed on frozen sections that were fixed in acetone. The aquaporin 3 antibody (1:50 dilution) was applied for 60 min followed by incubation with donkey anti-goat FITC-labelled secondary antibody (1:100 dilution) (Jackson ImmunoResearch Europe, Suffolk, UK) for 60 min.

Sections were enclosed with Vectashield mounting medium with DAPI (Vector Laboratories, Peterborough, UK).

Stratum corneum isolation and diffusion study

The SC of HSEs and human skin was isolated as described by De Jager *et al.* [41]. The diffusion study with benzocaine and further analysis with HPLC, to deteremine the flux of benzocaine through each SC sample, was performed as described earlier [41] with modification of the mobile phase to methanol:water (50:50 v/v). The diffusion study was performed with at least 4 SC sheets from each HSE type or human skin.

Lipid extraction and analysis

SC samples were consecutively extracted according to a modified Bligh and Dyer procedure with the addition of 0.25M KCl to extract polar lipids as described before [40, 42]. The extracted lipids were analyzed by means of one-dimensional high performance thin layer chromatography (HPTLC) as described before [40]. The ceramides are named according to the nomenclature defined by Motta *et al.* [43] and Masukawa *et al.* [44]. Briefly, ceramides with a sphingosine (S), phytosphingosine (P) or 6-hydroxysphingosine (H) are linked via an amide to a fatty acid chain, which can either be an estrified ω-hydroxy (EO), α-hydroxy (A) or non-hydroxy (N) fatty acid.

Fourier transform infrared spectroscopy (FTIR) and small angle x-ray diffraction (SAXD)

The SC samples for FTIR and SAXD measurements were hydrated at room temperature for 24 hours over a 27% (w/v) NaBr solution. The hydrated SC samples for FTIR were measured as described before [45]. The phase transitions of the SC lateral lipid organization were examined as a function of temperature from

0ºC to 90ºC with a heating rate of 1ºC/4 min. At least 3 SC sheets of each HSE type or human SC were measured.

SAXD measurements were performed at the European Synchrotron Radiation Facility (ESRF) in Grenoble as described before [45]. SC samples were clamped in specially designed holders and measured at room temperature for 10 minutes. The scattered intensity was measured as function of q. q is defined as $q= 4\pi\sin\theta/\lambda$, in which λ is the wavelength of the X-rays and θ the scattering angle. Repeat distances of lamellar phases are calculated from the peak positions; $d= 2\pi n/q_n$, in which n is the order of the peak and q_n its position. At least 2 samples of each HSE type or human SC were measured. A schematic overview of the FTIR and SAXD measurements is depicted in figure 1B and C, respectively.

Transmission electron microscopy (TEM)

HSEs were fixed in 2% paraformaldehyde-2.5% glutaraldehyde in 0.1M sodium cacodylate buffer (pH 7.4) followed by a first post-fixation in 1% osmium tetroxide in cacodylate buffer and a second post-fixation in 0.5% ruthenium tetroxide. Hereafter the samples were dehydrated in 70% ethanol and subsequently processed in a series of 70% ethanol/epoxy resin LX112 (LADD Research Industries, Williston, VT) dilutions and finally in 100% epoxy resin. Ultrathin sections were stained with uranyl-acetate and lead hydroxide and visualized with a Fei Tecnai 12 Twin (Spirit) (Fei Europa, Eindhoven, The Netherlands) electron microscope. At least 2 cultures per HSE type were examined and at least 20 images per culture were made.

Figure 2. Haematoxylin and eosin (HE) and immunohistochemical staining of the expression pattern of keratin 10, keratin 16, filaggrin, loricrin, involucrin and aquaporin 3 (green pattern in the image) in FDM, LEM, FTM and native human skin are shown. Scale bar represents 50 μm.

RESULTS

The morphology and differentiation process show similarities between HSEs and native human skin

FDM, LEM and FTM show a fairly similar morphology and expression of the investigated differentiation markers, except for two markers which are indicative of an activated epithelium, when compared to human skin (figure 2). All HSEs show the presence of all epidermal strata, including a SC. The keratinocytes become flat and elongated as they migrate and differentiate from the basal layer towards the upper spinous and granular layer. In the latter layer keratohyalin granules can be detected. Occasionally the stratum granulosum in the LEM consisted of more cell layers than observed for the FDM, FTM and human skin. Furthermore, all HSEs show similar expression of the early differentiation marker keratin 10, the water/glycerol transporting channel aquaporin 3 and the two terminal differentiation markers filaggrin and loricrin as human skin (figure 2). Filaggrin and loricrin are only detected in the stratum granulosum, while keratin 10 is detected in the suprabasal layers and aquaporin 3 in the cell membranes of all cells in the viable epidermis. In native human skin involucrin expression is confined to the granular layer and keratin 16 expression is absent. In all HSEs however, involucrin and keratin 16 are expressed throughout the suprabasal layers of the viable epidermis, which are signs of an activated epithelium.

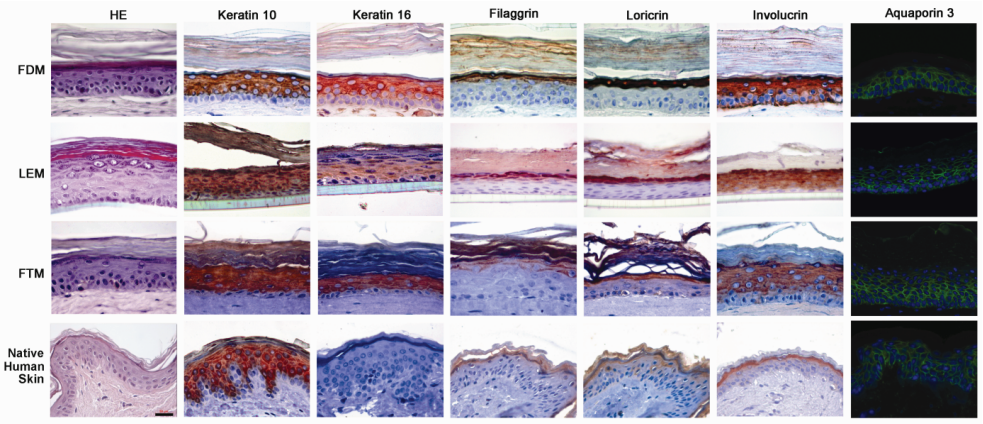

The SC of the HSEs contains all barrier lipid classes that are present in human skin

The three lipid classes present in human SC, namely cholesterol, free fatty acids and ceramides, are also present in the SC of the HSEs (figure 3). In addition, the HSEs show the presence of all ceramide subclasses that are present in native human SC. However, some differences can be noticed in the relative abundance of free fatty acids and ceramides when the different lipid profiles are compared. The FDM and LEM exhibit a relatively lower level of free fatty acids compared to human SC. However, the lipid profile of the FTM indicates that in this model the free fatty acid level is higher than in the LEM and FDM and appears to be comparable to native human SC. Furthermore, all HSEs seem to have a higher relative content of ceramides EOS and EOP. The LEM and FTM have an additional ceramide subclass, with a retention factor between that of ceramide NP and AS (figure 3; indicated by *), that is not present in the FDM or human SC.

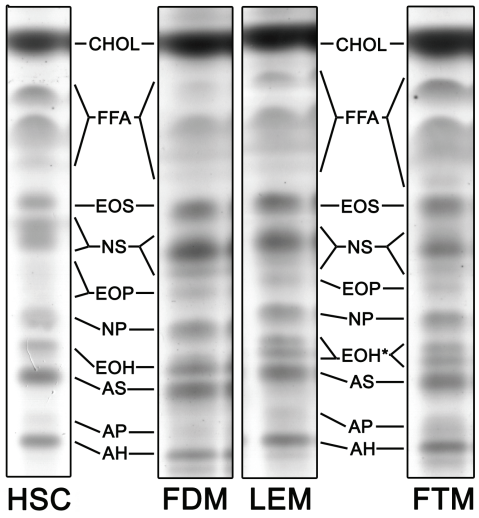

Figure 3. The SC barrier lipid profile of each HSE and human SC are shown. The HSEs contain all lipid classes that are also present in human SC, namely cholesterol (CHOL), free fatty acids (FFA) and ceramides. The FTM and LEM show the presence of an additional ceramide subclass (*) that is not detected in human SC or the FDM.

Permeability assessment of HSEs and native human skin

To investigate the barrier function of the HSEs a diffusion study was performed. Figure 4 shows the diffusion profile of benzocaine through the SC of the three HSEs and native human skin. These results show that the FDM and LEM have an improved barrier function compared to FTM. The calculated steady-state flux (figure 4) indicates that the SC of the FDM and LEM is approximately 3 times more permeable than native human SC, whereas the SC of FTM is about 5 times more permeable. The lag-time of the benzocaine flux through the SC of the FDM and FTM is slightly lower compared to native human SC.

	Human SC	FDM	LEM	FTM
$Flux_{ss}$ ($\mu g/hr/cm^2$)	13.6 ± 3.5	44.5 ± 4.6	47.0 ± 5.8	65.8 ± 4.0
T_{LAG} (hr)	0.5 ± 0.2	0.2 ± 0.1	0.6 ± 0.4	0.2 ± 0.0

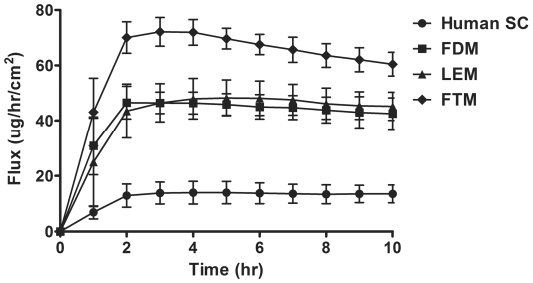

Figure 4. Benzocaine was used as a model drug to investigate the permeability of the three HSEs and human SC. The data represent the mean and standard deviation of at least 4 measurements. The estimated steady-state flux ($Flux_{ss}$) and lag-time (T_{lag}) of benzocaine through the SC of human skin and the three HSEs are also shown.

The lateral packing in the SC of the three HSEs differs from human SC

The lateral packing in the SC of the three HSEs and human skin were examined using FTIR. The lateral packing can be determined by monitoring the rocking bands in an FTIR spectrum. When lipids are in a crystalline orthorhombic packing the CH_2 rocking band consists of two vibrations at 719 cm^{-1} and 730 cm^{-1}, while a crystalline hexagonal lateral packing results in a single vibration at 719 cm^{-1}. An example of the thermotropic response of the CH_2 rocking band as a function of temperature in the FDM, LEM, FTM and native human SC are shown in figure 5. In general the HSEs show a strong peak at 719 cm^{-1} and a smaller peak at 730 cm^{-1} at lower temperatures. This indicates that in that temperature region the lipids in the SC mainly form a hexagonal lateral packing and a small population of lipids forms an orthorhombic packing. In human SC the high intensity of the 730 cm^{-1} peak indicates an abundant formation of the orthorhombic lateral packing. The temperature at which the orthorhombic packing transforms into the hexagonal packing, indicated by the disappearance of the 730 cm^{-1} peak, varies between each HSE type and also between samples of the same HSE type and native human skin.

Figure 5. Examples of the lateral lipid organization as a funtion of temperature are shown for the FDM, LEM, FTM and native human SC (HSC) (a, b, c and d, respectively). At lower temperatures the lipids in the FDM, LEM and FTM mainly form a hexagonal lateral packing (strong vibrations at 719 cm^{-1}) and a minor population of lipids forms an orthorhombic packing (weak vibrations at 730 cm^{-1}). The transition to a hexagonal packing, indicated by the disappearance of the 730 cm^{-1} peak, occurs at approximately 24ºC, 30ºC and 26ºC in the FDM, LEM and FTM, respectively. In human SC (d) a doublet is observed with a high intensity peak at 730 cm^{-1} , representing a dominant orthorhombic packing. The orthorhombic packing disappears between 28ºC to 40ºC. At higher temperatures only a singlet is observed signifying a hexagonal packing. Figure e shows the transition from a hexagonal to a liquid phase detected by the symmetric stretching vibrations. The liquid phase is formed between 56-84ºC in the HSEs and between 66-86ºC in human SC.

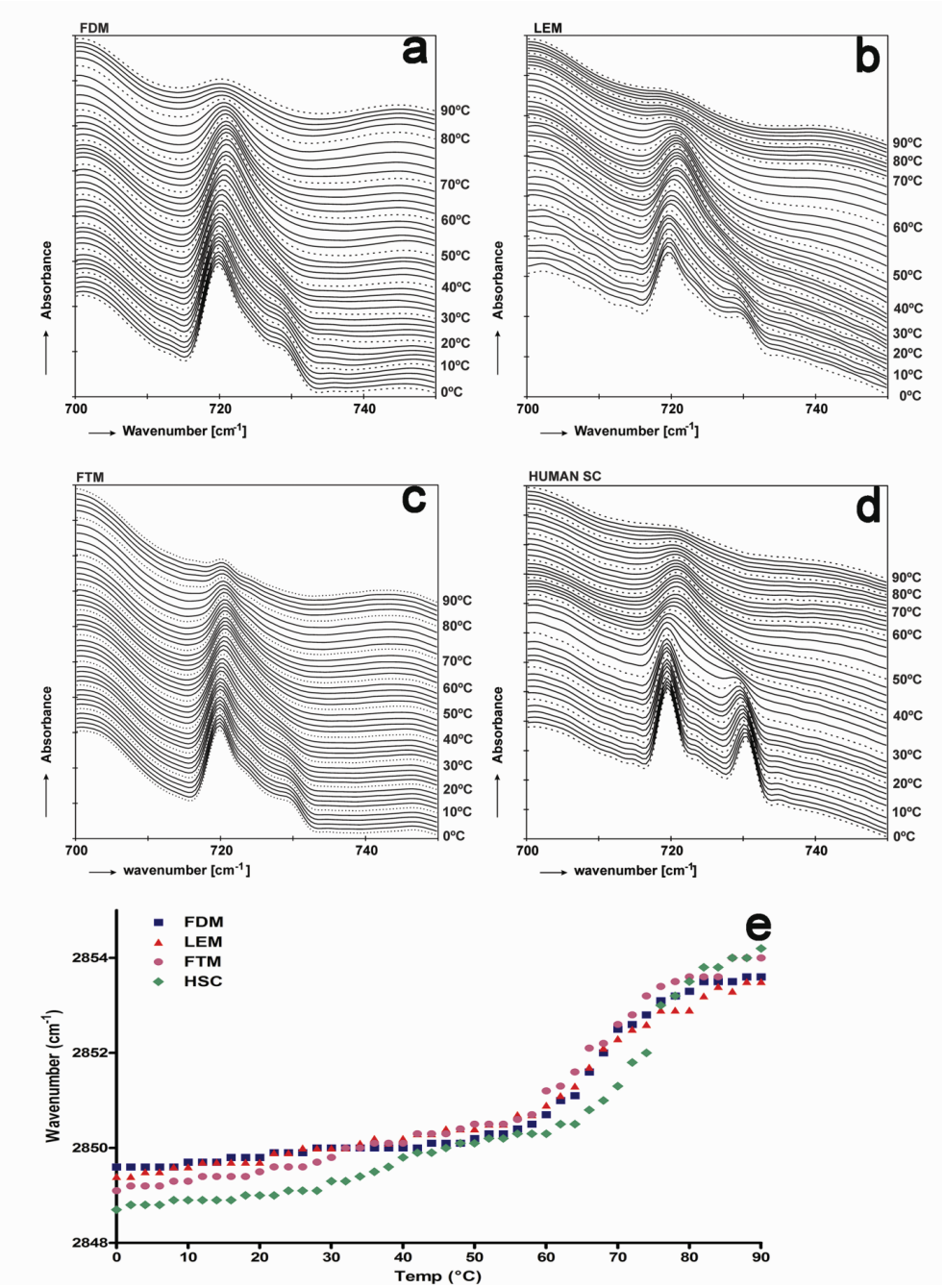
FDM
a
LEM
b
FTM
c
HUMAN SC
d
Absorbance
Wavenumber [cm-1]
wavenumber [cm-1]
90°C
80°C
70°C
60°C
50°C
40°C
30°C
20°C
10°C
0°C
700
720
740
e
FDM
LEM
FTM
HSC
Wavenumber (cm-1)
Temp (°C)
2854
2852
2850
2848
0
10
20
30
40
50
60
70
80
90

In FDM the orthorhombic packing disappears at a temperature that varies between 8-24ºC, in FTM between 14-26ºC, in LEM between 24-30ºC and in native human SC between 40-50ºC. At which temperature the lipids finally form a liquid phase can be determined from the CH_2 symmetric stretching mode, which provides information about the conformational disorder. In a crystalline phase (hexagonal or orthorhombic packing) the conformational disorder is low resulting in symmetric stretching frequencies below 2850 cm^{-1}. In a liquid phase, the conformational disordering is high resulting in symmetric stretching vibrations of around 2852-2854 cm^{-1}. The transition from a crystalline to a conformational disordered liquid phase can therefore be distinguished by a steep increase in wavenumber. In human SC the CH_2 symmetric stretching is around 2848.5 cm^{-1} at 0ºC and increases slightly when the temperature is raised. Between 30-40ºC there is a steeper shift, indicating the orthorhombic to hexagonal phase transition. A further increase to 66ºC results in a gradual shift in wavenumber. At 66ºC a steep shift is noticed from 2850.9 cm^{-1} to 2854.0 cm^{-1} at 86ºC, which corresponds to the formation of a liquid phase (figure 5e). When focussing on the HSEs, between 0ºC and 56ºC a gradual increase in wavenumber from around 2849.5 to 2850.4 cm^{-1} is observed. The symmetric stretching is located at higher wavenumbers than observed for native human SC. Above 56ºC a steep increase in wavenumber is observed to 2853.2 – 2853.6 cm^{-1} at 82-84ºC (figure 5e) demonstrating the formation of the liquid phase. The liquid phase is formed at a lower temperature in the SC of the HSEs compared to human SC.

The SC intercellular lipid regions of HSEs are composed of more lipid lamellae than native human skin

Transmission electron microscopy images taken at the stratum garnulosum/SC interface show the lamellar body extrusion process in the HSEs similarly as observed in native human skin (figure 6a, c, e and g). The extruded lipids are neatly arranged into lipid lamellae (figure 6b, d, f and h), which is characteristic for the SC

lipid organization. When compared to human SC it is evident that the HSEs contain a higher number of lipid lamellae between corneocytes. This finding indicates that the intercellular lipid regions in the SC of the HSEs are more pronounced than in human SC.

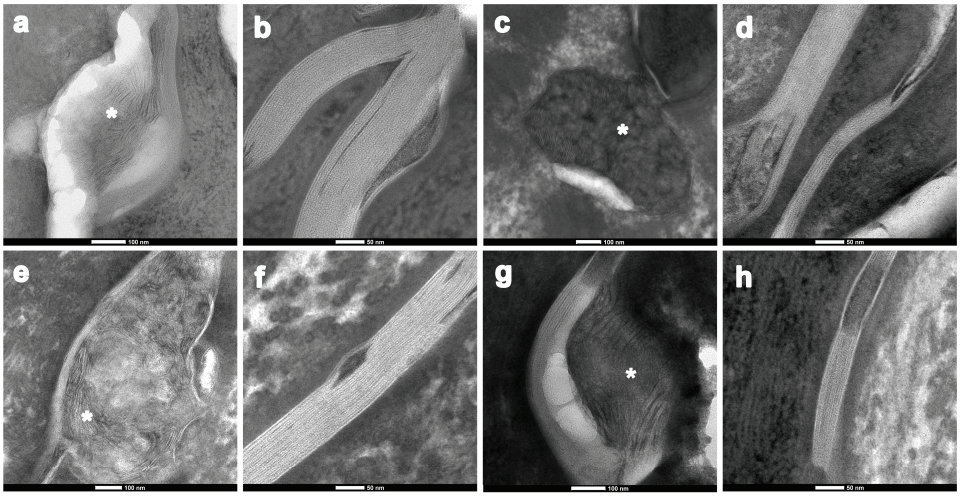

Figure 6. The lipid lamellae in the SC of the three HSEs and human skin were visualized with TEM. Representative images of each HSE and human SC are shown. Figure a, c, e and g represent the lamellar extrusion process in FDM, LEM, FTM and native human skin, respectively (scale bar represents 100 nm). Figure b, d, f and h show the formed lipid lamellae in the SC of FDM, LEM, FTM and native human skin, respectively (scale bar represent 50 nm). *= lamellar body.

The SC lipids in HSEs form the LPP similar to native human skin

The observed lamellar organization in the SC of the three HSEs and native human skin (figure 6) was also investigated by SAXD. The SAXD profiles of all three HSEs show the presence of three sharp diffraction peaks (figure 7; referred to as 1, 2 and 3) that can be attributed to the LPP with a corresponding repeat distance varying between 11.8 - 12.6 nm, 12.6 - 12.8 nm and 11.6 - 12.5 nm for the FDM, LEM and FTM, respectively. However, no peaks are observed that can be

attributed to the SPP. The presence of crystalline cholesterol can also be detected in the diffraction profiles of all three HSEs (figure 7; indicated by *).

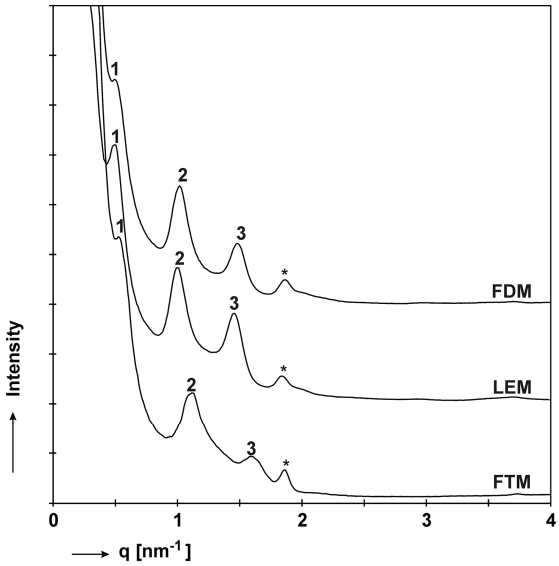

Figure 7. A representative SAXD profile of each HSE type is shown. The 1st, 2nd and 3rd order diffraction peaks of the LPP (indicated by 1, 2 and 3, respectively) are located at q= 0.50, q= 1.01 and q= 1.48 nm^{-1} for the FDM, corresponding to a repeat distance of 12.6 nm. For the LEM the various orders of the LPP are located at q= 0.50, q= 1.00 and q= 1.46 nm^{-1}, indicating a repeat distance of 12.7 nm. For the FTM the various orders of the LPP are located at q= 0.52, q= 1.01 and q= 1.59 nm^{-1}, which corresponds to a repeat distance of 11.7 nm. At q= 1.84 nm^{-1} a reflection is detected in all profiles demonstrating the presence of phase separated crystalline cholesterol (indicated by *).

Discussion

In order to obtain a suitable replacement of native human skin for penetration studies or for safety testing of compounds, we compared two novel in-house skin models with FTM and native human skin and evaluated their SC barrier properties. An overview of the SC barrier properties of the three HSEs and human skin is provided in table 1. Both FDM and LEM show an improved SC barrier function compared to FTM, indicated by the higher flux of benzocaine through the SC of

FTM. Although the SC barrier function of the novel HSEs has improved and mimics more closely the SC barrier function of native human skin, it is still reduced compared to native human skin. A reduced SC barrier function has also been reported for other HSE types, including the commercially available models Epiderm (Mattek), Episkin and SkinEthic [25-32]. As the lipid organization is a crucial determinant for the SC barrier function, we examined the lamellar phases and the lateral packing in all three HSEs and compared that to native human SC.

Table 1. Overview SC barrier properties human skin *vs* HSEs

	Lamellar Packing (RT)	***Lateral Packing (RT)***	***SC Lipid Composition***	***Benzocaine $Flux_{ss}$ ($\mu g/hr/cm^2$)***
Native HS	LPP + SPP	Orthorhombic	CHOL, FFA, CERs	13.6 ± 3.5
FDM	LPP	Hexagonal	CHOL, FFA ↓, CERs EOS and EOP ↑	44.5 ± 4.6
LEM	LPP	Hexagonal	CHOL, FFA ↓, CERs EOS and EOP ↑	47.0 ± 5.8
FTM	LPP	Hexagonal	CHOL, FFA, CERs EOS and EOP ↑	65.8 ± 4.0

An overview of the SC barrier properties of native human skin (HS) and SC of FDM, LEM and FTM are shown. RT = room temperature, CHOL= cholesterol, FFA= free fatty acid, CER= ceramides, $Flux_{ss}$= steady state flux, arrows indicate an increase (↑) or decrease (↓) compared to native human SC.

Morphology and expression of differentiation markers

All three HSEs show a similar morphology and expression of several differentiation markers as native human skin, except for the expression of involucrin and keratin 16, which were detected throughout the suprabasal viable epidermis in all three HSEs. The observed expression of keratin 16 and the early

start of the terminal differentiation program indicated by the premature expression of involucrin might be explained by an over-activated cell differentiation due to compounds or possible growth factors present in the commercial culture media, or by the number of fibroblasts present in the dermal matrices [15, 16]. The over-activated differentiation programme observed in the HSEs may have an effect on the barrier properties of the HSEs. An altered expression of differentiation markers has also been observed in the commercially available models [12]. These models showed a fully differentiated epidermis and an expression pattern for keratin 10 and loricrin that is mainly similar to native human skin. However, all commercial skin models showed a premature expression of involucrin compared to native human skin, indicating that homeostasis was not yet achieved in these models. Cheng *et al.* [46] and El Ghalbzouri *et al.*[13] showed that it is possible to generate HSEs that do not demonstrate the premature expression of involucrin and/or the presence of activation associated markers like keratin 6, 16 and 17. However, it still remains to be investigated whether a normalized involucrin expression or the absence of activation associated markers lead to improved SC barrier properties. Previous studies have shown that the SC of FTM is less hydrated than human SC [39]. The similar expression of the water/glycerol transporting channel aquaporin 3 in the HSEs and native human skin indicates that the reduced SC hydration in FTM is not caused by the absence of aquaporin 3.

Lamellar organization

Our results demonstrate that in all three HSEs the LPP is formed, similar to native human skin [21], while there is no indication of the formation of the SPP. The latter is present in native human SC. Previous studies demonstrated that the presence of acylceramides, such as acylceramides EOS and EOP, induce the formation of the LPP [22]. These ceramides are present in relatively higher amounts in the HSEs compared to native human skin and therefore may account for the abundant presence of the LPP. However, this most probably does not contribute to the

reduced skin barrier function of the HSEs, as the LPP plays a more prominent role in the skin barrier function than the SPP [41]. In 2000 Ponec *et al.*[14] reported the lamellar organization of the EpiSkin and EpiDerm penetration models. In the EpiDerm model an LPP with a repeat distance of 12 nm was clearly detected, while the EpiSkin model showed signs of a poor lamellar organization. Although both the EpiDerm and Episkin models had approximately the same relative amount of ceramide EOS as native human skin, ceramides EOP, AS, AP and AH were minimally present or even absent [6, 14].

When we examine the EM images, the SC of the HSEs seem to contain a larger number of lipid lamellae than observed for human SC. The sharp peaks observed in the SAXD profiles clearly indicate that the mean number of lipid lamellae between the cells is increased in the SC of the HSEs compared to native human SC; the width of half maximum is proportional to 1/N, in which N is the number of lamellae in a stack [47]. Since the penetration of substances through the SC mainly proceeds via the lipid domains we hypothesize that the increased number of lipid layers in the HSEs form wider intercellular 'channels' for compound penetration, which may attribute to the impaired skin barrier function of the HSEs. The SC intercellular lipid domains of the commercially available skin models have also been examined by EM [14]. All models showed the presence of lipid lamellae, however, this was not continuously observed throughout the SC in all models. Additionally, some EpiSkin models showed an incomplete lamellar body extrusion process.

Lateral packing

When focussing on the lateral packing, HSEs have a hexagonal packing rather than an orthorhombic packing that is present in native human SC. Previous studies [18] have shown that long-chain free fatty acids (e.g. free fatty acids with a chain length of 24 or 26 carbon atoms), promote the formation of an orthorhombic packing in SC lipid mixtures, while a reduction in these fatty acids results in a more prominent

formation of the hexagonal packing. These findings suggest that a reduced free fatty acid content in the FDM and LEM may contribute to the absence of an orthorhombic packing. The free fatty acid level in FTM mimics the free fatty acid content of human SC more closely, but nonetheless the lipids also form a hexagonal packing. Therefore other factors also play a role, such as a possible reduction in the chain length of the free fatty acids or the presence of unsaturated fatty acids. Based on previous studies, both of these aberrations are expected to reduce the formation of the orthorhombic packing [48]. To gain more insight in this phenomenon the free fatty acid chain length distribution and degree of saturation in the HSEs will be subject of future studies. Whether the hexagonal packing contributes to the increased permeability for substances like benzocaine is not yet clear. Although the hexagonal packing is less dense than the orthorhombic packing, very recently no difference in the benzoic acid permeability was observed between SC lipid membranes forming either a hexagonal packing or an orthorhombic packing [49].

Formation of a liquid phase

The higher degree of conformational disorder observed for the HSEs at 32ºC, which is the normal skin temperature, suggests an increased proportion of gauche conformations in the alkyl chains of the fatty acids or ceramides in the SC of HSEs compared to human SC. This may signify that relatively more lipids may already be in the liquid phase at 32ºC compared to lipids in the SC of native human skin. This may render the HSEs more permeable.

When examining the transition from a hexagonal to a liquid phase, this transition occurs at a lower temperature in the investigated HSEs compared to human SC. Previous studies show that a reduced free fatty acid content cannot explain this phenomenon, since a reduction in the free fatty acid level increases the temperature at which a liquid phase is formed [50]. However, a reduced chain length

of the free fatty acids or the presence of unsaturated chains may contribute to the decrease in transition temperature [48].

Optimization of the barrier properties of HSEs

The presented results show that the increased permeability of the investigated HSEs is likely caused by an increased conformational disordering of the lipids compared to the lipids in human SC. Furthermore, we hypothesize that a higher number of lipid lamellae between the cells may also reduce the SC barrier function. Whether the pronounced hexagonal packing also plays a role is not clear yet, but will be subject of future research. The change in lipid profile compared to native human SC indicates that the lipid metabolism in these HSEs differs from native human skin. Each HSE is generated under the same incubator conditions, but still shows (slight) differences in their lipid composition. Additionally, our in-house HSEs have an improved SC lipid composition and lamellar organization compared to the commercially available HSEs studied so far [14]. Taken together this implies that factors such as substrates used for HSE generation, culture media or other culture conditions can have an influence on the lipid metabolism in the viable epidermis resulting in changes in the SC barrier properties. Over the past years modulation of e.g. culture media or culture environment have improved epidermal development and consequently the lipid profiles and SC barrier formation of HSEs [15, 25, 35, 51]. Ponec *et al.* [35] showed that addition of vitamin C to the culture medium improved the lamellar body formation, extrusion and thus the intercellular lipid lamellae formation. The epidermal lipid metabolism was altered and resulted in an increased amount of ceramides AS and AP and detection of ceramide AH in the SC. Further optimization of culture media and culture conditions may lead to further improvements in the epidermal lipid metabolism in HSEs, such as an increase in the free fatty acid synthesis to induce the orthorhombic packing. Additionally, improvements made in the culture conditions may also enhance epidermal homeostasis, which in turn may lead to improved SC barrier properties.

Further optimization of the SC barrier properties of the presented HSEs, to resemble the SC barrier properties of native human skin more closely, will be subject of future research.

ACKNOWLEDGEMENTS

We would like to thank Dr. Maria Ponec for suggestions and discussions during our meetings and for proof reading the article. The Netherlands organization for Scientific Research is acknowledged for providing beam time at the ESRF in Grenoble. We would also like to thank Dr. W. Bras and co-workers for assistance at the ESRF. We are grateful to Evonik (Essen, Germany) for providing the ceramides. This research was financially supported by the Dutch Technology Foundation (STW; grant no. 7503).

REFERENCES

1. Brusselaers, N., Pirayesh, A., Hoeksema, H., Richters, C.D., Verbelen, J., Beele, H., Blot, S.I. and Monstrey, S. Skin replacement in burn wounds. J Trauma **68,** 490, 2010.
2. Shakespeare, P.G. The role of skin substitutes in the treatment of burn injuries. Clin Dermatol **23,** 413, 2005.
3. Supp, D.M. and Boyce, S.T. Engineered skin substitutes: practices and potentials. Clin Dermatol **23,** 403, 2005.
4. Alepee, N., Tornier, C., Robert, C., Amsellem, C., Roux, M.H., Doucet, O., Pachot, J., Meloni, M. and de Brugerolle de Fraissinette, A. A catch-up validation study on reconstructed human epidermis (SkinEthic RHE) for full replacement of the Draize skin irritation test. Toxicol In Vitro **24,** 257, 2009.
5. Gibbs, S. In vitro irritation models and immune reactions. Skin Pharmacol Physiol **22,** 103, 2009.
6. Netzlaff, F., Lehr, C.M., Wertz, P.W. and Schaefer, U.F. The human epidermis models EpiSkin, SkinEthic and EpiDerm: an evaluation of morphology and their suitability for testing phototoxicity, irritancy, corrosivity, and substance transport. Eur J Pharm Biopharm **60,** 167, 2005.
7. El Ghalbzouri, A., Siamari, R., Willemze, R. and Ponec, M. Leiden reconstructed human epidermal model as a tool for the evaluation of the skin corrosion and irritation potential according to the ECVAM guidelines. Toxicol In Vitro **22,** 1311, 2008.
8. Carlson, M.W., Alt-Holland, A., Egles, C. and Garlick, J.A. Three-dimensional tissue models of normal and diseased skin. Curr Protoc Cell Biol **Chapter 19,** Unit 19 9, 2008.
9. Engelhart, K., El Hindi, T., Biesalski, H.K. and Pfitzner, I. In vitro reproduction of clinical hallmarks of eczematous dermatitis in organotypic skin models. Arch Dermatol Res **297,** 1, 2005.
10. Garlick, J.A. Engineering skin to study human disease--tissue models for cancer biology and wound repair. Adv Biochem Eng Biotechnol **103,** 207, 2007.
11. Mildner, M., Jin, J., Eckhart, L., Kezic, S., Gruber, F., Barresi, C., Stremnitzer, C., Buchberger, M., Mlitz, V., Ballaun, C., Sterniczky, B., Fodinger, D. and Tschachler, E. Knockdown of filaggrin impairs diffusion barrier function and increases UV sensitivity in a human skin model. J Invest Dermatol **130,** 2286, 2010.
12. Boelsma, E., Gibbs, S., Faller, C. and Ponec, M. Characterization and comparison of reconstructed skin models: morphological and immunohistochemical evaluation. Acta Derm Venereol **80,** 82, 2000.

13. El-Ghalbzouri, A., Gibbs, S., Lamme, E., Van Blitterswijk, C.A. and Ponec, M. Effect of fibroblasts on epidermal regeneration. Br J Dermatol **147,** 230, 2002.
14. Ponec, M., Boelsma, E., Weerheim, A., Mulder, A., Bouwstra, J. and Mommaas, M. Lipid and ultrastructural characterization of reconstructed skin models. Int J Pharm **203,** 211, 2000.
15. El Ghalbzouri, A., Lamme, E. and Ponec, M. Crucial role of fibroblasts in regulating epidermal morphogenesis. Cell Tissue Res **310,** 189, 2002.
16. Boehnke, K., Mirancea, N., Pavesio, A., Fusenig, N.E., Boukamp, P. and Stark, H.J. Effects of fibroblasts and microenvironment on epidermal regeneration and tissue function in long-term skin equivalents. Eur J Cell Biol **86,** 731, 2007.
17. Stark, H.J., Boehnke, K., Mirancea, N., Willhauck, M.J., Pavesio, A., Fusenig, N.E. and Boukamp, P. Epidermal homeostasis in long-term scaffold-enforced skin equivalents. J Investig Dermatol Symp Proc **11,** 93, 2006.
18. Bouwstra, J., Pilgram, G., Gooris, G., Koerten, H. and Ponec, M. New aspects of the skin barrier organization. Skin Pharmacol Appl Skin Physiol **14 Suppl 1,** 52, 2001.
19. White, S.H., Mirejovsky, D. and King, G.I. Structure of lamellar lipid domains and corneocyte envelopes of murine stratum corneum. An X-ray diffraction study. Biochemistry **27,** 3725, 1988.
20. McIntosh, T.J., Stewart, M.E. and Downing, D.T. X-ray diffraction analysis of isolated skin lipids: reconstitution of intercellular lipid domains. Biochemistry **35,** 3649, 1996.
21. Bouwstra, J.A., Gooris, G.S., van der Spek, J.A. and Bras, W. Structural investigations of human stratum corneum by small-angle X-ray scattering. J Invest Dermatol **97,** 1005, 1991.
22. Bouwstra, J.A., Gooris, G.S., Dubbelaar, F.E. and Ponec, M. Phase behavior of lipid mixtures based on human ceramides: coexistence of crystalline and liquid phases. J Lipid Res **42,** 1759, 2001.
23. Goldsmith, L.A. and Baden, H.P. Uniquely oriented epidermal lipid. Nature **225,** 1052, 1970.
24. Damien, F. and Boncheva, M. The extent of orthorhombic lipid phases in the stratum corneum determines the barrier efficiency of human skin in vivo. J Invest Dermatol **130,** 611, 2010.
25. Batheja, P., Song, Y., Wertz, P. and Michniak-Kohn, B. Effects of growth conditions on the barrier properties of a human skin equivalent. Pharm Res **26,** 1689, 2009.
26. Schmook, F.P., Meingassner, J.G. and Billich, A. Comparison of human skin or epidermis models with human and animal skin in in-vitro percutaneous absorption. Int J Pharm **215,** 51, 2001.

27. Netzlaff, F., Kaca, M., Bock, U., Haltner-Ukomadu, E., Meiers, P., Lehr, C.M. and Schaefer, U.F. Permeability of the reconstructed human epidermis model Episkin in comparison to various human skin preparations. Eur J Pharm Biopharm **66,** 127, 2007.
28. Schafer-Korting, M., Bock, U., Diembeck, W., Dusing, H.J., Gamer, A., Haltner-Ukomadu, E., Hoffmann, C., Kaca, M., Kamp, H., Kersen, S., Kietzmann, M., Korting, H.C., Krachter, H.U., Lehr, C.M., Liebsch, M., Mehling, A., Muller-Goymann, C., Netzlaff, F., Niedorf, F., Rubbelke, M.K., Schafer, U., Schmidt, E., Schreiber, S., Spielmann, H., Vuia, A. and Weimer, M. The use of reconstructed human epidermis for skin absorption testing: Results of the validation study. Altern Lab Anim **36,** 161, 2008.
29. Asbill, C., Kim, N., El-Kattan, A., Creek, K., Wertz, P. and Michniak, B. Evaluation of a human bio-engineered skin equivalent for drug permeation studies. Pharm Res **17,** 1092, 2000.
30. Ackermann, K., Borgia, S.L., Korting, H.C., Mewes, K.R. and Schafer-Korting, M. The Phenion full-thickness skin model for percutaneous absorption testing. Skin Pharmacol Physiol **23,** 105, 2010.
31. Marjukka Suhonen, T., Pasonen-Seppanen, S., Kirjavainen, M., Tammi, M., Tammi, R. and Urtti, A. Epidermal cell culture model derived from rat keratinocytes with permeability characteristics comparable to human cadaver skin. Eur J Pharm Sci **20,** 107, 2003.
32. Zghoul, N., Fuchs, R., Lehr, C.M. and Schaefer, U.F. Reconstructed skin equivalents for assessing percutaneous drug absorption from pharmaceutical formulations. Altex **18,** 103, 2001.
33. Gibbs, S., Vicanova, J., Bouwstra, J., Valstar, D., Kempenaar, J. and Ponec, M. Culture of reconstructed epidermis in a defined medium at 33 degrees C shows a delayed epidermal maturation, prolonged lifespan and improved stratum corneum. Arch Dermatol Res **289,** 585, 1997.
34. Kennedy, A.H., Golden, G.M., Gay, C.L., Guy, R.H., Francoeur, M.L. and Mak, V.H. Stratum corneum lipids of human epidermal keratinocyte air-liquid cultures: implications for barrier function. Pharm Res **13,** 1162, 1996.
35. Ponec, M., Weerheim, A., Kempenaar, J., Mulder, A., Gooris, G.S., Bouwstra, J. and Mommaas, A.M. The formation of competent barrier lipids in reconstructed human epidermis requires the presence of vitamin C. J Invest Dermatol **109,** 348, 1997.
36. Pappinen, S., Hermansson, M., Kuntsche, J., Somerharju, P., Wertz, P., Urtti, A. and Suhonen, M. Comparison of rat epidermal keratinocyte organotypic culture (ROC) with

intact human skin: lipid composition and thermal phase behavior of the stratum corneum. Biochim Biophys Acta **1778,** 824, 2008.

37. Bouwstra, J.A., Gooris, G.S., Weerheim, A., Kempenaar, J. and Ponec, M. Characterization of stratum corneum structure in reconstructed epidermis by X-ray diffraction. J Lipid Res **36,** 496, 1995.
38. El Ghalbzouri, A., Commandeur, S., Rietveld, M.H., Mulder, A.A. and Willemze, R. Replacement of animal-derived collagen matrix by human fibroblast-derived dermal matrix for human skin equivalent products. Biomaterials **30,** 71, 2009.
39. Bouwstra, J.A., Groenink, H.W., Kempenaar, J.A., Romeijn, S.G. and Ponec, M. Water distribution and natural moisturizer factor content in human skin equivalents are regulated by environmental relative humidity. J Invest Dermatol **128,** 378, 2008.
40. Thakoersing, V.S., Ponec, M. and Bouwstra, J.A. Generation of human skin equivalents under submerged conditions-mimicking the in utero environment. Tissue Eng Part A **16,** 1433, 2009.
41. De Jager, M., Groenink, W., Bielsa i Guivernau, R., Andersson, E., Angelova, N., Ponec, M. and Bouwstra, J. A novel in vitro percutaneous penetration model: evaluation of barrier properties with p-aminobenzoic acid and two of its derivatives. Pharm Res **23,** 951, 2006.
42. Bligh, E.G. and Dyer, W.J. A rapid method of total lipid extraction and purification. Can J Biochem Physiol **37,** 911, 1959.
43. Motta, S., Monti, M., Sesana, S., Caputo, R., Carelli, S. and Ghidoni, R. Ceramide composition of the psoriatic scale. Biochim Biophys Acta **1182,** 147, 1993.
44. Masukawa, Y., Narita, H., Shimizu, E., Kondo, N., Sugai, Y., Oba, T., Homma, R., Ishikawa, J., Takagi, Y., Kitahara, T., Takema, Y. and Kita, K. Characterization of overall ceramide species in human stratum corneum. J Lipid Res **49,** 1466, 2008.
45. Caussin, J., Gooris, G.S., Janssens, M. and Bouwstra, J.A. Lipid organization in human and porcine stratum corneum differs widely, while lipid mixtures with porcine ceramides model human stratum corneum lipid organization very closely. Biochim Biophys Acta **1778,** 1472, 2008.
46. Cheng, T., Tjabringa, G.S., van Vlijmen-Willems, I.M., Hitomi, K., van Erp, P.E., Schalkwijk, J. and Zeeuwen, P.L. The cystatin M/E-controlled pathway of skin barrier formation: expression of its key components in psoriasis and atopic dermatitis. Br J Dermatol **161,** 253, 2009.
47. Bouwstra, J.A., Gooris, G.S., Bras, W. and Talsma, H. Small angle X-ray scattering: possibilities and limitations in characterization of vesicles. Chem Phys Lipids **64,** 83, 1993.

48. Janssens, M., Gooris, G.S. and Bouwstra, J.A. Infrared spectroscopy studies of mixtures prepared with synthetic ceramides varying in head group architecture: coexistence of liquid and crystalline phases. Biochim Biophys Acta **1788,** 732, 2009.
49. Groen, D., Poole, D.S., Gooris, G.S. and Bouwstra, J.A. Is an orthorhombic lateral packing and a proper lamellar organization important for the skin barrier function? Biochim Biophys Acta 2010.
50. Gooris, G.S. and Bouwstra, J.A. Infrared spectroscopic study of stratum corneum model membranes prepared from human ceramides, cholesterol, and fatty acids. Biophys J **92,** 2785, 2007.
51. Mak, V.H., Cumpstone, M.B., Kennedy, A.H., Harmon, C.S., Guy, R.H. and Potts, R.O. Barrier function of human keratinocyte cultures grown at the air-liquid interface. J Invest Dermatol **96,** 323, 1991.

4

NATURE *VS* NURTURE: DOES HUMAN SKIN MAINTAIN ITS BARRIER PROPERTIES *IN VITRO*?

Varsha S. Thakoersing[1], Mogbekeloluwa O. Danso[1], Aat Mulder[1], Gerrit Gooris[1], Abdoelwaheb El Ghalbzouri[2], Joke A. Bouwstra[1]

[1]Department of Drug Delivery Technology, Leiden Amsterdam Center for Drug Research, Leiden University, Leiden, 2333 CC, The Netherlands.

[2] Department of Dermatology, Leiden University Medical Center, Leiden, 2333 ZA, The Netherlands

Accepted for publication in Experimental Dermatology

ABSTRACT

Human skin equivalents (HSEs) mimic human skin closely, but show differences in their stratum corneum (SC) lipid properties. The aim of this study was to determine whether isolation of primary cells, which is needed to generate HSEs, influences the SC lipid properties of HSEs. For this purpose we expanded explants of intact full thickness human skin and isolated epidermal sheets *in vitro*. We investigated whether their outgrowths maintain barrier properties of human skin. The results reveal that the outgrowths and human skin have a similar morphology and expression of several differentiation markers, except for an increased expression of keratin 16 and involucrin. The outgrowths show a decreased SC fatty acid content compared to human skin. Additionally, SC lipids of the outgrowths have a predominantly hexagonal packing, whereas human skin has the dense orthorhombic packing. Furthermore, the outgrowths have lipid lamellae with a slightly reduced periodicity compared to human skin. These results demonstrate that the outgrowths do not maintain all properties observed in human skin, indicating that changes in properties of HSEs are not caused by isolation of primary cells, but by culture conditions.

INTRODUCTION

The stratum corneum (SC) is the outermost layer of the epidermis and consists of dead cells which are embedded in a lipid matrix. This lipid matrix plays a crucial role in the skin permeability barrier. Native human SC contains three main lipid classes which are cholesterol, free fatty acids and ceramides. In human SC the lipids form two lamellar phases with a repeat distance of approximately 13 nm and 6 nm, referred to as the long periodicity phase (LPP) and short periodicity phase (SPP), respectively [1-4]. The lipid organization within the lipid lamellae is referred to as the lateral lipid packing. In native human SC the lipids are mainly arranged in a dense orthorhombic packing [2, 5-7]. A schematic representation of the lipid organization in native human SC is provided in figure 1.

We have previously demonstrated that three different in-house human skin equivalents (HSEs) showed an increased permeability for benzocaine, even though they showed a comparable morphology and protein expression as native human skin [8]. To understand why these HSEs showed an increased permeability for benzocaine, the SC lipid properties of each HSE was investigated thoroughly. We found that two of the HSEs had a reduced free fatty acid content. Furthermore, all HSEs showed the presence of the LPP, but had a hexagonal lateral packing rather than the orthorhombic packing that is observed in human skin. In the present study we determined whether the observed differences in SC lipid properties between the HSEs and native human skin are caused by cell isolation procedures. In order to engineer HSEs primary cells of fibroblasts and keratinocytes are isolated from human skin by enzymes. These cells are cultured and subsequently used to generate HSEs. This procedure may disable the isolated cells to form a proper SC barrier that is found *in vivo*. We used full thickness (FT) human skin explants and human epidermal sheet (ES) explants and expanded them *in vitro*. In the FT explants the native tissue is left intact, whereas ES explants are obtained by enzymatic separation of the epidermis from the dermis. These skin cultures were generated under the same conditions as used for the previously investigated in-

house HSEs. The SC lipid properties of the FT explants, ES explants and the outgrowths that developed from these explants were evaluated to determine whether tissue dissociation is responsible for the altered SC lipid properties of HSEs.

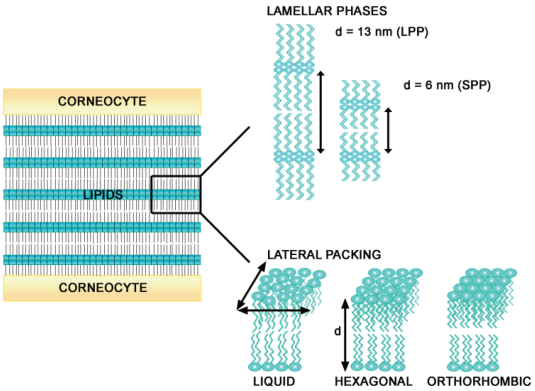

Figure 1. Human SC lipids are organized into lipid lamellae parallel to the skin surface. The repeat distance (d) is the distance over which the molecular structure is repeated. Native human SC lipids are arranged into two lamellar phases, the long periodicity phase (LPP) and the short periodicity phase (SPP), with repeat distances of around 13 and 6 nm, respectively. The lateral packing discloses information about the density of the lipids within the lipid lamellae. The liquid packing is the least dense packing, while the orthorhombic lateral packing has the highest density of lipids. In native human SC the lipids are mostly arranged in the orthorhombic packing.

MATERIALS AND METHODS

Generation of explant cultures

Dermal equivalents consisting of fibroblast-populated collagen matrices were generated as described previously [8-10]. Human skin used for the experiments was obtained from adults undergoing cosmetic mammary or abdomen surgery. The Declaration of Helsinki principles were followed when using human tissue.

Full thickness cultures (FT explants): 4 mm fat free punch biopsies of full thickness (FT) skin were gently pushed into the dermal equivalents on the same day the dermal equivalents were prepared. The cultures were directly grown at the air-liquid interface and were nourished with a 3:1 mixture of DMEM (Invitrogen, Leek, The Netherlands) and Ham's F12 (Invitrogen, Leek, The Netherlands) supplemented with 1% penicillin/streptomycin solution (Sigma), 0.5 μM hydrocortisone (Sigma), 1 μM isoproterenol (Sigma), 0.5 μg/mL insulin (Sigma), 0.053 μM selenious acid (Johnson Matthey, Maastricht, The Netherlands), 10 mM L-serine (Sigma), 10 μM L-carnitine (Sigma), 1 μM α-tocopherol acetate (Sigma), 25 mM vitamin C (Sigma) and a lipid mixture consisting of 7 μM arachidonic acid (Sigma), 30 μM linoleic acid (Sigma) and 25 μM palmitic acid (Sigma). The culture medium was refreshed twice a week. The cultures were grown for approximately 16 days at 37°C, 93% relative humidity and 8% CO_2.

Epidermal sheet cultures (ES explants): 4 mm punch biopsies of fat free full thickness human skin were incubated overnight at 4°C in a dispase II solution (2.4 AU/mL; Roche, Almere, The Netherlands) to separate the epidermis from the dermis. The obtained epidermal sheets (ES) were placed on the dermal equivalents one day after preparation of the dermal equivalents. The ES explant cultures were fed with the same media and were generated under the same conditions as the FT explant cultures.

Morphology and immunofluorescent staining

Harvested cultures were formalin-fixed and embedded in paraffin. 5 μm sections were cut, deparaffinized and rehydrated in preparation for haematoxylin and eosin staining. For immunofluorescent staining frozen sections were fixed with acetone. The sections were incubated at room temperature with the first antibody and the secondary antibody for 60 minutes each. The sections were enclosed with DAPI-Vectashield (Vector Laboratories, Peterborough, UK). The primary antibodies used were cytokeratin 10 (1:50) (Neomarkers, Fremont, CA), cytokeratin 16 (1:5)

(Neomarkers, Fremont, CA), filaggrin (1:75) (Neomarkers, Fremont, CA), involucrin (1:600) (Sanbio, Uden, The Netherlands), loricrin (1:400) (Covance, Princeton, NJ) and aquaporin 3 (1:50) (Santa Cruz Biotechnology, Santa Cruz, CA). The secondary antibodies used were Rhodamine conjugated bovine anti-mouse (Santa Cruz Biotechnology, Santa Cruz, CA), FITC conjugated donkey anti-goat (Jackson ImmunoResearch Europe, Suffolk, UK) and Texas Red conjugated chicken anti-rabbit (Santa Cruz Biotechnology, Santa Cruz, CA) in a 1:100 dilution.

Counting stratum corneum layers

HSEs were fixed in Tissue Tek O.C.T. compound (Sakura Finetek Europe, Zoeterwoude, The Netherlands) and frozen in liquid nitrogen. 5 μm sections were stained with a 1% (w/v) safranin (Sigma) solution for 1 minute followed by 20 minutes incubation with a 2% (w/v) KOH solution to allow the corneocytes to swell. Images of the sections were taken with a digital camera (Carl Zeiss axioskop, Jena, Germany) connected to a microscope. The number of SC layers of at least three different explants and outgrowths were counted. The data represent the mean and standard deviation.

Extraction and analysis of stratum corneum lipids

SC of native human skin, epidermal sheets and SC of the outgrowths of the FT and ES explant cultures were isolated by overnight incubation with a 0.1% trypsin solution at 4ºC followed by incubation at 37ºC for 1 hour. The lipid extracts of 2-4 outgrowth cultures from the same skin donor were pooled for lipid analysis. The SC lipid composition of the FT and ES explants could not be determined, because there was not enough material to extract. The extracted lipids were fractionated with high performance thin layer chromatography (HPTLC) using the solvent system described elsewhere [11]. The extracted ceramides are named according to the nomenclature of Motta *et al.* [12] and Masukawa *et al* [13]: ceramides with a sphingosine (S), phytosphingosine (P), 6-hydroxysphingosine (H) or dihydrosphingosine (dS)

base are linked to an esterified ω-hydroxy (EO), α-hydroxy (A) or non-hydroxy (N) fatty acid.

Fourier transform infrared spectroscopy (FTIR) and small angle x-ray diffraction (SAXD)

Isolated SC sheets were hydrated for 24 hours over a 27% NaBr solution (achieving a relative humidity level of 80%) at room temperature prior to the measurements. For FTIR measurements the hydrated SC sheets were sandwiched between AgBr windows and mounted into a specially designed heating/cooling cell. The IR spectra in the frequency range of 600-4000 cm^{-1} were obtained with a Varian 670-IR FTIR (Agilent Technologies, Santa Clara, CA) equipped with a mercury-cadmium-telluride detector. Each spectrum was collected for 4 minutes at a 1ºC interval within a temperature range of 0-90ºC. Each spectrum was acquired from the co-addition of 248 scans with a resolution of 1 cm^{-1}.

SAXD measurements were performed at the European Synchrotron Radiation Facility (ESRF) in Grenoble at station BM26B. The scattering intensity I (arbitrary units) was plotted against the scattering vector q (nm^{-1}). The repeat distance of a lamellar phase was calculated from the position of the diffraction peaks as described earlier [8]. At least 3 samples of the FT and ES explants, FT and ES outgrowths and human SC were examined with FTIR and SAXD. SAXD and FTIR data represent the mean and standard deviation.

Visualization of lipid lamellae

Approximately 1 mm^2 of human skin, explants and outgrowths were fixed as described previously [8]. Uranyl-acetate and lead hydroxide were used to stain ultrathin sections, which were visualized with a Fei Tecnai 12 Twin (Spirit) (Fei Europa, Eindhoven, The Netherlands) transmission electron microscope. At least 2 samples of each explant type and their corresponding outgrowths were examined and 10 to 51 images per sample were made.

RESULTS

Explants and their outgrowths have a similar morphology as native human skin

After 16 days of culturing, both FT and ES explants maintain a morphology that is comparable to native human skin (figure 2 and 3). The morphology of the outgrowths was investigated in two regions: 1) the centre of the outgrowth, which represents the main part of the outgrowth and 2) the periphery of the outgrowth. At the centre of the FT and ES outgrowths a completely stratified epidermis could be observed. Sometimes a SC was observed at the periphery of the outgrowths, while in other cultures a developing epidermis could be detected, indicated by the absence of a SC. No difference in morphology could be detected between the outgrowths of the FT and ES explants. Safranin red staining revealed that the FT and ES explants had a thicker SC than the majority of the outgrowth that developed from the explants (micrographs not shown). The FT and ES explants on average had 23.8 $\pm$ 2.8 and 32.7 $\pm$ 12.7 SC layers, while the centre of the FT and ES outgrowths had 11.0 $\pm$ 4.1 and 11.3 $\pm$ 1.5 SC layers, respectively. Native human skin has 11.4 $\pm$ 1.2 SC layers, which is similar to the number of SC layers observed for the FT and ES outgrowths.

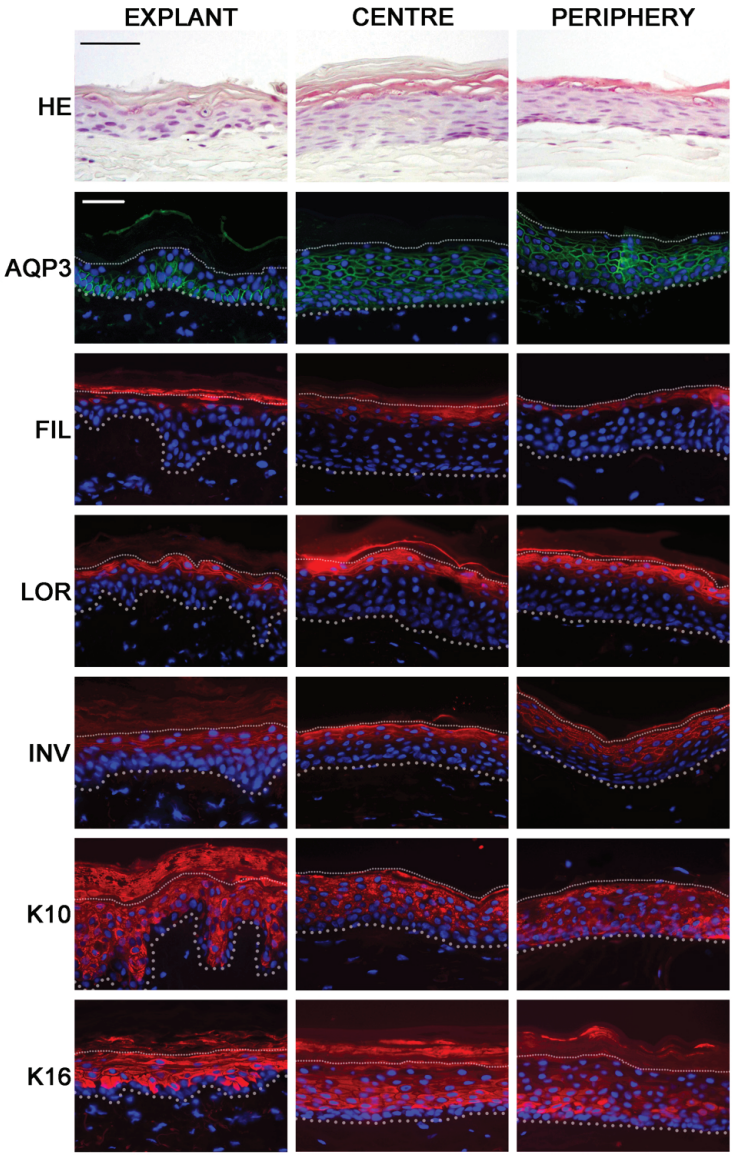

Figure 2. Haematoxylin and eosin (HE) and immunofluorescent stained sections showing aquaporin 3 (AQP3), filaggrin (FIL), loricrin (LOR), involucrin (INV), keratin 10 (K10) and keratin 16 (K16) expression in the FT explant and different regions of its outgrowth. Dotted lines indicate the dermal-epidermal border and stratum granulosum-SC border. HE and immunofluorescent images 20x magnification. Scale bars represent 50 μm.

Explants and their outgrowths show similar expression of differentiation markers

The expression pattern of several differentiation markers was investigated to determine whether the differentiation process of the explants and their outgrowths differs from native human skin (figure 2 and 3). The FT explant and its outgrowth at the centre and periphery mostly showed similar expression of the water/glycerol transporting channel aquaporin 3, filaggrin, loricrin and keratin 10 as native human skin. In native human skin involucrin is expressed in the granular layer, whereas keratin 16 expression is absent. In the FT explant and its entire outgrowth, however, keratin 16 is expressed throughout the suprabasal layers and involucrin is expressed in the granular layer and in the upper spinous layers.

The ES explant and the different regions of the outgrowth show a similar expression of most of the investigated differentiation markers. They show a suprabasal expression of involucrin and keratin 16, while expression of loricrin can be detected in the upper spinous layers and in the stratum granulosum. At the periphery of the outgrowth loricrin is expressed in the whole epidermis. In the ES outgrowth filaggrin expression is only detected in the stratum granulosum, while the ES explant also shows filaggrin expression in the upper spinous layers. The expression of aquaporin 3 and keratin 10 is similar between the ES explant, its outgrowth and native human skin. From these results it is evident that the FT outgrowths show a more normalized expression pattern of loricrin and involucrin compared to the ES outgrowths.

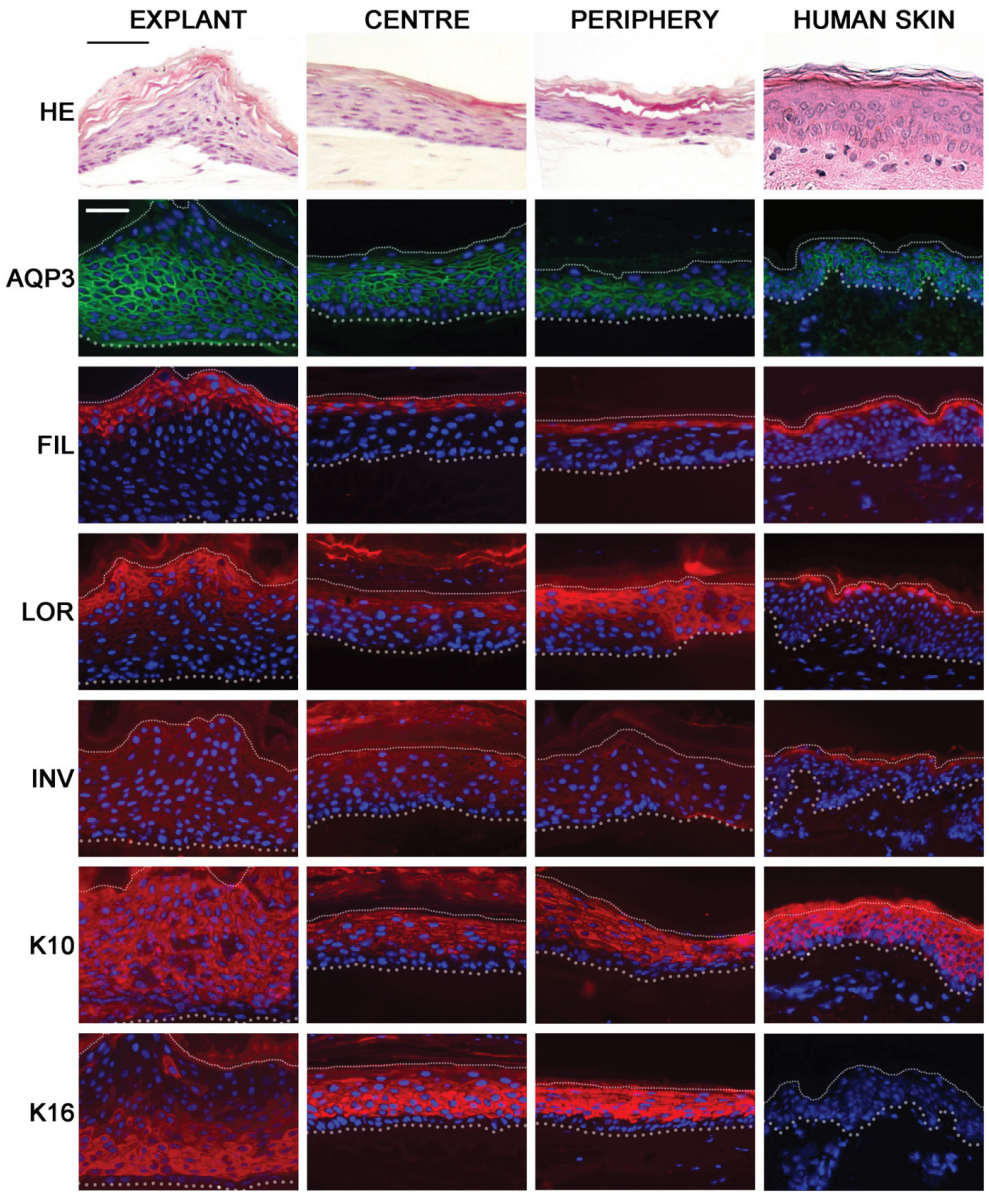

Figure 3. Haematoxylin and eosin (HE) and immunofluorescent stained sections showing aquaporin 3 (AQP3), filaggrin (FIL), loricrin (LOR), involucrin (INV), keratin 10 (K10) and keratin 16 (K16) expression in the ES explant, its outgrowth and native human skin. Dotted lines indicate the dermal-epidermal border and stratum granulosum-SC border. HE and immunofluorescent images 20x magnification. Scale bars represent 50 μm.

The FT and ES outgrowths show the presence of all SC barrier lipid classes

After examining the differentiation status of the outgrowths, we determined whether the outgrowths maintained the SC lipid properties as observed in native human skin. Therefore, we investigated the SC lipid composition of the outgrowths of the FT and ES explants. The FT and ES outgrowths have similar lipid profiles and contain all lipid classes that are present in native human skin, namely cholesterol, free fatty acids and ceramides (figure 4). However, the most apolar fragment of the free fatty acids appears to be present in a relatively lower quantity in both outgrowths compared to native human skin, while ceramides EOS and EOH are present in relatively higher quantities. Dispase treatment (used to obtain the ES explant) has no effect on the SC lipid profiles (figure 4).

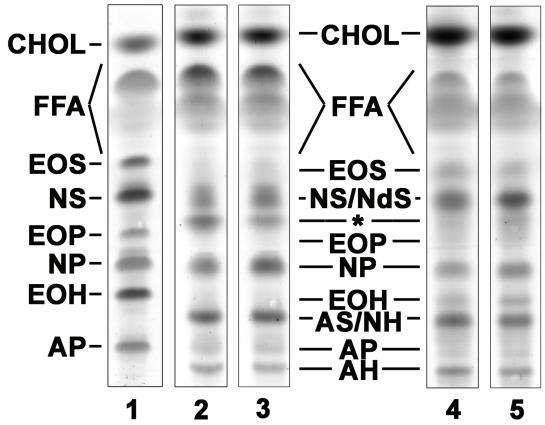

Figure 4. SC lipid profiles of native human skin obtained after trypsin digestion (lane 2), native human skin after dispase and trypsin digestion (lane 3), outgrowth of the FT explants (lane 4) and outgrowth of the ES explant (lane 5). The standards used to identify lipid classes are shown in lane 1. CHOL= cholesterol, FFA= free fatty acid, *= unidentified lipid. Ceramide nomenclature according to Motta *et al.* [12] and Masukawa *et al.*[13].

FT and ES outgrowths have a different lateral lipid organization compared to their respective explants

The lateral lipid organization in the SC of the FT and ES explants, their outgrowths and native human skin was examined by measuring the thermotropic response of the CH_2 rocking band in the FTIR spectrum (figure 5). An orthorhombic lipid packing can be recognized when the rocking bands consists of two peaks at 719 and 730 cm^{-1}, whereas a hexagonal lipid packing is characterized by a single peak at 719 cm^{-1}. Native human SC shows two strong peaks at 719 and 730 cm^{-1} at lower temperatures, indicating that the lipids mainly form an orthorhombic packing. Around 45.5ºC ± 4.4ºC a phase transition to a hexagonal packing, characterized by the presence of only a singlet at 719 cm^{-1}, is observed. The FT and ES explants show two vibrations at 719 and 730 cm^{-1} until 32.7ºC ± 4.6ºC and 32.7ºC ± 6.4ºC, respectively. However the peak intensity at 730 cm^{-1} is weaker than observed for native human SC. This indicates that the fraction of lipids forming an orthorhombic packing is less than in native human SC. The FT and ES outgrowths mainly show a strong peak at 719 cm^{-1} and a very weak shoulder at 730 cm^{-1}, which is only observed until a temperature of 11.0ºC ± 14.3ºC and 3.3 ± 5.8ºC, respectively. This indicates that the lipids are mainly organized in a hexagonal packing, but with the presence of some orthorhombic domains. This is different than observed for native human SC.

To determine at which temperatures the lipid domains transform into a liquid phase the CH_2 symmetric stretching frequency in the FTIR spectrum, which provides information about the conformational disorder, was investigated. When the SC lipids are organized in an ordered packing – the orthorhombic or hexagonal packing - the conformational disorder is low, reflected by CH_2 symmetric stretching frequencies below 2850 cm^{-1}. When the lipids are in a disordered packing - the liquid phase - the CH_2 symmetric stretching frequencies increase to 2852 cm^{-1} or higher values. As the order-disorder transition occurs in a temperature range, the

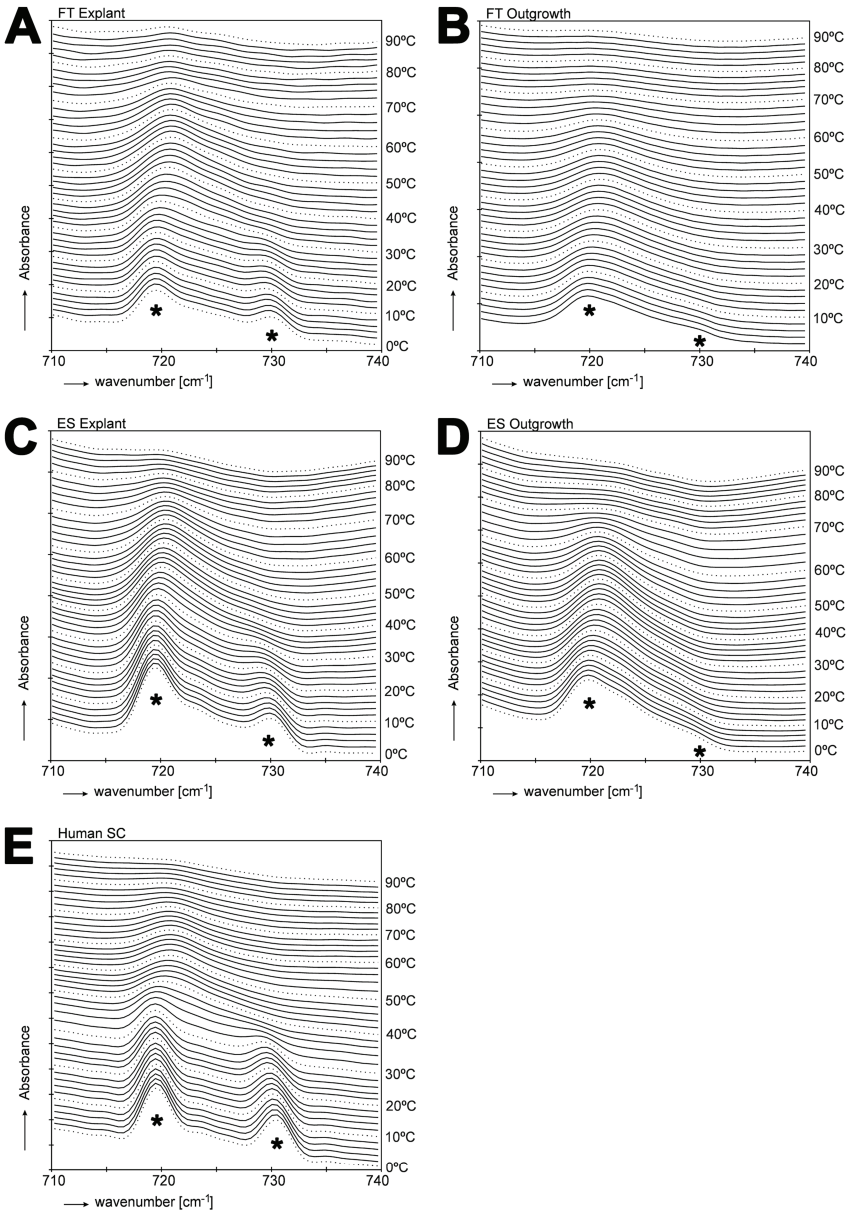

Figure 5. A, C, B and D: representative rocking vibrations in a temperature range from 0-90ºC in FT and ES explants and their outgrowths. The rocking vibrations of human SC are shown figure E. An orthorhombic packing is recognized by two contours at 719 and 730 cm^{-1}, whereas a hexagonal packing is indicated by a single contour at 719 cm^{-1}. * indicates the CH_2 rocking contours at 719 and 730 cm^{-1}.

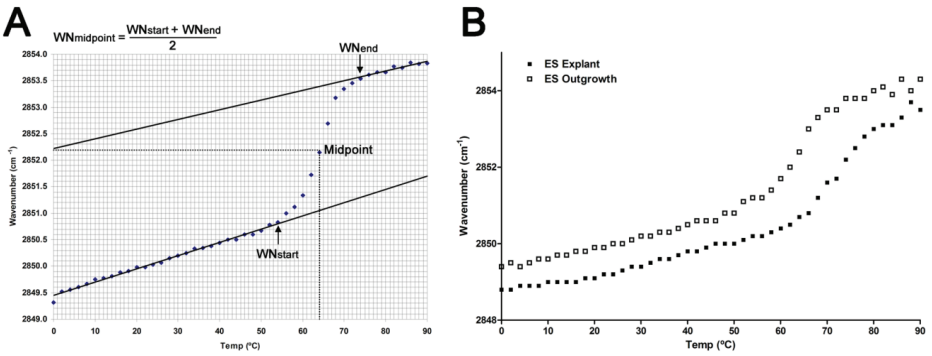

Sample	Midpoint Order-Disorder Transition	Symmetric Stretching (cm^{-1}) at 32ºC
FT Explants	63.7ºC ± 4.5ºC	2849.9 ± 0.2
ES Explants	66.7ºC ± 4.7ºC	2849.7 ± 0.2
FT Outgrowth	54.8ºC ± 8.0ºC	2850.6 ± 0.6
ES Outgrowth	59.3ºC ± 7.2ºC	2850.3 ± 0.2
Native HSC	76.8ºC ± 1.7ºC	2849.5 ± 0.1

Figure 6. A: the CH_2 symmetric stretching wavenumbers are plotted as function of the temperature. In this example the calculation is shown of the midpoint temperature of the order-disorder transition. $WN_{midpoint}$, WN_{start} and WN_{end} indicate the wavenumber corresponding to the midpoint, start and end of the order-disorder transition, respectively. B: an example is shown of the CH_2 symmetric stretching frequency as a function of temperature for an ES explant and its outgrowth. The higher symmetric stretching wavenumbers of the ES outgrowth compared to the explant illustrate that the ES outgrowth has an increased conformational disordering. Table: the order-disorder midpoint temperatures and the symmetric stretching frequency at 32ºC, which corresponds to the *in vivo* skin temperature, are shown for the FT explants, ES explants, FT outgrowths, ES outgrowths and native human SC. Data represent the mean and standard deviation of at least 3 samples.

midpoint temperature of this transition was determined for the FT and ES explants and their outgrowths and compared to native human skin. The table in figure 6 shows that the midpoint temperature of the steep shift in CH_2 symmetric stretching frequency of the order-disorder transition (an example profile is shown in figure 6A) occurs at lower temperatures in both explants compared to native human skin. This transition temperature is even lower in the outgrowths. These results clearly

show that the FT and ES explants and their outgrowths do not retain the same SC lipid properties as native human skin. We also observed that at temperatures ranging from 0ºC until the order-disorder transition the symmetric stretching CH_2 frequency of the outgrowths is higher compared to that of their respective explants and native human SC (figure 6B). This is indicative of an increased conformational disordering in the SC of the outgrowths.

FT and ES explants and their outgrowths show the presence of the LPP

The lamellar organization is an important determinant in the skin barrier function and was therefore examined in the FT and ES explants and their outgrowths. The SAXD profiles of the explants and their outgrowths show the presence of three diffraction peaks (figure 7) indicating the presence of only the LPP in the SC. The average repeat distance of the LPP in the FT and ES explants are 12.3 ± 0.2 nm and 12.1 ± 0.3 nm. The outgrowths of the FT and ES explants have a LPP with a repeat distance of 12.3 ± 0.3 nm and 11.7 ± 0.4 nm, respectively. The diffraction profiles of the explants and outgrowths also show the presence of crystalline cholesterol similar to human SC. Occasionally an additional peak with a q-value around q= 0.78 nm^{-1} could be observed in the SAXD profiles of the explants or outgrowths, which might be assigned to phase separated acylceramides [14]. In this and previous studies the diffraction profile of native human SC revealed the presence of both the SPP and the LPP (figure 7) [2]. The repeat distance of the LPP in human SC is around 13 nm, as published previously [2].

The lamellar lipid organization of the FT and ES explants and their outgrowths were visualized with transmission electron microscopy (figure 8). The FT and ES explants and their outgrowths show a similar lamellar body extrusion process at the stratum granulosum/SC interface as native human skin. The extruded lipids are subsequently neatly arranged into lipid lamellae. The lipid lamellae in the outgrowths are comparable to native human skin, but sometimes appear to have a higher number of intercellular lipid layers.

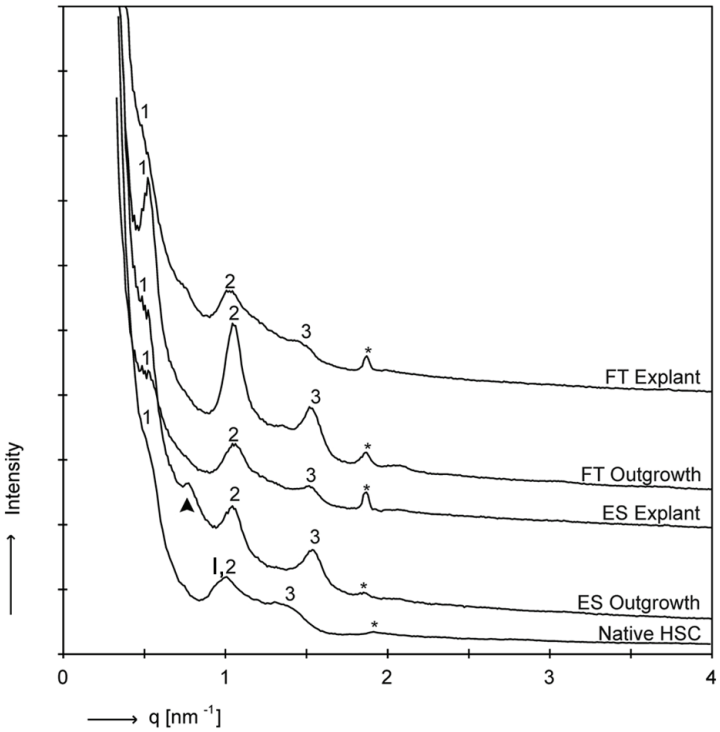

Figure 7. Example SAXD profiles of a FT and ES explant, their outgrowths and native human SC are shown. The first, second and third order diffraction peak of the LPP are indicated as 1, 2 and 3, respectively. Most probably the SPP (indicated by I) is also present in human SC, but the 1st order diffraction peak of the SPP is obscured by the 2nd order diffraction peak of the LPP. For this reason the repeat distance of the LPP or SPP in human SC cannot directly be calculated from the SAXD profile. The corresponding repeat distance of the LPP in the FT and ES explants and outgrowths of the FT and ES explants are 12.2 nm, 12.2 nm, 12.3 nm and 12.2 nm, respectively. The reflection indicated by * is attributed to phase separated crystalline cholesterol. The arrow head may indicate the presence of phase separated acylceramides.

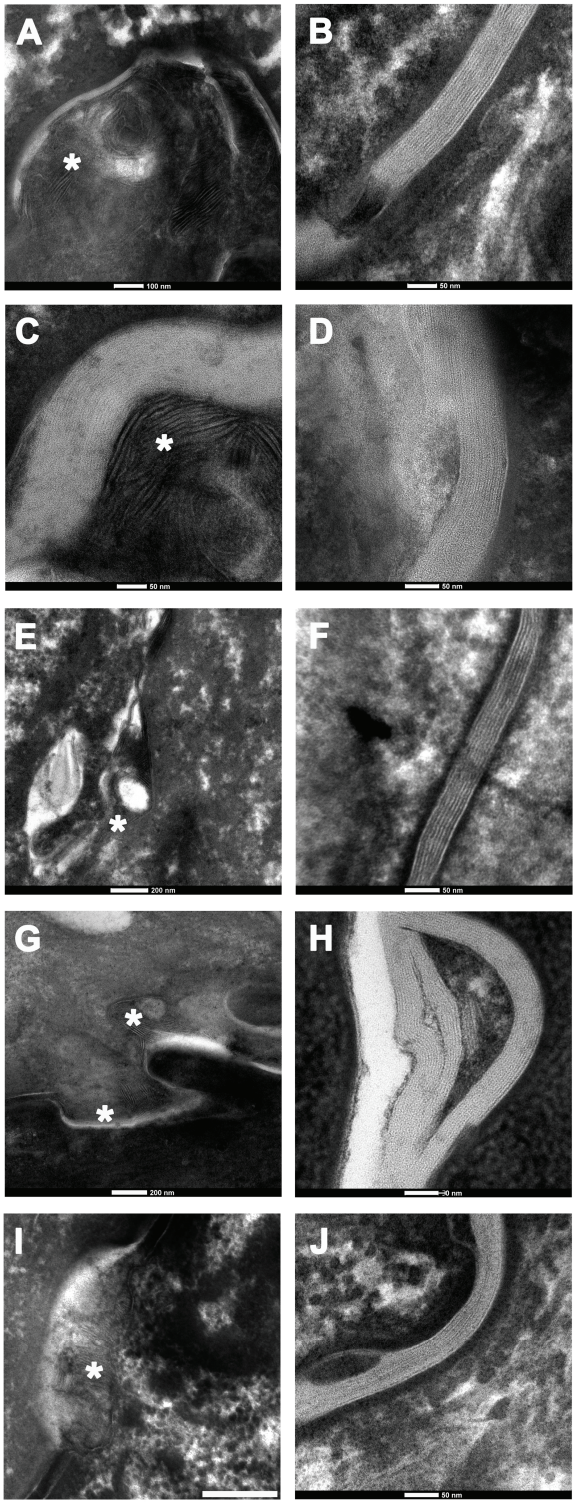

Figure 8. Figures a, c, e, g and i show the lamellar body extrusion process in the FT explant, FT outgrowth, ES explant, ES outgrowth and native human SC, respectively. Figures b, d, f, h and j show the arrangement of the extruded lipids in the SC in the FT explant, FT outgrowth, ES explant, ES outgrowth and native human SC, respectively. *= lamellar body. Figure a: scale bar represents 100 nm. Figures b, c, d, f, h, and j: scale bar represents 50 nm. Figures e, g and i: scale bar represents 200 nm.

DISCUSSION

The barrier properties of our previously investigated HSEs differ to some extent from native human skin [8]. In this study we determined whether the differences between the *in vitro* and *in vivo* barrier properties are caused by the isolation of keratinocytes prior to the generation of HSEs. The elevated expression of involucrin and/or loricrin indicate that the explants and their outgrowth are not in homeostasis [15, 16]. Additionally, the presence of keratin 16 in the explants and outgrowths indicates that the epidermis is in an activated state, since keratin 16 is only expressed in wounded or stressed skin [17-20]. The difference in expression of the investigated differentiation markers occasionally observed at the periphery of the outgrowths is due to the still developing epidermis, causing activation of the keratinocytes [10, 21]. The expression of keratin 16 and the premature expression of involucrin were also detected in our in-house HSEs [8].

The results reveal that the outgrowths contain relatively less free fatty acids, but higher levels of ceramides EOS and EOH compared to native skin. The decreased free fatty acid level was also observed in two in-house HSEs, while the increase in ceramide EOS was observed in all three investigated HSEs [8]. Examination of the lamellar lipid organization shows that in the FT and ES outgrowths the LPP is prominently present. Previous studies demonstrated that the formation of the LPP is promoted by increasing the level of acylceramides such as ceramide EOS [5]. The relatively higher ceramide EOS and EOH content in the SC of the outgrowths is therefore expected to enable the outgrowths to form only the LPP, similar as in the previously investigated HSEs [8].

The reduction of lipids forming an orthorhombic packing in the FT and ES outgrowths compared to their respective explants demonstrates that the outgrowths do not maintain the same lipid organization as the native tissue. The mainly hexagonal packing that is detected in the outgrowths may be caused by the reduced free fatty acid content as observed in previous studies [1]. However, the reduced fatty acid level cannot explain the reduction in temperature of the

crystalline to liquid phase transition and the increased symmetric stretching frequency at 32ºC. Other factors, such as an increased presence of short-chain free fatty acids and/or unsaturated free fatty acids may play a role in the decreased order-disorder midpoint temperature. All these differences were also detected in the previously examined HSEs [8]. Additionally, HSEs developed by other groups or commercially available models also have a reduced SC free fatty acid content, a mainly hexagonal packing and generally show the presence of the LPP [22-28]. It should be noted that the SC lipid properties of commercially available models were investigated several years ago. The current status of their SC lipid properties is therefore not known.

All our observations suggests that under the used culture conditions native human skin will not be able to form a SC with lipid properties similar to that observed *in vivo*. Moreover, the outgrowths that develop from human skin will mimic the lipid composition and organization of the previously investigated HSEs. This indicates that the SC lipid properties or epidermal morphogenesis of our in-house HSEs are not noticeably affected by the isolation procedure of primary cells, but are affected by the culture medium and/or environmental factors. This most probably also applies to other developed HSEs considering that they show some similar SC lipid properties as our in-house HSEs. The results of these studies therefore direct future research by offering the opportunity to further improve the culture medium and environmental factors to establish HSEs with improved epidermal homeostasis and SC barrier properties. The reduction in free fatty acid content and increase in acylceramide species in the FT and ES outgrowths and in HSEs demonstrate that the culture conditions lead to alterations in epidermal lipid metabolism. The altered lipid metabolism is also indicated by the presence of diacyl- and triacylglycerides in the SC of the HSEs and FT and ES outgrowths (data not shown). The specific cause for the different epidermal lipid metabolism remains to be established. However, it is known that peroxisome proliferator-activated receptors (PPARs) play a central role in the regulation of lipid homeostasis and differentiation in

human keratinocytes. These PPARs are activated by endogenous fatty acids and their derivatives [29-32]. Specifically polyunsaturated fatty acids such as arachidonic and linoleic acid are efficient activators of two PPAR isoforms, namely PPARα and PPARβ/δ [33]. The level of linoleic acid, arachidonic acid and palmitic acid in the culture media may therefore lead to a change in the activation of the various PPAR isoforms and subsequent alterations in epidermal homeostasis and SC lipid properties. Optimization of the levels of these lipids is a focus of future research.

The FT and ES explant cultures presented in this study may also serve as a model to study the wound healing process of the skin. These models can be used to determine the expression of basement membrane components and integrin subunits that play an important role in the re-epithilization process. Additionally, these models can be used to determine which exogenous factors can accelerate or improve epithelial cell migration.

ACKNOWLEDGEMENTS

VST designed the research study, performed the research, analyzed the data and wrote the paper. MOD, AM and GG performed the research, AEG and JAB designed the research study, supported the analysis of the data and wrote the paper. The authors thank Marion Rietveld and Ida Rasmussen for their technical assistance and Maria Ponec for her suggestions during the meetings. The Netherlands organization for Scientific Research is acknowledged for providing beam time at the ESRF in Grenoble. We are also grateful for Dr W. Bras and co-workers for assistance at the ESRF. We like to thank Evonik (Essen, Germany) for providing the ceramides. This research was financially supported by the Dutch Technology Foundation STW (grant no. 7503).

REFERENCES

1. Bouwstra, J., Pilgram, G., Gooris, G., Koerten, H. and Ponec, M. New aspects of the skin barrier organization. Skin Pharmacol Appl Skin Physiol **14 Suppl 1,** 52, 2001.
2. Bouwstra, J.A., Gooris, G.S., van der Spek, J.A. and Bras, W. Structural investigations of human stratum corneum by small-angle X-ray scattering. J Invest Dermatol **97,** 1005, 1991.
3. McIntosh, T.J., Stewart, M.E. and Downing, D.T. X-ray diffraction analysis of isolated skin lipids: reconstitution of intercellular lipid domains. Biochemistry **35,** 3649, 1996.
4. White, S.H., Mirejovsky, D. and King, G.I. Structure of lamellar lipid domains and corneocyte envelopes of murine stratum corneum. An X-ray diffraction study. Biochemistry **27,** 3725, 1988.
5. Bouwstra, J.A., Gooris, G.S., Dubbelaar, F.E. and Ponec, M. Phase behavior of lipid mixtures based on human ceramides: coexistence of crystalline and liquid phases. J Lipid Res **42,** 1759, 2001.
6. Goldsmith, L.A. and Baden, H.P. Uniquely oriented epidermal lipid. Nature **225,** 1052, 1970.
7. Damien, F. and Boncheva, M. The extent of orthorhombic lipid phases in the stratum corneum determines the barrier efficiency of human skin in vivo. J Invest Dermatol **130,** 611, 2010.
8. Thakoersing, V.S., Gooris, G., Mulder, A.A., Rietveld, M., El Ghalbzouri, A. and Bouwstra, J.A. Unravelling Barrier Properties of Three Different In-House Human Skin Equivalents. Tissue Eng Part C Methods **In press,** In press, 2011.
9. Bouwstra, J.A., Groenink, H.W., Kempenaar, J.A., Romeijn, S.G. and Ponec, M. Water distribution and natural moisturizer factor content in human skin equivalents are regulated by environmental relative humidity. J Invest Dermatol **128,** 378, 2008.
10. El Ghalbzouri, A., Lamme, E. and Ponec, M. Crucial role of fibroblasts in regulating epidermal morphogenesis. Cell Tissue Res **310,** 189, 2002.
11. Thakoersing, V.S., Ponec, M. and Bouwstra, J.A. Generation of human skin equivalents under submerged conditions-mimicking the in utero environment. Tissue Eng Part A **16,** 1433, 2010.
12. Motta, S., Monti, M., Sesana, S., Caputo, R., Carelli, S. and Ghidoni, R. Ceramide composition of the psoriatic scale. Biochim Biophys Acta **1182,** 147, 1993.
13. Masukawa, Y., Narita, H., Shimizu, E., Kondo, N., Sugai, Y., Oba, T., Homma, R., Ishikawa, J., Takagi, Y., Kitahara, T., Takema, Y. and Kita, K. Characterization of overall ceramide species in human stratum corneum. J Lipid Res **49,** 1466, 2008.

14. De Jager, M. Acylceramide head group architecture affects lipid organisation in synthetic ceramide mixture. Thesis **Chapter 5,** 95, 2006.
15. Hagemann, I. and Proksch, E. Topical treatment by urea reduces epidermal hyperproliferation and induces differentiation in psoriasis. Acta Derm Venereol **76,** 353, 1996.
16. Le, T.K., Schalkwijk, J., van de Kerkhof, P.C., van Haelst, U. and van der Valk, P.G. A histological and immunohistochemical study on chronic irritant contact dermatitis. Am J Contact Dermat **9,** 23, 1998.
17. Leigh, I.M., Navsaria, H., Purkis, P.E., McKay, I.A., Bowden, P.E. and Riddle, P.N. Keratins (K16 and K17) as markers of keratinocyte hyperproliferation in psoriasis in vivo and in vitro. Br J Dermatol **133,** 501, 1995.
18. Myers, S.R., Navsaria, H.A., Brain, A.N., Purkis, P.E. and Leigh, I.M. Epidermal differentiation and dermal changes in healing following treatment of surgical wounds with sheets of cultured allogeneic keratinocytes. J Clin Pathol **48,** 1087, 1995.
19. Paladini, R.D., Takahashi, K., Bravo, N.S. and Coulombe, P.A. Onset of re-epithelialization after skin injury correlates with a reorganization of keratin filaments in wound edge keratinocytes: defining a potential role for keratin 16. J Cell Biol **132,** 381, 1996.
20. Smiley, A.K., Klingenberg, J.M., Boyce, S.T. and Supp, D.M. Keratin expression in cultured skin substitutes suggests that the hyperproliferative phenotype observed in vitro is normalized after grafting. Burns **32,** 135, 2006.
21. Paramio, J.M., Casanova, M.L., Segrelles, C., Mittnacht, S., Lane, E.B. and Jorcano, J.L. Modulation of cell proliferation by cytokeratins K10 and K16. Mol Cell Biol **19,** 3086, 1999.
22. Batheja, P., Song, Y., Wertz, P. and Michniak-Kohn, B. Effects of growth conditions on the barrier properties of a human skin equivalent. Pharm Res **26,** 1689, 2009.
23. Bouwstra, J.A., Gooris, G.S., Weerheim, A., Kempenaar, J. and Ponec, M. Characterization of stratum corneum structure in reconstructed epidermis by X-ray diffraction. J Lipid Res **36,** 496, 1995.
24. Gibbs, S., Vicanova, J., Bouwstra, J., Valstar, D., Kempenaar, J. and Ponec, M. Culture of reconstructed epidermis in a defined medium at 33 degrees C shows a delayed epidermal maturation, prolonged lifespan and improved stratum corneum. Arch Dermatol Res **289,** 585, 1997.
25. Kennedy, A.H., Golden, G.M., Gay, C.L., Guy, R.H., Francoeur, M.L. and Mak, V.H. Stratum corneum lipids of human epidermal keratinocyte air-liquid cultures: implications for barrier function. Pharm Res **13,** 1162, 1996.

26. Pappinen, S., Hermansson, M., Kuntsche, J., Somerharju, P., Wertz, P., Urtti, A. and Suhonen, M. Comparison of rat epidermal keratinocyte organotypic culture (ROC) with intact human skin: lipid composition and thermal phase behavior of the stratum corneum. Biochim Biophys Acta **1778,** 824, 2008.
27. Ponec, M., Boelsma, E., Weerheim, A., Mulder, A., Bouwstra, J. and Mommaas, M. Lipid and ultrastructural characterization of reconstructed skin models. Int J Pharm **203,** 211, 2000.
28. Ponec, M., Weerheim, A., Kempenaar, J., Mulder, A., Gooris, G.S., Bouwstra, J. and Mommaas, A.M. The formation of competent barrier lipids in reconstructed human epidermis requires the presence of vitamin C. J Invest Dermatol **109,** 348, 1997.
29. Rivier, M., Castiel, I., Safonova, I., Ailhaud, G. and Michel, S. Peroxisome proliferator-activated receptor-alpha enhances lipid metabolism in a skin equivalent model. J Invest Dermatol **114,** 681, 2000.
30. Schmuth, M., Jiang, Y.J., Dubrac, S., Elias, P.M. and Feingold, K.R. Thematic review series: skin lipids. Peroxisome proliferator-activated receptors and liver X receptors in epidermal biology. J Lipid Res **49,** 499, 2008.
31. Sertznig, P., Seifert, M., Tilgen, W. and Reichrath, J. Peroxisome proliferator-activated receptors (PPARs) and the human skin: importance of PPARs in skin physiology and dermatologic diseases. Am J Clin Dermatol **9,** 15, 2008.
32. Feingold, K.R. and Jiang, Y.J. The mechanisms by which lipids coordinately regulate the formation of the protein and lipid domains of the stratum corneum: Role of fatty acids, oxysterols, cholesterol sulfate and ceramides as signaling molecules. Dermatoendocrinol **3,** 113, 2011.
33. Forman, B.M., Chen, J. and Evans, R.M. Hypolipidemic drugs, polyunsaturated fatty acids, and eicosanoids are ligands for peroxisome proliferator-activated receptors alpha and delta. Proc Natl Acad Sci U S A **94,** 4312, 1997.

5

INCREASED PRESENCE OF MONO-UNSATURATED FATTY ACIDS IN THE STRATUM CORNEUM OF HUMAN SKIN EQUIVALENTS

Varsha S. Thakoersing[1*], Jeroen van Smeden[1*], Aat Mulder[1], Rob Vreeken[2], Abdoelwaheb El Ghalbzouri[3], Joke A. Bouwstra[1]

[1]Department of Drug Delivery Technology, Leiden / Amsterdam Center for Drug Research, Leiden University, Leiden, 2333 CC, The Netherlands. [2]Department of Analytical Biosciences, Leiden / Amsterdam Center for Drug Research, Leiden University, Leiden, 2333 CC, The Netherlands. [3]Department of Dermatology, Leiden University Medical Center, Leiden, 2333 ZA, The Netherlands

[*] These two authors contributed equally to the paper

Manuscript submitted to The Journal of Investigative Dermatology

ABSTRACT

Previous results showed that our in-house human skin equivalents (HSEs) differ in their stratum corneum (SC) lipid organization compared to human SC. To elucidate the cause of the altered SC lipid organization in the HSEs a novel LC/MS method was used to study the free fatty acid (FFA) and ceramide composition in detail. In addition, the SC lipid composition of the HSEs and human skin was examined quantitatively with HPTLC. For the first time our results reveal that all our HSEs have an increased presence of mono-unsaturated FFAs compared to human SC. Moreover, the HSEs display the presence of ceramide species with a mono-unsaturated acyl chain, which are not detected in human SC. All HSEs also exhibit an altered expression of stearoyl-CoA desaturase 1, the enzyme that converts saturated FFAs to mono-unsaturated FFAs. Furthermore, the HSEs show the presence of twelve ceramide subclasses, similar to native human SC. However, the HSEs have increased levels of ceramides EOS and EOH, ceramide species with a short total carbon chain, and a reduced FFA level compared to human SC. The presence of unsaturated lipid chains in HSEs offers new opportunities to mimic the lipid properties of human SC more closely.

INTRODUCTION

Human skin equivalents (HSEs) provide a valuable tool to predict the permeation of substances through the skin [1-8] or to determine whether compounds are toxins, irritants or sensitizers for the skin [9-12]. However, in order to obtain a reliable *in vitro* – *in vivo* correlation it is a prerequisite that HSEs have a comparable skin barrier function as native human skin. The main barrier for compound penetration is located in the lipid matrix of the stratum corneum (SC). This lipid matrix is mainly composed of cholesterol, free fatty acids (FFAs) and ceramides [13, 14]. The lipid composition determines the lipid organization in the SC and is therefore a key factor in determining the skin barrier function [15]. We have previously investigated the SC lipid organization of four of our in-house HSEs, namely the fibroblast derived matrix model (FDM), Leiden Epidermal Model (LEM), Full Thickness collagen Model (FTM) and full thickness outgrowth (FTO). The LEM is a skin equivalent with only an epidermal compartment. The FDM is a model wherein fibroblasts produce their own extracellular matrix, while the FTM contains a dermal compartment that consists of rat tail collagen populated with human fibroblasts. In the FTO a full thickness explant of native human skin is placed onto rat tail collagen and is allowed to expand and develop an epidermis. The skin models mimic many aspects of native human skin. However, they display some differences in their SC lipid organization. These differences may play an important role in their decreased permeability barrier compared to human SC* [16]. As the lipid organization is dictated by the lipid composition, we determined the SC lipid composition of each HSE in detail to unravel the cause of their altered SC lipid organization. For this purpose we quantitatively assessed the SC lipid composition of our in-house HSEs and native human SC with high performance thin layer chromatography (HPTLC). Nine ceramide subclasses have been identified in native human SC using HPTLC [17], while twelve ceramide subclasses have been identified using a novel liquid chromatography/mass spectrometry (LC/MS)

* Chapter 4

method [18]. In this study we used LC/MS to determine whether all identified ceramide subclasses in native human SC are also present in the SC of our HSEs. In addition, detailed information on the chain length distribution and degree of saturation of each ceramide subclass and FFAs is provided and compared to SC of native human skin. The expression pattern of several enzymes involved in the FFA and ceramide synthesis was also investigated to examine the biological cause of the altered SC lipid properties observed in the HSEs. This study has led to the identification of novel targets that offer new opportunities to optimize the SC lipid properties of HSEs and mimic the barrier properties of native human skin even more closely.

MATERIALS AND METHODS

Cell culture

Native human mammary or abdomen skin was obtained from adults undergoing surgery. The collection of human skin was conducted after informed consent of the skin donors. The Declaration of Helsinki principles were followed when using human tissue. Normal human keratinocytes (NHKs) and human dermal fibroblasts were isolated as described before [19]. NHKs used to generate LEMs were cultured with Dermalife K medium complete kit (Lifeline Cell Technology, Walkersville, MD) supplemented with 1% penicillin/streptomycin (Sigma) until they reached a maximum confluency of 80%. NHKs used to generate the FDM and FTM were grown in medium consisting of DMEM and Hams's F12 (Invitrogen, Leek, The Netherlands) (3:1 v/v), 5% fetal bovine serum (FBS; Hyclone, Logan, UT) 1% penicillin/streptomycin (Sigma), 1 μM hydrocortisone (Sigma), 1 μM isoproterenol (Sigma) and 0.5 μg/mL insulin (Sigma). First and second passage NHKs were used to generate HSEs.

Human dermal fibroblasts were cultured in DMEM (Invitrogen, Leek, The Netherlands) supplemented with 5% FBS and 1% penicillin/streptomycin.

Dermal equivalents

Collagen-type I containing dermal equivalents: a 1 mg/mL collagen (isolated form rat tails) solution was obtained by mixing a 4 mg/mL collagen solution in 0.1% acetic acid with Hank's Buffered Salt Solution (Invitrogen, Leek, The Netherlands), 0.1% acetic acid, 1M NaOH and FBS on ice. One mL of this mixture was pipetted into a filter insert (Corning transwell cell culture inserts, membrane diameter 24 mm, pore size 3 μm, Corning Life Sciences, Amsterdam, The Netherlands) and polymerized for 15 minutes at 37ºC. Hereafter, a 2 mg/mL collagen layer was prepared as described, with the addition of fibroblasts to the FBS solution (final fibroblast cell density of $0.4x10^5$ cells/mL collagen solution). Three mL of this fibroblast-populated collagen mixture was pipetted onto the previous collagen layer and was polymerized as described. The dermal equivalents were transferred to a 6-well deep-well plate (Organogensis, Canton, MA) and cultured under submerged conditions in medium consisting of DMEM, 5% FBS, 1% penicillin/streptomycin and fresh supplementation of 45 mM vitamin C (Sigma). The medium was refreshed twice a week.

Fully human dermal equivalents: $0.4x10^6$ fibroblasts were seeded onto filter inserts (Corning Transwell culture inserts, membrane diameter 24 mm, pore size 0.4 μm; Corning Life Sciences, Amsterdam, The Netherlands) and were nourished with a similar medium as described for the collagen type I containing dermal equivalents. The fibroblasts were allowed to generate their own extracellular matrix for 3 weeks. The medium was refreshed twice a week.

Generation of human skin equivalents (HSEs)

HSEs generated on collagen dermal equivalents referred to as Full Thickness collagen Model (FTM): One week after preparation of the collagen type I containing dermal equivalents, $0.5x10^6$ NHKs were seeded on top of each dermal equivalent. The first two days the HSEs were kept submerged in medium consisting of DMEM and Ham's F12 (Invitrogen, Leek, The Netherlands) (3:1 v/v), 5% FBS, 1%

penicillin/streptomycin, 0.5 μM hydrocortisone, 1 μM isoproterenol and 0.5 μg/mL insulin. The following two days the HSEs were kept submerged in a similar medium, except that the FBS was reduced to 1% and 0.053 μM selenious acid (Johnson Matthey, Maastricht, The Netherlands), 10 mM L-serine (Sigma), 10 μM L-carnitine (Sigma), 1 μM α-tocopherol acetate (Sigma), 25 mM vitamin C and a lipid mixture of 3.5 μM arachidonic acid (Sigma), 30 μM linoleic acid (Sigma), 25 μM palmitic acid (Sigma) were added to the medium. Hereafter, the HSEs were lifted to the air/liquid interface and were nourished with a medium in which the FBS was omitted and the arachidonic acid concentration was increased to 7 μM. The medium was refreshed twice a week. The HSEs were harvested 16 days after seeding of the NHKs onto the dermal equivalents.

HSEs generated on fully human dermal equivalents referred to as Fibroblast Derived matrix Model (FDM): three weeks after seeding fibroblasts onto filter inserts, $0.5x10^6$ NHKs were seeded onto each dermal equivalent. The HSEs were further cultured as described for the FTMs.

HSEs generated on inert filter, referred to as Leiden Epidermal Model (LEM): LEMs were generated as described previously [10] with slight modifications. $0.2x10^6$ NHKs were seeded onto cell culture inserts (Corning tranwell cell culture inserts, membrane diameter 12 mm, pore size 0.4 μm, Corning Life Sciences, Amsterdam, The Netherlands). The cells were kept submerged for 2-3 days in Dermalife medium until confluency. The following 2 days the HSEs were kept submerged in CnT medium (CellnTec, Bern, Switzerland) supplemented according to the manufacturer's protocol and 1% penicillin/streptomycin solution, 1 μM α-tocopherol acetate, 25 mM vitamin C and a lipid mixture of 7 μM arachidonic acid, 30 μM linoleic acid and 25 μM palmitic acid. Hereafter, the cells were nourished with the same medium, but were grown at the air/liquid interface. The LEMs were harvested 16 days after seeding the NHKs onto the inserts.

Full thickness cultures (FTO): 4 mm full thickness fat free punch biopsies obtained from abdomen or mammary skin were gently pushed into freshly generated

collagen type 1 containing dermal equivalents. These HSEs were cultured similarly as described for the FTMs and FDMs, except that they were directly cultured at the air/liquid interface. The FTOs were grown for approximately 16 days.

Morphology and immunohistochemistry

Harvested HSEs were fixed in 4% (w/v) paraformaldehyde (Lommerse Pharma, Oss, The Netherlands), dehydrated and subsequently embedded in paraffin. 5 μm sections were cut and used for immunohistochemical staining of human stearoyl-CoA desaturase 1 (SCD1; 100x dilution) (Sigma), serine palmitoyltransferase (SPT; 400x dilution) (Cayman Chemicals, MI) and ceramide synthase 3 (CERS3; 10x dilution) (Atlas Antibodies, Stockholm, Sweden). The paraffin sections were deparaffinized and rehydrated through xylene and graded ethanol series and finally washed with PBS. Antigen retrieval was performed by immersion in sodium citrate buffer (pH 6) for 30 minutes close to the boiling point. After cooling, the sections were blocked with normal horse serum for 20 min, followed by incubation with the primary antibody (diluted to the appropriate concentration in 1% BSA in PBS) overnight at 4ºC. After washing with PBS the sections were incubated with the secondary antibody for 30 minutes, washed again and incubated with ABC reagent for 30 minutes. The sections were consecutively washed with PBS, 0.1 M sodium acetate buffer and incubated for 30 minutes in amino-ethylcarbazole (Sigma) dissolved in N,N-dimethylformamide (1g/250 mL) (Sigma) supplemented with 0.1% hydrogen peroxide and finally washed with water. Counterstaining was performed with haematoxylin. Incubations with normal horse serum, secondary antibody and ABC reagent were performed with the R.T.U. Vectastain Elite ABC Reagent Kit (Vector Laboratories, Burlingame, CA).

Stratum corneum isolation and lipid extraction

The SC of human abdomen or mammary skin was isolated as described previously [18]. The SC lipids were extracted according to the Bligh and Dyer procedure [20] with

a series of chloroform: methanol mixtures (1:2, 1:1 and 2:1 v/v) for 1 hour each. The extracts were combined and treated with 0.25M KCl and water. The organic phase was collected and evaporated under a stream of nitrogen at 40ºC. The obtained lipids were re-dissolved in a suitable volume of chloroform: methanol (2:1 v/v) and stored at -20ºC until use. To obtain enough lipids for quantification, the lipid extracts of 2 - 4 HSEs from the same experiment and donor were pooled. The SC lipid composition of the FT explant could not be determined, because there was not enough material to extract.

HPTLC lipid quantification

The extracted SC lipids were quantified using HPTLC. The used solvent system to separate the lipids is provided elsewhere [21]. Co-chromatography of serial dilutions of standards was used to identify and quantify each lipid class. The standards consisted of cholesterol, palmitic acid, stearic acid, arachidic acid, tricosanoic acid, behenic acid, lignoceric acid, cerotic acid and ceramides EOS, NS, NP, EOH and AP (ceramide nomenclature according to terminology of Motta *et al.* [22] and Masukawa *et al.* [23]). The ceramides were provided by Cosmoferm (The Netherlands). All other compounds were purchased from Sigma (The Netherlands). The lipid fractions were visualized and quantified as described before [24]. For quantification SC lipid samples of two donors were used of each HSE type and native human skin.

LC/MS lipid analysis

The SC lipid species in the pooled lipid extracts of the HSEs and native human skin were analyzed by LC/MS according to the method described elsewhere [18]. Briefly, an Alliance 2695 HPLC (Waters Corp., Milford, MA) was coupled to a TSQ Quantum MS (Thermo Finnigan, San Jose, CA) measuring in APCI mode. The total lipid concentration of all samples was around 1 mg/ml, the injection volume was set to 10 µl for the analysis of both ceramides and fatty acids.

Ceramides were separated using a PVA-Sil analytical column (5 μm particle size, 100 × 2.1 mm i.d. YMC, Kyoto, Japan) using a gradient mobile phase from heptane to heptane/IPA/EtOH at a flow rate of 0.8 mL/min. The scan range of the MS was set between 500-1200 amu, measuring in positive ion mode. FFAs were analyzed by introducing some adaptations to the setup used for ceramide analysis as will be described in detail elsewhere (Van Smeden *et al.*, in preparation). Separation was achieved using a LiChroCART Purospher STAR analytical column (55 x 2 mm i.d. Merck, Darmstadt, Germany) under a flow rate of 0.6 ml/min using a gradient system from ACN/H_2O to MeOH/Heptane. 1% $CHCl_3$ and 0.2% HAc were added to both mobile phases as ionization enhancers. The ionization mode and scan range was altered to negative mode and 200-600 amu, respectively.

RESULTS

HPTLC analysis reveals that the HSEs have a reduced SC free fatty acid content compared to human skin

The SC lipids of the HSEs and human skin were extracted and quantified with HPTLC to determine whether the HSEs show differences in their lipid composition compared to human skin. Figure 1a shows that SC of the HSEs contains cholesterol, FFAs and all ceramide subclasses, which are also observed in human SC. In the LEM and FTM an additional band of an unidentified lipid, with an R_f value close to that of ceramide EOH, can be observed. This unidentified lipid, which may represent an unidentified ceramide, was occasionally also observed in the FDM and FTO.

Figure 1b shows that human SC consists of approximately equal amounts of cholesterol, FFAs and ceramides. All HSEs, however, show a different distribution of the SC barrier lipids (figure 1b). The relative FFA content in the HSEs, especially in the FDM, LEM and FTO, is much lower compared to human SC. The SC lipid quantification also indicates that the ceramide/cholesterol ratio (table 1) in

the LEM is increased and reduced in FTO compared to human SC. This indicates that the relative ceramide and/or cholesterol levels in the SC of the LEM and FTO differ from the levels determined in human SC.

Table 1

	Ceramide/Cholesterol ratio
HSC Donor 1	1.3
HSC Donor 2	1.3
FDM Donor 1	1.3
FDM Donor 2	1.3
LEM Donor 1	1.8
LEM Donor 2	1.6
FTM Donor 1	1.5
FTM Donor 2	1.5
FTO Donor 1	0.8
FTO Donor 2	0.8

Most of the HSEs have an increased acylceramide content compared to native human SC

In human SC twelve ceramide subclasses are identified. Each subclass is named according to its chemical structure [22, 23]. In short, ceramides with a sphingosine (S), phytosphingosine (P), 6-hydroxysphingosine (H) or dihydrosphingosine (dS) backbone are linked via an amide to a fatty acid chain, which can either be an esterified ω-hydroxy (EO), α-hydroxy (A) or non-hydroxy (N) fatty acid. Figure 1c shows the ratio between the total acylceramides (EO ceramides) and the other ceramide classes (sum of all α-hydroxy + non-hydroxy ceramides) in the HSEs and native human skin. This figure clearly shows that the total acylceramides level is much higher in the FDM, LEM and FTO compared to native human skin. Focusing on the individual acylceramide levels, it is evident that the FDM, LEM and FTO have a higher content of ceramides EOS and EOH* compared to human

SC. The difference in EOP level between FDM, LEM, FTO and human SC is somewhat smaller compared to the other acylceramides (figure 1d). FTM has a small increase in ceramide EOS and EOH* level compared to human SC, while the EOP level is very similar (figure 1d).

On the TLC plate an unidentified lipid close to ceramide EOH is observed in the LEM and FTM (figure 1a). In the LC/MS ceramide profiles of the HSEs an unidentified group of lipids, which have a molecular weight similar to acylceramides, is also observed close to ceramide EOH (figure 2b, indicated by **). This suggests that the lipid band on the TLC plate most likely represents an acylceramide class. For this reason the unidentified lipid was quantified together with ceramide EOH (the two bands together are represented as EOH*).

Comparison of the α-hydroxy and non-hydroxy ceramides also shows some differences in distribution of these ceramide subclasses between the HSEs and human SC (figure 1e). Ceramide NP is the most abundant ceramide in human SC. Compared to human SC the ceramide NP content is reduced in the FTM and an even further reduction is observed in the FDM, LEM and FTO. Additionally, the ceramide AP content in FTM is close to the ceramide content in human SC, but reduced in the FDM, LEM and FTO. The relative content of ceramides NS + NdS, ceramides AS + NH and AH are similar in the HSEs and human SC. Ceramides NS + NdS and AS + NH were grouped together for quantification, because they co-migrate and therefore have a similar R_f value when using HPTLC.

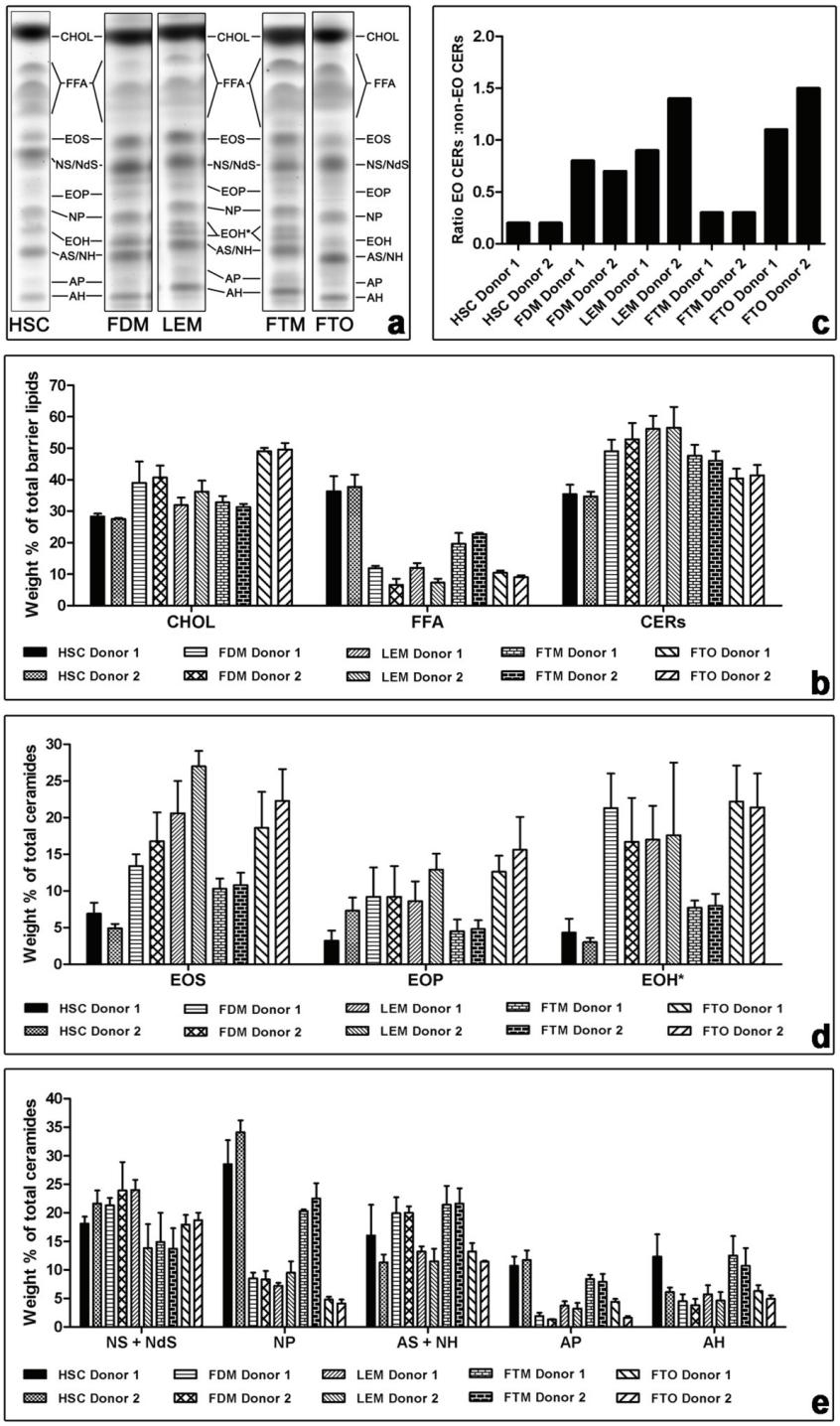
CHOL
FFA
EOS
NS/NdS
EOP
NP
EOH
EOH*
AS/NH
AP
AH
HSC
FDM
LEM
FTM
FTO
a
Ratio EO CERs :non-EO CERs
2.0
1.5
1.0
0.5
0.0
HSC Donor 1
HSC Donor 2
FDM Donor 1
FDM Donor 2
LEM Donor 1
LEM Donor 2
FTM Donor 1
FTM Donor 2
FTO Donor 1
FTO Donor 2
c
Weight % of total barrier lipids
70
60
50
40
30
20
10
0
CHOL
FFA
CERs
HSC Donor 1
HSC Donor 2
FDM Donor 1
FDM Donor 2
LEM Donor 1
LEM Donor 2
FTM Donor 1
FTM Donor 2
FTO Donor 1
FTO Donor 2
b
Weight % of total ceramides
30
25
20
15
10
5
0
EOS
EOP
EOH*
HSC Donor 1
HSC Donor 2
FDM Donor 1
FDM Donor 2
LEM Donor 1
LEM Donor 2
FTM Donor 1
FTM Donor 2
FTO Donor 1
FTO Donor 2
d
Weight % of total ceramides
40
35
30
25
20
15
10
5
0
NS + NdS
NP
AS + NH
AP
AH
HSC Donor 1
HSC Donor 2
FDM Donor 1
FDM Donor 2
LEM Donor 1
LEM Donor 2
FTM Donor 1
FTM Donor 2
FTO Donor 1
FTO Donor 2
e

All twelve ceramide subclasses detected in human SC are also observed in the HSEs

LC/MS analysis of native human SC lipids shows the presence of at least twelve ceramide subclasses, as reported previously [18] (figure 2a). Additionally, within one ceramide subclass a large number of peaks are observed in the multi-mass chromatogram. Each peak represents a ceramide specie that has the same head group, but a different total carbon chain length and therefore a different molecular weight. In descending order each specie has 14 mass units less, which represents a reduction in one CH_2-group compared to the previous specie. All twelve ceramide subclasses in human SC show a large variation in their total carbon chain length distribution. In human SC the acylceramides have a total chain length varying from 63 to 78 carbon atoms. The α-hydroxy and non-hydroxy ceramide subclasses have shorter total carbon chains which range from 34 to 50 and 34 to 56 carbon atoms, respectively. In addition to the twelve identified ceramide subclasses, human SC also shows the presence of some unidentified lipid classes. These unidentified lipid classes also consist of several species, indicated by the variation in total carbon chain length. The molecular structure of these lipids remains to be elucidated. The ceramide subclasses present in the FDM, including the total chain length distribution of each subclass, is provided in the multi mass chromatogram in figure

Figure 1. SC barrier lipids of human skin (HSC), FDM, LEM, FTM and FTO were fractionated and quantified by HPTLC and photo densitometry. A: barrier lipid composition of human SC and HSEs. B: relative level of each SC lipid class, c: ratio of acylceramides (EO CERs) and non-acylceramides (non-EO CERs), d: relative level of acylceramides, e: relative level of α-hydroxy and non-hydroxy ceramides. The data represents the sample mean + SD of at least 3 analytical points. CHOL= cholesterol, FFA= free fatty acids, CERs= ceramides, *= unidentified lipid. Ceramide nomenclature: A= α-hydroxy fatty acids, E= ester-linked fatty acids, H= 6-hydroxy sphingosine, dS= dihydrosphingosine, N= non-hydroxy fatty acids, O= ω-hydroxy fatty acids, P= phytosphingosine, S= sphingosine.

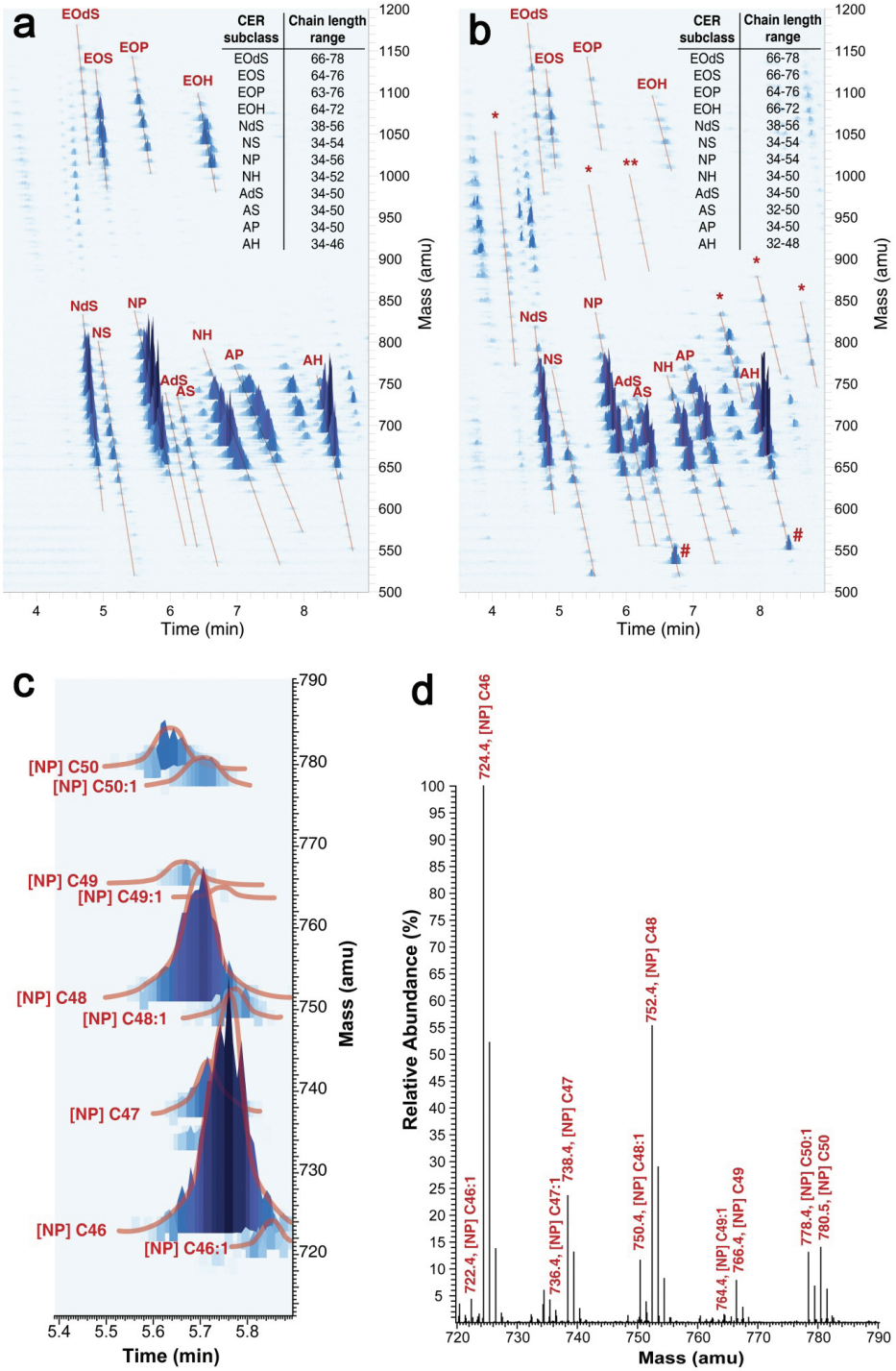
a
b
EOdS
EOS
EOP
EOH
NdS
NS
NP
NH
AdS
AS
AP
AH
CER subclass
Chain length range
EOdS 66-78
EOS 64-76
EOP 63-76
EOH 64-72
NdS 38-56
NS 34-54
NP 34-56
NH 34-52
AdS 34-50
AS 34-50
AP 34-50
AH 34-46
EOdS 66-78
EOS 66-76
EOP 64-76
EOH 66-72
NdS 38-56
NS 34-54
NP 34-54
NH 34-50
AdS 34-50
AS 32-50
AP 34-50
AH 32-48
Mass (amu)
Time (min)
c
[NP] C50
[NP] C50:1
[NP] C49
[NP] C49:1
[NP] C48
[NP] C48:1
[NP] C47
[NP] C46
[NP] C46:1
Mass (amu)
Time (min)
d
Relative Abundance (%)
Mass (amu)
724.4, [NP] C46
722.4, [NP] C46:1
736.4, [NP] C47:1
738.4, [NP] C47
750.4, [NP] C48:1
752.4, [NP] C48
764.4, [NP] C49:1
766.4, [NP] C49
778.4, [NP] C50:1
780.5, [NP] C50

2b. This figure shows that all twelve ceramide subclasses present in native human SC are also detected in FDM. The other HSEs show a very similar LC/MS profile as the FDM and also show the presence of all twelve ceramide subclasses (figure 4a-c). Each ceramide subclass in the HSEs shows a wide variation in total chain length distribution, similar to native human SC. In the HSEs the acylceramides have a total carbon chain that varies between 64 and 78 carbon atoms, which is almost similar to the chain length distribution observed for native human SC. The α-hydroxy and non-hydroxy ceramide subclasses have a total carbon chain between 32 and 50 and 34 and 56 carbon atoms, respectively. When focusing in more detail on the LC/MS profiles of the HSEs and native human SC some differences are observed. In the multi mass chromatograms of the HSEs a weak lipid band is located just below the stronger peaks of the ceramide species (figure 2c), which is observed for all ceramide subclasses. These additional weak lipid bands always have a mass of two units less than the stronger band of the ceramide specie above them (figure 2c, d). This specific difference of two mass units suggests that the lipid band represent a ceramide specie that contains a mono-unsaturated fatty acyl chain.

Figure 2. LC/MS chromatograms of ceramide subclasses in human SC (a) and FDM (b). The retention time, mass and intensity of each peak are shown on the X-axis, Y-axis and Z-axis, respectively. The total carbon chain length variation of each ceramide subclass is provided in the inset. Ceramides with a low total carbon chain length, which are present in lower quantities in human SC, are indicated by # in the chromatogram of FDM. Unidentified lipids only observed in the chromatogram of FDM are specified with *. The unidentified lipid quantified together with ceramide EOH using HPTLC is indicated by **. Examples of ceramide species containing a MUFA chain are shown in (c). The masses of ceramide species with a saturated or MUFA chain are shown in (d).

The multi mass chromatograms of the HSEs also show low molecular weight ceramide species which are not detected in human SC. Furthermore, some low molecular weight ceramide species which have a mass below approximately 620 amu have a higher intensity in the multi mass chromatograms of the HSEs compared to human skin. This is mainly observed for species of ceramides AS and AH which have a total chain length of 34 carbon atoms (figure 2b and 4a-c, indicated by #). The HSEs show the presence of several unidentified lipids, of which some are not present in the multi mass chromatogram of native human SC (figure 2b and 4a-c, indicated by *).

HSEs show an increased presence of mono-unsaturated fatty acids compared to native human SC

Figure 3 depicts the FFA chain length distribution and degree of saturation in human SC and FDM. The other HSEs showed a similar FFA composition as the FDM (figure 4d-f). Human SC shows a FFA chain length distribution from C16:0 to C30:0. All HSEs contain FFAs with chain lengths varying from C16:0 to C28:0. This indicates that the HSEs are able to synthesize similar FFAs as native human skin. However, the FFA LC/MS profiles of all HSEs additionally show the presence of mono-unsaturated fatty acids (MUFAs), which are hardly detected in human SC. The MUFAs detected in the LC/MS profiles of the HSEs have a chain length varying from C16:1 up to C34:1. All HSEs also show a reduced level of FFAs with an odd carbon chain length compared to human SC.

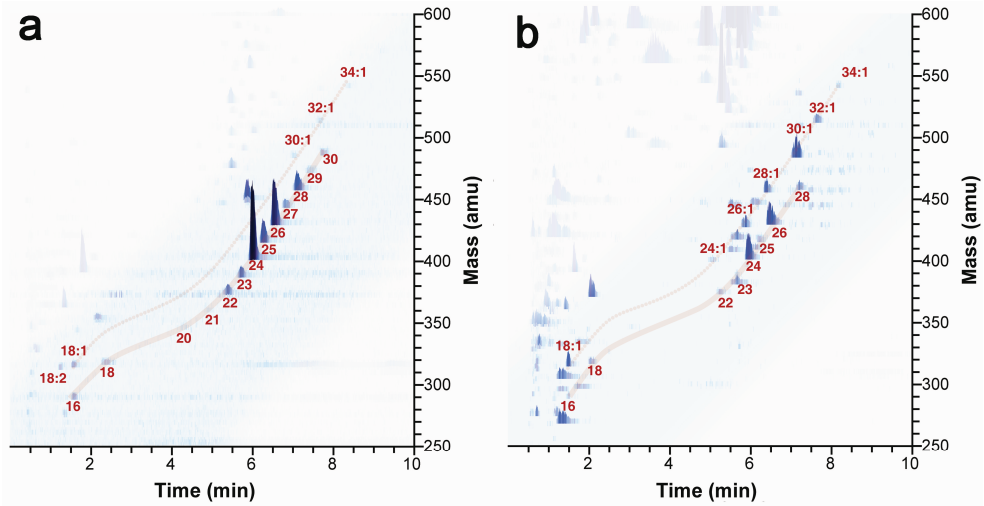

Figure 3. Three dimensional multi-mass LC/MS chromatograms of FFAs in native human SC (a) and FDM (b) are shown. The retention time is shown on the X-axis, the mass (in amu) is provided on the Y-axis and the intensity of each peak is depicted on the Z-axis. In human SC the FFA chain length distribution varies from C16:0 to C30:0. The FDM has a very similar FFA chain length distribution as human SC, but shows an increase in MUFAs with chain lengths varying from C16:1 to C34:1. Additionally, the odd chain length FFAs show a lower intensity in the chromatogram of FDM compared to human SC.

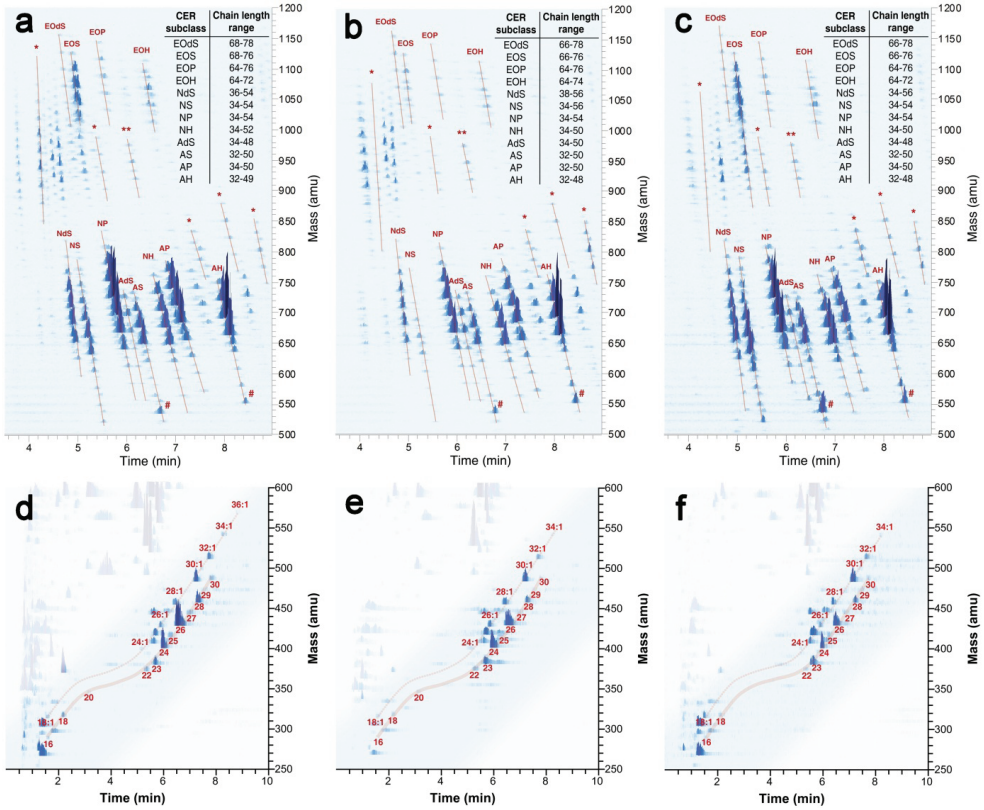

Figure 4. Three dimensional multi-mass LC/MS chromatograms of ceramide subclasses in LEM (a), FTM (b) and FTO (c). The retention time is shown on the X-axis, the mass is provided on the Y-axis and the intensity of each peak is depicted on the Z-axis. The total carbon chain length variation of each ceramide subclass is indicated in the inset. Ceramides with a low total carbon chain length which are present in lower quantities in human SC are indicated by #. Unidentified lipids observed in the chromatogram of the LEM, FTM and FTO which are not observed in human SC are specified with *. The unidentified lipid quantified together with ceramide EOH using HPTLC is indicated by **. The FFA chain length distribution and degree of saturation of LEM, FTM and FTO are shown in d, e and f, respectively.

The HSEs show an altered expression of stearoyl-CoA desaturase 1

To investigate the biological cause of the altered SC lipid organization of the HSEs, the expression pattern of some enzymes involved in the FFA and ceramide synthesis were examined. Stearoyl-CoA desaturase 1 (SCD1) is the rate-limiting enzyme that catalyzes the synthesis of MUFAs from saturated fatty acids [25, 26]. In native human epidermis SCD1 is only expressed in the basal layer (figure 5). In all HSEs the expression of SCD1 is observed in the basal layer as well as the in the differentiated layers of the viable epidermis (figure 5). This indicates that the expression of SCD1 is altered in the HSEs compared to human skin.

The first step in ceramide synthesis is the coupling of serine to palmitic acid by serine palmitoyltransferase (SPT) [27]. In human skin SPT expression is observed in the entire viable epidermis, showing both nucleic as well as cytoplasmic staining. No difference in expression pattern between human skin and the HSEs is observed (figure 5). Ceramide synthase 3 (CERS3), is one of the key enzymes involved in *de novo* ceramide synthesis pathway. CERS3 has a broad fatty acyl-coA preference and therefore n-acylates both long and very-long chain fatty acyl-CoAs to a sphingoid base. Among the six CERS members (CERS 1-6), the mRNA expression of CERS3 is found to be the highest in differentiated keratinocytes *in vitro* [28]. Additionally, a recent publication by Jennemann *et al.* [29] demonstrated that CERS3 is responsible for the synthesis of very-long chain ceramides in the skin. In human skin and in all HSEs CERS3 is expressed in the entire viable epidermis (figure 5). It should be noted that the expression of SCD1, SPT and CERS3 was weaker in the FTO samples compared to the other HSEs.

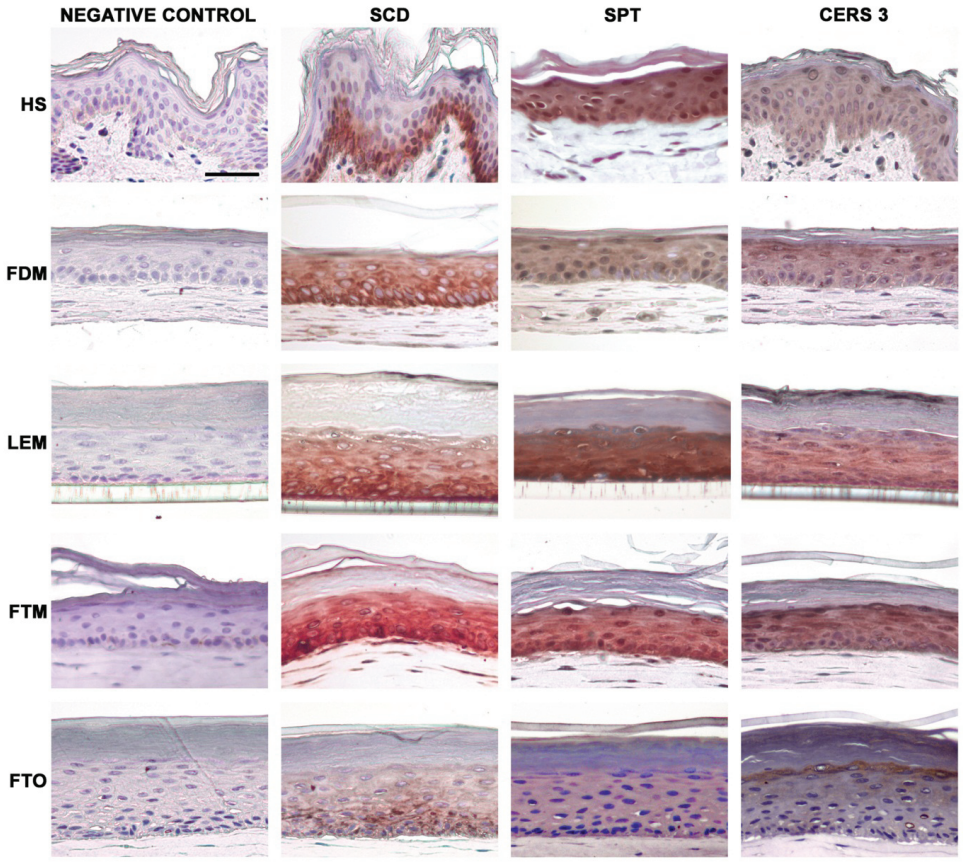

Figure 5. Immunohistochemical staining showing the expression pattern of stearoyl-CoA desaturase1 (SCD), serine palmitoyltransferase (SPT) and ceramide synthase 3 (CERS3) in human skin (HS), FDM, LEM, FTM and FTO. The negative control represents sections on which only the secondary antibody was applied. The micrographs were taken at a 20x magnification. Scale bar represents 50 μm.

DISCUSSION

In previous studies we have investigated the SC lipid organization of four in-house HSEs and native human skin. These studies showed that our in-house HSEs have a mainly hexagonal packing[*] [16], while human SC has the dense orthorhombic packing (a schematic representation of the SC lipid organization is depicted in figure 6). The presence of a hexagonal lipid organization has been correlated to a decreased skin barrier function as monitored by transepidermal water loss compared to the orthorhombic packing [30]. We examined the SC lipid composition of our HSEs in detail to verify the cause of their altered SC lipid properties and to determine how the latter can be optimized. In this study we show for the first time that the SC of HSEs contains MUFAs, which may be a key factor for their altered SC lipid organization. The increase in MUFA content in the SC of HSEs coincides with the altered expression of SCD1 in the viable epidermis of the HSEs compared to human epidermis. It has been demonstrated that lipid mixtures containing an equimolar ratio of cholesterol, FFAs and human ceramides predominantly form an orthorhombic packing [31]. However, a reduction in FFAs or the addition of MUFAs in such mixtures enhances the formation of a hexagonal lateral packing[†]. This indicates that the reduction in FFA level and an increased presence of MUFAs contribute to the formation of the hexagonal packing in our HSEs, which thus may be key factors in the observed increased benzocaine penetration across the SC of HSEs compared to native human skin. With respect to the lamellar phases, the HSEs show the predominant presence of the LPP[*] [16], whereas in human SC both the LPP and SPP are formed [32]. All HSEs have an increased relative content of ceramides EOS and EOH. As suggested in previous studies, these high acylceramide levels may favor the formation of the LPP in HSEs [33], but does not make the HSEs more permeable.

[*] Chapter 4
[†] Janssens *et al.*, unpublished results

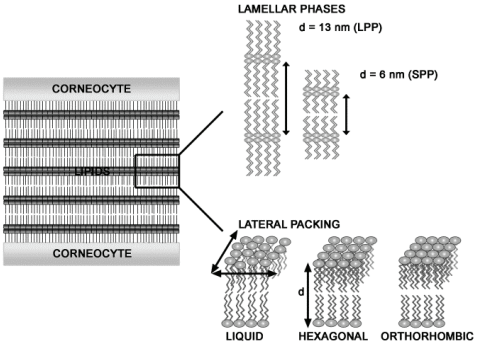

Figure 6. In human SC the lamellar phases refer to the stack of lipid layers (i.e. lipid lamellae) between the corneocytes. The distance over which one lipid layer is repeated is referred to as the repeat distance (d). In human SC the lipid lamellae have a repeat distance of approximately 13 or 6 nm, the long and short periodicity phase (LPP and SPP), respectively. The lateral packing discloses the density of the lipids within the lipid lamellae. The orthorhombic packing has the highest lipid density and the liquid packing the lowest. In human SC the lipids are arranged in the orthorhombic packing, although some lipid domains also form the hexagonal or liquid packing.

We show that all twelve ceramide subclasses observed in native human SC are also present in the SC of all HSEs. This indicates that the keratinocytes in our HSEs retain their ability to synthesize all ceramide subclasses that are also present in human SC. This observation represents a big step forward in the characterization of the SC lipid properties of HSEs, considering that until now a maximum of nine ceramide subclasses were detected in HSEs, while in the commercial HSEs even those nine ceramide classes were not always present [17, 34, 35].

Masukawa *et al.* quantified the ceramide composition in native human SC using LC/MS [36]. The relative prevalence of each ceramide class determined in this study and the study of Masukawa *et al.* are very similar. In this study five synthetic ceramides are used for quantification of the SC lipids in the HSEs and native human SC. The use of several ceramide subclasses for quantification is very important, since the charring intensities of the ceramide subclasses differ considerably when equal amounts are sprayed on TLC plates (figure 7).

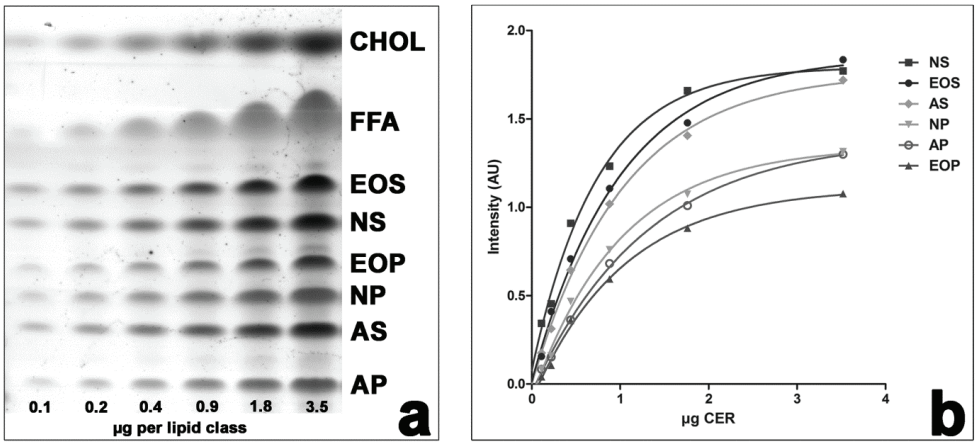

Figure 7. Figure a shows the charring intensities of the lipid standards used for the quantification of the SC lipid composition. The lipid standard contains equal weight amounts of each standard. The charring intensity of each spot was determined by densitometry and plotted against the amount sprayed to construct a calibration curve (b).

The different composition of ceramide subclasses in the FDM, LEM and FTO compared to human skin is indicative of an altered ceramide subclass synthesis in these HSEs. The reason for this difference remains to be elucidated.

Our results demonstrate that the HSEs show a similar expression of CERS3 as human skin. The LC/MS multi mass chromatograms indeed show that the HSEs are able to synthesize ceramides with a large variety in total carbon chain lengths, which are very similar to human skin. The expression of SCD1 in the proliferating and differentiating layers of the epidermis of the HSEs may result in an increased activity of SCD1 in the differentiated epidermal layers and thus an increased intracellular content of MUFAs in the keratinocytes. Due to the increase in intracellular MUFA content the CERS enzymes, including CERS3, n-acylate both MUFAs and saturated FFAs to the sphingoid bases. The observation that an increase in MUFA content in the SC is accompanied by the presence of ceramide species with a mono-unsaturated fatty acyl chain suggests that fatty acids present in

the SC and the fatty acyl chains of ceramides have a common source or synthetic pathway.

The results of this study indicate that the SC lipid properties of the HSEs can be improved by increasing the FFA content in the SC. The culture medium used to generate the HSEs is supplemented with FFAs. Optimization of FFA supplementation to the culture medium may lead to SC FFA levels that more closely resemble the SC FFA level of native human skin. It remains to be established whether increased expression of SCD1 in the suprabasal layers of the HSEs is truly associated with an increased activity of SCD1 compared to native human epidermis. If this appears to be true, the SC lipid properties can additionally be improved by reducing SCD1 activity and thereby the MUFA level in the SC of HSEs. SCD activity is regulated by many factors, such as insulin, temperature, leptin or synthetic inhibitors [25, 37]. SCD1 activity in the HSEs may therefore be reduced by using e.g. SCD inhibitors in the culture medium. Studies performed by Miyazaki *et al.* [38] have demonstrated that SCD deficient mice show skin permeability barrier defects, such as an insufficient lipid deposition in the SC due to the presence of immature lamellar bodies with a reduced lipid content, and a reduction in acylceramide content. The reduction in SCD1 activity should therefore be performed with care to prevent different types of SC barrier defects in HSEs that may occur by a too severe suppression of SCD1 activity. Optimization of the FFA content in the SC of HSEs will be the subject of future studies.

ACKNOWLEDGEMENTS

The authors would like to thank Maria Ponec for helpful suggestions during the meetings. This research was financially supported by the Dutch Technology Foundation STW (grant no. 7503).

REFERENCES

1. Ackermann, K., Borgia, S.L., Korting, H.C., Mewes, K.R. and Schafer-Korting, M. The Phenion full-thickness skin model for percutaneous absorption testing. Skin Pharmacol Physiol **23,** 105, 2010.
2. Asbill, C., Kim, N., El-Kattan, A., Creek, K., Wertz, P. and Michniak, B. Evaluation of a human bio-engineered skin equivalent for drug permeation studies. Pharm Res **17,** 1092, 2000.
3. Batheja, P., Song, Y., Wertz, P. and Michniak-Kohn, B. Effects of growth conditions on the barrier properties of a human skin equivalent. Pharm Res **26,** 1689, 2009.
4. Marjukka Suhonen, T., Pasonen-Seppanen, S., Kirjavainen, M., Tammi, M., Tammi, R. and Urtti, A. Epidermal cell culture model derived from rat keratinocytes with permeability characteristics comparable to human cadaver skin. Eur J Pharm Sci **20,** 107, 2003.
5. Netzlaff, F., Kaca, M., Bock, U., Haltner-Ukomadu, E., Meiers, P., Lehr, C.M. and Schaefer, U.F. Permeability of the reconstructed human epidermis model Episkin in comparison to various human skin preparations. Eur J Pharm Biopharm **66,** 127, 2007.
6. Schafer-Korting, M., Bock, U., Diembeck, W., Dusing, H.J., Gamer, A., Haltner-Ukomadu, E., Hoffmann, C., Kaca, M., Kamp, H., Kersen, S., Kietzmann, M., Korting, H.C., Krachter, H.U., Lehr, C.M., Liebsch, M., Mehling, A., Muller-Goymann, C., Netzlaff, F., Niedorf, F., Rubbelke, M.K., Schafer, U., Schmidt, E., Schreiber, S., Spielmann, H., Vuia, A. and Weimer, M. The use of reconstructed human epidermis for skin absorption testing: Results of the validation study. Altern Lab Anim **36,** 161, 2008.
7. Schmook, F.P., Meingassner, J.G. and Billich, A. Comparison of human skin or epidermis models with human and animal skin in in-vitro percutaneous absorption. Int J Pharm **215,** 51, 2001.
8. Zghoul, N., Fuchs, R., Lehr, C.M. and Schaefer, U.F. Reconstructed skin equivalents for assessing percutaneous drug absorption from pharmaceutical formulations. Altex **18,** 103, 2001.
9. Alepee, N., Tornier, C., Robert, C., Amsellem, C., Roux, M.H., Doucet, O., Pachot, J., Meloni, M. and de Brugerolle de Fraissinette, A. A catch-up validation study on reconstructed human epidermis (SkinEthic RHE) for full replacement of the Draize skin irritation test. Toxicol In Vitro **24,** 257, 2009.

10. El Ghalbzouri, A., Siamari, R., Willemze, R. and Ponec, M. Leiden reconstructed human epidermal model as a tool for the evaluation of the skin corrosion and irritation potential according to the ECVAM guidelines. Toxicol In Vitro **22,** 1311, 2008.
11. Gibbs, S. In vitro irritation models and immune reactions. Skin Pharmacol Physiol **22,** 103, 2009.
12. Netzlaff, F., Lehr, C.M., Wertz, P.W. and Schaefer, U.F. The human epidermis models EpiSkin, SkinEthic and EpiDerm: an evaluation of morphology and their suitability for testing phototoxicity, irritancy, corrosivity, and substance transport. Eur J Pharm Biopharm **60,** 167, 2005.
13. Feingold, K.R. The outer frontier: the importance of lipid metabolism in the skin. J Lipid Res **50 Suppl,** S417, 2009.
14. Wertz, P.W. Lipids and barrier function of the skin. Acta Derm Venereol Suppl (Stockh) **208,** 7, 2000.
15. Bouwstra, J.A. and Ponec, M. The skin barrier in healthy and diseased state. Biochim Biophys Acta **1758,** 2080, 2006.
16. Thakoersing, V.S., Gooris, G., Mulder, A.A., Rietveld, M., El Ghalbzouri, A. and Bouwstra, J.A. Unravelling Barrier Properties of Three Different In-House Human Skin Equivalents. Tissue Eng Part C Methods 2011.
17. Ponec, M., Weerheim, A., Lankhorst, P. and Wertz, P. New acylceramide in native and reconstructed epidermis. J Invest Dermatol **120,** 581, 2003.
18. Van Smeden, J., Hoppel, L., van der Heijden, R., Hankemeier, T., Vreeken, R.J. and Bouwstra, J.A. LC/MS analysis of stratum corneum lipids: ceramide profiling and discovery. J Lipid Res **52,** 1211, 2011.
19. Bouwstra, J.A., Groenink, H.W., Kempenaar, J.A., Romeijn, S.G. and Ponec, M. Water distribution and natural moisturizer factor content in human skin equivalents are regulated by environmental relative humidity. J Invest Dermatol **128,** 378, 2008.
20. Bligh, E.G. and Dyer, W.J. A rapid method of total lipid extraction and purification. Can J Biochem Physiol **37,** 911, 1959.
21. Thakoersing, V.S., Ponec, M. and Bouwstra, J.A. Generation of human skin equivalents under submerged conditions-mimicking the in utero environment. Tissue Eng Part A **16,** 1433, 2010.
22. Motta, S., Monti, M., Sesana, S., Caputo, R., Carelli, S. and Ghidoni, R. Ceramide composition of the psoriatic scale. Biochim Biophys Acta **1182,** 147, 1993.

23. Masukawa, Y., Narita, H., Shimizu, E., Kondo, N., Sugai, Y., Oba, T., Homma, R., Ishikawa, J., Takagi, Y., Kitahara, T., Takema, Y. and Kita, K. Characterization of overall ceramide species in human stratum corneum. J Lipid Res **49,** 1466, 2008.
24. Rissmann, R., Groenink, H.W., Weerheim, A.M., Hoath, S.B., Ponec, M. and Bouwstra, J.A. New insights into ultrastructure, lipid composition and organization of vernix caseosa. J Invest Dermatol **126,** 1823, 2006.
25. Ntambi, J.M., Miyazaki, M. and Dobrzyn, A. Regulation of stearoyl-CoA desaturase expression. Lipids **39,** 1061, 2004.
26. Zhang, L., Ge, L., Parimoo, S., Stenn, K. and Prouty, S.M. Human stearoyl-CoA desaturase: alternative transcripts generated from a single gene by usage of tandem polyadenylation sites. Biochem J **340 (Pt 1),** 255, 1999.
27. Gault, C.R., Obeid, L.M. and Hannun, Y.A. An overview of sphingolipid metabolism: from synthesis to breakdown. Adv Exp Med Biol **688,** 1, 2010.
28. Mizutani, Y., Mitsutake, S., Tsuji, K., Kihara, A. and Igarashi, Y. Ceramide biosynthesis in keratinocyte and its role in skin function. Biochimie **91,** 784, 2009.
29. Jennemann, R., Rabionet, M., Gorgas, K., Epstein, S., Dalpke, A., Rothermel, U., Bayerle, A., van der Hoeven, F., Imgrund, S., Kirsch, J., Nickel, W., Willecke, K., Riezman, H., Grone, H.J. and Sandhoff, R. Loss of ceramide synthase 3 causes lethal skin barrier disruption. Hum Mol Genet **21,** 586, 2012.
30. Damien, F. and Boncheva, M. The extent of orthorhombic lipid phases in the stratum corneum determines the barrier efficiency of human skin in vivo. J Invest Dermatol **130,** 611, 2010.
31. Bouwstra, J., Pilgram, G., Gooris, G., Koerten, H. and Ponec, M. New aspects of the skin barrier organization. Skin Pharmacol Appl Skin Physiol **14 Suppl 1,** 52, 2001.
32. Bouwstra, J.A., Gooris, G.S., van der Spek, J.A. and Bras, W. Structural investigations of human stratum corneum by small-angle X-ray scattering. J Invest Dermatol **97,** 1005, 1991.
33. De Jager, M., Gooris, G., Ponec, M. and Bouwstra, J. Acylceramide head group architecture affects lipid organization in synthetic ceramide mixtures. J Invest Dermatol **123,** 911, 2004.
34. Ponec, M., Boelsma, E., Gibbs, S. and Mommaas, M. Characterization of reconstructed skin models. Skin Pharmacol Appl Skin Physiol **15 Suppl 1,** 4, 2002.

35. Ponec, M., Weerheim, A., Kempenaar, J., Mulder, A., Gooris, G.S., Bouwstra, J. and Mommaas, A.M. The formation of competent barrier lipids in reconstructed human epidermis requires the presence of vitamin C. J Invest Dermatol **109,** 348, 1997.
36. Masukawa, Y., Narita, H., Sato, H., Naoe, A., Kondo, N., Sugai, Y., Oba, T., Homma, R., Ishikawa, J., Takagi, Y. and Kitahara, T. Comprehensive quantification of ceramide species in human stratum corneum. J Lipid Res **50,** 1708, 2009.
37. Liu, G. Stearoyl-CoA desaturase inhibitors: update on patented compounds. Expert Opin Ther Pat **19,** 1169, 2009.
38. Miyazaki, M., Dobrzyn, A., Elias, P.M. and Ntambi, J.M. Stearoyl-CoA desaturase-2 gene expression is required for lipid synthesis during early skin and liver development. Proc Natl Acad Sci U S A **102,** 12501, 2005.

6

MODULATION OF BARRIER PROPERTIES OF HUMAN SKIN EQUIVALENTS BY SPECIFIC MEDIUM SUPPLEMENTS

Varsha S. Thakoersing[1], Jeroen van Smeden[1], Walter Boiten[1], Gert Gooris[1], Aat Mulder[1], Rob J. Vreeken[2,3], Abdoelwaheb El Ghalbzouri[4], Joke A. Bouwstra[1]

[1]Department of Drug Delivery Technology, Leiden/Amsterdam Center for Drug Research, Leiden University, Leiden, 2333 CC, The Netherlands. [2]Department of Analytical Biosciences, Leiden/Amsterdam Center for Drug Research, Leiden University, Leiden, 2333 CC, The Netherlands. [4]Department of Dermatology, Leiden University Medical Center, Leiden, 2333 ZA, The Netherlands

ABSTRACT

Previous studies demonstrated that our in-house human skin equivalents show the presence of all stratum corneum (SC) barrier lipid classes, but show a reduced level of free fatty acids, of which a part is mono-unsaturated. In this study we aimed to improve the SC lipid properties of the Leiden Epidermal Model (LEM) by specific media supplements. For this purpose, the level of the fatty acid mixture (consisting of palmitic, linoleic and arachidonic acid) supplemented to the medium was increased four times or was modified by 1) replacing protonated palmitic acid with deuterated palmitic acid, 2) a fourfold increase in palmitic acid concentration or 3) addition of deuterated arachidic acid. Furthermore, the effect of insulin on the SC mono-unsaturated fatty acid content was studied. The results demonstrate that deuterated palmitic and arachidic acid are taken up into the LEM and are subsequently elongated and incorporated in the SC. Increasing the concentration of arachidonic and linoleic acid resulted in a decreased level of very long chain fatty acids and an increased level of mono-unsaturated fatty acids, while insulin did not affect the fatty acid profile. These results indicate that SC lipid properties can be modulated by specific supplements in the culture medium. This study therefore signifies the importance of medium composition on the SC lipid properties during culture of human skin equivalents.

INTRODUCTION

Human skin has a dual function: it prevents the entry of pathogens and harmful substances into the body and at the same time prevents excess water and electrolyte loss from the body. The permeability barrier of the skin is located in the extracellular lipid domains that surround the corneocytes in the stratum corneum (SC). The predominating lipid classes in human SC are cholesterol, free fatty acids and ceramides. The composition of these lipids in the SC plays an essential role in maintaining the permeability barrier [1-4].

In our previous studies we have demonstrated that our in-house human skin equivalents (HSEs) mimic many aspects of human skin, such as its morphology and the expression of early and late differentiation markers [5]. Nevertheless, these HSEs showed a decreased permeability barrier compared to human skin when the diffusion of bezocaine was analyzed [5]. Detailed examination of the SC lipids of the HSEs revealed that the total SC fatty acid content was reduced, while an increase in mono-unsaturated fatty acid (MUFA) content was observed (Thakoersing *et al., submitted*). Additionally, the SC of the HSEs contains ceramide species with a mono-unsaturated acyl chain. The observation of MUFAs and ceramides with a mono-unsaturated acyl chain indicates that both lipid classes have a common synthetic pathway.

In the previous studies the MUFA level in the SC of the HSEs was not quantified. It is therefore not known to which extent the MUFA level in the HSEs differs from native human SC and to which extent it affects the lipid properties of the SC. The altered fatty acid level and composition are expected to be the key factors for the presence of the mainly hexagonal packing in the HSEs [5] compared to the dense orthorhombic packing observed in human SC [6-8]. Optimization of the SC fatty acid level and composition of HSEs may therefore improve the SC barrier properties of HSEs to allow a better prediction of compound penetration through the skin.

Stearoyl-CoA desaturase (SCD) is an enzyme that catalyzes the biosynthesis of MUFAs from saturated fatty acids [9, 10]. The HSEs show the expression of SCD1 in

the basal and differentiated layers of the epidermis, while this protein is strictly localized in the basal layer of human skin (Thakoersing *et al., submitted*). The increase in MUFA content in the HSEs may therefore be attributed to the increased presence of SCD1 in the differentiated layers of the epidermis, which may result in an increased activity of SCD1. The culture medium used to generate HSEs is supplemented with a fatty acid mixture consisting of palmitic acid, arachidonic acid and linoleic acid. The supplementation of this mixture may influence the SC fatty acid level and composition in the HSEs. Furthermore, the activity of SCD is affected by a variety of factors, including insulin [9-12]. Since the culture medium is also supplemented with insulin, this may influence the activity of SCD1 and therefore affect the SC fatty acid composition of HSEs. In this study we aimed to improve the fatty acid composition and organization in the SC of the Leiden Epidermal Model (LEM) by supplementing and altering the fatty acid and insulin levels in the culture medium. To determine whether the supplemented fatty acids are incorporated in the SC of LEM, protonated palmitic acid was replaced by deuterated palmitic acid. In some experiments the medium of LEM was additionally supplemented with deuterated arachidic acid. SC fatty acid profiling of LEM was performed by a novel LC/MS method. To our knowledge we report for the first time the effect of fatty acid supplementation on the SC lipid organization and composition in epidermal skin models.

MATERIALS AND METHODS

Cell culture

Normal human keratinocytes (NHKs) were established from mammary or abdomen skin, obtained from adult donors undergoing surgery, as described previously [13]. The Declaration of Helsinki principles were followed when working with human tissue. The NHKs were cultured with the Dermalife K medium complete kit (Lifeline Cell Technology, Walkersville, MD) and grown to 80%

confluency before trypsin digestion. First and second passage NHKs were used to generate LEMs.

Generation of the Leiden Epidermal Model (LEM)

LEMs were generated as described previously [5] with minor changes. NHKs (0.2 x 10^6 cells/filter) were seeded onto cell culture inserts (Corning Transwell cell culture inserts, membrane diameter 12 mm, pore size 0.4 μm; Corning Life Sciences, Amsterdam, The Netherlands) and were kept submerged in Dermalife medium until confluency. Hereafter the HSEs were kept submerged in CnT medium (CellnTec, Bern, Switzerland), which was supplemented according to the manufacturer's protocol, and 1% penicillin/streptomycin solution (Sigma, Zwijndrecht, The Netherlands), 0.25 μg/mL insulin (Sigma) and a lipid mixture consisting of 7 μM arachidonic acid (Sigma), 30 μM linoleic acid (Sigma) and 25 μM palmitic acid (Sigma). The LEMs were lifted to the air-liquid interface after two days and were cultured for an additional 12 days before harvesting. In order to improve the SC lipid properties of LEMs, modifications were made to the culture medium that was used during the time the LEMs were air-exposed. The specific modifications are provided in table 1.

Immunohistochemistry

Harvested HSEs were fixed in 4% (w/v) paraformaldehyde (Lommerse Pharma, Oss, The Netherlands), dehydrated and embedded in paraffin. 5 μm sections were cut and used for immunohistochemical staining of stearoyl-CoA desaturase 1 (SCD1; 100x dilution) (Sigma), peroxisome proliferator-activated receptor α and β/δ (PPARα; 200x dilution and PPARβ/δ; 400x dilution) (Acris Antibodies, San Diego, CA). The sections were deparaffinized and rehydrated with xylene and graded ethanol series and finally washed with PBS. The sections were immersed in sodium citrate buffer (pH 6) for 30 minutes close to the boiling point for antigen retrieval. Hereafter the sections were blocked with normal horse serum for 20 min

and incubated overnight at 4ºC with the primary antibody. Next, the sections were incubated with the secondary antibody for 30 minutes, washed with PBS and incubated with ABC reagent for 30 minutes. The sections were consecutively washed with PBS, 0.1 M sodium acetate buffer and incubated for 30 minutes in amino-ethylcarbazole (Sigma) dissolved in N,N-dimethylformamide (1g/250 mL) (Sigma) supplemented with 0.1% hydrogen peroxide and finally washed with water. The sections were counterstained with haematoxylin. R.T.U. Vectastain Elite ABC Reagent Kit (Vector Laboratories, Burlingame, CA) was used for incubations with normal horse serum, secondary antibody and ABC reagent.

Table 1 Adjustment of the culture media

Modification	***Specification***
LEM Control	FFA mix: 25 μM palmitic acid, 30 μM linoleic acid, 7 μM arachidonic acid
LEM C16:0D31	Replacement of protonated palmitic acid with deuterated palmitic acid (C16:0D31) (Isotec, Sigma)
LEM 4x FFA mix	Supplementation of FFA mix increased 4x
LEM 4x C16:0	Supplementation of palmitic acid increased to 100 μM (4x increase)
LEM + C20:0D39	Addition of 47μM deuterated arachidic acid (C20:0D39) (Cambridge Isotope Laboratories, Andover, MA) to FFA mix
LEM No insulin	No insulin added to culture medium
LEM 0.5x insulin	Supplementation of insulin (Sigma) lowered to 0.125 μg/mL medium (2x reduction)

Modifications made to the culture medium during generation of LEMs under air-exposed conditions. C16:0D31= deuterated palmitic acid with 31 deuterium atoms. C20:0D39= deuterated arachidic acid with 39 deuterium atoms.

Stratum corneum isolation

SC of LEM was isolated by overnight incubation on a 0.1% trypsin (Sigma) soaked filter followed by incubation at 37ºC for 1 hour. The SC was separated from the viable epidermis and washed with a 0.1% trypsin inhibitor (Sigma) solution and water. The obtained SC sheets were dried and stored under argon. When using fresh human abdomen or mammary skin, fat tissue was removed and the skin was dermatomed to a thickness of approximately 300 μm. The SC was then isolated as described above.

Lipid extraction and HPTLC analysis

SC samples were extracted according to the Bligh and Dyer procedure with the addition of 0.25M KCl to extract polar lipids as described before [14, 15]. The extracted lipids were analyzed by means of one-dimensional high performance thin layer chromatography (HPTLC) as described before [15]. A standard lipid solution consisting of cholesterol, palmitic acid, stearic acid, arachidic acid, tricosanoic acid, behenic acid, lignoceric acid, cerotic acid and ceramides EOS, NS, NP, EOH and AP was used to identify each lipid (sub)class. Ceramides are named according to the nomenclature defined by Motta *et al.* [16] and extended by Masukawa *et al.* [17]. Briefly, sphingosine (S), dihydrosphingosine (dS), phytosphingosine (P) or 6-hydroxysphingosine (H) represent the sphingoid base structures to which an esterified ω-hydroxy (EO), α-hydroxy (A) or non-hydroxy (N) fatty acid specie is attached via an amide bond. The SC lipid composition of at least 2 human SC donors and 2 LEMs, each generated with the same modified medium, were examined.

Fourier transform infrared spectroscopy (FTIR)

SC samples for FTIR measurements were hydrated at room temperature for 24 hours over a 27% (w/v) NaBr solution. The hydrated SC samples were measured by FTIR as described before [5]. Each spectrum in the frequency range of 600 to

4000 cm^{-1} was obtained during 4 minutes in transmission mode as a co-addition of 256 scans with a resolution of 1 cm^{-1} with a Varian 670-IR FTIR (Agilent Technologies, Santa Clara, CA) equipped with a mercury-cadmium-telluride detector. The phase transitions of the SC lateral lipid organization were examined as a function of temperature from 0ºC to 90ºC with a heating rate of 1ºC/4 min. The FTIR spectra were analyzed with Win-IR pro 3.0 from Bio-Rad (Bio-Rad Laboratories, Cambridge, Massachusetts, USA). At least 2 SC sheets of human SC and LEMs generated with a modified medium composition were measured.

Small angle x-ray diffraction (SAXD)

SAXD measurements were performed at the European Synchrotron Radiation Facility (ESRF) at station BM26B in Grenoble as described before [2, 18]. Prior to the measurement, SC samples were hydrated as described above. The SC samples were placed in specially designed holders and measured at room temperature for 10 minutes. The intensity of scattered x-rays was measured as function of q. Repeat distances of lamellar phases are calculated from the peak positions (q-values) as described elsewhere [5]. At least 2 samples of human SC and LEMs generated with a modified medium content were measured.

Free fatty acid analysis and quantification by LC/MS

Extracted SC lipids were dissolved in chloroform/methanol/heptane (2½:2½:95) to obtain a final lipid concentration of 1 mg/ml. In addition, deuterated stearic acid and deuterated lignoceric acid were added to each sample as internal standards, both with a final concentration of 10 μM. An Alliance 2695 HPLC system (Waters Corp., Milford, MA) was used to inject 10 μl of each sample. A C18 analytical column (LiChroCART Purospher STAR, 55 x 2 mm i.d. Merck, Darmstadt, Germany) was used to separate all free fatty acids using gradient elution at a flow rate of 0.5 ml/min starting from acetonitrile: water (90:10) to methanol: heptane (90:10). In addition, 0.1% acetic acid and 1% chloroform were added to both

mobile phases to obtain chloro adducts, greatly enhancing the ionization efficiency [19, 20]. A TSQ Quantum MS (Thermo Finnigan, San Jose, CA) was used to analyze all free fatty acids as $[M+Cl]^-$ ions. Using an APCI source, the MS was scanning in negative ion mode using a scan range from 200-600 amu while maintaining a discharge current of 5 μA. The scan time was set to 500 ms while the resolution at full width half maximum was 0.7. The capillary and vaporizer temperature were set to respectively 250 and 450ºC. An extensive method description will be reported elsewhere (Van Smeden *et al.*, in preparation). Afterwards, data was analyzed and quantified using Xcalibur software (version 2.0.7, Thermo Scientific, San Jose, CA).

RESULTS

Human SC fatty acids mainly consists of saturated fatty acids, while the SC of LEM shows an increased presence of mono-unsaturated fatty acids

The SC fatty acid chain length distribution and saturation of LEM and human skin were quantified from LC/MS data to determine to which extent they differ from each other. Figure 1 shows the free fatty acid species present in human SC (A) and in LEM (B). In order to compare the relative chain length distribution of the fatty acids in human SC and LEM, the fatty acids were divided into two groups. The long chain fatty acids (LCFAs) are defined as fatty acids with 16-21 carbon atoms, while the very long chain fatty acids (VLCFAs) are defined as fatty acids with 22-38 carbon atoms. In these groups both the saturated fatty acids and MUFAs are included. LEM has an almost 1:1 molar distribution of VLCFAs and LCFAs, while human SC contains approximately three times more VLCFAs compared to LCFAs (figure 1C). The seven most prevailing fatty acid species in human SC and LEM are provided in table 2. In human SC lignoceric acid (C24:0) and cerotic acid (C26:0) account for more than 50% of the total amount of fatty acids. In LEM, however, a drastic reduction in lignoceric and especially cerotic acid (both account for approximately 33% of the total fatty acid level) is observed together with a

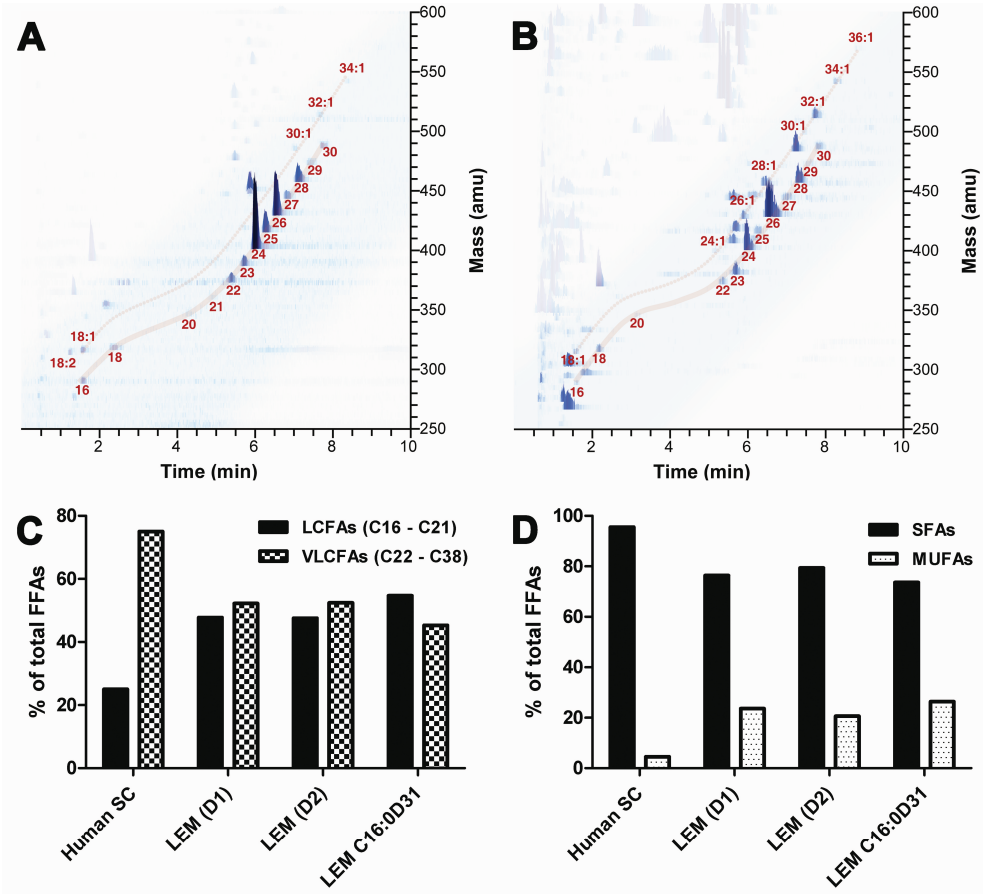

Figure 1. Three dimensional multi-mass LC/MS chromatogram of FFAs in native human SC (A) and control LEM (B) are shown. The retention time is shown on the X-axis, the mass (in amu) is provided on the Y-axis and the intensity of each peak is depicted on the Z-axis. Figure C: relative molar distribution of long chain fatty acids (LCFAs) and very long chain fatty acids (VLCFAs) in the SC of native human skin, control LEM (LEM) and LEM generated with deuterated palmitic acid (LEM C16:0D31). Figure D: relative molar distribution of saturated fatty acids (SFAs) and MUFAs. D1= donor 1, D2= donor2.

large increase in stearic (C18:0) and oleic (C18:1) acid. When comparing the MUFA level, LEM contains 21-26% MUFAs (figure 1D), while this is only 4% in native human SC. These results clearly demonstrate that LEMs have a decreased VLCFA content and an increased MUFA content compared to native human SC.

Substitution of protonated palmitic or arachidic acid with their deuterated counterparts does not alter the SC lipid composition or organization

It is unknown whether the fatty acids that are supplemented to the culture medium are taken up by keratinocytes and are subsequently incorporated into SC lipids. To investigate this fatty acid uptake, protonated palmitic acid (C16:0), which is part of the standard supplement of the LEM culture medium, was substituted by deuterated palmitic acid (C16:0D31). HPTLC analysis revealed that the SC lipid composition of the LEMs fed with deuterated palmitic acid does not differ from the control (data not shown). Both LEMs show the presence of all SC barrier lipid classes, namely cholesterol, free fatty acids and all ceramides subclasses. The free fatty acid chain length distribution and saturation remains similar compared to the control (figure 1C and D). Additionally, both the controls as well as the LEMs treated with deuterated palmitic acid show the presence of only the long periodicity phase with a repeat distance of approximately 12 nm. Additionally, from around 20ºC and higher the lipids form only a hexagonal packing (table 3). This indicates that the lipid composition and organization does not differ between the control and LEMs generated with deuterated palmitic acid.

Deuterated arachidic acid (C20:0D39) was used to determine whether fatty acids with carbon chains longer than that of palmitic acid are taken up from the medium and are incorporated in the SC lipids and thereby increase the fraction of SC fatty acids with longer acyl chains. The addition of deuterated arachidic acid does not affect the SC lateral and lamellar lipid organization (table 3) or SC fatty acid composition (figure 4A-C and table 2) compared to the control.

Table 2. Prevailing free fatty acids in human SC and LEMs

	C16:1	C16:0	C18:1	C18:0	C20:0	C22:0	C24:0	C25:0	C26:0	C28:0	SUM
Human skin	1.9	**11.5**	2.2	**8.5**	0.7	**4.5**	**34.8**	**6.0**	**20.9**	**4.0**	**93.1**
Control (D1)	ND	**11.2**	**14.4**	**16.9**	**4.0**	**8.4**	**24.2**	0.2	**9.5**	1.6	**90.5**
Control (D2)	2.7	**12.8**	**10.7**	**16.1**	**4.6**	**9.2**	**23.4**	0.7	**9.5**	2.0	**89.1**
+C20:0D39 (D1)	0.8	**9.1**	**9.4**	**13.7**	**3.6**	**8.9**	**29.5**	0.4	**15.7**	2.7	**93.0**
+C20:0D39 (D2)	2.1	**14.6**	**17.4**	**16.1**	**4.1**	**8.3**	**19.8**	0.4	**8.1**	1.4	**90.3**
4x FFA mix (D1)	**4.2**	**18.0**	**25.2**	**19.8**	2.8	**4.8**	**12.5**	0.1	**4.3**	0.7	**88.2**
4x FFA mix (D2)	**5.3**	**17.8**	**33.9**	**17.3**	2.5	**4.1**	**9.1**	0.5	**3.1**	0.6	**88.9**
4x C16:0 (D1)	1.2	**11.3**	**7.5**	**15.4**	**3.6**	**9.0**	**28.2**	0.4	**15.2**	2.5	**93.1**
4x C16:0 (D2)	**4.8**	**17.2**	**23.3**	**14.4**	2.5	**5.7**	**16.8**	0.2	**8.0**	1.3	**89.3**
1/2 insulin (D1)	1.6	**16.3**	**13.8**	**18.8**	**3.9**	**7.7**	**21.2**	0.2	**7.9**	1.3	**91.1**
1/2 insulin (D2)	1.1	**12.6**	**12.8**	**15.7**	**3.6**	**8.3**	**24.0**	0.5	**11.1**	1.8	**90.4**
No insulin (D1)	1.2	**14.9**	**16.6**	**19.4**	**4.0**	**7.7**	**19.7**	0.3	**7.1**	1.1	**90.7**
No insulin (D2)	2.1	**20.4**	**13.9**	**24.3**	**3.0**	**6.0**	**15.8**	0.3	**6.7**	1.1	**91.4**

Table 2 shows an overview of the relative prevalence (mole %) of free fatty acid species in human skin and LEMs generated with a different medium composition. The seven most prevailing free fatty acids in each sample (highlighted in bold) were determined to examine shifts in prevailing free fatty acid species between different samples. D1= donor 1, D2= donor2, ND= not detected.

Table 3. SC lipid properties of LEMs generated with different media suppelemts

	2nd order LPP (nm)		Hexagonal packing (ºC)	
	Donor 1	Donor 2	Donor 1	Donor 2
LEM control	6.0 ± 0.1 (n=8)		23.4 ± 3.8 (n=7)	
LEM C16:0D31	5.9	6.0	20	22
LEM +C20:0D39	5.9	5.9	28	20
LEM 4x FFAs	5.3	5.5	12	0
LEM 4x C16:0	5.9	5.9	30	24
LEM no insulin	5.7	5.9	12	18
LEM 0.5x insulin	5.8	5.7	20	20

Deuterated palmitic and arachidic acid are incorporated in the SC lipid matrix of LEM

FTIR offers the opportunity to determine whether deuterated palmitic and arachidic acid are incorporated in the SC lipids. The vibrations of the deuterated lipids result in shifted peak positions in the FTIR spectrum compared to the peak positions belonging to the vibrations of their protonated counterparts. The FTIR symmetric CH_2 stretching vibration observed around 2850 cm^{-1} provides information about the conformational disordering. The frequency of the CH_2 symmetric stretching vibration indicates whether the lipids are present in a crystalline phase, namely the orthorhombic or hexagonal phase, or in the liquid phase [21, 22]. When lipids are arranged in a crystalline packing the symmetric CH_2 stretching frequency is below 2850 cm^{-1}, but when they are in a liquid packing the conformational disorder increases. This is reflected in a steep increase in symmetric stretching frequency to 2852-2854 cm^{-1}. In the FTIR spectrum the symmetric stretching frequency of deuterated lipids is located around 2090 cm^{-1}. The transition from a crystalline to liquid phase can be recognized by a steep increase in wavenumber to 2096 cm^{-1}. The order-disorder transition temperature observed for the controls and LEMs treated with deuterated palmitic or arachidic acid overlap (figure 2A). The presence of the 2090 cm^{-1} CD_2 stretching vibration peak in the spectrum of the LEMs cultured with deuterated palmitic or arachidic acid clearly demonstrates that the deuterated fatty acids added to the culture medium are taken up by basal keratinocytes and are present in the SC lipids. To determine whether the deuterated lipids were incorporated into the SC lipid phases or formed separate lipid domains, the CD_2 scissoring vibrations around 1090 cm^{-1} were examined. If deuterated palmitic or arachidic acid form separate lipid domains an orthorhombic lateral packing is observed, which is characterized by two vibrations. However, only one peak is observed in the FTIR spectrum of the LEMs treated with deuterated palmitic or arachidic acid (figure 2B). Therefore there are no indications

that separate domains of palmitic or arachidic acid are present in the SC of the LEMs.

The deuterated symmetric stretching vibration around 2090 cm^{-1} and scissoring vibration around 1090 cm^{-1} of LEMs treated with deuterated arachidic acid have a lower intensity than observed for LEMs treated with deuterated palmitic acid. This indicates that a higher amount of deuterated palmitic acid is present in the SC of LEM, even though a higher molar amount of deuterated arachidic acid is added to the medium. Taking this into consideration, it is of more interest to supplement the medium with palmitic acid than arachidic acid.

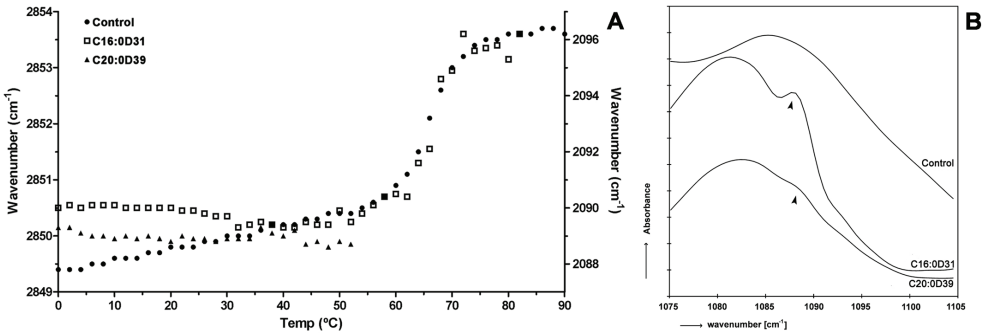

Figure 2. A: protonated and deuterated symmetric stretching frequencies around 2850 and 2090 cm^{-1}, respectively. B: deuterated scissoring vibration in the control LEM and LEM treated with deuterated palmitic or arachidic acid. The arrow head indicates the deuterated scissoring vibration at 1088 cm^{-1}.

Deuterated palmitic and arachidic acid are present as various elongated fatty acid species in the SC of LEM

The SC fatty acid composition of LEMs treated with deuterated palmitic or arachidic acid was studied by LC/MS to verify whether deuterated lipids are indeed present in the SC. As can be observed from figure 3, the LC/MS method is able to detect deuterium labelled fatty acids since the added internal standard (C24:0D47) is observed in the chromatograms, bearing a mass of 47.3 amu higher than protonated lignoceric acid (C24:0). The LC/MS profile of LEMs treated with

deuterated palmitic acid show the presence of lipid peaks (figure 3B) which are not observed in the control LEM (figure 3A). The molecular weight of these lipids corresponds exactly to the molecular weight of saturated fatty acid species with a chain length varying from C20:0 to C28:0 with the addition of 31.2 mass units. The increase in 31.2 mass units corresponds to the higher molecular weight of deuterated palmitic acid compared to protonated palmitic acid. These results demonstrate that palmitic acid added to the culture medium is taken up by the keratinocytes and is subsequently elongated in the viable epidermis to longer fatty

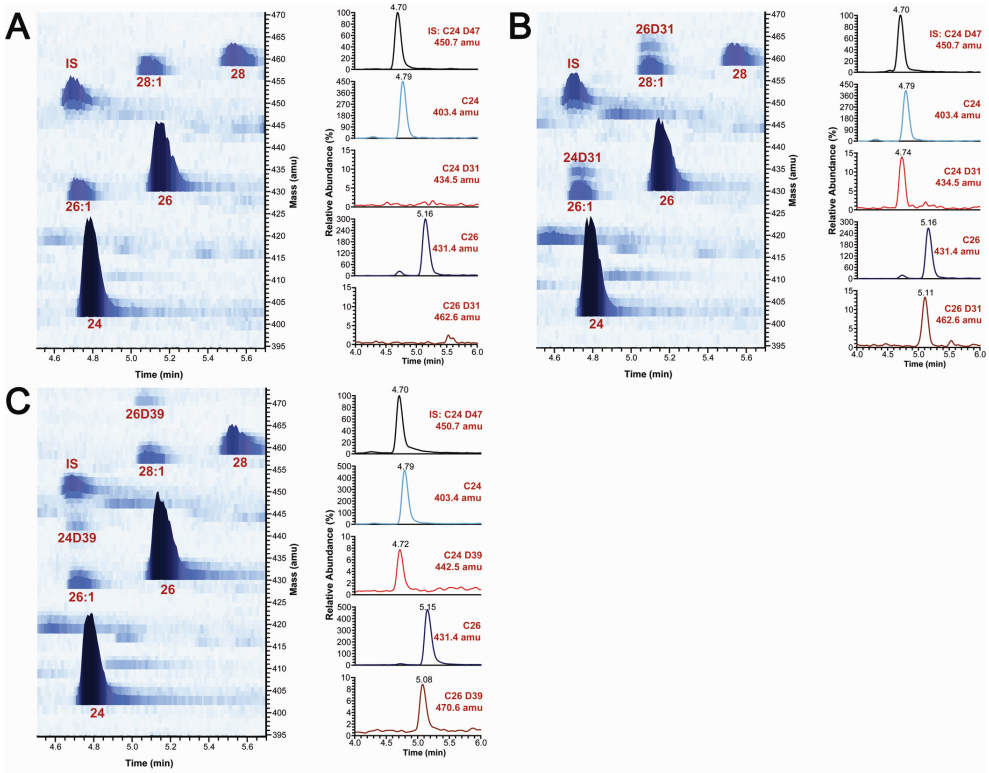

Figure 3. Three dimensional multi mass chromatogram and retention times of individual fatty acids in the SC of control LEM (A) and LEM generated with deuterated palmitic (B) or arachidic acid (C). The deuterated fatty acids have a slightly shifted retention time compared to the corresponding protonated fatty acids, similarly as observed for the deuterated internal standard C24:0D47 (IS) and protonated C24:0.

acid species. At the final differentiation step it is used to generate the extracellular lipid matrix in the SC. The LC/MS fatty acid profile of LEMs treated with deuterated arachidic acid also shows the presence of lipid peaks which are not present in the control (figure 3C and A, respectively). These lipid peaks have an increase of 39.2 mass units compared to protonated fatty acids (ranging from C20:0 to C28:0), which corresponds to the molecular weight difference between deuterated and protonated archidic acid. This indicates that arachidic acid can also be elongated to longer fatty acid species in LEM.

High amounts of polyunsaturated fatty acids added to the culture medium result in a deteriorated SC lipid organization and free fatty acid composition

After having demonstrated that palmitic acid in the culture medium can be elongated and incorporated in the SC lipids of LEMs, different approaches were used to increase the SC fatty acid content and to shift their composition in the direction of the VLCFA level observed for human SC. The total fatty acid mixture (palmitic acid, arachidonic acid and linoleic acid; FFA mix) concentration in the culture medium was increased four times. Since we observed elongation of supplemented deuterated palmitic acid to fatty acids with longer carbon chains in the viable epidermis of LEMs, the addition of extra palmitic acid may not only increase the total fatty acid content, but also increase the content of VLCFAs.

HPTLC analysis reveals that the intensity of cholesterol and free fatty acid bands are similar in the control and one LEM donor generated with a fourfold increased FFA mix, while the other donor even showed a reduced free fatty acid intensity compared to the control (figure 4A). This indicates that there is no increase in fatty acid content in SC of LEM when the fatty acid mixture is increased four times. FTIR and SAXD analyses, however, show that the SC lipid organization is altered, albeit not in the desired manner. A fourfold increase in FFA mix supplementation reduces the repeat distance of the lipid lamellae and the temperature at which only a hexagonal phase is present (table 3). The LC/MS results demonstrate that the

increased addition of the FFA mix markedly reduces the level of VLCFAs and increases the MUFA content (figure 4B and C). The main differences in fatty acid composition between the LEMs treated with a fourfold higher FFA mix and the control is an increase in oleic acid and a decrease in lignoceric acid (table 2). Although the palmitic acid concentration is increased in the culture medium, no major increase in palmitic acid level is observed compared to the control (table 2). This study demonstrates that the VLCFA and MUFA content in LEM even further deviates from the VLCFA and MUFA content of human SC when supplementation of linoleic, arachidonic acid and palmitic acid is increased.

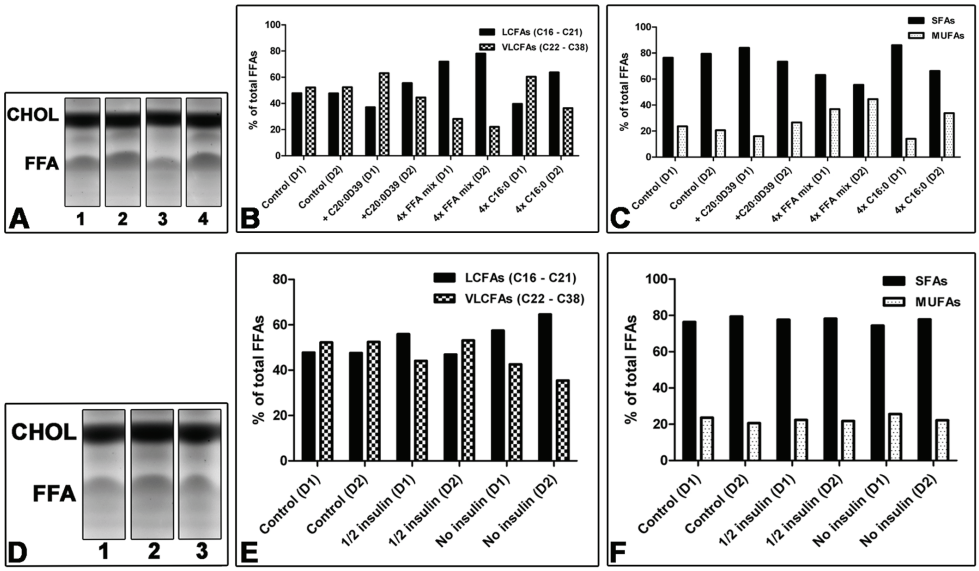

Figure 4. A: SC cholesterol (CHOL) and free fatty acid (FFA) content of control LEM (lane 1), LEM with deuterated arachidic acid (lane 2), LEM with a fourfold higher fatty acid mixture (lane 3) and LEM with a fourfold higher palmitic acid content (lane 4). D: SC cholesterol and free fatty acid content of control LEM (lane 1), LEM with a twofold reduction in medium insulin concentration (lane 2) and LEM with medium containing no supplemented insulin (lane 3). B and E: relative molar distribution of long chain fatty acids (LCFAs) and very long chain fatty acids (VLCFAs). C and F: relative molar distribution of saturated fatty acids (SFAs) and mono-unsaturated fatty acids (MUFAs).

Increase of palmitic acid supplementation does not alter SC lipid composition and organization in LEM

Another approach to increase the SC fatty acid content of LEMs was to increase the palmitic acid concentration four times, while the arachidonic (C20:4) and linoleic acid (C18:2) concentration remained similar. These LEMs show no differences in intensity of the fatty acid and cholesterol bands compared to the control in their HPTLC lipid profile (figure 4A). This indicates that the increase in palmitic acid concentration does not lead to dramatic differences in the total free fatty acid level in SC. The increase in palmitic acid concentration also did not affect the lamellar lipid organization or lead to a pronounced difference in the temperature at which only the hexagonal phase is present compared to the controls (table 3). LEMs treated with a fourfold increase in palmitic acid concentration also show no considerable difference in their VLCFA and MUFA content compared to the controls (figure 4B and C). Furthermore, they do not show marked differences in the relative content of individual fatty acid species, including palmitic acid (table 2), compared to the controls. This demonstrates that no pronounced differences in the fatty acid chain length distribution or degree of saturation occurs by only increasing the palmitic acid concentration in the medium four times.

The fourfold increased FFA mix has four times more arachidonic and linoleic acid compared to the four fold increase in palmitic acid supplementation. This indicates that the increased addition of these two polyunsaturated fatty acids to the medium is probably the cause of the deteriorated lipid organization observed in LEMs treated with a fourfold higher FFA mix.

Reduction of insulin concentration in the medium does not reduce SCD1 expression

It has been reported that a reduction in insulin level leads to decreased SCD activity [10, 11] and thus a reduction in MUFA levels. For this reason the insulin concentration of the medium was lowered. No difference in free fatty acid content can be detected with HPTLC (figure 4D) regardless of the insulin concentration in the medium. Additionally, reduction of insulin supplementation does not lead to differences in lipid organization (table 3), fatty acid chain length distribution or a decrease in MUFA level compared to the control (figure 4E and F). Concurrently, expression of SCD1 in LEMs generated with media containing a reduced insulin concentration remains unaltered compared to the control (figure 5A). Under these conditions SCD1 is expressed in the basal and differentiated layers in LEM, while in human skin the expression of SCD1 is strictly localized in the basal layer.

Peroxisome proliferator-activated receptors (PPARs) are important in the regulation of lipid homeostasis in human keratinocytes. Endogenous fatty acids and their derivatives are activators of PPARs [23-25]. Forman *et al.* [26] demonstrated that polyunsaturated fatty acids such as arachidonic and linoleic acid are efficient activators of two PPAR isoforms, namely PPARα and PPARβ/δ. The expression pattern of these two PPARs were therefore determined in LEM (control) and compared to native human skin. LEM shows a similar expression pattern of PPARα and PPARβ/δ in the viable epidermis as native human skin (figure 5B). PPARα is mainly expressed in the nuclei of the keratinocytes in the viable epidermis, but also shows some staining of the cytosol. PPARβ/δ is detected in the nuclei and cytosol of the entire viable epidermis. Altering the free fatty acid supplementation or reducing the insulin concentration in the medium did not result in changes in PPARα and PPARβ/δ expression in LEM (data not shown).

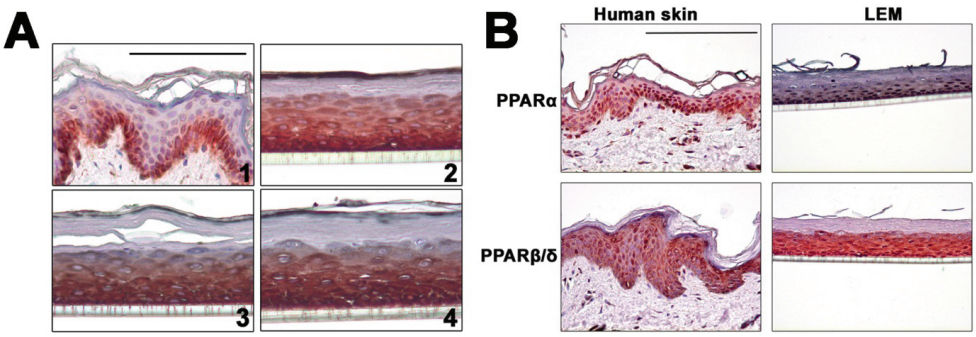

Figure 5. A: Immunohistochemical staining showing the expression pattern of stearoyl-CoA desaturase 1 in native human skin (1), control LEM (2), LEM generated in medium with a twofold lower insulin concentration (3) and LEM generated without insulin in the culture medium (4). B: Immunohistochemical staining showing the expression pattern of PPARα and PPARβ/δ in native human skin and control LEM. Scale bars represent 50 μm.

DISCUSSION

Reconstructed epidermal models mimic epidermal morphogenesis of human skin to a high degree. For this reason a number of commercial HSEs have been used for safety testing of compounds [27-30]. However, these models do not fully mimic the SC barrier properties of human skin and therefore can provide an overestimation of compound penetration [31-36]. Only a few studies have been dedicated to optimize the SC barrier properties of HSEs [31, 37]. Generally the culture medium is modulated by supplementing compounds that have beneficial effects on the SC lipid properties of HSEs. This indicates that optimization of the culture medium shows potential to improve the SC barrier properties of HSEs. We demonstrated that the SC of LEM, our in-house HSE, has a decreased free fatty acid level and an increased presence of MUFAs compared to human SC. These two factors may be key factors for the decreased permeability barrier observed for LEM [5]. We aimed to improve the SC fatty acid composition of LEM by adding fatty acids to the culture medium or reducing the medium insulin level. A number of SC barrier properties were examined in great detail by different techniques.

Additionally, a novel LC/MS method was used to quantitatively determine the MUFA level and distribution of FFA species in the SC of LEM. The presented results show that LEM has approximately 1.5x less VLCFAs and 5-6x more MUFAs than observed in human SC. The detection of elongated deuterated fatty acid species in the SC of LEMs after supplementation of the medium with deuterated palmitic or arachidic acid explicitly demonstrates that SC lipids do not necessarily need to be derived from *de novo* synthesis, but may also originate from external sources. Increasing the amount of fatty acids added to the culture medium therefore appeared to be a straightforward approach to increase the SC fatty acid level in LEM. Increasing the palmitic acid supplementation four times, however, does not result in an improved chain length distribution of free fatty acids in LEM. This indicates that the altered free fatty acid distribution observed in LEM compared to human SC is not caused by a deficiency of palmitic acid in the culture medium.

Palmitic acid is a building block for many lipid species, such as longer fatty acids, phospholipids, ceramides, diacylglycerides (DAG) and triacylglycerides (TAG). It is possible that the extra palmitic acid added to the culture medium is incorporated into the latter two lipid species, considering that LEMs have an increased DAG and TAG content (data not shown). Fatty acids may therefore be available to a lesser extent for the synthesis of phospholipids, which are degraded to fatty acids at the stratum granulosum/SC interface [38].

LEMs generated without fatty acids supplemented to the culture medium did not show reproducible results concerning their morphology, SC lipid organization and composition. This indicates that fatty acid supplementation is required to generate LEMs. The irreproducible results may be due to keratinocyte donor variations in fatty acid synthesis or differentiation and proliferation responses when free fatty acids are omitted from the culture medium.

LEM has a reduced VLCFA content compared to native human SC. Increasing the VLCFA content in the SC of LEM cannot be achieved by supplementation of the

medium with fatty acids longer than palmitic acid, since they are taken up to a lesser extent by keratinocytes than palmitic acid. In native human epidermis VLCFAs are generated by the activity of several elongases [39, 40]. The reduction of VLCFAs in LEMs may therefore be caused by a reduced activity of elongases.

The deteriorated SC lipid organization of LEMs in which the FFA mix supplementation was increased four times is most probably due to the increased MUFA level. As far as the increased hexagonal packing is concerned, we observed that an increased level of MUFAs in lipid mixtures comprised of fatty acids, ceramides and cholesterol increases the formation of the hexagonal packing (Janssens *et al.*, unpublished data). By increasing the supplementation of the FFA mix four times, the endogenous levels of palmitic, linoleic and arachidonic acid in the keratinocytes may have increased. This may have led to an imbalanced activation of PPARs and consequently an altered SC lipid composition and organization in LEMs treated with a fourfold higher FFA mix.

Insulin is a potent hormone that regulates carbohydrate and fat metabolism in the body. However, the reduction or complete omission of insulin supplementation to the culture medium does not lead to apparent changes in the SC lipid organization or fatty acid composition. It still remains to be established why the LEMs generated with lower insulin concentrations compared to the control show only minor changes in the SC lipid composition and organization. However, several studies have shown that the accumulation of e.g. DAG decrease insulin action [41, 42]. Since LEM have an increased DAG content in the SC compared to human SC, it may indicate that the keratinocytes may have a reduced response to insulin.

Novel approaches are required to improve the SC lipid properties of LEM. SCD1 activity in HSEs needs to be determined and compared to native human skin. If needed, a reduction of SCD1 activity to decrease the MUFA content may be achieved by adding (synthetic) SCD inhibitors [10, 11, 43] to the culture medium.

LEMs show a relatively higher content of DAG and TAG in their SC compared to human SC. DAG and TAG are generated through the action of monoacylglycerol

acyltransferase (MGAT) and diacylglycerol acyltransferase (DGAT), respectively [44]. An increase in total fatty acid content may be achieved by partial inhibition of MGAT and DGAT activity [44].

In conclusion, we have clearly shown that modification of lipid supplementation is not sufficient to improve the SC lipid composition and consequently the SC barrier function of LEM. Therefore, different approaches are needed to optimize the SC lipid composition of LEM. The increased content of MUFAs, DAG and TAG in SC of LEM suggest that the SC lipid composition might be improved by modulating the activity of enzymes such as SCD1, MGAT en DGAT. This may contribute to the development of a new generation of HSEs that harbor a competent SC barrier that even more closely resembles the SC lipid composition and organization of native human SC than the current LEMs.

ACKNOWLEDGEMENTS

The authors would like to thank Maria Ponec for helpful suggestions during the meetings. We would also like to thank the personnel at the DUBBLE beam line at the ESRF for their support with the x-ray measurements. This research was financially supported by the Dutch Technology Foundation STW (grant no. 7503).

REFERENCES

1. Choi, M.J. and Maibach, H.I. Role of ceramides in barrier function of healthy and diseased skin. Am J Clin Dermatol **6,** 215, 2005.
2. Janssens, M., van Smeden, J., Gooris, G.S., Bras, W., Portale, G., Caspers, P.J., Vreeken, R.J., Kezic, S., Lavrijsen, A.P. and Bouwstra, J.A. Lamellar lipid organization and ceramide composition in the stratum corneum of patients with atopic eczema. J Invest Dermatol **131,** 2136, 2011.
3. Lavrijsen, A.P., Bouwstra, J.A., Gooris, G.S., Weerheim, A., Bodde, H.E. and Ponec, M. Reduced skin barrier function parallels abnormal stratum corneum lipid organization in patients with lamellar ichthyosis. J Invest Dermatol **105,** 619, 1995.
4. Proksch, E., Folster-Holst, R., Brautigam, M., Sepehrmanesh, M., Pfeiffer, S. and Jensen, J.M. Role of the epidermal barrier in atopic dermatitis. J Dtsch Dermatol Ges **7,** 899, 2009.
5. Thakoersing, V.S., Gooris, G., Mulder, A.A., Rietveld, M., El Ghalbzouri, A. and Bouwstra, J.A. Unravelling Barrier Properties of Three Different In-House Human Skin Equivalents. Tissue Eng Part C Methods 2011.
6. Bouwstra, J.A., Gooris, G.S., Dubbelaar, F.E. and Ponec, M. Phase behavior of lipid mixtures based on human ceramides: coexistence of crystalline and liquid phases. J Lipid Res **42,** 1759, 2001.
7. Bouwstra, J.A., Gooris, G.S., van der Spek, J.A. and Bras, W. Structural investigations of human stratum corneum by small-angle X-ray scattering. J Invest Dermatol **97,** 1005, 1991.
8. Damien, F. and Boncheva, M. The extent of orthorhombic lipid phases in the stratum corneum determines the barrier efficiency of human skin in vivo. J Invest Dermatol **130,** 611, 2010.
9. Flowers, M.T. and Ntambi, J.M. Role of stearoyl-coenzyme A desaturase in regulating lipid metabolism. Curr Opin Lipidol **19,** 248, 2008.
10. Ntambi, J.M. and Miyazaki, M. Regulation of stearoyl-CoA desaturases and role in metabolism. Prog Lipid Res **43,** 91, 2004.
11. Mauvoisin, D. and Mounier, C. Hormonal and nutritional regulation of SCD1 gene expression. Biochimie **93,** 78, 2011.
12. Ntambi, J.M. Regulation of stearoyl-CoA desaturase by polyunsaturated fatty acids and cholesterol. J Lipid Res **40,** 1549, 1999.

13. Bouwstra, J.A., Groenink, H.W., Kempenaar, J.A., Romeijn, S.G. and Ponec, M. Water distribution and natural moisturizer factor content in human skin equivalents are regulated by environmental relative humidity. J Invest Dermatol **128,** 378, 2008.
14. Bligh, E.G. and Dyer, W.J. A rapid method of total lipid extraction and purification. Can J Biochem Physiol **37,** 911, 1959.
15. Thakoersing, V.S., Ponec, M. and Bouwstra, J.A. Generation of human skin equivalents under submerged conditions-mimicking the in utero environment. Tissue Eng Part A **16,** 1433, 2010.
16. Motta, S., Monti, M., Sesana, S., Caputo, R., Carelli, S. and Ghidoni, R. Ceramide composition of the psoriatic scale. Biochim Biophys Acta **1182,** 147, 1993.
17. Masukawa, Y., Narita, H., Shimizu, E., Kondo, N., Sugai, Y., Oba, T., Homma, R., Ishikawa, J., Takagi, Y., Kitahara, T., Takema, Y. and Kita, K. Characterization of overall ceramide species in human stratum corneum. J Lipid Res **49,** 1466, 2008.
18. Bras, W., Dolbnya, I.P., Detollenaere, D., Van Tol, R., Malfois, M., Greaves, G.N., Ryan, A.J. and Heeley, E. Recent experiments on a combined small-angle/wide-angle X-ray scattering beam line at the ESRF. Journal of Applied Crystallography **36,** 791, 2003.
19. Gao, S., Zhang, Z.P. and Karnes, H.T. Sensitivity enhancement in liquid chromatography/atmospheric pressure ionization mass spectrometry using derivatization and mobile phase additives. J Chromatogr B Analyt Technol Biomed Life Sci **825,** 98, 2005.
20. Kato, Y. and Numajiri, Y. Chloride attachment negative-ion mass spectra of sugars by combined liquid chromatography and atmospheric pressure chemical ionization mass spectrometry. J Chromatogr **562,** 81, 1991.
21. Mendelsohn, R. and Moore, D.J. Infrared determination of conformational order and phase behavior in ceramides and stratum corneum models. Methods Enzymol **312,** 228, 2000.
22. Moore, D.J., Rerek, M.E. and Mendelsohn, R. Lipid domains and orthorhombic phases in model stratum corneum: evidence from Fourier transform infrared spectroscopy studies. Biochem Biophys Res Commun **231,** 797, 1997.
23. Feingold, K.R. and Jiang, Y.J. The mechanisms by which lipids coordinately regulate the formation of the protein and lipid domains of the stratum corneum: Role of fatty acids, oxysterols, cholesterol sulfate and ceramides as signaling molecules. Dermatoendocrinol **3,** 113, 2011.

24. Schmuth, M., Jiang, Y.J., Dubrac, S., Elias, P.M. and Feingold, K.R. Thematic review series: skin lipids. Peroxisome proliferator-activated receptors and liver X receptors in epidermal biology. J Lipid Res **49,** 499, 2008.
25. Sertznig, P., Seifert, M., Tilgen, W. and Reichrath, J. Peroxisome proliferator-activated receptors (PPARs) and the human skin: importance of PPARs in skin physiology and dermatologic diseases. Am J Clin Dermatol **9,** 15, 2008.
26. Forman, B.M., Chen, J. and Evans, R.M. Hypolipidemic drugs, polyunsaturated fatty acids, and eicosanoids are ligands for peroxisome proliferator-activated receptors alpha and delta. Proc Natl Acad Sci U S A **94,** 4312, 1997.
27. Alepee, N., Tornier, C., Robert, C., Amsellem, C., Roux, M.H., Doucet, O., Pachot, J., Meloni, M. and de Brugerolle de Fraissinette, A. A catch-up validation study on reconstructed human epidermis (SkinEthic RHE) for full replacement of the Draize skin irritation test. Toxicol In Vitro **24,** 257, 2010.
28. Gibbs, S. In vitro irritation models and immune reactions. Skin Pharmacol Physiol **22,** 103, 2009.
29. Netzlaff, F., Lehr, C.M., Wertz, P.W. and Schaefer, U.F. The human epidermis models EpiSkin, SkinEthic and EpiDerm: an evaluation of morphology and their suitability for testing phototoxicity, irritancy, corrosivity, and substance transport. Eur J Pharm Biopharm **60,** 167, 2005.
30. El Ghalbzouri, A., Siamari, R., Willemze, R. and Ponec, M. Leiden reconstructed human epidermal model as a tool for the evaluation of the skin corrosion and irritation potential according to the ECVAM guidelines. Toxicol In Vitro **22,** 1311, 2008.
31. Batheja, P., Song, Y., Wertz, P. and Michniak-Kohn, B. Effects of growth conditions on the barrier properties of a human skin equivalent. Pharm Res **26,** 1689, 2009.
32. Schmook, F.P., Meingassner, J.G. and Billich, A. Comparison of human skin or epidermis models with human and animal skin in in-vitro percutaneous absorption. Int J Pharm **215,** 51, 2001.
33. Netzlaff, F., Kaca, M., Bock, U., Haltner-Ukomadu, E., Meiers, P., Lehr, C.M. and Schaefer, U.F. Permeability of the reconstructed human epidermis model Episkin in comparison to various human skin preparations. Eur J Pharm Biopharm **66,** 127, 2007.
34. Schafer-Korting, M., Bock, U., Diembeck, W., Dusing, H.J., Gamer, A., Haltner-Ukomadu, E., Hoffmann, C., Kaca, M., Kamp, H., Kersen, S., Kietzmann, M., Korting, H.C., Krachter, H.U., Lehr, C.M., Liebsch, M., Mehling, A., Muller-Goymann, C., Netzlaff, F., Niedorf, F., Rubbelke, M.K., Schafer, U., Schmidt, E., Schreiber, S.,

Spielmann, H., Vuia, A. and Weimer, M. The use of reconstructed human epidermis for skin absorption testing: Results of the validation study. Altern Lab Anim **36,** 161, 2008.

35. Asbill, C., Kim, N., El-Kattan, A., Creek, K., Wertz, P. and Michniak, B. Evaluation of a human bio-engineered skin equivalent for drug permeation studies. Pharm Res **17,** 1092, 2000.
36. Zghoul, N., Fuchs, R., Lehr, C.M. and Schaefer, U.F. Reconstructed skin equivalents for assessing percutaneous drug absorption from pharmaceutical formulations. Altex **18,** 103, 2001.
37. Ponec, M., Weerheim, A., Kempenaar, J., Mulder, A., Gooris, G.S., Bouwstra, J. and Mommaas, A.M. The formation of competent barrier lipids in reconstructed human epidermis requires the presence of vitamin C. J Invest Dermatol **109,** 348, 1997.
38. Mao-Qiang, M., Feingold, K.R., Jain, M. and Elias, P.M. Extracellular processing of phospholipids is required for permeability barrier homeostasis. J Lipid Res **36,** 1925, 1995.
39. Jakobsson, A., Westerberg, R. and Jacobsson, A. Fatty acid elongases in mammals: their regulation and roles in metabolism. Prog Lipid Res **45,** 237, 2006.
40. Ohno, Y., Suto, S., Yamanaka, M., Mizutani, Y., Mitsutake, S., Igarashi, Y., Sassa, T. and Kihara, A. ELOVL1 production of C24 acyl-CoAs is linked to C24 sphingolipid synthesis. Proc Natl Acad Sci U S A **107,** 18439, 2010.
41. Samuel, V.T., Petersen, K.F. and Shulman, G.I. Lipid-induced insulin resistance: unravelling the mechanism. Lancet **375,** 2267, 2010.
42. Timmers, S., Schrauwen, P. and de Vogel, J. Muscular diacylglycerol metabolism and insulin resistance. Physiol Behav **94,** 242, 2008.
43. Liu, G. Stearoyl-CoA desaturase inhibitors: update on patented compounds. Expert Opin Ther Pat **19,** 1169, 2009.
44. Shi, Y. and Cheng, D. Beyond triglyceride synthesis: the dynamic functional roles of MGAT and DGAT enzymes in energy metabolism. Am J Physiol Endocrinol Metab **297,** E10, 2009.

7

Shedding Light on the Expression and Activity of Specific Desquamatory Enzymes in Human Skin Equivalents

ABSTRACT

Human skin equivalents (HSEs) resemble human skin to a great extent. However, one limitation of HSEs is their increasing stratum corneum (SC) thickness as the culture period is prolonged. In human skin the superficial layers of the SC are normally shed off in a process referred to as desquamation. The aim of this study was to identify possible causes for the impaired desquamation process observed for HSEs. For this purpose the number of SC layers, expression pattern and activity of specific desquamatory enzymes of our in-house HSEs, fresh native human skin and native human skin cultured for one or two weeks were determined. The results demonstrate that the HSEs and human skin cultured for two weeks have an increased number of SC layers compared to native human skin. All HSEs and cultured human skin show a similar expression of kallikrein 5 as native human skin. However, almost all HSEs show the expression of Lympho-epithelial Kazal type related inhibitor (LEKTI) in more differentiated epidermal layers compared to native human skin. In one of the HSEs the activity of kallikrein 5 and 7 was determined in the uppermost SC layers: a decreased kallikrein 5 activity was observed compared to native human SC. These results suggest that a reduced kallikrein 5 activity and altered expression of LEKTI may contribute to the impaired desquamation process in some HSEs.

INTRODUCTION

The stratum corneum (SC) is the outermost layer of the epidermis. It is composed of dead cells, referred to as corneocytes, which are embedded in a lipid matrix. The SC forms the first and main barrier against penetration of exogenous substances and pathogens into the body. In order to maintain a proper skin barrier function, the SC is continuously renewed and thereby maintains approximately the same number of SC layers. The inner SC layers are replenished by new corneocytes, while the upper SC layers are shed off. The latter is referred to as the desquamation process. The turnover time of the SC depends on the anatomical location and takes around four weeks [1].

The adhesion of corneocytes in the SC is maintained by corneodesmosomes and lipid lamellae. In order to shed off the most superficial SC layers corneodesmosomes are degraded by several proteases. In this process cadherins and kallikreins (KLKs) play a central role [1-4]. When focusing on kallikreins especially KLK 5 (stratum corneum tryptic enzyme) and KLK 7 (stratum corneum chymotryptic enzyme) are involved in the desquamation process. In the viable epidermis the KLKs are located in lamellar bodies. Once the lamellar bodies are extruded at the stratum granulosum/SC interface, KLK 5 will activate KLK 7 and itself. However, the proteolytic activity of the KLKs is regulated by Lympho-epithelial Kazal type related inhibitor (LEKTI) in a pH dependent matter [5]. Human SC has a pH gradient that ranges from pH 7.5 at the inner SC layers to ~pH 5 at the SC surface [6]. At a physiological pH LEKTI and the KLKs form a stable complex. The association of LEKTI and KLKs at this pH therefore prevents premature proteolysis of corneodesmosomes in the inner SC layers. As the pH decreases towards the SC surface, LEKTI dissociates from the KLKs and thereby enables the start of the desquamation process. At acidic pH KLK activity is sufficient to complete corneodesmolysis.

Human skin equivalents (HSEs) form a fully differentiated epidermis, which includes a SC. However, as the culture period is prolonged, the SC of HSEs

increases in thickness, indicating that the desquamation process does not occur *in vitro* [7, 8]. A proper desquamation process is important, as the gradual increase in SC thickness affects skin permeation and thus the outcome of studies in which the effect of topical agents is examined when using HSEs. Although the absence of desquamation is unwanted for the latter purpose, HSEs provide a unique opportunity to investigate the mechanisms involved in the desquamation process. HSEs can for instance be used to determine whether their impaired desquamation process is caused by the inhibitory effects of LEKTI.

To investigate the desquamation process *in vitro* three different in-house HSEs were generated: the full-thickness collagen model (FTM), fibroblast-derived matrix model (FDM) and Leiden epidermal model (LEM). These HSEs are cultured at a constant temperature of 37ºC, a high relative humidity of approximately 92% and are not exposed to daily stressors that occur *in vivo,* such as exposure to friction, tension and washing. To determine whether the desquamation process is maintained if the formed epidermis is derived from the native tissue rather than from isolated cells (used to generate HSEs), small explants of full-thickness (FT) native human skin were expanded *in vitro*. Additionally, *ex vivo* human skin was cultured to determine whether the superficial SC layers of human skin will desquamate *in vitro* when it is cultured under the same conditions as the HSEs. The expression pattern of KLK 5 and LEKTI was determined in the above mentioned cultures. Additionally, KLK 5 and KLK 7 activity in the superficial SC layers of FTM was compared to *in vivo* KLK 5 and KLK 7 activity. This study provides new insights on the expression and activity of specific desquamatory enzymes in HSEs and could therefore contribute to a better understanding of the desquamation process *in vitro* and *in vivo*.

MATERIALS AND METHODS

Cell culture

Normal human keratinocytes (NHKs) and human dermal fibroblasts were obtained from adult donors undergoing mammary or abdomen surgery. The Declaration of Helsinki principles were followed when working with human tissue. NHKs were cultured in medium consisting of a 3:1 mixture of Dulbecco's Modified Eagle Medium (DMEM) (Invitrogen, Leek, The Netherlands) and Ham's F12 medium (Invitrogen, Leek, The Netherlands) supplemented with 5% newborn fetal bovine serum (FBS) (Hyclone, Logan, UT), 1% penicillin/streptomycin solution (Sigma), 0.4 μg/mL hydrocortisone (Sigma), 0.5 μM isoproterenol (Sigma) and 0.5 μg/mL insulin (Sigma). The cells were grown to at least 80% confluency (but never reaching full confluency) and were harvested by trypsin digestion. First and second passage NHKs were used to generate HSEs. NHKs used to create HSEs with only an epidermal compartment were cultured with the Dermalife K medium complete kit (Lifeline Cell Technology, Walkersville, MD) supplemented with 1% penicillin/streptomycin (Sigma) until they reached a maximum confluency of 80%. First and second passage NHKs were used to generate HSEs.

Human dermal fibroblasts were cultured in DMEM, supplemented with 5% FBS and 1% penicillin/streptomycin solution. This medium is further referred to as F-medium. The cultures were grown to full confluence and were harvested by trypsin digestion. First to fifth passage fibroblasts were used for the generation of HSEs.

Dermal equivalents

Collagen-type I containing dermal equivalents: these dermal equivalents were generated as described earlier [9]. A 4 mg/mL collagen solution, isolated from rat tails, was mixed at 4°C with Hank's Buffered Salt Solution to obtain a final collagen concentration of 1 mg/mL or 2 mg/mL. 1 mL of the 1 mg/mL collagen solution was pipetted into a filter insert (Corning Transwell cell culture inserts, membrane diameter 24 mm, pore size 3 μm; Amsterdam, The Netherlands) and was allowed

to polymerize for 15 minutes at 37°C. Subsequently, 3 mL of the 2 mg/mL collagen solution, mixed at 4°C with a fibroblast suspension (final density of 0.4 x 10^5 cells/mL collagen solution) was pipetted into the inserts. After polymerization, the dermal compartments were kept submerged in F-medium supplemented with 0.45 mM vitamin C (Sigma). The dermal compartments were either used on the same day or after one week.

Fully human dermal equivalents: the dermal matrices for the FDMs were generated as described previously [10]. In short, 0.4x10^6 fibroblasts were seeded onto filter inserts (Corning transwell culture inserts, membrane diameter 24 mm, pore size 0.4 μm, Corning Life Sciences, Amsterdam, The Netherlands). The fibroblasts were kept submerged in the medium described for the collagen type I containing dermal equivalents for three weeks. During this period the fibroblasts developed their own dermal matrix. The medium was refreshed twice a week.

Generation of human skin equivalents (HSEs)

Full Thickness collagen Model (FTM): One week after preparation of the fibroblast populated collagen dermal equivalents, 0.5x10^6 NHKs were seeded on top of each dermal equivalent. The first two days the HSEs were kept submerged in medium consisting of DMEM and Ham's F12 (Invitrogen, Leek, The Netherlands) (3:1 v/v) supplemented with 5% FBS, 1% penicillin/streptomycin solution, 0.5 μM hydrocortisone, 1 μM isoproterenol and 0.5 μg/mL insulin. The following two days the HSEs were kept submerged in a similar medium, except that the FBS was reduced to 1% and 0.053 μM selenious acid (Johnson Matthey, Maastricht, The Netherlands), 10 mM L-serine (Sigma), 10 μM L-carnitine (Sigma), 1 μM α-tocopherol acetate (Sigma), 25 mM vitamin C and a lipid mixture of 3.5 μM arachidonic acid (Sigma), 30 μM linoleic acid (Sigma), 25 μM palmitic acid (Sigma) were added to the medium. Hereafter, the HSEs were lifted to the air/liquid interface and were nourished with medium in which the FBS was omitted and the arachidonic acid concentration was increased to 7 μM. The medium was refreshed

twice a week. The HSEs were grown at 37°C, 92% relative humidity and 8% CO_2 for 16 days after seeding the NHKs onto the dermal equivalents.

Fibroblast Derived matrix Model (FDM): three weeks after seeding fibroblasts onto filter inserts $0.5x10^6$ NHKs were seeded onto each dermal equivalent. The HSEs were further cultured as described for the FTMs.

Leiden Epidermal Model (LEM): LEMs were generated as described previously [11] with slight modifications. $0.2x10^6$ NHKs were seeded onto cell culture inserts (Corning tranwell cell culture inserts, membrane diameter 12 mm, pore size 0.4 μm, Corning Life Sciences, Amsterdam, The Netherlands). The cells were kept submerged for 2-3 days in Dermalife medium until confluency. The following 2 days the HSEs were kept submerged in CnT medium (CellnTec, Bern, Switzerland) supplemented according to the manufacturer's protocol and 1% penicillin/streptomycin solution, 1 μM α-tocopherol acetate, 25 mM vitamin C and a lipid mixture of 7 μM arachidonic acid, 30 μM linoleic acid and 25 μM palmitic acid. Hereafter, the cells were nourished with the same medium, but were grown at the air/liquid interface. The LEMs were harvested 16 days after seeding the NHKs onto the inserts.

Full Thickness Outgrowth (FTO): 4 mm full thickness fat free punch biopsies obtained from abdomen or mammary skin were transferred onto freshly generated collagen type 1 containing dermal equivalents. These HSEs were cultured similarly as described for the FTMs except that they were directly cultured at the air/liquid interface. The FTOs were grown for approximately 16 days.

Ex vivo human skin

20 mm punch biopsies of dermatomed abdomen and mammary human skin were placed onto filter inserts (Corning Transwell cell culture inserts, membrane diameter 24 mm, pore size 3 μm; Amsterdam, The Netherlands). The biopsies were cultured at the air/liquid interface for 1 or 2 weeks with the serum-free medium and culture conditions described for the FTM.

Counting of stratum corneum layers

Harvested FTMs, FDMs, LEMs, FTOs and native human skin cultured for one or two weeks were fixed in Tissue Tek O.C.T. compound (Sakura Finetek Europe, Zoeterwoude, The Netherlands) and frozen in liquid nitrogen. 5 μm sections were cut and stained with an aqueous 1% safranin red (Sigma) solution (w/v) for 1 minute and were subsequently washed with deionized water. A 2% KOH solution (w/v) was applied on the sections for 20 minutes to allow the corneocytes to swell. The sections were visualized with a light microscope and at least five images per sample were taken with a digital camera (Carl Zeiss axioskop, Jena, Germany) connected to the microscope. The number of SC layers of at least three different skin cultures or *ex vivo* skin samples were counted. The provided data represent the mean and standard deviation.

Immunohistochemistry

Harvested HSEs were fixed in 4% (w/v) paraformaldehyde (Lommerse Pharma, Oss, The Netherlands), dehydrated and embedded in paraffin. 5 μm sections were cut and used for immunohistochemical staining of kallikrein 5 (KLK 5; 400x dilution) (Santa Cruz, CA) and LEKTI (20x dilution) (Invitrogen, Leek, The Netherlands). The sections were deparaffinized and rehydrated through xylene and graded ethanol series and finally with PBS. Antigen retrieval was performed by immersion in sodium citrate buffer (pH 6) for 30 minutes close to the boiling point. After cooling the sections were blocked with normal horse serum for 20 min, followed by incubation with the primary antibody overnight at 4ºC. The sections were successively incubated with the secondary antibody and ABC reagent for 30 minutes each. Between each incubation step the sections were washed with PBS. Hereafter the sections were consecutively washed with PBS, 0.1 M sodium acetate buffer and incubated for 30 minutes in amino-ethylcarbazole (Sigma) dissolved in N,N-dimethylformamide (1g/250 mL) (Sigma) supplemented with 0.1% hydrogen peroxide and finally washed with water. Counterstaining was

performed with haematoxylin. Incubations with normal horse serum, secondary antibody and ABC reagent were performed with the R.T.U. Vectastain Elite ABC Reagent Kit (Vector Laboratories, Burlingame, CA).

Kallikrein activity assay

FTMs were tape-stripped as described previously [9]. The tape-strips were extracted as described by Voegeli *et al.* [12]. Tape-strips were transferred to Eppendorf tubes, to which 250 μL buffer was added. The buffer was composed of 0.1 M Tris/HCl and 0.5% Triton X-100 at pH 8. Blank tape strips were used as a negative control. The tape-strips were extracted for 15 minutes at 25ºC while shaking at 1000 rpm. To obtain enough sample for analysis, the extracts (200 μL) of four tape strips were pooled together. Aminomethyl coumarin (AMC) labelled peptide substrate (kindly provided by DSM, Basel, Switzerland) Boc-Phe-Ser-Arg-AMC for KLK5 or MEOSuc-Arg-Pro-Tyr-AMC for KLK7 were each added to 200 μL of the pooled extracts. The final substrate concentration in the pooled extracts was 25 μM. The pooled extracts were incubated with the substrates for 2 hours at 37ºC while shaking at 1000 rpm. The enzymatic reaction was stopped by addition of 200 μL of 1% acetic acid. The KLK activity was determined by the release of AMC from the peptides. The released AMC was quantified by reverse phase high performance liquid chromatography. A gradient elution system of H_2O: acetonitrile: trifluoroacetic acid (TFA) (80: 20: 0.07) and H_2O: acetonitrile: TFA (50: 50: 0.07) was used (see table 1 for details of the gradient system) with a flow rate of 1 mL/ min and injection volume of 5 μL. The column used was a Symmetry C18, 3.5 μm, 4.6 mm x 75 mm (Waters, Milford, MA). The excitation and emission wavelengths were set at 354 nm and 442 nm, respectively.

The protein content of the pooled extracts was determined with the micro BCA protein assay reagent (Pierce, Rockford, IL) according to the manufacturer's protocol. A calibration curve of BSA was used to quantify the protein content of each sample. The 96-wells plates were incubated for 2 hours at 37ºC. The

absorbance was measured at 562 nm with a plate reader (Tecan Infinite M1000, Männedorf, Switzerland). The activity of KLK 5 and KLK 7 in FTM was compared to *in vivo* KLK 5 and KLK 7 activity in two healthy Caucasian volunteers between 25 and 30 years. No MEC approval was needed to perform the kallikrein activity assay on human volunteers, since tape-stripping represents a non-invasive technique.

Table 1. Gradient elution system

Time	*Gradient*
6 minutes	100% solvent A
10 minutes	100% solvent B
13 minutes	100% solvent A
15 minutes	100% solvent A

Solvent A consists of H_2O: acetonitrile: trifluoroacetic acid (TFA) (80: 20: 0.07). Solvent B consists of H_2O: acetonitrile: TFA (50: 50: 0.07).

RESULTS

Neither HSEs nor native human skin desquamate in vitro

First we determined the number of SC layers in HSEs and *ex vivo* human skin using safranin red staining. The results revealed that after 16 days of culture FTM, FDM and LEM have 25.4 ± 0.6, 21.7 ± 3.0 and 30.9 ± 10.4 SC layers respectively, while native human skin has 11.3 ± 1.9 SC layers (table 2). The increased number of SC layers in the HSEs compared to native human skin indicates that the desquamation process is impaired *in vitro*. To investigate whether the culture conditions influence the desquamation process FT skin explants were expanded *in vitro*. After two weeks of culture the FT explants have 24.1 ± 1.4 SC layers, while the FT outgrowths (FTOs) that developed from the explants have 13.9 ± 0.9 SC layers (table 2). Additionally, when *ex vivo* human skin is placed in the incubator, the number of SC layers remains similar to native human skin after one week (11.8 ± 1.0 SC layers).

However, after two weeks the number of SC layers of *ex vivo* skin (16.9 ± 0.4 SC layers) is increased compared to native human skin (table 2). These results clearly demonstrate that native human skin does not desquamate under the selected culture conditions.

Table 2. Number of stratum corneum layers

Sample	*Number of SC layers*
Native human skin	11.3 ± 1.9
FTM	25.4 ± 0.6
FDM	21.7 ± 3.0
LEM	30.9 ± 10.4
FT explant	24.1 ± 1.4
FT outgrowth	13.9 ± 0.9
Ex vivo human skin 1 week	11.8 ± 1.0
Ex vivo human skin 2 weeks	16.9 ± 0.4

The number of stratum corneum (SC) layers per sample are provided. The data represent the mean ± STD of at least three different cultures.

Most HSEs show expression of LEKTI in deeper layers of the viable epidermis compared to native human skin

Next we evaluated the expression of KLK 5 and LEKTI by immunohistochemistry to compare the expression pattern of these desquamatory proteins between native human skin, FTM, FDM, LEM, FTO and *ex vivo* human skin cultured for one or two weeks (figure 1).

In native human skin KLK 5 expression is detected as a thin layer in the uppermost stratum granulosum layers. When focussing on the HSEs and cultured human skin, KLK 5 expression in FTM, FDM, FTO and cultured skin is similar to that observed for native human skin. In LEM, however, KLK 5 expression is observed in the stratum granulosum as well as in the upper stratum spinosum,

indicating that LEM has a different KLK 5 expression compared to native human skin.

When focussing on LEKTI expression, in human skin the expression is confined to the stratum granulosum. However, the expression of LEKTI is observed in deeper layers of the stratum granulosum compared to KLK 5. In the HSEs the expression of LEKTI is detected in the stratum granulosum and in the (upper) stratum spinosum layers in FTM, FDM and LEM. This indicates that these HSEs have an altered expression of LEKTI compared to native human skin. FTO on the other hand shows the expression of LEKTI only in the stratum granulosum, which is similar to native human skin. *Ex vivo* human skin that is cultured for one week shows the expression of LEKTI only in the granular layer, just as native human skin. After placing *ex vivo* human skin in the incubator for two weeks, LEKTI expression is observed in the granular layer, but occasionally also extends into the upper stratum spinosum layers.

FTM has decreased KLK 5 activity in the superficial SC layers compared to in vivo human skin

The activity of KLK 5 and KLK 7 was investigated in the superficial SC layers (the first four tape-strips) of FTM and healthy volunteers. The activity of KLK 5 and KLK 7 is expressed as the AMC/protein ratio. The AMC content reflects the amount of AMC that has been cleaved from the AMC-labelled substrates of KLK 5 and KLK 7. The measured activity is corrected for the total amount of proteins present in the pooled samples of the first four tape-strips. In the superficial layers of native human skin KLK 5 activity is approximately six times higher compared to KLK 7 activity (figure 2). In the superficial layers of FTM, however, the activity of KLK 5 and KLK 7 are found to be equal (figure 2). Compared to human skin FTM shows a drastic reduction in KLK 5 activity, while KLK 7 activity appears to be equal.

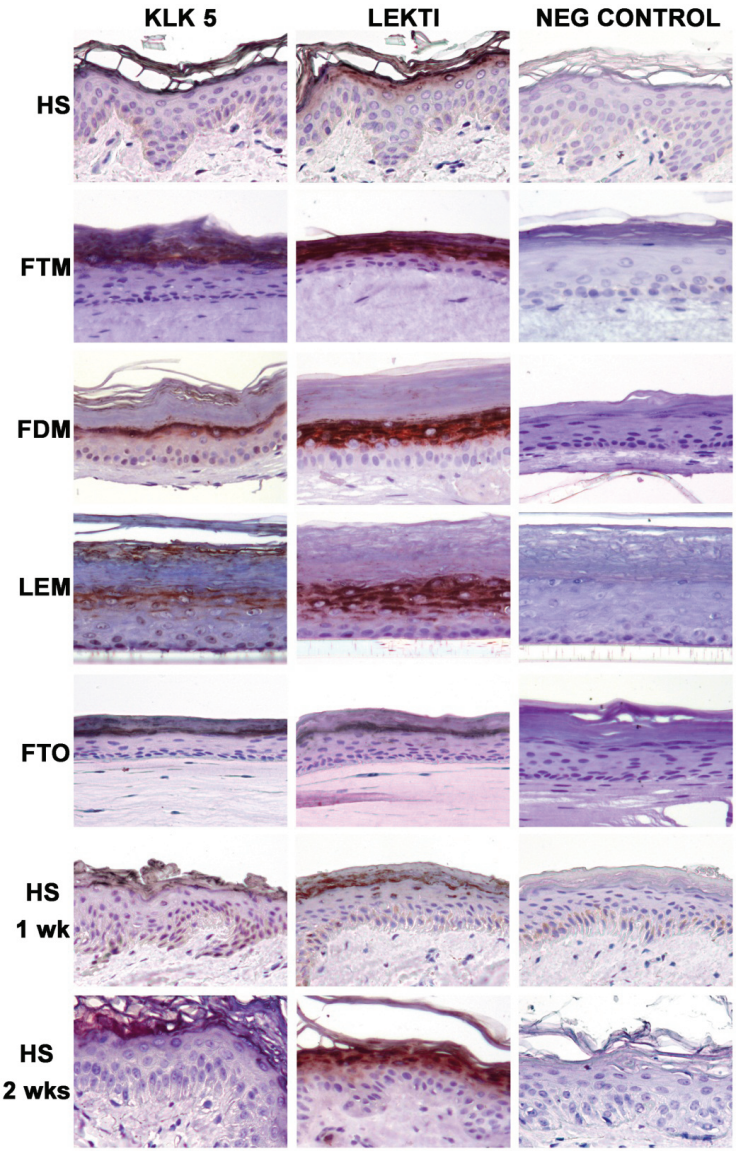

Figure 1. Immunohistochemical staining was performed to determine the expression pattern of KLK 5 and LEKTI in fresh native human skin (HS), FTM, FDM, LEM, FTO and native human skin cultured for one week (HS 1 wk) or two weeks (HS 2 wks). The negative controls are sections to which only the secondary antibody was applied. Original magnification: 20x.

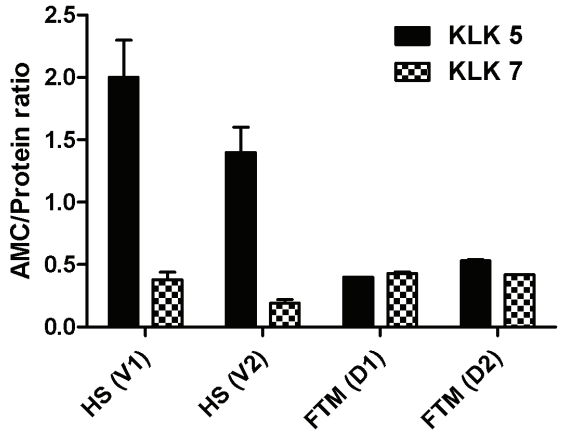

Figure 2. The activity of KLK 5 and KLK 7 in the first four SC tape-strips from two healthy Caucasian volunteers (HS V1 and HS V2) and from two FTMs (FTM D1 and FTM D2) have been determined. The KLK activity is presented as the amount of AMC that has been cleaved from the AMC-labelled KLK 5 and KLK 7 substrates. The cleaved amount of AMC is corrected for the total amount of protein that is tape-stripped. The data represent the sample mean + STD of 3 analytical points.

DISCUSSION

The observed increase in SC thickness in all HSEs indicates that the desquamation process does not occur *in vitro*. Moreover, even human skin will not retain its ability to desquamate under the used culture conditions. The increased number of SC layers observed for FTM correlates well with the decreased KLK 5 activity in the superficial SC layers compared to native human skin. The decreased KLK 5 activity may partially be caused by the altered expression profile of LEKTI observed in most HSEs. The expression of LEKTI observed in the upper stratum spinosum and stratum granulosum may result in a stronger inhibition of corneodesmolysis by KLKs. The reason for the altered expression of LEKTI in most of the HSEs remains to be established. It is known that inhibition of KLK activity by LEKTI depends on the environmental pH [5] and water content [4, 13]. Factors that contribute to the SC surface acidification are thought to be proton

donors from free amino acids, urocanic acid, pyrrolidone carboxylic acid (all collectively referred to as natural moisturizaing factors), lactic acid, free fatty acids and the skin moisture level [14, 15]. These components may be derived from sebum, sweat or degradation of filaggrin. The latter is needed to generate natural moisturizing factors that regulate SC hydration [16, 17]. HSEs do not contain skin appendages like sweat glands or sebaceous glands. Additionally, the SC of FTM and FDM contain less natural moisturizing factors and are therefore less hydrated [9, 10]. These findings suggest that a reduction in SC water content and/or SC surface pH may be the cause of the impaired desquamation process in HSEs. In order to increase the SC hydration level of FTM, the cultures were repeatedly treated with topical application of glycerol. This treatment increased the SC hydration level of FTM, as observed from cryo-scanning electron micrographs, but no desquamation of the superficial SC layers was observed (Bouwstra *et al.*, unpublished data). Additionally, Ponec *et al.* [7] used various repetitive treatments, such as mechanical scraping of the SC surface and topical application of acids and trypsin, to induce desquamation *in vitro*. From all these treatments only mechanical scraping was shown to be effective in reducing the number of SC layers in HSEs. This indicates that friction plays an important role in shedding of the superficial SC layers. This correlates well with the results demonstrating that *ex vivo* human skin cultured for two weeks in the incubator does not desquamate, despite its mostly similar expression of LEKTI as native human skin. It is possible that the absence of others factors, such as tension, washing, UV exposure, changes in environmental conditions and other daily stressors human skin is normally exposed, also have an inhibitory effect on the desquamation process *in vitro*.

It should be noted that KLK 7 activity in the superficial SC layers is similar between native human skin and FTM. This indicates that the impaired desquamation observed for HSEs is not caused by a decreased activity of KLK 7.

The simplest method to maintain a physiological number of SC layers *in vitro* can be achieved by applying friction on the SC surface. However, this procedure may

be time consuming and is not desirable when topical treatments are tested *in vitro*. Therefore additional studies are required to determine how desquamation can be induced *in vitro* and how LEKTI expression and KLK activity can be improved in HSEs.

ACKNOWLEDGEMENT

The authors would like to thank Rainer Voegeli and Stephan Doppler (DSM; former Pentapharm, Basel, Switzerland) for their support with the KLK activity assay, Maria Ponec for helpful suggestions during the meetings and Ida Rasmussen and Naila Akram for their practical support. This research was financially supported by the Dutch Technology Foundation STW (grant no. 7503).

REFERENCES

1. Egelrud, T. Desquamation in the stratum corneum. Acta Derm Venereol Suppl (Stockh) **208,** 44, 2000.
2. Borgono, C.A., Michael, I.P., Komatsu, N., Jayakumar, A., Kapadia, R., Clayman, G.L., Sotiropoulou, G. and Diamandis, E.P. A potential role for multiple tissue kallikrein serine proteases in epidermal desquamation. J Biol Chem **282,** 3640, 2007.
3. Eissa, A. and Diamandis, E.P. Human tissue kallikreins as promiscuous modulators of homeostatic skin barrier functions. Biol Chem **389,** 669, 2008.
4. Harding, C.R., Watkinson, A., Rawlings, A.V. and Scott, I.R. Dry skin, moisturization and corneodesmolysis. Int J Cosmet Sci **22,** 21, 2000.
5. Deraison, C., Bonnart, C., Lopez, F., Besson, C., Robinson, R., Jayakumar, A., Wagberg, F., Brattsand, M., Hachem, J.P., Leonardsson, G. and Hovnanian, A. LEKTI fragments specifically inhibit KLK5, KLK7, and KLK14 and control desquamation through a pH-dependent interaction. Mol Biol Cell **18,** 3607, 2007.
6. Hanson, K.M., Behne, M.J., Barry, N.P., Mauro, T.M., Gratton, E. and Clegg, R.M. Two-photon fluorescence lifetime imaging of the skin stratum corneum pH gradient. Biophys J **83,** 1682, 2002.
7. Ponec, M., Kempenaar, J. and Weerheim, A. Lack of desquamation - the Achilles heel of the reconstructed epidermis. Int J Cosmet Sci **24,** 263, 2002.
8. Vicanova, J., Mommaas, A.M., Mulder, A.A., Koerten, H.K. and Ponec, M. Impaired desquamation in the in vitro reconstructed human epidermis. Cell Tissue Res **286,** 115, 1996.
9. Bouwstra, J.A., Groenink, H.W., Kempenaar, J.A., Romeijn, S.G. and Ponec, M. Water distribution and natural moisturizer factor content in human skin equivalents are regulated by environmental relative humidity. J Invest Dermatol **128,** 378, 2008.
10. El Ghalbzouri, A., Commandeur, S., Rietveld, M.H., Mulder, A.A. and Willemze, R. Replacement of animal-derived collagen matrix by human fibroblast-derived dermal matrix for human skin equivalent products. Biomaterials **30,** 71, 2009.
11. El Ghalbzouri, A., Siamari, R., Willemze, R. and Ponec, M. Leiden reconstructed human epidermal model as a tool for the evaluation of the skin corrosion and irritation potential according to the ECVAM guidelines. Toxicol In Vitro **22,** 1311, 2008.
12. Voegeli, R., Rawlings, A.V., Breternitz, M., Doppler, S., Schreier, T. and Fluhr, J.W. Increased stratum corneum serine protease activity in acute eczematous atopic skin. Br J Dermatol **161,** 70, 2009.

13. Watkinson, A., Harding, C., Moore, A. and Coan, P. Water modulation of stratum corneum chymotryptic enzyme activity and desquamation. Arch Dermatol Res **293,** 470, 2001.
14. Rippke, F., Schreiner, V. and Schwanitz, H.J. The acidic milieu of the horny layer: new findings on the physiology and pathophysiology of skin pH. Am J Clin Dermatol **3,** 261, 2002.
15. Schmid-Wendtner, M.H. and Korting, H.C. The pH of the skin surface and its impact on the barrier function. Skin Pharmacol Physiol **19,** 296, 2006.
16. Rawlings, A.V. and Harding, C.R. Moisturization and skin barrier function. Dermatol Ther **17 Suppl 1,** 43, 2004.
17. Verdier-Sevrain, S. and Bonte, F. Skin hydration: a review on its molecular mechanisms. J Cosmet Dermatol **6,** 75, 2007.

8

Summary and Perspectives

SUMMARY

The skin forms an effective permeability barrier against penetration of foreign substances into the body and excessive water loss from the body. To generate this barrier the keratinocytes in the basal layer of the epidermis undergo a complex maturation process that finally results in the formation of the stratum corneum (SC), the outermost layer of the epidermis [1, 2]. The SC is the main permeability barrier of the skin and consists of terminally differentiated dead keratinocytes, called corneocytes, which are embedded in a lipid-rich extracellular environment. Due to the rather impermeable character of the cornified envelope surrounding the corneocytes, the main penetration pathway of most substances is suggested to proceed via the SC lipid domains [3, 4]. This is the reason why the SC lipids are considered to play a crucial role in the barrier function of the skin. The SC lipids are primarily composed of cholesterol, free fatty acids and ceramides in an approximately equimolar ratio [5]. The lipids are organized in lipid layers (referred to as lamellae) stacked on top of each other approximately parallel to the skin surface. In human SC two lamellar phases are formed with repeat distances of approximately 13 and 6 nm, referred to as the long and short periodicity phase (LPP and SPP), respectively [6]. The LPP is characteristic for the SC lipid organization and is considered to be important for a competent skin barrier function [7, 8]. The lipids within the lamellae are predominantly arranged in the dense orthorhombic packing, while a subpopulation of lipids also forms the less dense hexagonal or liquid organization [9, 10]. In order to determine whether active compounds hold potential for (trans)dermal application, their penetration through the skin has to be investigated. *Ex vivo* human or animal skin has extensively been used for this purpose. However, the use of human skin is limited due to its scarce availability. Furthermore, animal skin shows differences in e.g. dermal and epidermal thickness, hair density and SC lipid composition and therefore in skin barrier function. Additionally, from March 2013 a complete ban on animal testing of cosmetic products and their ingredients will be adopted within the EU. This

means that there is an urgent need for a suitable replacement for human or animal skin, which may be provided by three-dimensional human skin equivalents (HSEs). When HSEs were initially developed, keratinocytes were seeded in culture vessels and grown under submerged conditions. This resulted in an incomplete differentiation of the keratinocytes and consequently an epithelium that did not fully resemble native human skin. A major step forward in the development of HSEs was achieved by generating HSEs at the air-liquid interface [11]. Due to this and many other modifications of the culture conditions HSEs nowadays mimic many aspects of native human skin and have improved SC barrier properties. They show great resemblance in tissue morphology and have an almost similar expression of early and late differentiation markers as native human skin. Furthermore, the SC barrier lipids of native human skin are also detected in the SC of HSEs.

It is more than a decade ago that the SC lipid composition and organization of HSEs were reported extensively. The published reports demonstrated that the SC lipid composition and organization of HSEs differed to some extent from native human SC [12]. Due to the differences in SC lipid properties, HSEs have a decreased SC barrier function compared to native human SC [12-14]. They generally overestimate compound penetration and therefore do not provide a reliable *in vitro - in vivo* correlation with regard to permeation studies [15-18]. Additionally, the desquamation process, which regulates the shedding of the superficial SC layers, is impaired in HSEs [19, 20]. This leads to gradual thickening of the SC as the culture period is prolonged, which may also influence the outcome of permeation studies. This indicates that HSEs can be improved further to achieve an even higher resemblance to native human skin. During the last few years the culture conditions have been further optimized and two novel in-house HSEs have been developed in Leiden. The novel fibroblast-derived matrix model (FDM) and Leiden epidermal model (LEM) were generated together with the full thickness collagen model

(FTM). These models were used to answer the main questions of this thesis, namely:

1. Can fully differentiated HSEs be generated under submerged conditions and how does this affect the epidermal differentiation and lipid composition?
2. Do the SC barrier properties of our novel in-house HSEs resemble the SC barrier properties of native human skin?
3. How does the SC lipid composition of the in-house HSEs relate to the SC lipid organization?
4. To what extent do the culture conditions influence the SC barrier properties of HSEs?
5. How can the SC barrier properties of HSEs be improved?

Submerged versus air-exposed HSEs

In *chapter 2* studies are reported in which HSEs were generated under submerged and air-exposed conditions. The aim of the study was to determine whether the difference in micro-environment during keratincoyte differentiation affects skin architecture of HSEs. HSEs generated under submerged conditions have a similar tissue morphology, expression of several differentiation markers and show the presence of all SC barrier lipids as their air-exposed counterparts. However, they contain less fatty acids and one of the ceramide subclasses with a very long fatty acid chain (referred to as acylceramides) than the air-exposed HSEs. Additionally, the results demonstrate that the SC of FTMs generated under air-exposed conditions contain more natural moisturizing factors than FTMs generated under submerged conditions, but nevertheless has a reduced SC hydration level. The results presented in *chapter 2* show for the first time that HSEs can form a well-organized epidermis, including a SC, when generated under submerged conditions.

SC barrier properties of the novel HSEs

In *chapter 3* the SC barrier function, SC lipid composition and organization of FDM, LEM and FTM are presented. The HSEs have a similar morphology and expression of several early and late differentiation markers as native human skin, except for the observed expression of keratin 16 and premature expression of involucrin. To compare the SC barrier function of FDM, LEM, FTM and native human skin permeation studies, using benzocaine as a model drug, were performed. The SC of FDM and LEM showed a three times higher permeability, while the SC of FTM showed a five time higher permeability for benzocaine compared to native human SC. These results indicate that all HSEs have a decreased barrier function compared to native human SC. Therefore, the SC lipid organization and composition of the HSEs was investigated. All HSEs showed the presence of the LPP, which is considered to be important for a competent skin barrier. However, no indication of the presence of the SPP was observed. Furthermore, all HSEs have a mainly hexagonal arrangement of the SC lipids, a less dense packing than the orthorhombic packing observed in human SC. Additionally, the HSEs have an increased lipid disordering and form a liquid phase at a lower temperature compared to native human SC. All HSEs showed the presence of cholesterol, free fatty acids and eight ceramide subclasses that can be distinguished using high performance thin layer chromatography (HPTLC), similarly as human SC. Although the lipid composition was not determined in a quantitative manner, the results strongly indicate that the HSEs have a reduced free fatty acid content and an increased level of some acylceramides compared to human SC.

The effect of culture conditions on the SC barrier properties of HSEs

After establishing that the HSEs show differences in their SC barrier properties compared to native human SC, we examined whether these differences are caused by culture conditions or by the isolation procedure used to obtain single cells. The

latter involves enzymatic digestion of native human skin and is required to generate HSEs. The experiments conducted to answer this question are described in *chapter 4*. Intact full-thickness native human skin explants and epidermal sheets were expanded on fibroblast-populated collagen matrices. The morphology, differentiation process and barrier properties of the explants and outgrowths were examined. The outgrowths from the skin explants have a similar morphology and expression of several differentiation markers, except for an increased expression of involucrin and observed expression of keratin 16, as native human skin. The presence of keratin 16 indicates that the keratinocytes in the outgrowths are activated. Interestingly, the SC of the explants increased during the culture period, exceeding the number of SC layers found *in vivo*. This indicates that the desquamation process is impaired when native human skin is cultured *in vitro*. HPTLC results show that the SC lipid profiles of the outgrowths are very similar to that of HSEs. They also have a reduced free fatty acid content in their SC compared to native human skin. All ceramide classes are present in the outgrowths of these cultures, but an increase in the very long chain acylceramides is observed compared to native human SC. The SC lipid organization of the outgrowths is also similar to that of HSEs, which includes a predominant presence of the LPP and a mainly hexagonal lateral lipid organization. In addition, there is an indication of an increased presence of a liquid phase. This unambiguously demonstrates that the observed differences in SC barrier properties between the HSEs and native human skin are not caused by isolation of primary cells, but by the culture conditions. Efforts made to improve the SC lipid properties of HSEs should therefore be focused on optimizing the culture conditions.

The correlation between the SC lipid composition and SC lipid organization of HSEs

In the studies described in *chapter 3*, the SC lipid composition of HSEs was examined. In these studies the lipid profiles of the HSEs showed some changes

compared to native human skin. In order to provide more insight in these differences, quantitative analysis of the SC lipid composition was performed using HPTLC. As no information was obtained concerning the chain lengths of the ceramides and free fatty acids, a novel liquid chromatography/mass spectroscopy (LC/MS) method was additionally used to further analyze the SC lipids of the HSEs. These experiments are described in *chapter 5*. Quantification of the SC lipids showed that all HSEs have a reduced free fatty acid content compared to human SC. Additionally, LC/MS analysis revealed that all HSEs have an increased presence of mono-unsaturated fatty acids (MUFAs) compared to human SC. Fatty acids induce the orthorhombic packing [21] and their reduced level and altered composition are expected to be the key factors for the presence of the mainly hexagonal packing observed in the HSEs. Therefore these two changes in fatty acid profile may play an important role in the decreased permeability barrier observed for FDM, LEM and FTM. Additionally, the increased presence of MUFAs are at least partially responsible for the increased lipid disordering of the SC lipids of HSEs and the reduction in temperature at which the formation of the liquid phase occurs.

With respect to the ceramides, the LC/MS results demonstrated for the first time that the HSEs show the presence of twelve ceramide subclasses in their SC, similar to native human SC. However, the HSEs have increased levels of two ceramide subclasses with a very long fatty acid chain and ceramide species with an exceptionally short total carbon chain length. In addition, low fractions of ceramides with a mono-unsaturated acyl chain were detected. The latter ceramide species are not detected in human SC. Previous studies have shown that acylceramides induce the formation of the LPP [22]. The increased presence of the two acylceramide subclasses in the SC of the HSEs may therefore favour the formation of the LPP over the SPP.

All HSEs also show the expression of stearoyl-CoA desaturase 1 (SCD1), the enzyme that converts saturated fatty acids into MUFAs, in the basal and

differentiated layers of the viable epidermis. In native human skin, however, the expression of SCD1 is strictly localized in the basal layer. This suggests that the HSEs may have an increased MUFA content in their SC due to increased activity of SCD1 in the suprabasal layers of the viable epidermis. The results described in *chapter 5* indicate that the SC lipid properties of the HSEs can be improved by increasing the free fatty acid content in the SC and by reducing the SCD1 activity to decrease the amount of MUFAs in the SC.

Examining ways to improve the SC barrier properties of LEMs

After establishing that the SC barrier properties of HSEs may be improved by increasing the free fatty acid content and by reducing the MUFA content, we aimed to improve the SC lipid properties of LEM by specific media supplements. These studies are described in *chapter 6*. The SC fatty acid chain length distribution and saturation of LEM and human skin were quantified with LC/MS to determine to which extent they differ from each other. The results demonstrate that LEMs have a ~1.5x decreased very long chain fatty acid (fatty acids with 22-38 carbon atoms) content and a ~5x increased MUFA content compared to native human SC. The culture medium of LEM is supplemented with palmitic (C16:0), linoleic (C18:2) and arachidonic acid (C20:4). To examine the fatty acid uptake from the medium, protonated palmitic acid (C16:0) was substituted by deuterated palmitic acid, or deuterated arachidic acid (C20:0) was added to the fatty acid mixture which was supplemented to the culture medium. LC/MS analysis revealed that deuterated palmitic and arachidic acid are taken up, elongated and incorporated in the SC of LEM. However, fatty acids with a deuterated arachidic acid backbone were present in lower quantities in the SC of LEM than fatty acids with a deuterated palmitic acid backbone. In subsequent studies the level of the fatty acid mixture supplemented to the medium was increased four times or was modified by a fourfold increase in palmitic acid concentration. Furthermore, the effect of insulin on the SC MUFA content and SCD1 expression in the viable epidermis was

studied. The results demonstrate that increasing the concentration of arachidonic and linoleic acid results in a decreased content of very long chain fatty acids and an increase in MUFAs, whereas increasing the supplementation of palmitic acid had no effect on the fatty acid profile compared to the control. Additionally, modification of the insulin content in the culture medium did not affect the fatty acid profile or reduce the expression of SCD1 compared to the controls. All modifications in medium supplements did not affect the lateral or lamellar lipid organization compared to the control, except the condition wherein arachidonic and linoleic acid supplementation was increased. In the latter case the LEMs showed a reduction in the repeat distance of the LPP and the temperature at which the SC lipids are only arranged in a hexagonal packing compared to the controls.

The HSEs are known to have an increased triacyl- (TAG) and diacylglyceride (DAG) content compared to native human SC. TAG and DAG are formed by linking fatty acids to a glycerol backbone. The increased presence of TAG and DAG in the SC may be a reason why the LEM has a decreased SC fatty acid content.

Chapter 6 demonstrates that the medium composition can have a considerable influence on the SC lipid properties of HSEs. However, modifications made to the culture medium so far did not lead to an improved SC barrier in LEMs. This indicates that other media modifications are required to improve the SC lipid properties of HSEs.

Impairment of the desquamation process in vitro

The results presented in *chapter 4* indicated that the desquamation process is impaired *in vitro*. Based on these findings the expression and activity of specific desquamatory enzymes were further investigated in native human skin, HSEs and native human skin cultured for one or two weeks. These studies are described in *chapter* 7. The results demonstrate that the HSEs and human skin cultured for two weeks at the air-liquid interface do not desquamate. All HSEs and cultured human

skin show a similar expression of kallikrein 5, one of the important enzymes involved in the desquamation process, as native human skin. However, almost all HSEs show the expression of Lympho-epithelial Kazal type related inhibitor (LEKTI), an inhibitor of kallikreins, in more differentiated epidermal layers compared to native human skin. In FTM a decreased kallikrein 5 activity was observed in the superficial SC layers compared to native human skin. These results suggest that the impairment of the desquamation process in HSEs may partially be caused by an increased LEKTI expression.

CONCLUSIONS

The results presented in this thesis demonstrate that HSEs are able to form a completely stratified epidermis, including a SC, when generated under submerged conditions. However, under these conditions the HSEs have a reduced SC fatty acid and acylceramide content compared to HSEs generated at the air-liquid interface. This is an important finding since the SC is formed under submerged conditions *in utero*. The presented data also show that the culture conditions are of crucial importance concerning the protein expression and SC lipid properties of HSEs. Furthermore, we demonstrate that the SC lipid composition and organization of HSEs can be affected by the composition of the culture media.

Novel targets (e.g. SCD1) have been identified or proposed, which can guide future research focused on improving the SC barrier function of HSEs. Optimization of the culture conditions may improve the epidermal lipid metabolism in HSEs. This may contribute to the development of a new generation of HSEs that harbor a competent SC barrier that even more closely resembles the SC lipid composition and organization of native human SC than the current HSEs.

PERSPECTIVES

Further investigation of the SC lipid properties and barrier function of HSEs

In order to achieve more insight into the correlation between the SC lipid composition, organization and barrier function of each HSE type, it would be interesting to quantify the SC fatty acid chain length distribution and saturation of FDM and FTM, just as performed for LEM. This is of importance since the fatty acid composition plays an important role in the lateral lipid organization [21], which is different in all HSEs compared to native human skin. Quantification of the SC fatty acid species may also provide indications as to why FTM has a higher fatty acid level, but nevertheless does not show improved SC barrier properties, and even has a decreased SC permeability barrier for benzocaine compared to FDM and LEM.

The permeation pathway of compounds through the SC is suggested to mainly proceed through the lipid domains [3, 4]. Therefore our studies are primarily focused on the SC lipids of HSEs to understand and improve their impaired barrier function. Whether the cornified envelope also contributes to the increased permeability across HSEs compared to native human skin, should also be investigated. This can be done by visualizing the permeation pathway of a fluorescent marker through the SC of HSEs and native human skin using confocal laser scanning microscopy. Such studies are needed to determine whether changes in the SC lipid composition are the only cause of the decreased barrier function observed for the HSEs.

The SC barrier function of the HSEs was examined with benzocaine, which has been chosen for its low molecular weight and medium lipophilicity (mw = 165.2 g/mole, LogP = 1.44), resulting in an efficient permeation through human SC. In future studies the permeation of compounds with a broad range of lipophilicity and molecular weights should be assessed as well to compare the SC permeability barrier of the HSEs with human SC further. Additionally, the SC barrier function of FDM and LEM should be compared to commercially available HSEs in order

to determine whether the novel HSEs show an improved *in vitro - in vivo* correlation when they are used for permeability studies.

Identifying differences in epidermal lipid metabolism between HSEs and native human skin

The results presented in this thesis demonstrate that HSEs resemble human skin to a great extent with regard to their morphology, expression of various differentiation markers and ability to synthesize all SC barrier lipids. However, the SC lipid composition of HSEs shows some differences compared to native human SC. These differences indicate that epidermal lipid metabolism of HSEs deviates in some aspects from native human skin. In order to improve the SC lipid properties of HSEs, it is essential to bring the epidermal lipid metabolism of HSEs closer to the *in vivo* situation. To achieve this, it is first important to understand how epidermal lipid metabolism of HSEs differs from native human skin. This can be done by quantifying the mRNA expression level (using RealTime PCR) or protein abundance (using gel electrophoresis or mass spectrometry) of enzymes involved in epidermal lipid metabolism and their expression/activity regulators. Peroxisome proliferator-activated receptors (PPARs) play a central role in regulation of epidermal differentiation and lipid metabolism [23, 24]. Although our results showed that PPARα and PPARβ/δ have a similar expression pattern in the HSEs as native human skin, they might be expressed at different levels, which may lead to disturbance of epidermal homeostasis. It would also be of particular interest to determine the expression level of enzymes involved in the fatty acid synthesis, elongation and desaturation (such as SCD1) or synthesis and degradation of DAG and TAG, since all HSEs have a reduced fatty acid content and increased MUFA, DAG and TAG level in their SC compared to human SC. These differences in SC lipid composition are partially the cause of the altered SC lipid organization observed for HSEs, which may consequently be the cause of their decreased barrier function.

A more accurate method to assess the differences in epidermal lipid metabolism between HSEs and native human skin would be to quantify enzyme activity. However, determining enzyme activity in a 3D tissue may prove to be quite challenging. Identification of enzymes involved in epidermal lipid metabolism that are differentially expressed or active in human skin and HSEs can be considered as targets to improve the SC lipid properties of HSEs.

One potential enzymatic target could be SCD1. Immunohistochemical staining revealed that the HSEs show suprabasal expression of SCD1, whereas native human skin only shows expression of SCD1 in the basal layer. It is likely that the increased expression of SCD1 in the suprabasal layers of the viable epidermis in HSEs coincides with an increased SCD1 activity, resulting in higher SC MUFA levels compared to native human skin. SCD activity depends on various factors, such as the insulin level [25]. However, reduction of insulin content in the culture medium of LEM did not result in changes in SC MUFA content.

Optimization of culture conditions to improve SC lipid properties of HSEs

Optimization of the culture environment and/or culture media provides an opportunity to improve epidermal lipid metabolism of HSEs and thereby their SC lipid properties. A decrease in SCD1 activity in HSEs may be achieved by addition of specific SCD inhibitors to the culture medium. This may lead to a decrease in SC MUFA content of HSEs and thereby improve their SC lipid properties. An advantage of using specific SCD inhibitors rather than general changes made to the culture medium is the absence or reduction of any off-target effects. Changes observed in HSE morphology, differentiation or SC lipid properties can therefore more easily be correlated to the activity of one enzyme.

We showed that the SC lipid properties of HSEs can differ depending on the culture conditions. HSEs generated under submerged conditions show a reduction in SC free fatty acid level compared to HSEs generated at the air-liquid interface. HSEs generated under submerged conditions develop in an environment with

100% relative humidity (RH), while air-exposed HSEs are generated at a RH of 92%. The mechanism underlying the difference in SC fatty acid level between the submerged and air-exposed HSEs is unknown. However, it is possible that a reduction in environmental humidity below 92% will further increase the SC fatty acid level in HSEs. An increase in SC fatty acid level may promote the formation of the orthorhombic packing, as shown by Bouwstra *et al* [21]. This may consequently lead to improved SC barrier properties in HSEs.

The described HSEs show an altered expression of involucrin and presence of keratin 16 expression, which indicates that epidermal homeostasis is not reached. This may be due to the fast maturation of keratinocytes *in vitro*. The culture conditions used to generate HSEs do not reflect the *in vivo* situation. An improved balance between proliferation and differentiation in HSEs may therefore be achieved by adopting culture conditions that mimic the *in vivo* environment of human skin more closely. HSEs are generally cultured at 37ºC, while in daily life human skin is exposed to a fluctuating environmental temperature. Additionally, the skin surface has a temperature of approximately 32ºC, while the body's interior has a temperature of 37ºC. Studies performed by Gibbs *et al.* [26] showed that generating HSEs at 33ºC instead of 37ºC results in an improved balance between epidermal proliferation and differentiation. Furthermore, the oxygen level of *in vivo* skin ranges from 1.5-5%, while ambient oxygen concentration is around 21% [27]. It is thus also reasonable to take the environmental oxygen tension into consideration when HSEs are generated. It has been shown that low oxygen levels enhance fibroblasts growth [28]. Furthermore, an oxygen level of 5% has a minor effect on keratinocyte proliferation, but impedes keratinocyte differentiation compared to keratinocytes grown at atmospheric oxygen levels [29]. It is possible that fine tuning of the environmental temperature and/or oxygen level, at different stages of HSE generation, is needed to optimize fibroblast and keratinocyte growth and differentiation. This may lead to an improved epidermal homeostasis and consequently result in the formation of a competent skin barrier.

A closer look at the in vitro desquamation process

HSEs show an increased expression of LEKTI in the suprabasal layers of the epidermis compared to native human skin. Additionally, FTM shows a reduced KLK 5 activity compared to *in vivo* human skin. This suggests that the impaired desquamation process in HSEs, specifically in FTM, may be caused by an increased LEKTI inhibition of KLK 5 activity. Studies described by Deraison *et al.* [30] demonstrated that LEKTI inhibition occurs in a pH dependent manner. The SC of native human skin has a pH gradient that ranges from approximately pH 7.5 in the inner SC and pH 5 in the superficial SC layers [31]. At physiological pH LEKTI binds to KLKs and thereby inhibits corneodesmolysis. At lower pH LEKTI disassociates from KLKs rendering them free to degrade corneodesmosomes. The SC pH gradient is therefore essential for a proper desquamation process. In order to investigate whether impairment of the desquamation process in HSEs is caused by an increased KLK inhibition by LEKTI, it is necessary to determine whether HSEs also have a similar pH gradient as native human SC. Accurate determination of SC pH in HSEs can be done by using a pH-sensitive fluorescent probe in conjunction with two-photon fluorescence lifetime imaging microscopy as described by Hanson *et al.* [31].

REFERENCES

1. Eckert, R.L. and Rorke, E.A. Molecular biology of keratinocyte differentiation. Environ Health Perspect **80,** 109, 1989.
2. Fuchs, E. Epidermal differentiation: the bare essentials. J Cell Biol **111,** 2807, 1990.
3. Johnson, M.E., Blankschtein, D. and Langer, R. Evaluation of solute permeation through the stratum corneum: lateral bilayer diffusion as the primary transport mechanism. J Pharm Sci **86,** 1162, 1997.
4. Meuwissen, M.E., Janssen, J., Cullander, C., Junginger, H.E. and Bouwstra, J.A. A cross-section device to improve visualization of fluorescent probe penetration into the skin by confocal laser scanning microscopy. Pharm Res **15,** 352, 1998.
5. Wertz, P.W. Lipids and barrier function of the skin. Acta Derm Venereol Suppl (Stockh) **208,** 7, 2000.
6. Bouwstra, J.A., Gooris, G.S., van der Spek, J.A. and Bras, W. Structural investigations of human stratum corneum by small-angle X-ray scattering. J Invest Dermatol **97,** 1005, 1991.
7. De Jager, M., Groenink, W., Bielsa i Guivernau, R., Andersson, E., Angelova, N., Ponec, M. and Bouwstra, J. A novel in vitro percutaneous penetration model: evaluation of barrier properties with p-aminobenzoic acid and two of its derivatives. Pharm Res **23,** 951, 2006.
8. Groen, D., Poole, D.S., Gooris, G.S. and Bouwstra, J.A. Is an orthorhombic lateral packing and a proper lamellar organization important for the skin barrier function? Biochim Biophys Acta 2010.
9. Bouwstra, J.A., Gooris, G.S., Dubbelaar, F.E. and Ponec, M. Phase behavior of lipid mixtures based on human ceramides: coexistence of crystalline and liquid phases. J Lipid Res **42,** 1759, 2001.
10. Damien, F. and Boncheva, M. The extent of orthorhombic lipid phases in the stratum corneum determines the barrier efficiency of human skin in vivo. J Invest Dermatol **130,** 611, 2010.
11. Prunieras, M., Regnier, M. and Woodley, D. Methods for cultivation of keratinocytes with an air-liquid interface. J Invest Dermatol **81,** 28s, 1983.
12. Ponec, M., Boelsma, E., Weerheim, A., Mulder, A., Bouwstra, J. and Mommaas, M. Lipid and ultrastructural characterization of reconstructed skin models. Int J Pharm **203,** 211, 2000.

13. Bouwstra, J.A., Gooris, G.S., Weerheim, A., Kempenaar, J. and Ponec, M. Characterization of stratum corneum structure in reconstructed epidermis by X-ray diffraction. J Lipid Res **36,** 496, 1995.
14. Ponec, M., Weerheim, A., Kempenaar, J., Mulder, A., Gooris, G.S., Bouwstra, J. and Mommaas, A.M. The formation of competent barrier lipids in reconstructed human epidermis requires the presence of vitamin C. J Invest Dermatol **109,** 348, 1997.
15. Ackermann, K., Borgia, S.L., Korting, H.C., Mewes, K.R. and Schafer-Korting, M. The Phenion full-thickness skin model for percutaneous absorption testing. Skin Pharmacol Physiol **23,** 105, 2010.
16. Asbill, C., Kim, N., El-Kattan, A., Creek, K., Wertz, P. and Michniak, B. Evaluation of a human bio-engineered skin equivalent for drug permeation studies. Pharm Res **17,** 1092, 2000.
17. Netzlaff, F., Lehr, C.M., Wertz, P.W. and Schaefer, U.F. The human epidermis models EpiSkin, SkinEthic and EpiDerm: an evaluation of morphology and their suitability for testing phototoxicity, irritancy, corrosivity, and substance transport. Eur J Pharm Biopharm **60,** 167, 2005.
18. Schafer-Korting, M., Bock, U., Diembeck, W., Dusing, H.J., Gamer, A., Haltner-Ukomadu, E., Hoffmann, C., Kaca, M., Kamp, H., Kersen, S., Kietzmann, M., Korting, H.C., Krachter, H.U., Lehr, C.M., Liebsch, M., Mehling, A., Muller-Goymann, C., Netzlaff, F., Niedorf, F., Rubbelke, M.K., Schafer, U., Schmidt, E., Schreiber, S., Spielmann, H., Vuia, A. and Weimer, M. The use of reconstructed human epidermis for skin absorption testing: Results of the validation study. Altern Lab Anim **36,** 161, 2008.
19. Ponec, M., Kempenaar, J. and Weerheim, A. Lack of desquamation - the Achilles heel of the reconstructed epidermis. Int J Cosmet Sci **24,** 263, 2002.
20. Vicanova, J., Mommaas, A.M., Mulder, A.A., Koerten, H.K. and Ponec, M. Impaired desquamation in the in vitro reconstructed human epidermis. Cell Tissue Res **286,** 115, 1996.
21. Bouwstra, J., Pilgram, G., Gooris, G., Koerten, H. and Ponec, M. New aspects of the skin barrier organization. Skin Pharmacol Appl Skin Physiol **14 Suppl 1,** 52, 2001.
22. De Jager, M., Gooris, G., Ponec, M. and Bouwstra, J. Acylceramide head group architecture affects lipid organization in synthetic ceramide mixtures. J Invest Dermatol **123,** 911, 2004.
23. Feingold, K.R. and Jiang, Y.J. The mechanisms by which lipids coordinately regulate the formation of the protein and lipid domains of the stratum corneum: Role of fatty acids,

oxysterols, cholesterol sulfate and ceramides as signaling molecules. Dermatoendocrinol **3,** 113, 2011.

24. Schmuth, M., Jiang, Y.J., Dubrac, S., Elias, P.M. and Feingold, K.R. Thematic review series: skin lipids. Peroxisome proliferator-activated receptors and liver X receptors in epidermal biology. J Lipid Res **49,** 499, 2008.
25. Mauvoisin, D. and Mounier, C. Hormonal and nutritional regulation of SCD1 gene expression. Biochimie **93,** 78, 2011.
26. Gibbs, S., Vicanova, J., Bouwstra, J., Valstar, D., Kempenaar, J. and Ponec, M. Culture of reconstructed epidermis in a defined medium at 33 degrees C shows a delayed epidermal maturation, prolonged lifespan and improved stratum corneum. Arch Dermatol Res **289,** 585, 1997.
27. Evans, N.T. and Naylor, P.F. The systemic oxygen supply to the surface of human skin. Respir Physiol **3,** 21, 1967.
28. Balin, A.K. and Pratt, L. Oxygen modulates the growth of skin fibroblasts. In Vitro Cell Dev Biol Anim **38,** 305, 2002.
29. Ngo, M.A., Sinitsyna, N.N., Qin, Q. and Rice, R.H. Oxygen-dependent differentiation of human keratinocytes. J Invest Dermatol **127,** 354, 2007.
30. Deraison, C., Bonnart, C., Lopez, F., Besson, C., Robinson, R., Jayakumar, A., Wagberg, F., Brattsand, M., Hachem, J.P., Leonardsson, G. and Hovnanian, A. LEKTI fragments specifically inhibit KLK5, KLK7, and KLK14 and control desquamation through a pH-dependent interaction. Mol Biol Cell **18,** 3607, 2007.
31. Hanson, K.M., Behne, M.J., Barry, N.P., Mauro, T.M., Gratton, E. and Clegg, R.M. Two-photon fluorescence lifetime imaging of the skin stratum corneum pH gradient. Biophys J **83,** 1682, 2002.

Appendix

SAMENVATTING

De huid vormt een effectieve barrière tegen het binnendringen van ongewenste stoffen en het uitdrogen van het lichaam. Om deze barrière te vormen ondergaan de keratinocyten in de basale laag van de epidermis een complex differentiatieproces (d.w.z. een veranderingsproces) dat uiteindelijk resulteert in de vorming van het stratum corneum (SC), ook wel bekend als de hoornlaag, de bovenste laag van de epidermis [1, 2]. Het SC vormt de voornaamste transportbarrière van de huid. Het bestaat uit dode keratinocyten, genaamd corneocyten, die ingebed zijn in een lipidrijke, oftewel vetrijke, extracellulaire matrix. Aangezien de corneocyten een redelijk ondoordringbare structuur hebben, wordt aangenomen dat stoffen voornamelijk via de lipiddomeinen tusen de corneocyten het SC passeren [3, 4]. De SC lipiden zijn daarom van cruciaal belang voor de barrièrefunctie van de huid. De SC lipiden bestaan voornamelijk uit cholesterol, vrije vetzuren en ceramiden in een ongeveer equimolaire verhouding [5]. Ze zijn gerangschikt in lamellaire structuren (d.w.z. lipidenlagen) die op elkaar gestapeld zijn parallel aan het huidoppervlak. De lamellaire structuren kunnen een repeterende afstand van ongeveer 13 en 6 nm hebben, de lange periodiciteitsfase (LPP) en korte periodiciteitsfase (SPP), respectievelijk [6]. De LPP is een karakteristieke eigenschap van de SC lipiden en is belangrijk voor een competente barrièrefunctie [7, 8]. De lipiden binnen deze lagen vormen een dichte regelmatige (kristallijn) structuur en zijn voornamelijk gerangschikt in een zogenaamd orthorhombisch rooster, hoewel enkele lipidendomeinen ook een minder dichte regelmatige structuur (een hexagonaal) of zelfs een vloeibare structuur vormen [9, 10]. De orthorhombische rooster heeft de hoogste lipiddichtheid en de vloeibare rooster de laagste.

Het is van belang om het transport van stoffen door de huid te bepalen om vast te stellen of deze gebruikt kunnen worden voor toepassingen via de huid. *Ex vivo* humane huid en dierlijk huid wordt veelvuldig gebruikt om het transport van stoffen door de huid te onderzoeken. Het gebruik van humane huid wordt echter

beperkt door de geringe beschikbaarheid. Dierlijk huid verschilt van humane huid in een aantal aspecten, zoals epidermale en dermale dikte, haardichtheid en SC lipidensamenstelling, en daardoor dus ook in barrièrefunctie. Bovendien is het vanaf 2013 binnen de EU verboden om cosmetische producten en ingrediënten daarvan te testen op dierlijke modellen. Er is daarom een dringende behoefte aan een adequate vervanging voor humane en dierlijke huid. Het gebruik van huid gekweekt met behulp van geïsoleerde huidcellen, de zogenaamde 3-dimensionale humane huidequivalenten (HHEs), zou dit probleem kunnen oplossen.

HHEs werden in eerste instantie gegenereerd door keratinocyten in te zaaien op kweekplaten en deze in z'n geheel in het kweekmedium te houden. Dit resulteerde in een onvolledige differentiatie van keratinocyten en de vorming van een epidermis dat niet vergelijkbaar was met natieve humane huid. Een grote stap voorwaarts in de ontwikkeling van HHEs werd gerealiseerd door tijdens het kweken HHEs bloot te stellen aan de lucht [11]. Door deze en vele andere modificaties in de kweekcondities lijken HHEs tegenwoordig in veel opzichten op humane huid en hebben ze sterk verbeterde barrière-eigenschappen. HHEs hebben een vergelijkbare morfologie en brengen veel vroege en late differentiatiemarkers tot expressie op dezelfde manier als gezonde humane huid. Verder zijn de SC lipiden die aanwezig zijn in normale humane huid ook aanwezig in HHEs.

Het is meer dan een decennium geleden dat de SC lipidensamenstelling en -organisatie van HHEs uitgebreid onderzocht zijn. Uit literatuur blijkt dat de SC lipidensamenstelling en –organisatie van HHEs enige mate afwijken van humane huid [12]. Door de afwijkingen in SC lipideneigenschappen is de barrièrefunctie van HHEs minder efficient dan die van humane huid [12-14]. Hierdoor geven ze vaak een overschatting van de hoeveelheid stof dat door de huid getransporteerd wordt, waardoor er geen goede correlatie bestaat tussen *in vitro* en *in vivo* resultaten die betrekking hebben op transportstudies [15-18]. Bovendien is het desquamatieproces, het afschilferen van de dode corneocyten aan het huidoppervlak, verstoord in de

HHEs. Dit leidt geleidelijk tot verdikking van het SC als de kweekperiode verlengd wordt [19, 20]. Dit is ook van invloed op het transport van stoffen door HHEs. Hieruit blijkt dat de barrièrefunctie van HHEs verder verbeterd kan worden om humane huid nog beter na te bootsen. De afgelopen jaren zijn er in het Leids Universitair Medisch Centrum twee nieuwe HHEs ontwikkeld. De nieuwe 'fibroblast-derived matrix model' (FDM) en de 'Leiden epidermal model' (LEM) werden gekweekt samen met de 'full thickness collagen model' (FTM). Deze HHEs werden gebruikt om de hoofdvragen van dit proefschrift te beantwoorden, namelijk:

1. Kunnen HHEs gekweekt worden in een waterrijke omgeving, zoals *in uterus*, en hoe beïnvloedt dit de epidermale differentiatie en lipidensamenstelling?
2. Zijn de SC barrière-eigenschappen van de nieuw ontwikkelde HHEs en humane huid vergelijkbaar?
3. Wat is de correlatie tussen de SC lipidensamenstelling en lipidenorganisatie in de HHEs?
4. In hoeverre beïnvloeden de kweekcondities de SC barrière-eigenschappen van HHEs?
5. Hoe kunnen de SC barrière-eigenschappen van HHEs verbeterd worden?

HHEs gekweekt in een waterrijke omgeving en HHEs gekweekt aan het luchtoppervlak

In *hoofdstuk 2* staan studies beschreven waarin HHEs gekweekt worden in een volledig waterrijke omgeving, door onderdompeling in kweekmedium of vruchtwater, om de vorming van huid in de uterus na te bootsen. Het doel van deze studies was om vast te stellen of de micro-omgeving invloed heeft op de morfologie van HHEs tijdens het differentiatieproces van keratinocyten. HHEs gegenereerd in een volledig waterrijke omgeving, waarbij de keratinocyten van onder gevoed worden met medium, hebben een vergelijkbare morfologie en expressie van differentiatiemarkers als HHEs die gekweekt worden aan het

luchtoppervlak. Bovendien bevat het SC alle barrièrelipiden net als de HHEs die gekweekt worden door blootstelling aan de lucht. HHEs gekweekt in een waterrijke omgeving hebben echter een lager gehalte aan vrije vetzuren en een lager gehalte aan één van de ceramide subklassen met een zeer lange vetzuurketen (een van de acylceramides) in het SC ten opzichte van HHEs gekweekt aan de lucht. Verder blijkt uit de resultaten dat het SC van HHEs die blootgesteld worden aan de lucht tijdens het kweken meer waterminnende stoffen (natural moisturizing factors) bevatten dan HHEs gekweekt in een volledig waterrijke omgeving, maar desondanks een minder gehydrateerde SC hebben. De resultaten van *hoofdstuk 2* laten voor het eerst zien dat HHEs die gegenereerd worden in een waterrijke omgeving een volledig gedifferentieerde epidermis kunnen vormen.

SC barrière-eigenschappen van de nieuwe HHEs

In *hoofdstuk 3* worden de SC barrièrefunctie, SC lipidensamenstelling en –organisatie van FDM, LEM en FTM beschreven. De HHEs hebben een vergelijkbare morfologie en expressie van een aantal belangrijke differentiatiemarkers als normale humane huid, afgezien van de expressie van keratine 16 en de vroegtijdige expressie van involucrine. Om de barrièrefunctie van FDM, LEM, FTM en humane huid te vergelijken, werd het transport van benzocaine door het SC van de HHEs en humane huid onderzocht. Het SC van FDM en LEM heeft een driemaal hogere doorlaatbaarheid van benzocaine in vergelijking met humaan SC, terwijl de FTM een vijfmaal hogere doorlaatbaarheid heeft. Deze resultaten geven aan dat de HHEs een verminderde barrièrefunctie hebben in vergelijking met humane huid. Om de oorzaak van de verminderde barrièrefunctie van de HHEs te onderzoeken werden de SC lipidenorganisatie en –samenstelling onderzocht. De SC lipiden van alle HHEs vormen de LPP, wat belangrijk wordt geacht voor de barrièrefunctie. Er is echter geen indicatie voor de vorming van de SPP. Verder zijn de SC lipiden van HHEs voornamelijk gerangschikt in een hexagonale structuur, terwijl in humaan SC de lipiden

gerangschikt zijn in de dichtere orthorhombische structuur. Bovendien gaan de SC lipiden van HHEs bij een lagere temperatuur al over naar de vloeibare fase in vergelijking met humane huid. Alle HHEs bevatten net als humaan SC cholesterol, vrije vetzuren en alle acht ceramide subklassen die met dunnelaag chromatografie (HPTLC) gemeten kunnen worden. Hoewel de lipidencompositie niet quantitatief bepaald is, blijkt uit de resultaten dat het SC van de HHEs minder vrije vetzuren en meer acylceramides bevat dan humaan SC.

De invloed van kweekcondities op de SC barrière-eigenschappen van HHEs

Nadat bleek dat SC barrière-eigenschappen van de HHEs niet hetzelfde zijn als die van natief humaan SC, werd onderzocht of deze verschillen veroorzaakt worden door de kweekcondities of door de isolatieprocedure van de huidcellen. De experimenten die zijn uitgevoerd om deze vraag te beantwoorden staan beschreven in *hoofdstuk 4*. Biopten bestaande uit intacte huid of alleen de epidermale laag werden geplaatst op een fibroblast-bevattende collageen matrix. Uit deze studies blijkt dat de epidermale uitgroei van beide type biopten een vergelijkbare morfologie en expressie van de onderzochte differentiatiemarkers heeft als natieve humane huid. Er was echter wel sprake van vroegtijdige expressie van involucrine en aanwezigheid van keratine 16. De detectie van keratine 16 in de uitgroei van de biopten geeft aan dat de keratinocyten geactiveerd zijn. Het aantal SC lagen in de biopten nam toe gedurende de kweekperiode en was groter dan het aantal SC lagen in natief humaan SC. Hieruit blijkt dat het desquamatieproces niet op dezelfde manier plaatsvindt in de biopten als in natieve humane huid. Uit de lipidenanalyse blijkt dat de uitgroei van beide type biopten en de in *hoofdstuk 3* beschreven HHEs een vergelijkbare lipidensamenstelling hebben. De uitgegroeide epidermis van beide typen biopten heeft een lager vetzuurgehalte ten opzichte van humaan SC. Beide typen uitgroei bevatten alle ceramide subklassen, maar hebben een toename in acylceramides in vergelijking met humaan SC. Ook de SC lipidenorganisatie van

beide typen uitgroei is te vergelijken met die van de HHEs. De SC lipiden van de uitgegroeide epidermis vormen alleen de LPP en zijn voornamelijk gerangschikt in een hexagonale structuur. Bovendien zijn er aanwijzingen dat de lipiden iets meer vloeibare lipiddomeinen vormen dan in humaan SC. Deze resultaten laten overtuigend zien dat de verschillen in SC barrière-eigenschappen tussen de HHEs en humane huid niet het gevolg zijn van de celisolatie procedure, maar veroorzaakt worden door de kweekcondities. Dit is een positief resultaat, omdat hieruit blijkt dat een verdere verbetering van de SC lipideneigenschappen van HHEs gerealiseerd zou kunnen worden door vooral de kweekcondities te optimaliseren.

De correlatie tussen de SC lipidensamenstelling en SC lipidenorganisatie in HHEs

In de studies beschreven in *hoofdstuk* 3 zijn de SC lipidensamenstelling van HHEs onderzocht. In deze studies werden enkele verschillen in lipidenprofielen gevonden tussen de HHEs en natief humaan SC. Om meer inzicht te verkrijgen in deze verschillen werden de SC lipiden kwantitatief geanalyseerd met behulp van HPTLC. Bovendien werd er gebruik gemaakt van een recent ontwikkelde vloeistofchromatografie/massaspectrometrie (LC/MS) methode om de ketenlengtes van de vrije vetzuren en ceramides te bepalen. Deze experimenten staan beschreven in *hoofdstuk 5*. Uit de kwantificatie van de SC lipiden met HPTLC blijkt dat het SC van de HHEs inderdaad minder vrije vetzuren bevat dan SC van natieve humane huid. Bovendien blijkt uit de LC/MS resultaten dat de HHEs meer enkel onverzadigde vrije vetzuren bevatten dan humaan SC. Vrije vetzuren induceren de orthorhombische fase [21]. Het verlaagde vrije vetzuurgehalte en het verhoogde gehalte aan onverzadigde vetzuren spelen naar verwachting een cruciale rol bij de vorming van de hexagonale structuur in de SC lipidenorganisatie van HHEs. Deze twee veranderingen in de vrije vetzuursamenstelling in HHEs spelen waarschijnlijk ook een essentiële rol in de verminderde barrièrefunctie van de FDM, LEM en FTM. De verhoogde aanwezigheid van onverzadigde vrije vetzuren

in het SC van HHEs is waarschijnlijk ook deels verantwoordelijk voor de toegenomen lipidenwanorde en de verlaagde temperatuursovergang waarbij de vloeibare fase wordt gevormd.

Humaan SC bevat twaalf verschillende ceramide subklassen. Echter met behulp van HPTLC kunnen er acht ceramide klassen gescheiden worden, terwijl met LC/MS alle twaalf ceramide klassen gedetecteerd worden. Uit de LC/MS resultaten blijkt dat ook in het SC van de HHEs alle twaalf ceramide subklassen aanwezig zijn. In HHEs zijn echter twee acylceramides en ceramides met een uitzonderlijk korte totale koolstofketen in een verhoogde hoeveelheid aanwezig. Bovendien werden lage fracties onverzadigde ceramides gedetecteerd in HHEs. Deze werden niet gedetecteerd in humaan SC. Uit voorgaande studies blijkt dat acylceramides de vorming van de LPP induceren [22]. Hieruit mogen we concluderen dat de relatief hogere aanwezigheid van de twee acylceramide subklassen waarschijnlijk verantwoordelijk is voor de vorming van alleen de LPP in het SC van de HHEs.

Alle HHEs laten een verhoogde expressie zien van stearoyl-CoA desaturase 1 (SCD1), het enzym dat verantwoordelijk is voor de omzetting van verzadigde vrije vetzuren in enkel onverzadigde vrije vetzuren. SCD1 is aanwezig in zowel de basale als de gedifferentieerde lagen van de vitale epidermis in HHEs, terwijl in natieve huid SCD1 alleen aanwezig is in de basale laag. Dit suggereert dat de toename van enkel onverzadigde vrije vetzuren in het SC van HHEs veroorzaakt kan worden door een toegenomen activiteit van SCD1 in de suprabasale lagen van de vitale epidermis. Uit de resultaten van *hoofdstuk 5* blijkt dat de SC lipideneigenschappen verbeterd zouden kunnen worden door het vrije vetzuurgehalte in het SC te verhogen en de activiteit van SCD1 te verlagen, om zodoende de hoeveelheid enkel onverzadigde vrije vetzuren in het SC van de HHEs te reduceren.

Het onderzoeken van methodes om de SC barrière-eigenschappen te verbeteren

Omdat uit de in hoofdstuk 5 beschreven resultaten blijkt dat de SC barrière-eigenschappen verbeterd zouden kunnen worden door het totale SC vetzuurgehalte te verhogen en het enkel onverzadigde vetzuurgehalte te verlagen, besloten we de SC lipideneigenschappen van de LEM te optimaliseren door de samenstelling van het kweekmedium aan te passen. Deze studies staan beschreven in *hoofdstuk 6*. Om te bepalen in hoeverre de ketenlengtes en verzadigingsgraad van de vetzuren in LEM en humaan SC van elkaar verschillen, werd het vetzuurgehalte gekwantificeerd met behulp van LC/MS. Hieruit blijkt dat de LEMs ongeveer een 1.5x lagere hele lange vrije vetzuurgehalte (vrije vetzuren met 22-38 koolstofatomen) en ongeveer een 5x hogere enkel onverzadigde vrije vetzuurgehalte hebben in vergelijking met humaan SC.

Aan het medium van LEM wordt standaard palmitinezuur (C16:0), linolzuur (C18:2) en arachidonzuur (C20:4) toegevoegd. Om uit te zoeken of er vrije vetzuren uit het kweekmedium worden opgenomen door kweekjes, werd geprotoneerde palmitinezuur vervangen door gedeutereerde palmitinezuur, of werd er gedeutereerde arachidinezuur (C20:0) toegevoegd aan het standaard medium lipidensupplement. Uit de LC/MS analyse blijkt dat gedeutereerde palmitinezuur en arachidinezuur worden opgenomen. Deze vetzuren worden verlengd tot langere vrije vetzuren en worden vervolgens geïncorporeerd in het SC van LEM. Lipiden die afkomstig zijn van gedeuteerde arachidinezuur zijn echter in mindere mate aanwezig dan lipiden die afkomstig zijn van gedeutereerde palmitinezuur. In vervolgstudies werd i) de hoeveelheid lipidensupplement viermaal verhoogd of ii) het gehalte arachidonzuur en linolzuur gelijk gehouden, maar de hoeveelheid palmitinezuur viermaal verhoogd. Verder werden er verschillende concentraties insuline toegevoegd aan het medium om het effect van insuline op het gehalte van enkel onverzadigde vrije vetzuren in het SC van LEM en de expressie van SCD1 in de vitale epidermis te onderzoeken. Uit de resultaten blijkt dat een toename in de

supplementatie van arachidonzuur en linolzuur resulteert in een vermindering van de hoeveelheid hele lange vrije vetzuren en een toename in het gehalte van enkel onverzadigde vrije vetzuren. Het verhogen van de palmitinezuur in het kweekmedium had geen effect op het vetzuurprofiel in vergelijking met de controle. Ook de verandering in insuline concentratie in het kweekmedium had geen effect op het vetzuurprofiel van LEM of op de expressie van SCD1 ten opzichte van de controles. Alle veranderingen in het kweekmedium hadden geen invloed op de lipidenorganisatie van LEM, met uitzondering van de conditie waarbij arachidonzuur en linolzuur supplementatie viermaal verhoogd was. In het laatste geval vormden de SC lipiden van de LEMs een LPP met een kortere repetitieafstand en waren de lipiden al bij een lagere temperatuur volledig gerangschikt in een hexagonale fase in vergelijking met de controles.

HHEs hebben een toegenomen hoeveelheid di- en triglyceriden in het SC ten opzichte van humaan SC. Di- en triglyceriden worden gevormd door vrije vetzuren te koppelen aan een glycerol molecuul. De verhoogde aanwezigheid van di- en triglyceriden zou een reden kunnen zijn voor het verlaagde vrije vetzuurgehalte in het SC van LEM. De studies beschreven in *hoofdstuk 6* tonen aan dat de mediumsamenstelling een grote invloed kan hebben op de SC lipideneigenschappen van HHEs. Echter, de modificaties in het kweekmedium hebben tot dusver niet geleid tot een verbetering in de SC barrièrefunctie van LEMs. Dit geeft aan dat andere aanpassingen aan het medium of kweekomstandigheden nodig zijn om de SC lipideigenschappen van HHEs te verbeteren.

De afwezigheid van het desquamatieproces in vitro

Uit de resultaten beschreven in *hoofdstuk 4* blijkt dat het desquamatieproces niet plaatsvindt *in vitro*. Daarom werd er vervolgonderzoek uitgevoerd naar de expressie en activiteit van specifieke enzymen die betrokken zijn bij het desquamatieproces in natieve humane huid, HHEs en humane huid gekweekt voor één of twee weken

in de incubator. Deze studies staan beschreven in *hoofdstuk 7*. Uit de resultaten blijkt dat de HHEs en humane huid gekweekt gedurende twee weken nagenoeg geen desquamatie vertonen. Alle HHEs en humane huid in dezelfde kweekomstandigheden hebben dezelfde expressie van kallikreine 5, een van de belangrijke enzymen in het desquamatieproces, als humane huid. Bijna alle HHEs tonen echter de expressie van Lympho-epithelial Kazal type related inhibitor (LEKTI), een eiwit dat de activiteit van kallikreines inhibeert, in meerdere lagen van de vitale epidermis in vergelijking met natieve humane epidermis. In de FTM werd een verminderde kallikreine 5 activiteit gemeten in de oppervlakkige SC lagen in vergelijking met natieve humane huid. Uit deze resultaten blijkt dat de afwezigheid van het desquamatieproces in HHEs gedeeltelijk veroorzaakt zou kunnen worden door een verhoogde LEKTI expressie.

CONCLUSIES

Uit de resultaten in dit proefschrift blijkt dat HHEs een compleet gedifferentieerde epidermis vormen wanneer ze gekweekt worden in een waterrijke omgeving. Onder deze kweekomstandigheden hebben HHEs echter een verlaagde vrije vetzuur- en acylceramidegehalte in het SC ten opzichte van HHEs die gekweekt worden door blootstelling aan de lucht. Dit is een belangrijke bevinding, aangezien *in vivo* de huid gevormd wordt *in uterus*. Uit de gepresenteerde data blijkt dat de kweekomstandigheden van cruciaal belang zijn voor de eiwitexpressie en SC lipideneigenschappen van HHEs. Verder blijkt dat de SC lipidencompositie en –organisatie van HHEs beïnvloed wordt door de mediumsamenstelling.

In de studies beschreven in dit proefschrift zijn nieuwe aangrijpingspunten (zoals SCD1) geïdentificeerd die als richtlijn kunnen dienen voor toekomstig onderzoek gericht op het optimaliseren van de barrièrefunctie van HHEs. Optimalisatie van de kweekcondities kan leiden tot een verbetering in epidermale lipidmetabolisme van HHEs. Dit kan bijdragen tot de ontwikkeling van een nieuwe generatie HHEs

die beschikken over een competent SC barrière dat nog meer overeenkomsten heeft met natief humaan SC in vergelijking met de huidige HHEs.

REFERENTIES

1. Eckert, R.L. and Rorke, E.A. Molecular biology of keratinocyte differentiation. Environ Health Perspect **80,** 109, 1989.
2. Fuchs, E. Epidermal differentiation: the bare essentials. J Cell Biol **111,** 2807, 1990.
3. Johnson, M.E., Blankschtein, D. and Langer, R. Evaluation of solute permeation through the stratum corneum: lateral bilayer diffusion as the primary transport mechanism. J Pharm Sci **86,** 1162, 1997.
4. Meuwissen, M.E., Janssen, J., Cullander, C., Junginger, H.E. and Bouwstra, J.A. A cross-section device to improve visualization of fluorescent probe penetration into the skin by confocal laser scanning microscopy. Pharm Res **15,** 352, 1998.
5. Wertz, P.W. Lipids and barrier function of the skin. Acta Derm Venereol Suppl (Stockh) **208,** 7, 2000.
6. Bouwstra, J.A., Gooris, G.S., van der Spek, J.A. and Bras, W. Structural investigations of human stratum corneum by small-angle X-ray scattering. J Invest Dermatol **97,** 1005, 1991.
7. De Jager, M., Groenink, W., Bielsa i Guivernau, R., Andersson, E., Angelova, N., Ponec, M. and Bouwstra, J. A novel in vitro percutaneous penetration model: evaluation of barrier properties with p-aminobenzoic acid and two of its derivatives. Pharm Res **23,** 951, 2006.
8. Groen, D., Poole, D.S., Gooris, G.S. and Bouwstra, J.A. Is an orthorhombic lateral packing and a proper lamellar organization important for the skin barrier function? Biochim Biophys Acta 2010.
9. Bouwstra, J.A., Gooris, G.S., Dubbelaar, F.E. and Ponec, M. Phase behavior of lipid mixtures based on human ceramides: coexistence of crystalline and liquid phases. J Lipid Res **42,** 1759, 2001.
10. Damien, F. and Boncheva, M. The extent of orthorhombic lipid phases in the stratum corneum determines the barrier efficiency of human skin in vivo. J Invest Dermatol **130,** 611, 2010.
11. Prunieras, M., Regnier, M. and Woodley, D. Methods for cultivation of keratinocytes with an air-liquid interface. J Invest Dermatol **81,** 28s, 1983.
12. Ponec, M., Boelsma, E., Weerheim, A., Mulder, A., Bouwstra, J. and Mommaas, M. Lipid and ultrastructural characterization of reconstructed skin models. Int J Pharm **203,** 211, 2000.

13. Bouwstra, J.A., Gooris, G.S., Weerheim, A., Kempenaar, J. and Ponec, M. Characterization of stratum corneum structure in reconstructed epidermis by X-ray diffraction. J Lipid Res **36,** 496, 1995.
14. Ponec, M., Weerheim, A., Kempenaar, J., Mulder, A., Gooris, G.S., Bouwstra, J. and Mommaas, A.M. The formation of competent barrier lipids in reconstructed human epidermis requires the presence of vitamin C. J Invest Dermatol **109,** 348, 1997.
15. Ackermann, K., Borgia, S.L., Korting, H.C., Mewes, K.R. and Schafer-Korting, M. The Phenion full-thickness skin model for percutaneous absorption testing. Skin Pharmacol Physiol **23,** 105, 2010.
16. Asbill, C., Kim, N., El-Kattan, A., Creek, K., Wertz, P. and Michniak, B. Evaluation of a human bio-engineered skin equivalent for drug permeation studies. Pharm Res **17,** 1092, 2000.
17. Netzlaff, F., Lehr, C.M., Wertz, P.W. and Schaefer, U.F. The human epidermis models EpiSkin, SkinEthic and EpiDerm: an evaluation of morphology and their suitability for testing phototoxicity, irritancy, corrosivity, and substance transport. Eur J Pharm Biopharm **60,** 167, 2005.
18. Schafer-Korting, M., Bock, U., Diembeck, W., Dusing, H.J., Gamer, A., Haltner-Ukomadu, E., Hoffmann, C., Kaca, M., Kamp, H., Kersen, S., Kietzmann, M., Korting, H.C., Krachter, H.U., Lehr, C.M., Liebsch, M., Mehling, A., Muller-Goymann, C., Netzlaff, F., Niedorf, F., Rubbelke, M.K., Schafer, U., Schmidt, E., Schreiber, S., Spielmann, H., Vuia, A. and Weimer, M. The use of reconstructed human epidermis for skin absorption testing: Results of the validation study. Altern Lab Anim **36,** 161, 2008.
19. Ponec, M., Kempenaar, J. and Weerheim, A. Lack of desquamation - the Achilles heel of the reconstructed epidermis. Int J Cosmet Sci **24,** 263, 2002.
20. Vicanova, J., Mommaas, A.M., Mulder, A.A., Koerten, H.K. and Ponec, M. Impaired desquamation in the in vitro reconstructed human epidermis. Cell Tissue Res **286,** 115, 1996.
21. Bouwstra, J., Pilgram, G., Gooris, G., Koerten, H. and Ponec, M. New aspects of the skin barrier organization. Skin Pharmacol Appl Skin Physiol **14 Suppl 1,** 52, 2001.
22. De Jager, M., Gooris, G., Ponec, M. and Bouwstra, J. Acylceramide head group architecture affects lipid organization in synthetic ceramide mixtures. J Invest Dermatol **123,** 911, 2004.

LIST OF PUBLICATIONS

Varsha S. Thakoersing, Jeroen van Smeden, Walter Boiten, Gert Gooris, Aat Mulder, Rob J. Vreeken, Abdoelwaheb El Ghalbzouri, Joke A. Bouwstra, Modulation of barrier properties of human skin equivalents by specific medium supplements. *(Manuscript prepared for submission)*

Varsha S. Thakoersing[*], Jeroen van Smeden[*], Aat Mulder, Rob Vreeken, Abdoelwaheb El Ghalbzouri, Joke A. Bouwstra, Increased presence of mono-unsaturated fatty acids in the stratum corneum of human skin equivalents. *(Manuscript submitted to the Journal of Investigative Dermatology)*

Varsha S. Thakoersing, Mogbekeloluwa O. Danso, Aat Mulder, Gerrit Gooris, Abdoelwaheb El Ghalbzouri, Joke A. Bouwstra, Nature *vs* nurture: does human skin maintain its barrier properties *in vitro*? *(Accepted in the Journal of Experimental Dermatology)*

Thakoersing VS, Gooris G, Mulder AA, Rietveld M, El Ghalbzouri A, Bouwstra JA, 2012, Unraveling barrier properties of three different in-house human skin equivalents. Tissue Eng Part C Methods 18(1):1-11.

Thakoersing VS, Ponec M, Bouwstra JA, 2010, Generation of human skin equivalents under submerged conditions - mimicking the in utero environment. Tissue Eng Part A 16(4):1433-41.

[*]Contributed equally as first author

CURRICULUM VITAE

Varsha Thakoersing was born on January 22nd in 1984 in Paramaribo, Suriname. After graduating from Segbroek College in The Hague in 2002 she started her study Bio-Pharmaceutical Sciences at Leiden University. During her studies she did two internships. The first internship was performed at the department of Drug Delivery Technology at the Leiden/Amsterdam Center for Drug Research (LACDR), during which she established an *in vitro* model that mimics the *in utero* development of human skin. She did her second internship at the Dutch Discoveries Disclosed Foundation and the Dutch Clinical Trial Foundation within Science Alliance. During this internship she developed and implemented strategies to commercialize inventions from Dutch Universities and spin-off companies and to improve the position of The Netherlands as a clinical trial country. In August 2007 she obtained her Master's degree with honors. She started her PhD in September 2007 at the department of Drug Delivery Technology under the supervision of Prof. Dr. Joke Bouwstra, Dr. Abdoelwaheb El Ghalbzouri and Dr. Maria Ponec, which resulted in this thesis. From November 2011 she started as a research scientist at the Bioavailability and ADME group at Unilever in Vlaardingen.

NAWOORD

Na zo lang gezwoegd te hebben kan ik nu dan eindelijk beginnen met het laatste - maar zeker niet het minst belangrijke – gedeelte van mijn proefschrift. De afgelopen vier jaren waren fantastische jaren en hebben mij veel bijzondere ervaringen opgeleverd, zowel op wetenschappelijk als persoonlijk vlak. Ik heb veel mensen leren kennen en dankzij jullie zal ik altijd met een brede lach en fijn gevoel terug denken aan mijn AIO-tijd.

Wouter, jij bent mijn 'guru' wat celkweek betreft. Jij was een goede leraar, want tijdens mijn stage heb ik nooit een infectie gehad in mijn kweekjes! Zonder jouw training zou ik niet in staat zijn om de honderden kweekjes te maken tijdens mijn AIO-periode. Aan het begin van mijn AIO-tijd heeft ook Nazmoen mij het een en ander bijgebracht over huidkweek. Nazmoen, ook jij bedankt hiervoor. Dennis, jij stond altijd klaar om IHC kleuringen te doen voor mij. Mojgan, jij hebt mij ingewijd in de wereld van de diffusiestudies. Beiden bedankt voor jullie hulp tijdens onze korte tijd samen bij DDT.

Robert, jij was een super goede begeleider en later een fijne collega en kamergenoot. Jij hebt mij laten zien dat DDT een gezellige en boven alles een zeer sociale vakgroep is. Juul, wij zijn gelukkig ook een paar weekjes collega's geweest van elkaar (want ook jij was ooit mijn begeleider tijdens het GTA blok). Ik heb veel van jou geleerd en heb met veel plezier achter 'ons' bureau gewerkt. Ook nu na mijn AIO-tijd voorzie je me nog van advies.

Suus, wat hebben wij veel beleefd samen! Naast het werken hebben wij ook gefeest, gekookt en vakantie gevierd. Het cellab was onze toevluchtsoord als het leven even iets te spannend of frustrerend werd. Het was een vanzelfsprekende beslissing dat jij een van mijn paranimfen zou worden. Ik ben blij dat je me ook bijstaat tijdens mijn laatste momenten als AIO.

Bram, werken in het cellab was altijd veel leuker als jij er ook bezig was. Jij was onze radio, informant (!), adviseur en was altijd bereid om voor mijn cellen te zorgen. Het voelde alsof ik een grote broer had bij DDT.

Daniel, dankzij jou heb ik erg veel gelachen en ook steun gehad in de wat moeilijkere tijden. Samen hebben wij enkele DDT events georganiseerd. Al zeg ik het zelf, dat hebben we best goed gedaan. In ons laatste jaar bij DDT zorgde jij voor de organisatie van de vrijdagmiddagborrels of BBQs en daardoor voor de nodige ontspanningsmomenten. Olly, ook jij zorgde voor een gezellige sfeer in het lab. Jij was altijd vrolijk en voorzag ons van goede stapplaatsen tijdens onze congressen in België. Daarnaast heb je mij samen met Mojgan geleerd hoe ik huid moet dermatomiseren, een kunst dat nu zeer gewaardeerd wordt.

Na enige tijd veranderde ik van junior AIO naar senior AIO in kamer 718. Jeroen jij was 'ying' en ik was 'yang' (of was het andersom?). Het klinkt voor anderen misschien raar, maar wij weten wat karma met je kan doen! Het zal wel duidelijk zijn dat wij heel goed met elkaar hebben samengewerkt, aangezien jij een van mijn paranimfen bent. Onze trip naar New York en de Gordon was erg gezellig! Dankzij jouw LC/MS methode heb ik leuke resultaten gekregen dat heeft geleid tot twee gezamenlijke artikelen. Michelle, jij bracht orde in onze kamer. Onze tripjes naar conferenties waren ook altijd goed gepland en gezellig. Aat, jij was en bent altijd bereid om mij zo goed en zo snel mogelijk te helpen. Veel van de mooie IHC en TEM plaatjes in mijn proefschrift heb ik aan jou te danken. Jeroen, Michelle en Aat, het was erg fijn om een kamer met jullie te delen. Met z'n vieren hadden we leuke discussies over werk en andere zaken en konden we bij elkaar ons hart luchten of frustraties uiten.

Sun, we have some great memories together: France road trip, trip to Euro Disney, improving our cooking skills and all the great talks about whatever was on our minds. I'm happy you came to our lab and luckily you are not too far away to visit. Miranda, jij had het ook vaak heel druk, maar bleef altijd kalm en had altijd een glimlach op je gezicht. Jij hebt ook bijgedragen aan de parties van DDT: ons onvergetelijke uitstapje naar de Baja Beachclub en je geweldige bruiloft aan het strand! Andrea, wij hadden op wetenschappelijke vlak niet vaak met elkaar te maken, maar op het sociale vlak natuurlijk wel. Ons avondje cocktail drinken in München blijft nog heel lang in mijn herinneringen.

Vasco and Christophe, we started our PhD around the same time. I really had a lot of fun thanks to you guys. Even the conferences we went to felt like going to parties. Christophe, you hosted many dinners at your (old) place and Vasco, luckily you moved often and threw many house-warming parties. ☺ Thank you for all the parties, talks and cool programs.

Lolu, it was nice to finally have another person in the lab who was also working on skin cultures and who could understand the frustration when the cells did not grow well. Thank you for the nice discussions and the chance to be a bride's maid.

Diogenes and Tomo, you were also my room mates for a while. We had so much fun together. I could always count on you guys to leave the lab even later than I did! Hopefully our paths will cross again in the future.

I would like to thank the students who helped me with my project: Ida, Naila, Soedish and Walter. You worked very hard and sometimes experienced some bad luck. Thank you for all your effort and good luck with your (scientific) careers.

One of the things that I like so much about DDT is its international character. We had/have such an eclectic mix of nationalities of PhDs, post-docs, technicians, visiting scientists and students. Ana, Riccardo, Koen, Enamul, Eleni, Ding, Elly, Myrra, Robert P, Basak, Romano, Line, Anna, Tue, Nuch, Guri, Iwan, Hugo, Fransisco, Christian, Maria Chiara, Andreas, Abdoel, Ahmed, Anthippi and Daniel thank you all for the great moments. For those who are left, I hope you keep the DDT spirit alive.

En dan hebben we nog de vaste kern van DDT: Stefan, Connie en Gert. Stefan, ik kon altijd bij jou terecht voor technische hulp, vooral als het ging om de HPLC of de microscoop. Connie, jij maakt het leven van AIO's vaak (ongemerkt) veel makkelijker. Daarnaast biedt jij ook een luisterend oor. Bedankt voor alle hulp en steun! Gert, ook van jou heb ik veel geleerd. Onze tripjes naar Grenoble waren gezellig, zelfs tot in de late uurtjes. Ik kon altijd bij jou terecht voor mijn vraagjes over lipiden en voor discussies over films. Zoals ik altijd al zei "Jammer dat ik je niet mee kan nemen naar mijn nieuwe werkplek".

Natuurlijk mag ik mijn 'buren' bij Dermatologie in het LUMC niet vergeten. Marion, jij hebt me vooral in het begin flink geholpen. Bedankt voor alle tips en tricks. Vincent, jij ook bedankt voor alle hulp in je studententijd en als AIO. Suzan en Coby, jullie ook bedankt voor het delen van kennis en lenen van spullen.

During my PhD I was lucky enough to visit the ESRF twice to measure my samples. I would like to thank Dr. Wim Bras and co-workers for their kind assistance during these measurements.

Tish, jou kan ik natuurlijk niet vergeten. Heel erg bedankt voor het ontwerpen van de cover van mijn proefschrift. Pieter, jij ook bedankt voor het meedenken over de design van mijn cover.

Lieve familie, ook jullie wil ik heel graag bedanken voor jullie steun. Jullie boden me de noodzakelijke ontspanning tussen al het werken door. Soms kwamen jullie zelfs met ideeën om mijn doelen voor dit project te realiseren. Het is fijn om te weten dat er zo veel mensen zijn die mij steunen en succes toe wensen.

Died (Arshana), ook jij hebt mij de afgelopen vier jaar gesteund. Hoewel ik het niet vaak – misschien zelfs nooit – zeg, wil ik je hiervoor bedanken. Ook jij bent druk bezig met het opbouwen van een goede carrière. Veel succes! Met jouw inzet weet ik zeker dat je het nog veel verder zult schoppen.

Als allerlaatste zou ik dan mijn lieve pap en mam willen bedanken. Jullie liefde en steun kent geen grenzen. Jullie hebben Suriname verlaten voor een betere toekomst voor mij en Died. Het opbouwen van een nieuw bestaan in Nederland was moeilijk in het begin, maar jullie hebben met wilskracht en doorzettingsvermogen het uiteindelijk heel goed voor elkaar gekregen. Ik kan niet in woorden uitdrukken wat jullie voor mij betekenen. Een simpel bedankje is bij lange na niet voldoende en dat is dan ook de reden waarom ik dit proefschrift aan jullie opdraag. Als het in de toekomst mijn beurt is om een ouder te zijn, hoop ik het net zo goed te doen als jullie!